# A method for transient simulation of integrated ventilation and cooling systems in deep-level mines

**R Fair**

orcid.org/0000-0002-5286-9045

Thesis accepted in fulfilment of the requirements for the degree Doctor of Philosophy in Mechanical Engineering at the North-West University

Supervisor: Dr K. Nell

Co-supervisor: Dr J. C. Vosloo

Graduation: November 2022

Student number: 33596484

# ABSTRACT

Mine ventilation and cooling systems ensure adequate air temperature and flow in underground working areas. These are large and complicated systems that are integrated and interdependent. As underground mines expand to deeper and hotter levels where ore reserves are found, the efficient operation of ventilation and cooling systems becomes increasingly important.

Simulations are vital tools in the planning and optimisation of mine ventilation and cooling systems. The dynamic nature of underground mining operations, fluctuating ambient conditions, and dynamic cooling systems lead to a system that is seldomly in a steady state. Only a simulation that incorporates a true instantaneous heat flux model can simulate the thermal history effect seen in deep-level mines accurately.

Literature has shown the benefits of using true transient simulations that incorporate the thermal history effect. These studies applied true transient ventilation simulations to theoretical models or sections of deep-level mines and compared them with conventional steady-state simulations. There was therefore a need to apply a true transient simulation to entire mine ventilation systems and to integrate transient cooling simulation.

This study developed a novel methodology for simulating integrated true transient ventilation and cooling systems for underground mines. This method incorporated the thermal history effect and can practically be applied to entire deep-level mine ventilation and cooling systems with different infrastructure and mining methods.

The new methodology was used to develop simulations of three case study deep-level mine ventilation systems. Two of these case studies had integrated cooling systems providing secondary cooling to the mine. The case studies showed that a true transient simulation could accurately predict the underground airflow and temperatures.

Comparisons with a conventional steady-state simulation showed that the new true transient simulation had increased accuracy, which improved planning and optimisation. The case study simulation showed an average improvement of 1.0°C in the maximum error of temperature predictions. The improved accuracy further validated the true transient simulation in real-life applications.


**Key words:** Deep-level mines, ventilation, cooling, simulation, transient simulation.

# LIST OF PUBLICATIONS

The following publication has emanated from this research work so far:

- **R. Fair**, J. H. van Laar, K. Nell, D. Nell, and E. H. Mathews, “Simulating the sensitivity of underground ventilation networks to fluctuating ambient conditions,” S. Afr. J. Ind. Eng., vol. 32, no. 3, pp. 42–51, 2021. [1]

## ACKNOWLEDGEMENTS

This thesis would not have been possible without the support and guidance of the following people:

- I would like to thank my supervisors, Dr Kristy Nell and Dr Jan Vosloo for their support and guidance. I appreciate your contributions immensely.

- A big thank you to Prof. Eddie Mathews, Dr Jean van Laar, and Dr Diaan Nell for guiding me in writing up this thesis and the technical aspects thereof.

- To all my friends and colleagues, thanks for your support, contributions and encouragement. A special thanks to Austin Labuschagne, Juan van Wyk, JJ Swanepoel, and Marco le Roux for their assistance in the case studies.

- A big thanks to my family. I appreciate your support and understanding throughout this process. I would not have been able to complete this study without your love and understanding.

- Thanks to ETA Operations (Pty) Ltd for support to complete this study.

- Maryke du Toit, thank you for your love and support through this journey. Thank you for the constant perspective and balance you brought to my life.

- My heavenly Father, who has blessed me with the opportunity and drive to pursue post-graduate studies. All I have I owe to You.

## TABLE OF CONTENTS

## LIST OF FIGURES

** Figures marked with an asterisk were the author's work.*

## LIST OF TABLES

# LIST OF SYMBOLS

| Symbol | Description | Unit |
|---|---|---|
| $C_p$ | Specific heat of water | kJ/kg·K |
| *CV* | Calorific value of diesel | kJ/ℓ |
| *EEF* | Effective electrical heat | kW |
| *EHL* | Explosive heat load | kW |
| *FWHL* | Fissure water heat load | kW |
| *g* | Gravitational constant | $m/s^2$ |
| *HP* | Heat produced by explosive type | kJ/kg |
| *m* | Total mass of explosives used | kg |
| $\dot{m}$ | Mass flow of water/rock | kg/s |
| $\dot{m}_f$ | Fuel usage | ℓ/s |
| $\dot{m}_a$ | Air mass flow | kg/s |
| *MH* | Mechanised heat | kW |
| *MHL* | Metabolic heat load | kW |
| *MHR* | Metabolic heat rate | kW |
| *n* | Number of data points | – |
| *NE* | Number of employees | – |
| *PE* | Potential energy | kW |
| *q* | Water-cooling duty | kW |
| *Q* | Air volumetric flow | $m^3/s$ |
| *RP* | Release period | sec |
| $R^2$ | Coefficient of determination | – |
| *T* | Water temperature | °C |
| *VRT* | Virgin rock temperature | °C |
| *w* | Air density | $kg/m^3$ |
| *y* | Measured data | – |
| $\hat{y}$ | Simulation result | – |
| *Z* | Elevation | m |
| $\eta_{Com}$ | Combustion efficiency | % |

# LIST OF EQUATIONS

# LIST OF ABBREVIATIONS

| **Abbreviation** | **Description** |
| --- | --- |
| 3D | Three-dimensional |
| BAC | Bulk air cooler |
| DB | Dry bulb |
| FP1, …, FP5 | Fridge Plant 1, …, Fridge Plant 5 |
| GUI | Graphical user interface |
| KPI | Key performance indicator |
| L | Level (for example, 55L) |
| MSE | Mean square error |
| PTB | Process toolbox |
| SAJIE | South African Journal of Industrial Engineering |
| SCADA | Supervisory control and data acquisition |
| VRT | Virgin rock temperature |
| WB | Wet bulb |

# GLOSSARY

| Glossary | Description |
|---|---|
| *Air-cooling capacity* | The capacity of air to absorb heat in the mining environment. |
| *Auto-compression* | The conversion of potential energy to thermal energy by the compression of a fluid, such as air, moving downward, such as in a shaft. |
| *Blasting* | Setting off explosive charges in mining areas. |
| *Block-caving* | A mining method predominantly used on large, relatively low grade, ore deposits. |
| *Conventional mining* | Typical narrow reef with trackbound mining equipment. |
| *Cross-cut* | Drifts driven from the footwall across the ore body. |
| *Drift* | The generic name for all horizontal or subhorizontal developments made in a mine. |
| *Footwall* | A drift running parallel to the ore body. |
| *Geothermal* | Heat stored in the surrounding rock body. |
| *Hoisting* | The activity of extracting (bringing out) ore from the mine to surface. |
| *Intake airway* | Underground tunnels where fresh air flows to the working areas. |
| *Level* | A set of mining tunnels at a specific depth below surface. |
| *Mechanised mining* | A mining technique involving mobile mechanised equipment. |
| *Narrow reef mining* | The mining of a narrow hardrock ore reefs. |
| *Ore* | A naturally occurring solid material from which a metal or valuable mineral e.g. Gold can be extracted profitably. |
| *Quasi-steady-state simulation* | Consecutive steady-state simulation to form a transient output. |
| *Reject temperature* | Air temperature after the working areas. |
| *Return airway* | Underground tunnels where contaminated air flows out of the working areas to the surface. |
| *Shaft* | Vertical or incluined access tunnels used for transporting air, people, and materials. |

| | |
|---|---|
| *Steady state* | A condition of a system or process that does not change with time. |
| *Steady-state simulation* | A simulation where variables are constant with time. |
| *Transient simulation* | A simulation where variables are time-dependent. |
| *True transient simulation* | Time-dependent simulations that take the thermal history effect into account. |

# CHAPTER 1: INTRODUCTION

## 1.1 Background

Ventilation systems are essential for the operations of underground mines [2]. These systems and supplementary cooling systems ensure conducive underground environmental conditions [3]–[5]. Mine ventilation councils enforce ever-stricter regulations to ensure the health and safety of underground workers [5]–[11].

Ensuring good underground environmental conditions is becoming increasingly difficult as shallower mineral resources are depleted. The increasing depth of underground mines requires a constant increase in infrastructure and intensification of underground mining equipment use such as refrigeration, localised refrigeration, ventilation, administrative controls, and engineering controls [5], [6], [12]–[15]. The average depth of South African metal mines is over 2 km, with the deepest reaching up to 4.8 km [16], [17].

Ventilation and cooling systems, which require electricity to operate fans and refrigeration networks, use a significant portion of a mine's overall power consumption [7]. These systems may account for up to 40–50% of the total energy costs in mining [16], [18]. For deep South African mines, the extensive use of ventilation and cooling systems is a significant cost driver [11], [19].

In 2020, the mining industry made up 15% of Eskom's electricity sales [20]. Eskom is the power utility for the energy-constrained South Africa and has had extraordinarily high electricity price increases of 9.4%[1] per year over the past decade [21]–[23]. Figure 1-1 illustrates the historical and predicted (dashed lines) Eskom electricity tariffs against inflation in South Africa.

The increasing cost of ventilating and cooling resulting from an increase in electricity tariffs and inflation adds to the financial strain and uncertainties of the future of mining operations [24]. The mining industry is required to look at all possible improvements to make long-term financial sense [25].

---

[1] *Compiled from https://www.eskom.co.za/distribution/rates-in-excel-format/*

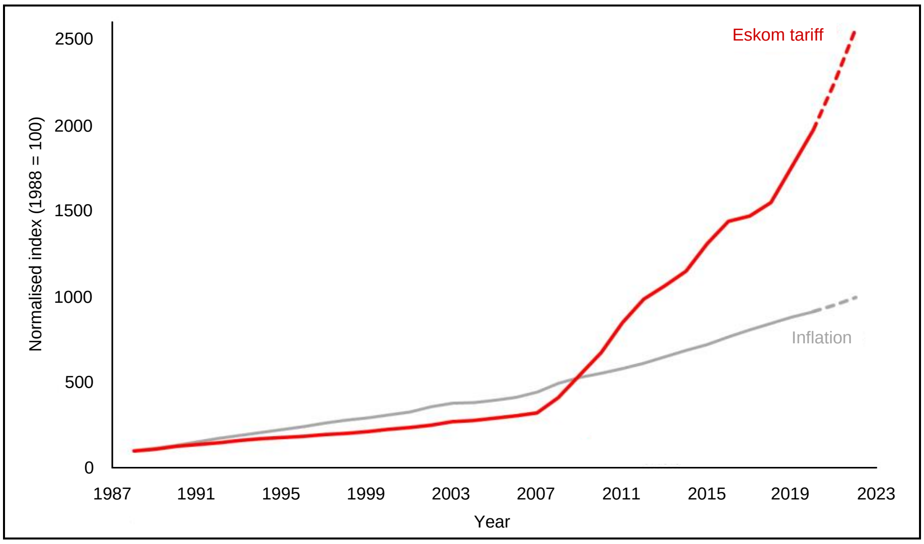


**Figure 1-1: South Africa electricity cost versus inflation[1]**

## 1.2 Mine ventilation and cooling systems

### 1.2.1 Overview

A mine ventilation system provides fresh air to underground workplaces that is used as a source of oxygen as well as to dilute and exhaust hot and contaminated air [26], [27]. An adequate quantity good quality fresh air is required to maintain ambient temperatures that provide a conducive and safe working environment [27]–[29]. Proper mine ventilation minimises and possibly prevents mine disasters [3], [30]. McPherson [31] described ventilation as the lifeblood of a mine. The intake airways are arteries that carry oxygen to the working areas, and the return airways are the veins that conduct pollutants from underground to be expelled to surface.

In South Africa, the Mine Health and Safety Act 29 of 2006 stipulates rigid temperature exposure limits that apply to underground workplaces [10], [32]. Mines must adhere to these exposure limits to continue mining and prevent heat stress on equipment and personnel [13]. Table 1-1 shows the maximum allowable temperatures for underground working areas in South Africa.

**Table 1-1: Temperature limits in South African mines [10]**

| Parameter | Limit |
|---|---|
| Maximum wet-bulb (WB) temperature | 32.5°C |
| Maximum dry-bulb (DB) temperature | 37.0°C |

[1] *Adapted from https://greeneconomy.media/the-price-of-water-and-electricity-in-south-africa-a-tale-of-two-tragedies/*

Deep underground mines use a network of tunnels and ventilation equipment to control airflow [33]. Conventional mining involves rock being excavated by drilling and blasting, usually from a narrow reef ore bodies, and transported by track bound machinery [11], [34], [35]. Figure 1-2 illustrates a simplified ventilation system on a conventional narrow-reef mine.

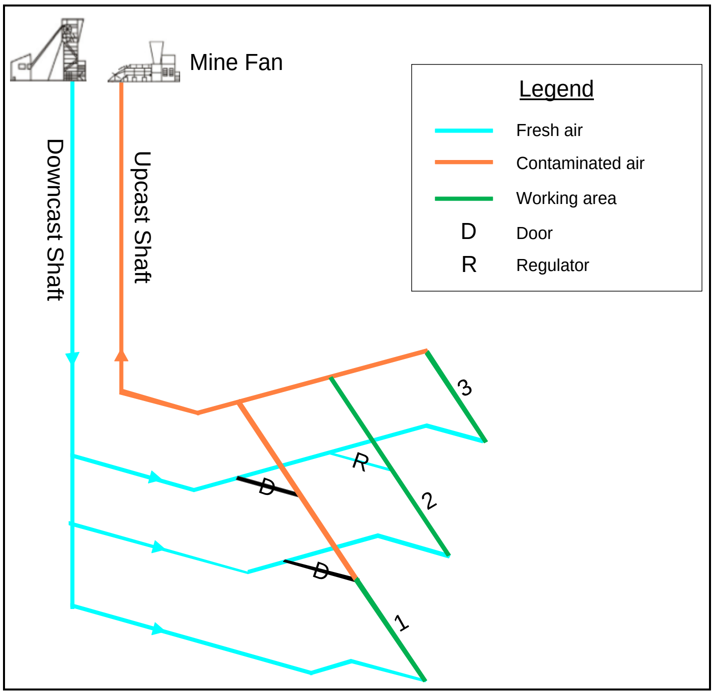


**Figure 1-2: Simplified schematic of a conventional mine ventilation system**

Block-caving mining method is used to mine large vertical and relatively low-grade ore deposits. This method undermines the orebody with undercut drifts and progressively collapses ore under its weight [36]. Mechanised mines use mobile diesel or electric machinery, which can be a significant contributor to the overall heat load and increase the ventilation and cooling requirements of an underground mine [11], [31], [35].

The mine ventilation system is the primary method of removing heat and contamination from the mine. Artificial mine cooling systems are incorporated when the ventilation system cannot provide acceptable and adequate working conditions [37]. Refrigeration and cooling systems supply artificial cooling to the underground ventilation system [38].

Figure 1-3 illustrates a simplified mine refrigeration cycle. The heat from the condenser side of the cycle is rejected to ambient air with cooling towers or to the return airway systems with condenser ponds.

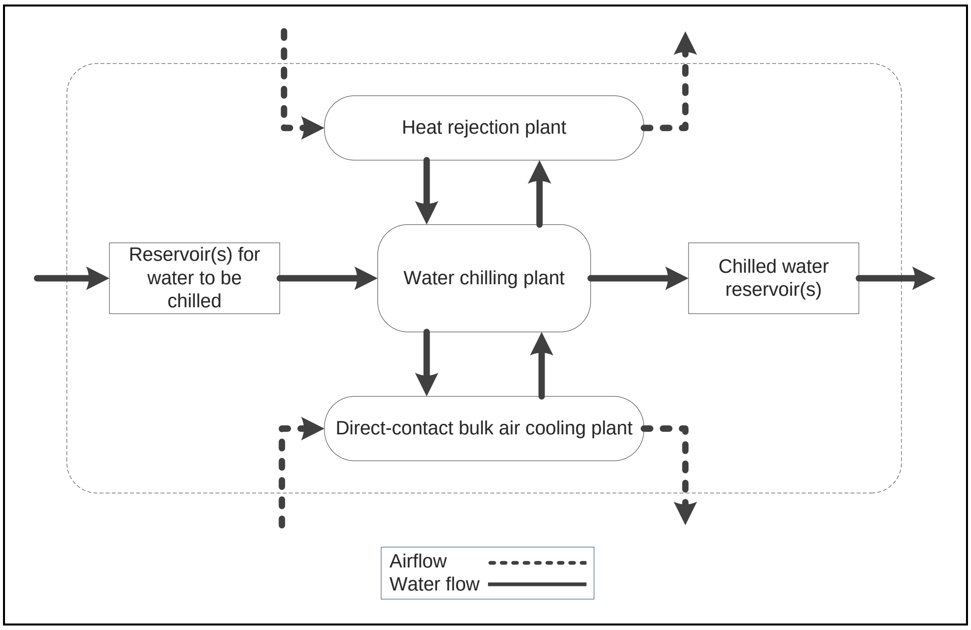


**Figure 1-3: Simplified schematic mine fluid cooling system(adapted from [35])**

Cooling can be applied to underground mines in many different ways, such as surface bulk air coolers (BACs), underground BACs, ice storage and spot coolers. Each has its advantages and disadvantages [39].

In deep and hot underground mines, the ventilation and cooling systems are integrated and interdependent [37], [40]. The planning and optimisation of these systems go hand in hand when planning the life-of-mine of an underground mine [41]. Mine ventilation and cooling are often investigated separately due to the complexity of the system [39], [42].

### 1.2.2 Heat loads in underground mines

Many potential heat sources contribute to elevated temperatures in deep underground mines [13]. Heat sources can differ considerably between mines, so all sources must be identified and quantified to determine the cooling requirements [24], [31]. Heat sources include geothermal (strata) heat, auto-compression, electrical, diesel machinery, human metabolism, explosives and fissure water. The average heat balance for hot mines is 48% from geothermal heat, 11% from auto-compression, 20% from equipment and 21% from other sources [5].

The ventilation system must supply adequate cooling to mitigate the identified heat sources. Cooling sources are also called heat sinks; defined as the phenomenon that extracts heat from the environment [11]. Heat sinks include air-cooling power, refrigeration and water-cooling duty [31].

Detailed heat load studies are used as a design tool for life-of-mine planning [11], [24]. Climatic monitoring and simulation software programs are vital tools for managing heat loads in underground mines [43].

### 1.2.3 Monitoring of ventilation and cooling systems

Traditional techniques for monitoring mine ventilation systems involve manual measurements that can be time-consuming [44], [45]. Although these methods often involve travelling on foot through the mine, they are still used in some mines today [46], [47]. Numerous handheld instruments are available to measure the different parameters of underground air [43], [47]:

- Vane anemometer – air velocity (m/s),
- Tube manometers – differential pressure (Pa),
- Sling hygrometer – WB and DB temperature (°C),
- Barometric pressure – digital barometer (kPa), and
- Temperature loggers (°C).

The integration of Industry 4.0 technologies provides improved monitoring and management of mine ventilation systems [24]. This paradigm is crucial for ensuring that the mining sector can remain profitable [48]. Underground climatic monitoring technology is critical for evaluating climatic conditions and developing heat control strategies [49], [50].

Climatic monitoring systems continuously record their data to a central supervisory control and data acquisition (SCADA) system [51]. These systems allow for the time-dependent assessment of cooling systems and underground climatic conditions [38], [43], [52]. The dynamic nature of mining and temperature variations requires the time-dependent assessment of ventilation networks [41], [50].

### 1.2.4 Dynamic nature of mine ventilation and cooling systems

Typical mine ventilation systems are complicated and comprise hundreds of airways with numerous branches and connections. Multiple controlling equipment such as doors, fans and regulators control the airflow to and from working areas. The dynamic nature of underground operations, fluctuating ambient conditions and dynamic cooling systems lead to a system that is seldom in a steady state [43], [53], [38].

The underground rock mass has a heat capacity that stores and releases heat to the air flowing underground. Heat storage and release cause thermodynamic dampening processes in an underground mine [24], [43]. Diurnal temperature fluctuation is reduced as the rock absorbs and releases heat [54]. The cyclic time-based heat-dampening processes in underground mines are widely known as the thermal damping effect and thermal flywheel effect [52], [55].

Figure 1-4 illustrates the surface intake DB temperatures and the DB temperatures at 1 290 m below surface of a mine over 24 hours. The thermal damping and thermal flywheel effects can be seen in the decrease in amplitude and phase shift of the 24-hour time cycle.

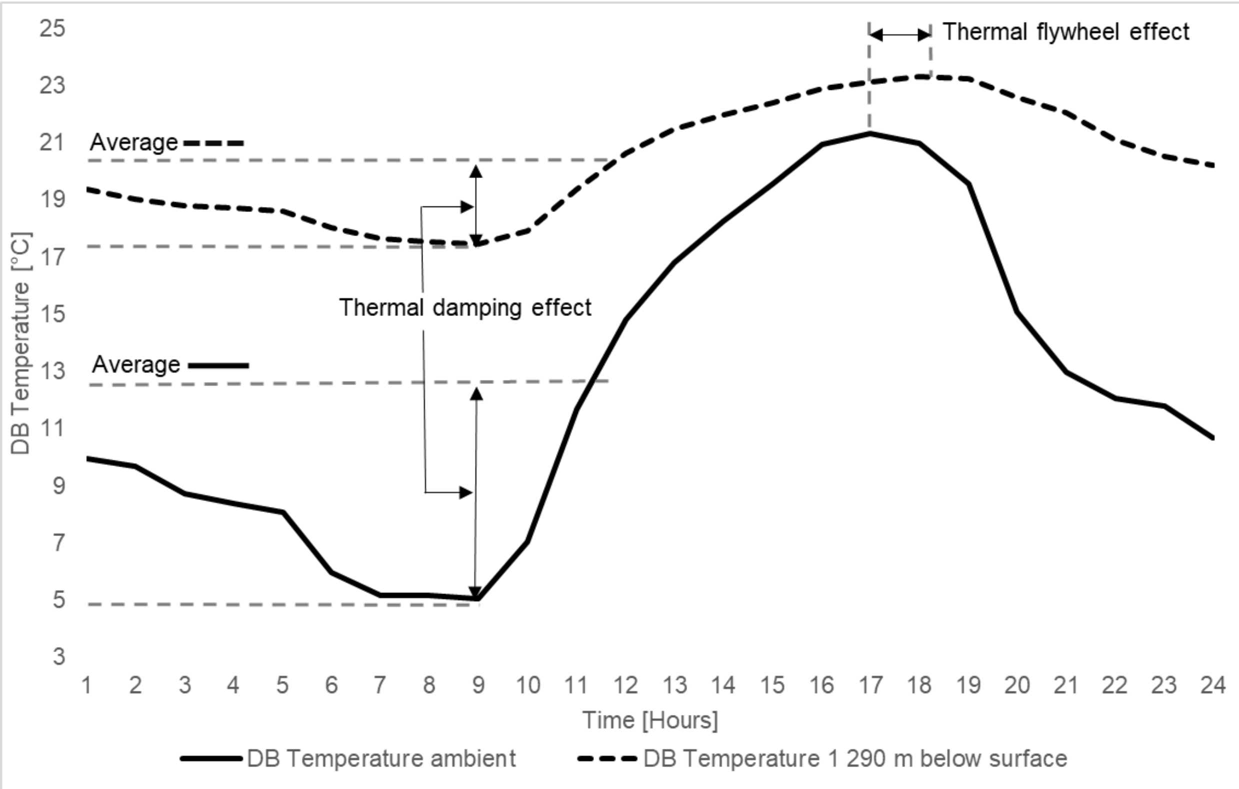


**Figure 1-4: Thermal history effect at 1 290 m below surface over 24h***

The decrease in the amplitude of the temperature fluctuation as air travels down the mine is the thermal damping effect. The intake air temperature is higher than the virgin rock temperature (VRT) at some locations during the daytime. At these times, the sensible heat is transferred from the intake air to the surrounding rock, cooling the surrounding air. With lower temperatures during the night, there is an increased potential for heat flow from the rock to the ventilating air, increasing the air's temperature [43], [52], [54].

The heat capacity of the surrounding rock and the distance that the ventilation air travels result in a time lag of temperature fluctuations. This time lag or phase shift in temperatures peaks as the air travels through the mine is the thermal flywheel effect [43]. The collective phenomenon is referred to as the thermal history effect [4], [56].

Dynamic underground operations and thermodynamic processes make it difficult to measure and optimise these systems. Specialised software can be used to capture and quantify the dynamic nature of mine ventilation and cooling systems [8], [32].

## 1.3 Mine ventilation and cooling simulation

### 1.3.1 History of mine ventilation simulation

Mine ventilation systems have been around for centuries, with the first texts dating to 1556 [57]. During the mid-1800s, Atkinson developed formulas for calculating pressure and airflow in underground tunnels [58]. These formulas formed the foundation for solving fundamental ventilation design problems [55].

The complexity of an underground ventilation system meant that the ability to predict ventilation conditions accurately was only realised with the development of analogue and digital computers [55]. During the second half of the twentieth century, the use of digital computers for ventilation planning became widespread throughout the mining industry [59], [60].

Historically, fires and explosions contributed to mining accidents and deaths, which were often caused by poor ventilation practices [55], [61]. Conventional steady-state modelling could not simulate the outcome of time-dependent ventilation problems like fires and explosions. This prompted the development of non-steady-state or transient behaviour simulations [59].

The main focus of transient ventilation simulations was on gas and fires. In the late 1970s, transient heat and airflow were successfully introduced into simulations [59]. During this time, the US Bureau of Mines developed the MFIRE program. MFIRE software is still widely accepted as the standard for the transient simulation of ventilation systems and underground fires [62].

Today, mine ventilation simulation is an indispensable tool used for planning and optimising mine ventilation systems across the world [7], [32], [63]. These simulations have proven to be reliable and flexible when applied to complex ventilation systems [47]. It is a valuable tool for making the right decisions and ensuring compliance with legislative requirements [42].

In his research on transient ventilation simulations, Stewart noted that there had been remarkably little research on improving transient network simulations since the 1990s, as a result of the computing power required. There has been, however, further research and validation on the MFIRE code. Only a few transient ventilation simulation software packages are available, namely VUMA, MFIRE, MineFire, VentGraph, Ventsim, Multiflux, and Process Toolbox (PTB) [55], [63].

These transient ventilation simulation software packages can solve non-steady-state solutions but not all can incorporate true transient heat exchange. In standard transient ventilation simulations, short time variations in ambient temperatures can induce significant modelling errors [43]. Only software that incorporates a true instantaneous heat flux model is capable of simulating the thermal history effect seen in underground mines and can solve true transient heat exchange processes [43], [55], [56].

The first documented use of true transient mine ventilation simulation was in 2012 when Danko et al. developed Multiflux [64]. This software incorporates a true instantaneous heat flux model to simulate heat from strata accurately. Since then, little research has been published on applying true transient mine ventilation simulations, possibly a testament to the computing power required for transient simulation [55].

Figure 1-5 shows the cumulative number of studies on transient mine ventilation simulations from 1987 until 2021. Since the first publication in 2012, there has been a growing interest in the true transient simulation of mine ventilation systems.

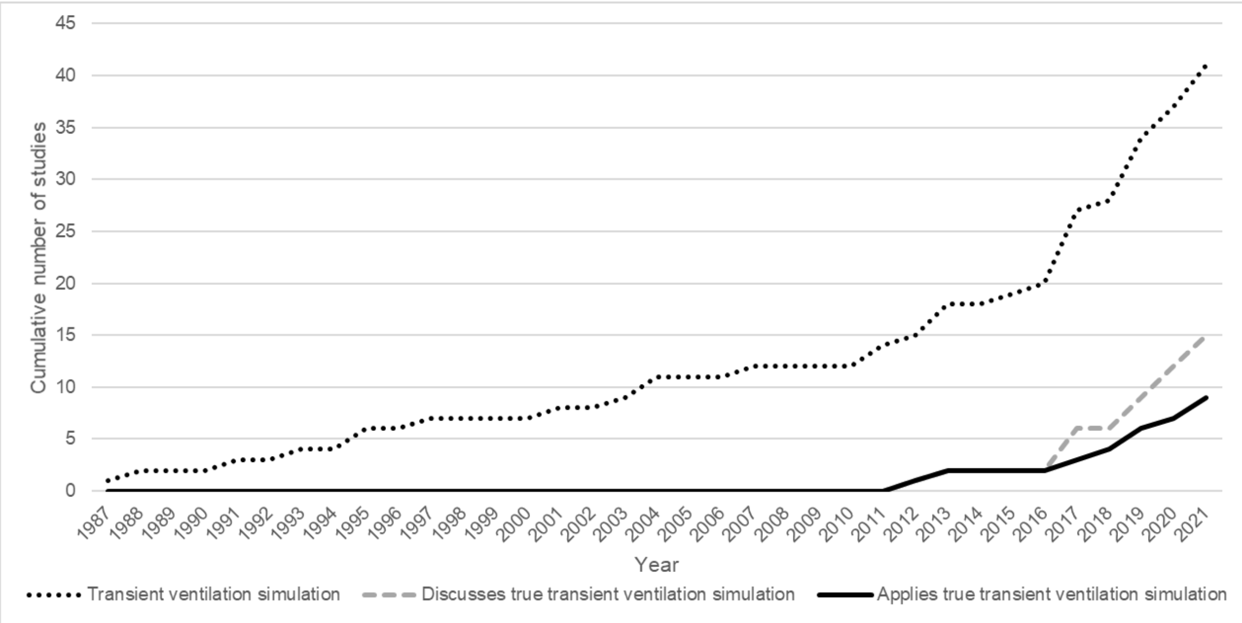


**Figure 1-5: Cumulative transient mine ventilation simulation literature***

Figure 1-6 shows the full chronological record of literature on transient mine ventilation simulation (see Appendix A for literature descriptions). Most recent studies from 2017 discussed or applied a true transient simulation.

Only a handful of simulation software packages are capable of solving true transient heat exchange processes. Table 1-2 shows a summary of true transient mine ventilation simulation software and the studies in the literature that applied each software.

**Table 1-2: True transient mine ventilation simulation software literature (2022)**

| Name | Owner | Studies that applied true transient simulation |
|---|---|---|
| Multiflux | University of Reno | • Analysis of the effects of thermal history of the strata upon temperature variations in underground airways [4]<br>• Temperature variations in underground tunnels [64]<br>• Subsurface flow and transport process model for time dependent mine ventilation simulations [65] |
| MFIRE | National Institute for Occupational Safety & Health | • Rapid dynamic ventilation modelling for improving health and safety in underground mining [55] |
| Ventsim | Chasm Consulting | • Managing heat in underground mines: The importance of incorporating the thermal flywheel effect into climatic modelling [2]<br>• Rapid dynamic ventilation modelling for improving health and safety in underground mining [55] |

These studies have shown the benefits of using true transient ventilation simulations. Incorporating thermal history will allow these simulations to consider true transient heat exchange processes such as the thermal damping and the thermal flywheel effects [4]. This is necessary to predict underground temperatures accurately [2], [65]. True transient mine ventilation simulation is an important research topic that may apply to many other uses [55].

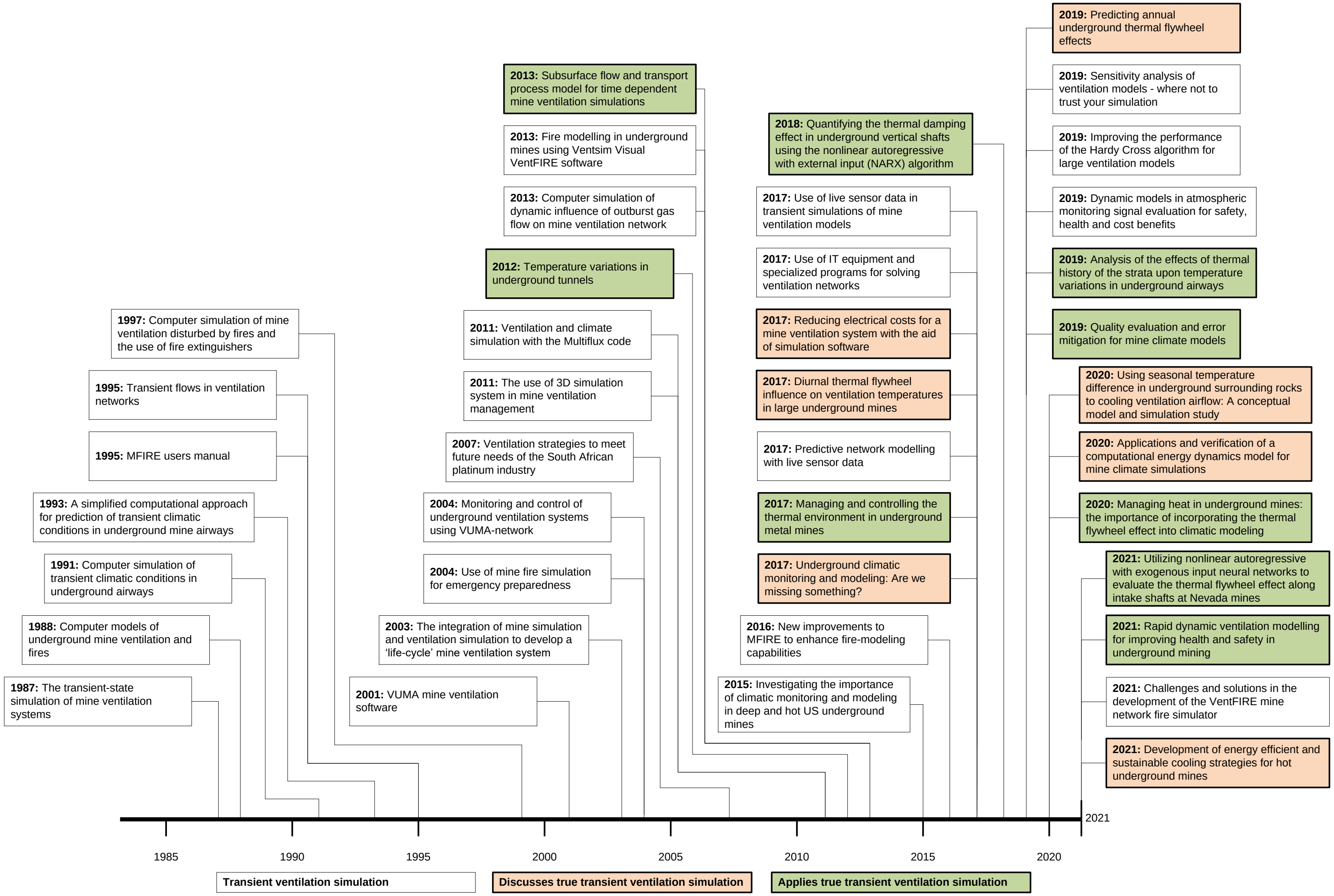


**Figure 1-6: Chronological record of transient mine ventilation simulation literature***

### 1.3.2 History of mine cooling simulations

Like mine ventilation simulations, the simulation of mine cooling systems became more prevalent with the advancement of computers during the late twentieth century [66], [67]. These simulation models solve various thermal equations by calculating the operating variables (temperature, pressure, and flow rates of energy and fluids). Conventional simulations solve for a thermal system in a steady state [21].

Mine cooling system simulation has proven to be crucial in the planning and optimising of mine cooling systems [66], [68]. Today, various software packages can simulate mine cooling systems accurately. Some well-known software packages include PTB, VUMA, Flownex, REMS, MVB, ENVIRON, QuickControl, VisualQEC, and WinMOD [21]. Of these softwares, only VUMA, PTB, Flownex, QuickControl, and VisualQEC can simulate transient systems [21]. Transient simulation is needed to evaluate the true operation of a mine cooling system and has been proved beneficial for energy management, future planning and optimisation [38], [66].

### 1.3.3 Integrated mine ventilation and cooling simulation

Mine ventilation and cooling simulations are vital tools in the planning and optimisation of these systems [31], [62], [65], [67], [68]. The integration of these system simulations allows for an iterative process to determine cooling needs. It is used to select the most viable size and position of air coolers and refrigeration components [40], [41].

Various mine ventilation simulation software has integrated components of refrigeration and cooling systems [21]. For example, VUMA mine ventilation software has steady-state and transient software that can integrate ventilation and cooling [41], [68]. PTB is also a component-based model capable of integrated ventilation and cooling simulations [21].

## 1.4 State of the art

The literature that incorporated true transient heat exchange processes plays a critical role in the current state-of-the-art simulation of ventilation and cooling networks. The studies in Section 1.3.1 that investigated the true transient simulation of mine ventilation systems are critical for improved environmental predictions.

Literature was reviewed according to a set of criteria. These criteria are determined by investigating how these simulations are used in the mining industry. The first criterion is to incorporate a true transient ventilation simulation. Literature has discussed the advantages of true transient simulation, which incorporates the thermal history effect.

True transient simulation incorporates the transient heat exchange between the underground rock and the ventilating air. These simulations can simulate the thermal history effect caused by the transient heat exchange to improve the accuracy of simulated environmental conditions. Accurate simulations are vital in the planning and optimisation of mine ventilation and cooling systems.

The development of transient ventilation models can be laborious and time-consuming [68]. A sound methodology to develop mine ventilation simulations is essential to enable accurate simulation and improved decision-making [58]. The second criterion is to investigate studies that include a methodology for developing true transient ventilation and cooling simulations.

Deep-level mine ventilation systems are complicated and dynamic, and simulations of these systems are used for planning and optimisation, which require an accurate representation of the entire system [7], [32], [63], [66], [68], [69]. These systems must ensure adequate underground environmental conditions to all areas of the mine [3]–[5]. The third criterion is to investigate studies that apply a true transient simulation to an entire mine ventilation system.

Cooling systems are incorporated when the ventilation system cannot adequately mitigate the heat in an underground mine ventilation system [37]. Ventilation and cooling systems are interdependent and are integrated using conventional simulations [21], [37], [40]. The fourth criterion is to investigate studies that integrate transient mine cooling simulations into the true transient mine ventilation simulation. Table 1-3 gives a summary of the criteria used.

**Table 1-3: Literature review criteria**

| Criteria | Description |
|---|---|
| 1. True transient ventilation | Studies that incorporate the thermal history effect in the simulation of a ventilation system. |
| 2. True transient methodology | Studies that include a methodology on building and calibrating an integrated true transient simulation. |
| 3. Entire mine ventilation network | Studies that are applied to an entire mine ventilation network. |
| 4. Integrated transient cooling simulation | Studies that integrate the transient simulation of cooling systems into the true transient simulation of ventilation networks. |

The following sections investigate the literature incorporating true transient heat exchange into simulations of underground mine ventilation systems. Each section gives an overview of the study and highlights the key outcomes relevant to this study.

### *1.4.1* Temperature variations in underground tunnels [64]

#### *i) Overview*

| | |
|---|---|
| **Year** | 2012 |
| **Authors** | G. Danko, D. Bahrami, W. Asante, R. Grymko, and P. Rostami |
| **Type** | Conference proceedings |
| **Conference** | 14th US/North American Mine Ventilation Symposium |

This was the first study during which the thermal history effect was investigated using simulation software. Danko et al. developed simulation software named Multiflux, which incorporated a “true temperature history model”.

A 3 km long theoretical tunnel was modelled to investigate the true temperature and heat flow variations over 25 months. This tunnel had a width of 3.5 m and a height of 5.7 m. The VRT was set to 57°C. The inlet was supplied with an airflow rate of 50 $m^3/s$ with a mean temperature of 28°C and a variation of 5°C amplitude.

The results from the Multiflux model were compared with other commercial mine ventilation simulation software available at the time, namely Climsim, Ventsim and VUMA. The true transient simulation was referred to as “with history”, and the quasi-steady-state simulation was referred to as “without history”. This method is called quasi-steady-state as it is time-dependent but does not fully incorporate the thermal history effect.

#### *ii) Key outcomes*

This study showed that the Multiflux's true temperature history model could incorporate the thermal history effect. The model further showed that seasonal temperature variations remain significant at a distance of 3 km.

The comparison of Multiflux with other commercially available software illustrated that none of the software packages incorporated the thermal history effect. Figure 1-7, 1-8, and 1-9 and compare Multiflux with Climsim, Ventsim, and VUMA, respectively.

The main findings from this study were that the short time and seasonal temperature variation are subject to significant modelling errors in steady-state models. It was further discovered that a phase shift accompanies an amplitude change in temperature predictions. Finally, these results have implications for future model solutions.

From the review criteria, the limitations of this study are that it did not include a methodology, was not applied to an entire mine ventilation system, and did not integrate transient cooling simulations. Furthermore, conference papers are not peer-reviewed and their findings can be questionable.

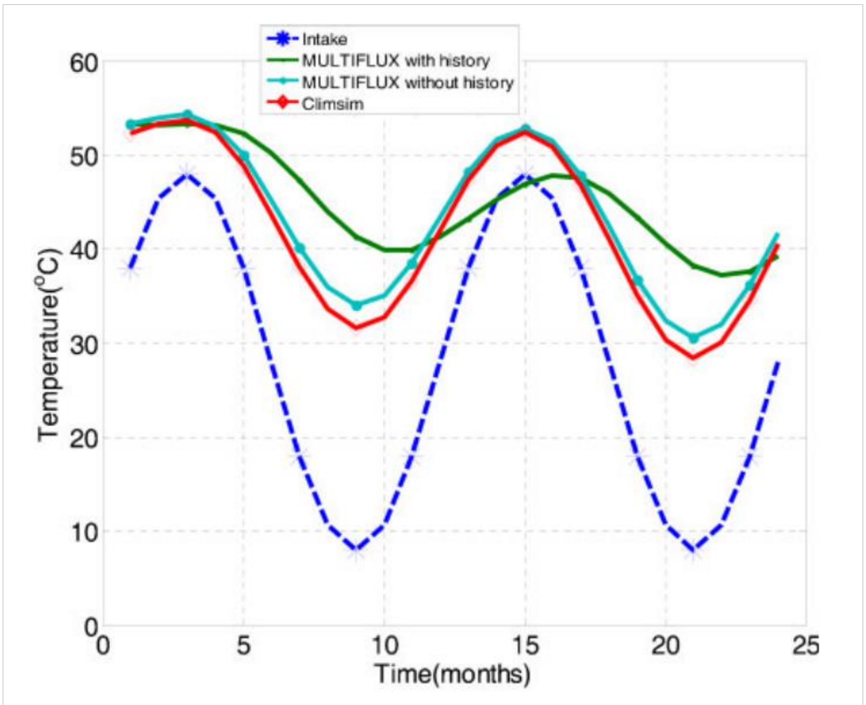


**Figure 1-7: Critical literature – Comparison between Multiflux and Climsim [64]**

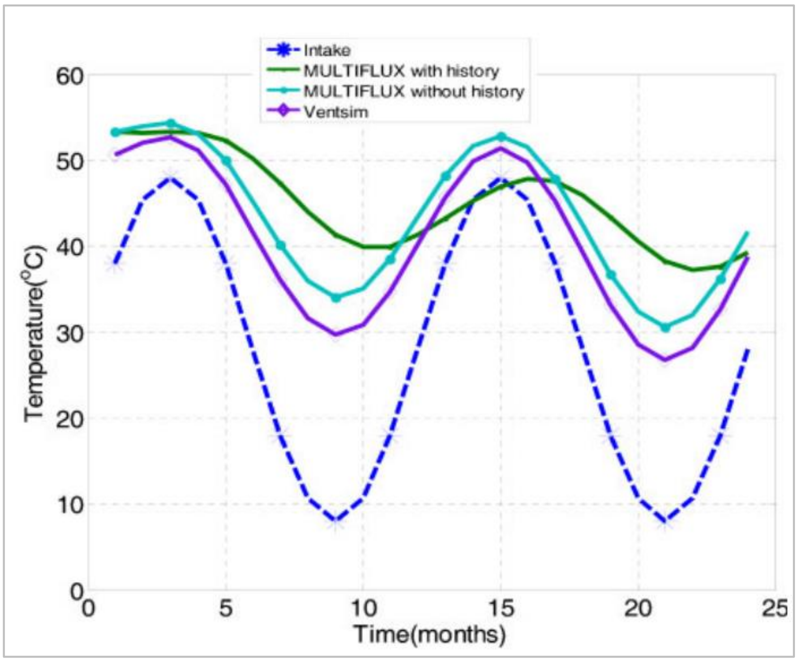


**Figure 1-8: Critical literature – Comparison between Multiflux and Ventsim [64]**

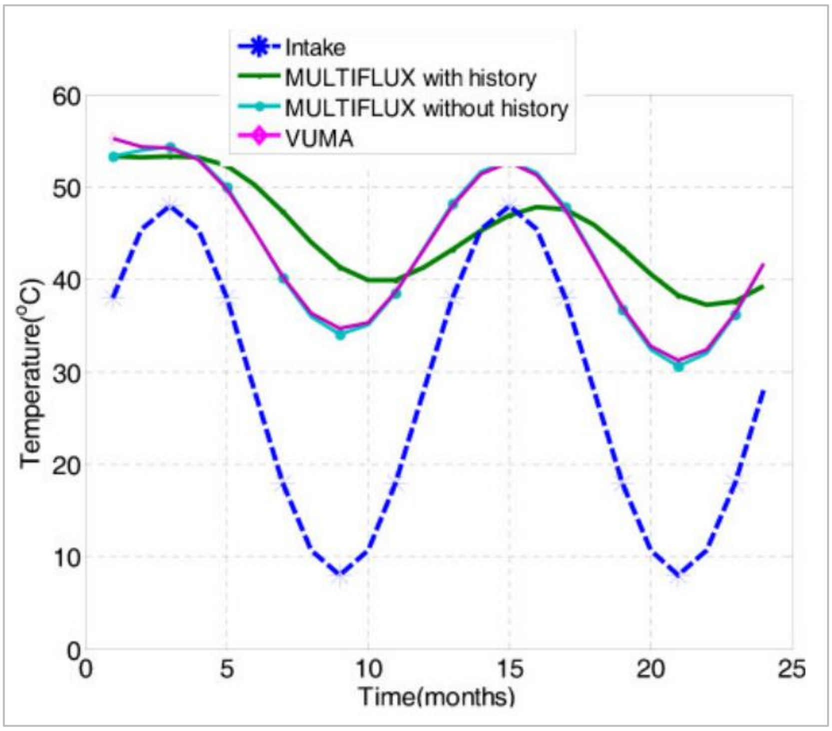


**Figure 1-9: Critical literature – Comparison between Multiflux and VUMA [64]**

### *1.4.2* Subsurface flow and transport process model for time dependent mine ventilation simulations [65]

#### *i) Overview*

| | |
|---|---|
| **Year** | 2013 |
| **Authors** | G. Danko |
| **Type** | Journal article |
| **Journal** | Transactions of the Institutions of Mining and Metallurgy, Section A: Mining Technology |

In this study, Danko built on his previous study, “Temperature variations in underground tunnels”, by incorporating the time-dependent simulation of contaminants. His previous study used a theoretical underground tunnel to simulate the time-dependent transport of ventilation, climate and contaminants [64].

#### *ii) Key outcomes*

The results and findings from the study “Temperature variations in underground tunnels” were reiterated in this study. The new findings primarily focused on the dispersion of contaminants in the model. These findings included methods to reduce the numerical and systematic errors and that the Multiflux model is prepared for real-time gas concentration predictions in ventilation-on-demand scenarios.

According to the review criteria, the limitations of this study are that it did not include a methodology for building a true transient simulation, was not applied to an entire mine ventilation system, and did not integrate transient cooling simulations.

### *1.4.3* Managing and controlling the thermal environment in underground metal mines [70]

#### *i) Overview*

| | |
|---|---|
| **Year** | 2017 |
| **Authors** | P. Roghanchi |
| **Type** | PhD dissertation |
| **University** | University of Nevada |

The main aim of this dissertation was to discuss methods for identifying and controlling heat in underground environments. The research contained three main sections, of which the last was to quantify the thermal damping effect in underground vertical openings (downcast shaft).

#### *ii) Key outcomes*

The author demonstrated that artificial neural network models can predict the temperature at the bottom of a shaft accurately. Further research was completed with linear regression models to quantify the damping coefficients of production and ventilation shafts.

This study further investigated the accuracy of the standard ventilation software programs, Climsim and Ventsim. A comparison between measured climatic conditions and the climatic predictions at the bottom of the intake shaft from this study is shown in Figure 1-10. The comparison indicates that commercially available mine ventilation software did not consider the thermal history effect at the time of this study.

From the review criteria, the limitations of this study are that it did not include a methodology, was not applied to an entire mine ventilation system, and did not integrate transient cooling simulations.

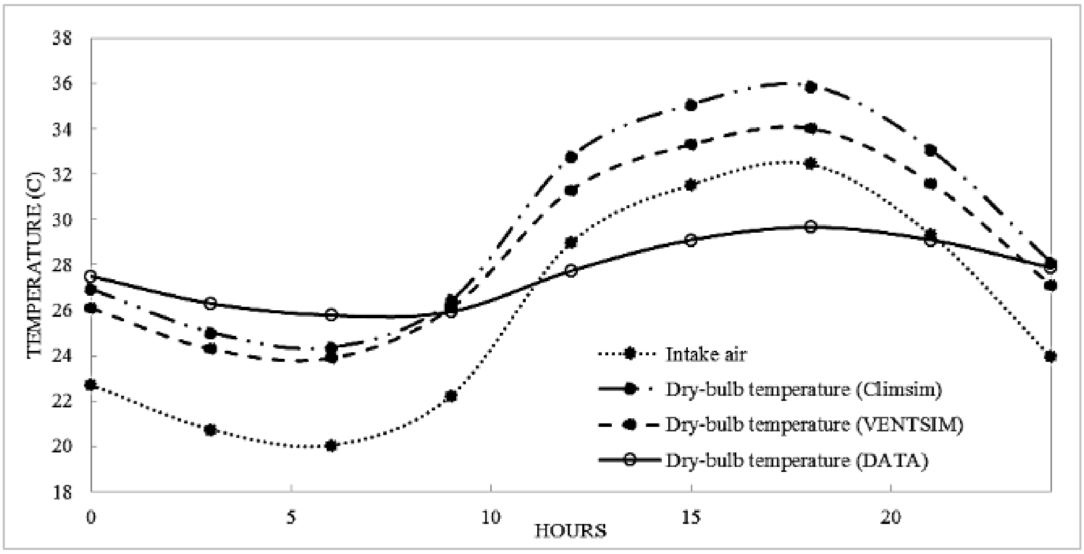


**Figure 1-10: Critical literature – Comparison between standard ventilation software [70]**

### *1.4.4* Quantifying the thermal damping effect in underground vertical shafts using the nonlinear autoregressive with external input (NARX) algorithm [52]

#### *i) Overview*

| | |
|---|---|
| **Year** | 2018 |
| **Authors** | P. Roghanchi and K. C. Kocsis |
| **Type** | Journal article |
| **Journal** | International Journal of Mining Science and Technology |

This study continued from the previous study but published in a journal format. It is important to note that these studies were only applied to vertical downcast shafts of an underground mine ventilation system.

#### *ii) Key outcomes*

This study had the same outcomes as the previous study.

### *1.4.5* Analysis of the effects of thermal history of the strata upon temperature variations in underground airways [4]

#### *i) Overview*

| | |
|---|---|
| **Year** | 2019 |
| **Authors** | C. Lu |

| | |
|---|---|
| **Type** | PhD dissertation |
| **University** | University of Nevada |

The objective of this dissertation was to investigate and compare ventilation simulation programs based on their dynamic capabilities. The goal was to understand the magnitude of modelling errors if the wrong inputs are used or if a software that cannot simulate the thermal history effect is used. Different scenarios were tested with Multiflux mine ventilation simulation software on theoretical underground tunnels.

#### *ii) Key outcomes*

There were multiple valuable outcomes and conclusions from this study:

- Mine ventilation software that does not consider the thermal history effect gives erroneous predictions, even if constant maximum or minimum constant temperatures are used.
- The mean absolute error of conventional steady-state mine ventilation software increases with the size of the mine. This shows that the thermal history effect is more important for deep and large underground mines.
- Mine ventilation software at the time of this study could not conduct dynamic ventilation simulations accurately.

From the review criteria, the limitations of this study are that it did not include a methodology, was not applied to an entire mine ventilation system, and did not integrate transient cooling simulations.

### *1.4.6* Quality evaluation and error mitigation for mine climate models [56]

#### *i) Overview*

| | |
|---|---|
| **Year** | 2019 |
| **Authors** | G. Danko |
| **Type** | Journal article |
| **Journal** | Quality – Access to Success |

It is well recognised that mine ventilation software without a thermal history component give erroneous results; however, simulations with a thermal history component are rarely available. This study aimed to find the best way to use simulation software that does not incorporate the thermal history effect. A long single-drift theoretical model was used to model three different scenarios.

***ii) Key outcomes***

An accurate solution model was set up that included a thermal history component and was used as the baseline for the other scenarios. Outcomes included recommendations for mine ventilation engineers to improve the predictions of simplified simulations.

From the review criteria, the limitations of this study are that it did not include a methodology, was not applied to an entire mine ventilation system, and did not integrate transient cooling simulations.

### *1.4.7* Managing heat in underground mines: The importance of incorporating the thermal flywheel effect into climatic modelling [2]

***i) Overview***

| | |
|---|---|
| **Year** | 2020 |
| **Authors** | K. A. Scalise, M. B. Teixeira and K. C. Kocsis |
| **Type** | Journal article |
| **Journal** | Mining, Metallurgy and Exploration |

This paper investigated two popular modelling softwares on how well they incorporate the thermal damping and thermal flywheel effects. A case study intake shaft model was developed in both simulation software packages. Actual weather data was used as the surface ambient conditions to compare the simulation with the temperatures measured at the bottom of the intake shaft.

***ii) Key outcomes***

Results showed that Ventsim could simulate the thermal flywheel effect on an annual flywheel heat simulation, while Climsim could not. The functionality to perform an annual flywheel heat simulation in Ventsim was new at the time of this study as it has not been used in previous studies [64], [70].

Figure 1-11 illustrates the Ventsim annual average temperatures simulation results in this study. The dashed red and blue lines are the ambient DB and WB temperatures, respectively. The solid red and blue lines are the DB and WB temperatures at the bottom of the shaft, respectively. The figure shows the average monthly WB and DB temperatures.

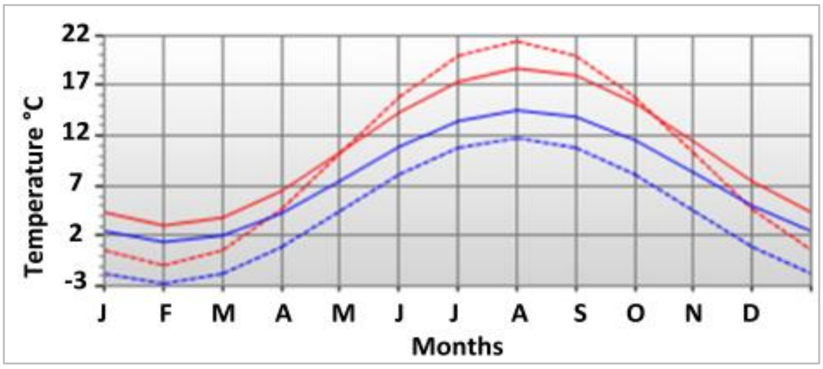


**Figure 1-11: Critical literature – Ventsim annual average temperatures [2]**

This study showed that Ventsim can incorporate the thermal flywheel to some extent. When compared with the actual measurements at the bottom of the shaft, the Ventsim model had an average WB temperature error of 7.9°C. The authors attributed this error to out-of-date continuous temperature data.

From the review criteria, the limitations of this study are that it did not include a methodology, was not applied to an entire mine ventilation system, and did not integrate transient cooling simulations.

### *1.4.8* Utilizing nonlinear autoregressive with exogenous input neural networks to evaluate the thermal flywheel effect along intake shafts at Nevada mines [71]

#### *i) Overview*

| | |
|---|---|
| **Year** | 2021 |
| **Authors** | K. Scalise and K. Kocsis |
| **Type** | Journal article |
| **Journal** | Mining Metallurgy & Exploration |

This study proposed a new method for using neural networks to determine the WB temperatures at the bottom of an intake shaft. WB temperature was selected as the crucial parameter as it significantly affects the working conditions and cooling capacity of ventilating air.

#### *ii) Key outcomes*

The neural network accurately predicted the WB temperature at the bottom of the intake shaft. However, this program only provides accurate results if it is kept up to date with large data sets collected with data loggers placed at the bottom of the shaft.

From the review criteria, the limitations of this study are that it did not include a methodology, was not applied to an entire mine ventilation system, and did not integrate transient cooling simulations.

### *1.4.9* Rapid dynamic ventilation modelling for improving health and safety in underground mining [55]

#### *i) Overview*

| | |
|---|---|
| **Year** | 2021 |
| **Authors** | C. Stewart |
| **Type** | PhD dissertation |
| **University** | The University of Queensland |

In this study, the author identified a need for real-time dynamic ventilation modelling with the main goal of predicting environmental conditions in the case of underground emergencies such as fires. The study aimed to develop a new method of dynamic ventilation modelling that can rapidly predict ventilation hazards.

#### *ii) Key outcomes*

New algorithms and methods provided rapid transient simulation modelling while maintaining sufficient accuracy. The rapid dynamic network algorithm was validated with a range of randomised models prepared for this study.

A new method was developed to estimate the dynamic heat transfer from rock strata. This model comes with the caveat that it is an approximation that lacks a complete air temperature history. This model was validated with the actual measurement of a section of Waldo mine fire experiments.

The research presented several applications that demonstrate the value of rapid dynamic network simulation. The applications include the simulation of:

- Explosive fume spread and clearance,
- Enhanced dynamic fire simulation,
- Real-time mine atmospheric monitoring, and
- Escapeway prediction.

From the review criteria, the limitations of this study are that it did not include a methodology, was not applied to an entire mine ventilation system, and did not integrate transient cooling simulations.

### 1.4.10 Summary of the literature

The true transient simulation of underground mine ventilation systems has improved and progressed since the first study in 2012. Appendix B shows how these critical studies have cited one another to get to the current practices.

Table 1-4 reviews the literature with the criteria listed in Table 1-3. These studies incorporate true transient ventilation simulation. The key outcomes of these studies were to show the advantages of true transient mine ventilation simulation.

The literature showed that there are currently no methods available for developing a true transient mine ventilation and cooling simulation. The studies have not been applied to entire mine ventilation systems, and none of the studies incorporated cooling simulations.

**Table 1-4: Summary of the literature**

| Reference | Year | Type | Study | 1. True transient ventilation | 2. True transient methodology | 3. Entire mine ventilation network | 4. Integrated transient cooling simulation |
|---|---|---|---|---|---|---|---|
| [64] | 2012 | Conference proceedings | Temperature variations in underground tunnels | | | | |
| [65] | 2013 | Journal article | Subsurface flow and transport process model for time dependent mine ventilation simulations | | | | |
| [70] | 2017 | PhD dissertation | Managing and controlling the thermal environment in underground metal mines | | | | |
| [52] | 2018 | Journal article | Quantifying the thermal damping effect in underground vertical shafts using the nonlinear autoregressive with external input (NARX) algorithm | | | | |
| [4] | 2019 | PhD dissertation | Analysis of the effects of thermal history of the strata upon temperature variations in underground airways | | | | |
| [56] | 2019 | Journal article | Quality evaluation and error mitigation for mine climate models | | | | |
| [2] | 2020 | Journal article | Managing heat in underground mines: the importance of incorporating the thermal flywheel effect into climatic modeling | | | | |
| [71] | 2021 | Journal article | Utilizing nonlinear autoregressive with exogenous input neural networks to evaluate the thermal flywheel effect along intake shafts at Nevada mines | | | | |
| [55] | 2021 | PhD dissertation | Rapid dynamic ventilation modelling for improving health and safety in underground mining | | | | |

| |
|---|
| The study contains information on this criterion |
| The study does not contain information on this criterion |

## 1.5 Need for this study

The literature and the fundamental shortcomings were highlighted in Section 1.4. Three critical problems were identified. The current needs in literature can be summarised as follows:

- A methodology needs to be developed to apply a true transient simulation to the integrated mine ventilation and cooling system. This methodology should be practical so that it can be applied to real-life case studies.
- True transient ventilation simulation has been proven to improve the prediction of the underground environment. There is a need for these simulations to be applied to an entire mine ventilation network. This will give insight into the feasibility of applying complicated true transient simulations to a large real-life case study.
- The integration of ventilation and cooling simulation is standard practice with conventional simulation. There is a need to integrate transient cooling simulation with true transient ventilation simulations. This will improve the environmental prediction for an integrated ventilation and cooling system to improve optimisation and life-of-mine planning.

The need for this study forms the foundation of the novel contributions discussed in the next section.

## 1.6 Novel contributions

### 1.6.1 Development of a methodology for integrated true transient mine ventilation and cooling simulations

#### *i) Need*

Developing ventilation simulations that incorporate the thermal history effect can be complicated and time-consuming [68]. A sound methodology is essential to enable accurate simulation and improved decision-making [58].

#### *ii) State of the art*

Steady-state and conventional transient ventilation and cooling simulations are widely used in the mining industry [7], [32], [63]. Numerous studies discuss a method for developing conventional ventilation and cooling simulations.

#### *iii) Shortcomings*

Current mine ventilation and cooling simulation methodologies do not take into account the development of a true transient simulation, which requires the detailed calibration of the thermal history effect. The literature that considers true transient simulation, as discussed in Section 1.4, does not provide a clear framework for the application of the simulation software.

#### *iv) The outcome of this study*

This study aims to develop a practical methodology for developing a true transient mine ventilation and cooling simulation for deep-level mines. An additional literature study will be conducted to determine the state-of-the-art methodologies for conventional mine ventilation and cooling simulations.

The new methodology should be practical so that it can be applied to real-life case studies. It should also take into account that deep-level mines have different instrumentation, layouts and mining methods. The simulation developed with this methodology should be as accurate as possible as it will be used for optimisation and future life-of-mine planning of underground ventilation and cooling systems.

### 1.6.2 Application of true transient ventilation simulation to an entire deep-level mine

#### *i) Need*

Mine ventilation planning and optimisation must ensure adequate underground environmental conditions for all areas of the mine. Simulations of these systems require an accurate representation of the entire system [7], [32], [63], [66], [68], [69].

#### *ii) State of the art*

State-of-the-art true transient ventilation simulation applied to sections of mine ventilation systems has improved the accuracy of environmental predictions compared with conventional ventilation simulations [2], [4], [52], [64], [65], [70], [71].

#### *iii) Shortcomings*

Section 1.4 investigated the studies that applied true transient mine ventilation software to underground mining networks. These studies applied the software to a theoretical model or a section of an underground mine. None of these studies applied the software to an entire mine ventilation network for comprehensive optimisation and life-of-mine planning simulations.

#### *iv) The outcome of this study*

This study aims to apply a true transient ventilation simulation to an entire deep-level mine ventilation network. The accuracy and feasibility of the simulation will be discussed. The result will be compared with conventional simulations to determine the benefit of this software on real-life applications.

### 1.6.3 Integration of a transient cooling simulation with a true transient ventilation simulation on a deep-level mine

#### *i) Need*

The integration of ventilation and cooling simulations allows for the detailed optimisation and planning of deep-level mine cooling systems [40], [41].

#### *ii) State of the art*

Integrating ventilation and cooling simulations is standard practice with conventional simulation [21], [40], [41], [68]. The second novel contribution aims to apply a true transient simulation to an entire mine ventilation system, which applies to deep-level mines that do not require secondary cooling systems.

#### *iii) Shortcomings*

Current studies have not integrated transient cooling simulations into true transient ventilation simulations. Integrating a cooling simulation will allow for improved prediction of environmental conditions, which is required when determining and optimising the cooling needs of deep-level mines.

#### *iv) The outcome of this study*

This study aims to develop an integrated true transient ventilation and cooling simulation for an entire mine. The results will be compared with that of a conventional simulation to determine the accuracy improvement and feasibility.

## 1.7 Conclusion

Mine ventilation and cooling systems are essential to the operation of deep underground mines [2]. These systems ensure adequate underground environmental temperatures and airflows as enforced by strict regulations [3]–[11]. Ensuring that these environmental conditions are achieved is becoming increasingly difficult as mines become deeper and more complex [5], [6], [12]–[15].

Mine ventilation and cooling simulations are vital tools in the planning and optimising of these systems [7], [32], [63], [66], [68]. Section 1.2.4 described the dynamic nature of underground mines and the resulting cyclic time-based heat-dampening processes known as the thermal history effect [4], [52], [55], [56]. Only a handful of simulation software packages can incorporate the thermal history effect, as discussed in Table 1-2.

The literature study in Section 1.4 investigated the application of modern true transient simulation to mine ventilation systems. This literature was reviewed according to a set of criteria, and the following gaps were identified [2], [4], [52], [55], [56], [64], [65], [70], [71]:

- No methods are currently available for the development of true transient mine ventilation and cooling simulations,
- True transient simulation has not been applied to an entire mine ventilation system, and
- No studies have incorporated transient cooling simulation into true transient ventilation simulation.

These shortcomings formed the foundation of the need for this study, discussed in Section 1.5. Developing a methodology and applying a true transient simulation to real-life mine ventilation and cooling system will give insight into the feasibility and advantages of these complicated simulations. Section 1.6 described the three novel contributions of this study, namely:

- Development of a methodology for integrated true transient mine ventilation and cooling simulations,
- Application of a true transient ventilation simulation to an entire deep-level mine, and
- Integration of a transient cooling simulation with a true transient ventilation simulation on a deep-level mine.

### 1.7.1 Thesis overview

#### *i) Chapter 1: Introduction*

Chapter 1 focused on the background of ventilation and cooling systems simulation of deep-level mines. A critical review of the literature has revealed a few shortcomings in applying true transient simulations. A need for the study was derived from these shortcomings, and three novel contributions were discussed.

#### *ii) Chapter 2: Methodology*

Chapter 1 showed a shortcoming in the literature for a methodology to develop true transient mine ventilation and cooling simulations. Chapter 2 aims to develop a methodology that incorporates the thermal history effect, which is fundamental to true transient simulations. This chapter will review the available literature on steady-state and transient mine ventilation and cooling simulation methodologies. The four main tasks of conventional simulation methodologies are data collection, building of the model, calibration and verification.

Each task was reviewed to incorporate the thermal history effect while remaining practically applicable to real-life scenarios. The novel true transient methodology developed in Chapter 2 considered data collection, calibration, and verification of cyclic time-based heat-dampening processes, which have not been considered in conventional methodologies.

#### *iii) Chapter 3: Results*

Chapter 1 determined a need from the literature to apply a true transient simulation to an entire mine ventilation and cooling system. Chapter 3 aimed to meet this need by applying the new methodology and true transient simulation to three case study mines.

The case studies were done on mines with different infrastructure and mining techniques, which gave insight into the advantages and disadvantages of applying true transient simulation. The results from these case study simulations aimed to validate the novel contributions of this study.

#### *iv) Chapter 4: Conclusion*

Chapter 4 included a review of how the needs for this study, identified in Chapter 1, were met in Chapter 2 and Chapter 3. The study was concluded by discussing this study's limitations, recommendations for further work, and a final conclusion.

# CHAPTER 2: METHODOLOGY

## 2.1 Preamble

Chapter 1 highlighted the importance of mine ventilation and cooling simulations in the planning and optimisation of these systems [7], [32], [63], [66], [68]. State-of-the-art simulations demonstrated the benefit of incorporating the thermal history effect when simulating underground environmental conditions [2], [4], [52], [64], [70]. Literature was reviewed in Section 1.4 according to a set of criteria and the following objectives were determined:

- Development of a methodology for integrated true transient mine ventilation and cooling simulations,
- Application of a true transient ventilation simulation to an entire deep-level mine, and
- Integration of a transient cooling simulation with a true transient ventilation simulation on a deep-level mine.

This chapter aims to meet the first outcome of this study and will start by investigating conventional mine ventilation and cooling simulation methodologies. These conventional methodologies will be adapted for integrated true transient mine ventilation and cooling simulations. The simulation software used in this study will also be discussed.

## 2.2 Conventional simulation methodologies

Simulations are vital in the modern-day planning and optimisation of mine ventilation and cooling systems [32], [45]. Multiple frameworks and methodologies are available in literature to develop and calibrate these models. A sound methodology is essential to enable accurate simulation and improved decision-making [67].

A literature study on mine ventilation and ventilation simulation methodologies showed four main tasks in developing a model, namely: data collection, building of the model, calibration and verification. The literature available for each task must be investigated to determine the current state-of-the-art practices. These tasks have many sub-task variations. The following sections will discuss a summary of the literature for each task.

### 2.2.1 Data collection

A comprehensive strategy for collecting data is crucial to calibrate an underground ventilation model accurately. The collected data will be compared with environmental predictions such as temperature, airflow,  and barometric pressure to determine the accuracy of the ventilation model [43].

Data can be collected at different levels of detail. Table 2-1 describes these different levels and gives examples of the data points to be collected for each. It is ideal to have a complete data set. However, collecting data at all levels can be a costly and time-intensive undertaking [24], [43], [67]. In the event of restricted data collection cases, only the key data points (as mentioned I the table below) can be used in conjunction with environmental prediction simulation [31], [60].

**Table 2-1: Data collection detail levels [11], [24], [43], [67]**

| Level | Description | Data measurement points examples |
|---|---|---|
| Level 1 | High-level data aimed at giving a holistic evaluation of the mine. | Primary intake and return airways, main fans, ambient conditions, fridge plants and BACs. |
| Level 2 | Intermediate data aimed at evaluating each specific mining level. | Level intake and return airways, level-specific cooling. |
| Level 3 | Low-level data that evaluates specific workplaces. | Working area intake and return airways, mobile coolers. Leaks in the underground network. |

Steady-state and transient data are required for steady-state and transient simulations, respectively [4]. A wide variety of data collection instruments is available. Some instrumentation requires manual measurements, which involve handheld instruments for taking spot measurements and logging data throughout the mine [43]. Climatic monitoring systems, sometimes called non-handheld instruments, allow for real-time and continuous monitoring of environmental conditions [60], [5].

As discussed in Section 1.2.2, mine ventilation systems have many potential heat sources contributing to the heat load. Conventional methodologies account for the heat load by adding heat to the ventilation simulation in the calibration process. Bluhm et al. [41] conducted a heat load study and distributed the heat on the relevant sections instead of conventional trial-and-error heat calibration.

The accuracy and reliability of ventilation and cooling simulation is dependent on the input data [72]. The input data is verified by establishing the accuracy of the measurements. Some instruments have known accuracy specifications [43], and other accuracies can be determined from previous empirical studies or field tests [44], [73]. Unwil et al. [74] conducted a detailed review of underground ventilation measurements and determined the associated accuracy of measurements.

### 2.2.2 Building of the model

The building of mine ventilation and cooling simulations is not discussed in detail often since typical software incorporates intuitive building functions. Some software, such as PTB, uses a component-based drag-and-drop graphical user interface (GUI) to simplify the building process [48]. This allows the user to import the digital survey plan files to the simulation software to create a three-dimensional (3D) network [50], [70]. Thereafter, other components such as fans, BACs and spot coolers are linked to the main ventilation systems.

The final step of building the model is to define all components with their standard parameters. This includes using empirical standards from various texts for each component [31], [75]. The components used to build ventilation simulations are tunnels, air pipes, and air fans. The components used to build cooling simulations are water-water chillers (fridge plants), water air-cooling towers, water-air heat exchangers, water dams, ice dams, water pipes, water pumps, and water demand [21].

### 2.2.3 Calibration

A well-calibrated model has a critical role in planning, optimising and controlling mine ventilation systems [45]. The calibration of networks differs between simulation software. Most calibration methods include manual iteration to determine unknown parameters [6], [21], [41], [53], [67], [76]. Some methods apply a dimensionless calibration factor to underground components to increase the accuracy of environmental predictions [75].

The accuracy of ventilation and cooling simulation predictions is critical, particularly when the parameters are close to allowable limits [43]. The required accuracy of the simulation depends on the desired outputs of the model [21]. The model accuracy is further limited by the accuracy of measured data [50], [75]. A study on mine cooling systems has shown that a simulation accuracy of 95% ensures an accurate representation of the actual system [38].

### 2.2.4 Verification

The predicted simulation outputs can be compared with actual measurements to verify the accuracy of a ventilation and cooling simulation model. For a steady-state simulation, this involves a simple comparison between a single value for each location and parameter [67]. For a transient-state simulation, this includes comparisons of time-dependent outputs [21], [45].

The accuracy of a steady-state simulation is determined by calculating the absolute error between the measured and simulated conditions [2], [51], [67], [75]. The time-dependent outputs can be compared with measurements in a few ways to determine the accuracy of a transient simulation. It might be necessary for mines with dynamic underground operations to compare averages over a time period [25], [54]. In other cases, the performance of the model is determined with statistical estimators such as the mean square error (MSE) and coefficient of determination ($R^2$) [52].

### 2.2.5 Summary

Table 2-2 summarises the literature on mine ventilation and cooling simulation, including a methodology or application framework (See Appendix C for literature descriptions).

**Table 2-2: Ventilation and cooling simulation methodologies**

| | | | Data collection | | | | Building of the model | | Calibration | Verification | |
|---|---|---|---|---|---|---|---|---|---|---|---|
| Number | Reference | Year | Collect steady-state data | Verify steady-state data | Collect transient data | Verify transient data | Build the model | Define the system with standard data | Perform iteration to determine unknown parameters | Compare results with measured data | Measure accuracy |
| 1 | [77] | 2001 | ■ | | | | | ■ | ■ | ■ | |
| 2 | [78] | 2002 | ■ | | | | ■ | ■ | | ■ | |
| 3 | [50] | 2004 | ■ | | ■ | ■ | ■ | ■ | ■ | ■ | |
| 4 | [32] | 2004 | | | | | ■ | ■ | | | |
| 5 | [53] | 2007 | ■ | ■ | | | ■ | ■ | ■ | ■ | ■ |
| 6 | [79] | 2011 | ■ | | | | ■ | ■ | ■ | ■ | |
| 7 | [80] | 2011 | ■ | | | | ■ | ■ | | ■ | |
| 8 | [41] | 2014 | ■ | | | | | ■ | ■ | | |
| 9 | [42] | 2014 | ■ | | | | ■ | ■ | | | |
| 10 | [43] | 2017 | | | ■ | ■ | | | | | |
| 11 | [70] | 2017 | ■ | | ■ | ■ | | | | ■ | ■ |
| 12 | [21] | 2017 | | | ■ | | ■ | ■ | ■ | ■ | ■ |
| 13 | [81] | 2017 | ■ | | ■ | ■ | | | ■ | ■ | ■ |
| 14 | [54] | 2017 | | | ■ | ■ | | ■ | | ■ | ■ |
| 15 | [67] | 2018 | ■ | ■ | | | ■ | | ■ | ■ | ■ |
| 16 | [76] | 2018 | | | | | ■ | ■ | ■ | | |
| 17 | [52] | 2018 | | | ■ | ■ | | | | ■ | ■ |
| 18 | [6] | 2019 | | | ■ | | | | ■ | ■ | ■ |
| 19 | [24] | 2019 | ■ | | ■ | | | | | | |
| 20 | [82] | 2021 | | | | | | ■ | | | |
| 21 | [47] | 2021 | ■ | ■ | | | | | | | |
| 22 | [55] | 2021 | | | ■ | ■ | | | | ■ | ■ |
| 23 | [75] | 2021 | ■ | | | | | ■ | ■ | ■ | |
| 24 | [45] | 2021 | ■ | | ■ | ■ | | | | | |
| 25 | [2] | 2021 | | | ■ | | | | | ■ | ■ |

| | |
|---|---|
| ■ | The study contains information on this step |
| | The study does not contain information on this step |

Figure 2-1 summarises the conventional simulation development process in a flow sheet. The percentage shown next to each step is the percentage of studies that described that step, as in Table 2-2.

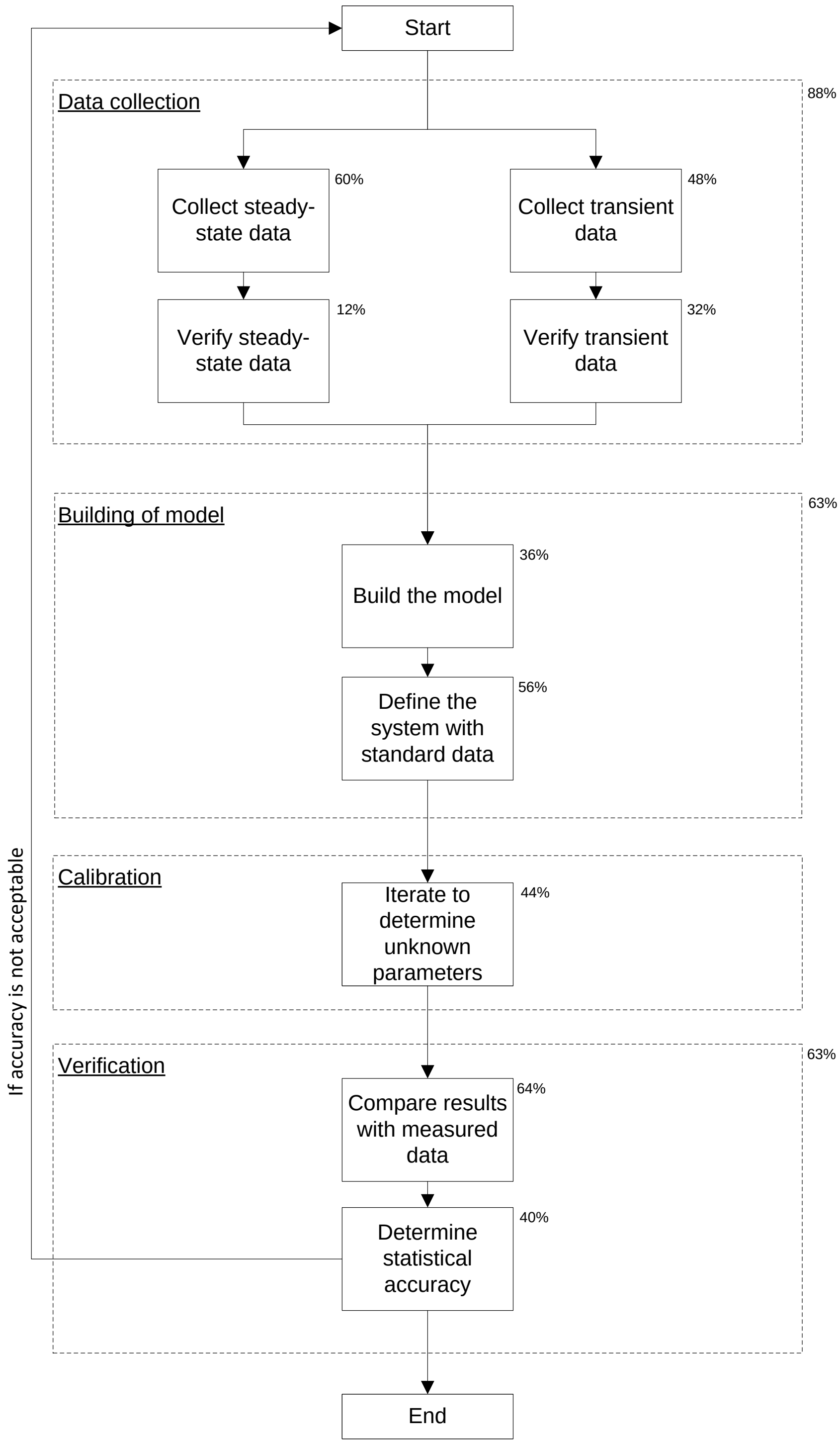


**Figure 2-1: Conventional ventilation and cooling simulation flow sheet***

### 2.3 True transient simulation methodology

The literature in Section 1.4 showed a shortcoming for a framework that applies a true transient simulation to mine ventilation and cooling systems. This section aims to develop a methodology to address the shortcoming. The conventional mine ventilation and cooling simulation must be adapted to incorporate true transient simulation, while remaining practically applicable.

In order to incorporate true transient simulation, the simulation software used for this method must include a time-dependent underground rock mass model with heat capacity. This will allow the simulation of thermodynamic processes seen in the thermal history effect. The methodology must consider the infrastructure available for the methodology to remain practically applicable.

This true transient methodology will primarily be based on the conventional methodologies seen in Section 2.2. Each of the four main tasks will be investigated separately to determine how it can be adapted for a true transient simulation.

#### 2.3.1 Data collection

Conventional methods have shown that the data collection strategy is crucial to calibrate a ventilation and cooling simulation accurately. Data should be collected according to the level of detail required for simulation outcomes. These methods have shown how steady-state, transient and heat load data can be used to improve the calibration of ventilation and cooling simulations. Figure 2-2 shows the data collection steps involved in conventional simulation methodologies.

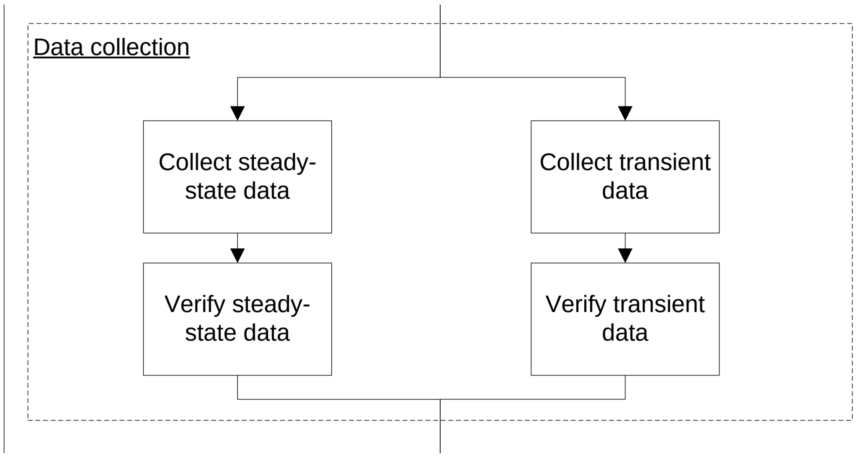


**Figure 2-2: Conventional data collection flow sheet***

### *i) Incorporate true transient simulation*

In literature, the calibration of true transient heat transfer processes requires enough time-dependent data to define the thermal history effect. Fluctuating ambient temperatures affect underground conditions significantly and time-dependent measurement is crucial for calibrating mine ventilation simulations. Underground time-dependent temperature measurements are compared with simulated predictions to calibrate the thermal history effect [2], [4], [43], [52], [54], [65].

From the studies in Chapter 1, the following is required to calibrate the true transient heat transfer processes:

- Transient ambient temperature data,
- Transient underground temperature data,
- Transient cooling and refrigeration component data, and
- Enough data to define the thermal history effect accurately.

The amount of data required will differ between mines as the thermal history effect will result in different amounts of damping in the mine. Data must be collected to define the full extent of the thermal history effect for all mine sections.

### *ii) Be practically applicable*

The data collection and development of transient ventilation models can be time-consuming. Some studies have used weeks or even years' worth of data to calibrate and verify models accurately [55], [65]. Environmental sensors allow for continuous monitoring of the underground environment, reducing the time required for manual data measurement. This technology is relatively new and not all mines have a complete set of instrumentation for capturing all the necessary data [24], [49]. Outstanding data has to be measured manually, making the data collection process laborious [43], [55].

The data collection should be prioritised according to the desired outcomes of the simulation while ensuring that enough data is collected to define the thermal history effect accurately. Before the data is collected, the level of detail and key performance indicators (KPIs) should be determined. This ensures that no unnecessary data is collected and less time is spent on data collection. The accuracy of the data should be determined to ensure that the simulation is calibrated to a realistic accuracy.

For mines with limited data collection infrastructure, it might be necessary to collect steady-state data to supplement the transient data. Airflow is an example of an environmental condition that is measured and calibrated in a steady state for cases where manual measurements are required [43].

True transient simulation models have longer simulation times [55]. Conventional methodologies have shown that steady-state heat load calculations can be used to calibrate the heat added to a ventilation model [41]. Other studies have shown that Industry 4.0 technology can determine and monitor dynamic heat loads [24]. Determining the dynamic heat load before the calibration reduces the simulation time by eliminating an unknown parameter that requires simulation iterations. The heat load calculation and data required are discussed in the following section:

#### *iii) Calculate heat load*

Heat load studies focused on identifying and quantifying heat sources in underground mines [11], [31]. True transient ventilation simulations can accurately account for geothermal and auto-compression heat sources. The heat added by the remaining secondary heat sources is added to the relevant sections of a mine ventilation simulation as a kW/m heat value [41]. The secondary heat sources to be determined in this heat load calculation are heat added by mechanised machinery, electrical, human metabolism, blasting, and fissure water. The most significant contributors to the heat load in deep mines are usually geothermal heat, auto-compression and machinery [11], [31]. Mechanised machinery can be either electricity- or fuel-driven [11], [31].

In underground mines, heat exchangers such as BACs or mobile coolers remove the heat from the ventilation airflow [35]. Simulation software integrates this cooling infrastructure into the ventilation model as heat exchanger components [32]. In cases where a chilled water reticulation system supplies cooling, heat is transferred between the ventilation airflow and chilled water pipes if the pipes are not insulated adequately [35]. The simulation accounts for this heat transfer by subtracting the chilled water pipe cooling duty from the secondary heat load.

The first step in the heat load calculation is to determine which of the heat sources listed above are present in the mine ventilation system. When all the heat sources have been identified, each source's amount of heat added can be calculated. Heat added by fuel-driven machinery is calculated if fuel-driven machinery operates in the underground ventilation network. The design duty is used to determine the transient heat of fuel-driven machinery. Detailed machine operating times and motor efficiencies are required to account for the transient nature of fuel-driven machinery [11].

It is important to account for all useful work conducted by fuel-driven machinery. This includes any work that increases the potential energy of a mass in the underground system. This usually includes transporting ore or pumping water to a higher elevation. The potential energy gain of the mass is calculated using Equation 2-1 and is subtracted from the heat from fuel-driven machinery [11], [83].

$$PE = m^{\cdot} \times g \times Z \qquad 2\text{-}1$$

Where:

| | | | |
|---|---|---|---|
| $PE$ | = | Potential energy rate | $kW$ |
| $\dot{m}$ | = | Rock mass flow/water mass flow | $kg/s$ |
| $g$ | = | Gravitational constant | $m/s^2$ |
| $Z$ | = | Elevation | $m$ |

In cases where operating time records are not kept, the average heat releases for diesel are calculated. This requires the average fuel consumption data for a typical mining day. The heat from the combustion of fuel is calculated using Equation 2-2.

During the operation of fuel-driven machinery, the average heat load from fuel consumption must be multiplied by a factor of between 2 and 3 for an accurate representation of the maximum temperatures that may be expected [11], [83].

$$MH = \dot{m}_f \times \eta_{Com} \times CV \qquad 2\text{-}2$$

Where:

| | | | |
|---|---|---|---|
| $MH$ | = | Mechanised heat | $kW$ |
| $\dot{m}_f$ | = | Fuel usage | $litre/s$ |
| $\eta_{Com}$ | = | Combustion efficiency | % |
| $CV$ | = | Calorific value of fuel | $kJ/litre$ |

Thereafter, the effective mechanised heat is calculated using Equation 2-3.

$$Effective\ mechanised\ heat = MH - PE \quad (2\text{-}3)$$

Where:

| | | | |
|---|---|---|---|
| $MH$ | = | Mechanised heat | $kW$ |

The electrical heat load includes mechanised and passive electric machinery that uses electricity but does not transport ore or water underground. As with fuel-driven machinery, it is essential to account for all useful work with Equation 2-1. Some electric equipment discharges its heat to the return airway system of the mine and should also be excluded from the electrical heat load [11], [83].

The effective electrical energy used in a mine is transformed into sensible heat. The effective electrical heat load is calculated using the total electrical energy supplied to the mine and excluding the potential energy gain and specific equipment as in Equation 2-4.

$$EEF = Total\ electrical\ supply - PE - Excluded\ equipment \quad (2\text{-}4)$$

Where:

| | | | |
|---|---|---|---|
| $EEF$ | = | Effective electrical heat | $kW$ |

The remaining heat sources are less significant contributors to the overall heat load. The heat from the human metabolism of underground workers is calculated using Equation 2-5.

$$MHL = NE \times MHR \qquad 2\text{-}5$$

Where:

| | | | |
|---|---|---|---|
| $MHL$ | = | Metabolic heat load | $kW$ |
| $NE$ | = | Number of employees | – |
| $MHR$ | = | Metabolic heat rate | $kW$ |

The explosive heat load is calculated using Equation 2-6. This method assumes that the heat energy released by an explosion is absorbed by the rock and released over a prolonged period.

$$EHL = \frac{HP \times m}{RP} \qquad 2\text{-}6$$

Where:

| | | | |
|---|---|---|---|
| $EHL$ | = | Explosive heat load | $kW$ |
| $HP$ | = | Heat produced by explosive type | $kJ/kg$ |
| $m$ | = | Total mass of explosive used | $kg$ |
| $RP$ | = | Release period | $sec$ |

Finally, the heat added to the ventilation system by fissure water is calculated using Equation 2-7. The mass flow of the fissure water is determined by the difference in water flow entering and leaving the mine. The fissure water temperature entering the system is equal to that of the temperature of the rock at the depth that the water enters the mine. The temperature at which the fissure water exits the mine is assumed to be equal to the rejected air temperature of the mine working areas [11], [35].

$$FWHL = \dot{m} \times C_p \times (T_2 - T_1) \quad 2\text{-}7$$

Where:

| | | | |
|---|---|---|---|
| $FWHL$ | = | Fissure water heat load | $kW$ |
| $\dot{m}$ | = | Mass flow rate of fissure water | $kg/s$ |
| $C_p$ | = | Specific heat of water | $kJ/kg \cdot K$ |
| $T_2$ | = | Inlet fissure water temperature | $°C$ |
| $T_1$ | = | Exit fissure water temperature | $°C$ |

These heat sources account for the heat load in the mine ventilation system. For mines that have chilled water reticulation systems, the cooling duty of the pipes is included in the secondary heat load to ensure that the final kW/m is an accurate representation of the actual system. The cooling duty of the chilled water reticulation systems is determined with Equation 2-8 [31].

$$q = \dot{m} \times C_p \times (T_2 - T_1) \quad 2\text{-}8$$

Where:

| | | | |
|---|---|---|---|
| $q$ | = | Water-cooling duty | $kW$ |
| $\dot{m}$ | = | Mass flow rate of chilled water | $kg/s$ |
| $C_p$ | = | Specific heat of water | $kJ/kg \cdot K$ |
| $T_2$ | = | Inlet chilled water temperature | $°C$ |
| $T_1$ | = | Exit chilled water temperature | $°C$ |

#### *iv) A new approach to data collection*

Figure 2-3 shows an adapted data collection method flow sheet for true transient simulations. To ensure that the true transient simulation is incorporated, the transient data is prioritised, and the steady-state data is only collected when there is no means to collect transient data for each parameter. For the method to remain practical, an additional step is added to determine the level of detail and KPIs before starting data collection.

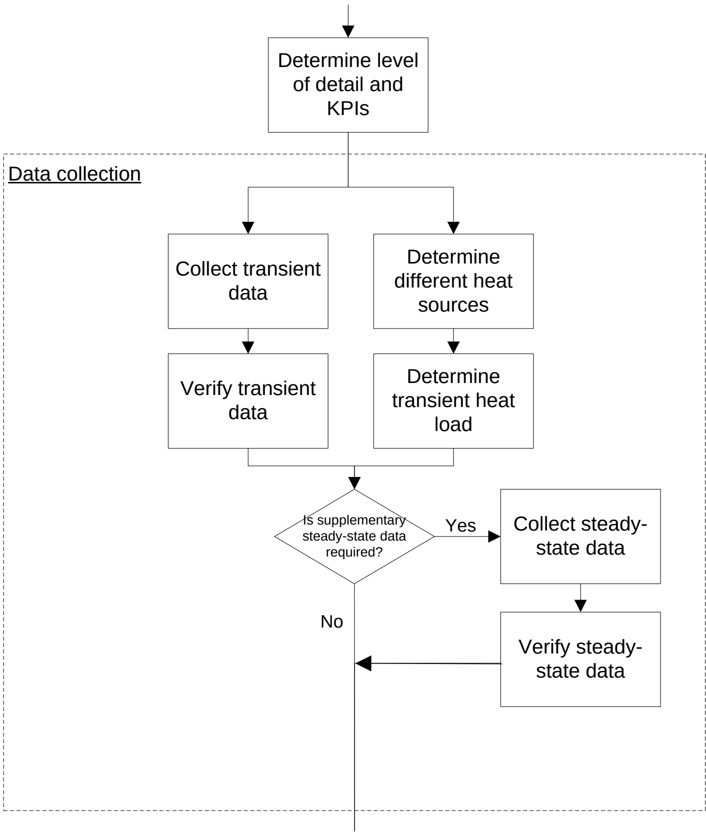


**Figure 2-3: Adapted true transient data collection flow sheet***

### 2.3.2 Data collection on an entire mine ventilation and cooling system

As stated in Section 1.5, there is a need to apply this methodology to an entire mine ventilation and cooling system. This section will discuss the requirements for each step in Figure 2-3 when the method is applied to the entire integrated system.

#### *i) Determine level of detail and KPIs*

To fully capture all areas of the mine ventilation and cooling system, data from all levels of detail is required. Table 2-1 shows the data points required for conventional deep-level mine ventilation and cooling systems. These will vary according to the infrastructure at the mine.

The KPIs are selected to meet the objectives of the simulation. The working area environmental conditions result from the aggregation of heat and cooling sources encountered by the intake air up to that point. For the simulation to accurately predict the environmental conditions of the intake air in the working area, the entire mine ventilation network has to be calibrated accurately. The main KPIs when simulating an entire mine ventilation and cooling network are the intake conditions of the working area, as shown in Table 2-3.

**Table 2-3: Main KPIs**

| Area | KPI | Unit |
|---|---|---|
| Working area intakes | Air mass flow rate | [kg/s] |
| | DB temperature | [°C] |
| | WB temperature | [°C] |

The KPIs of the critical ventilation and cooling components are added to ensure that the simulation represents the actual components accurately. Table 2-4 shows these KPIs, available in mine simulation software [11], [21], [51]. Depending on the available infrastructure, additional KPIs might be required for each individual mine.

**Table 2-4: Component KPIs**

| Component | KPI | Unit |
|---|---|---|
| Return fans operating condition | Air mass flow rate | [kg/s] |
| | Static pressure | [kPa] |
| Fridge plants | Condenser water flow rate | [ℓ/s] |
| | Condenser inlet water temperature | [°C] |
| | Condenser outlet water temperature | [°C] |
| | Evaporator water flow rate | [ℓ/s] |
| | Evaporator inlet water temperature | [°C] |
| | Evaporator outlet water temperature | [°C] |
| BAC | Air outlet WB temperature | [°C] |
| | Air mass flow rate | [kg/s] |
| Cold/ice dams | Outlet water temperature | [°C] |
| | Water outlet flow rate | [ℓ/s] |

The main and component KPIs are used to measure the performance of true transient mine ventilation and cooling simulations. The KPIs required also depend on the available data at the mine.

### *ii) Collect transient data*

Continuous, accurate ambient and underground transient temperature data is required to define the thermal history effect. All data will be available on a SCADA system in an optimal case. The data quality is determined by performing checks on the data, which entail maximum and minimum limits checks and balance checking [38].

In cases where not all the data is available on the SCADA system or data has poor quality, manual measurements are required. Manual measurements make the data collection process laborious and time-consuming. Only the necessary data should be collected to meet the desired outcomes of the simulation. Handheld temperature loggers are used to measure WB and DB temperature. Air psychrometric charts or psychrometric calculators can be used to determine the WB temperature, if the temperature logger only measures the DB temperature and humidity [31], [84]. Appendix D shows an example of air psychrometric calculator outputs.

#### *iii) Collect steady-state data*

Steady-state data is measured with the use of handheld instruments. Table 2-5 shows the handheld instruments required to measure each of the parameters where supplementary steady-state data is required. Standard measurement procedures are used to measure these parameters [31].

**Table 2-5: Handheld instrumentation required for steady-state data collection**

| Parameter | Unit | Handheld instrument required |
|---|---|---|
| Barometric pressure | [kPa] | • Digital barometer |
| Air mass flow rate | [kg/s] | • Vane anemometer<br>• Stopwatch<br>• Laser distance meter/tape measure<br>• Digital barometer<br>• Whirling hygrometer |
| Fan static pressure | [kPa] | • Pitot tube<br>• Vertical/digital manometer |
| Water temperatures | [°C] | • Infrared thermometer<br>• Thermometer |

The air mass flow rate is calculated using Equation 2-9. The air density is determined from the DB temperature, WB temperature and barometric pressure using the psychrometric charts or the PTB air psychrometric calculator [31].

$$\dot{m}_a = w \times Q \qquad 2\text{-}9$$

Where:

| | | | |
|---|---|---|---|
| $\dot{m}_a$ | = | Air mass flow rate | $kg/s$ |
| $w$ | = | Air density | $kg/m^3$ |
| $Q$ | = | Air volumetric flow rate | $m^3/s$ |

### 2.3.3 Building of the model

No significant changes in the steps are required from conventional methods when building an entire true transient-state simulation. Figure 2-4 shows the flow sheet to build the model.

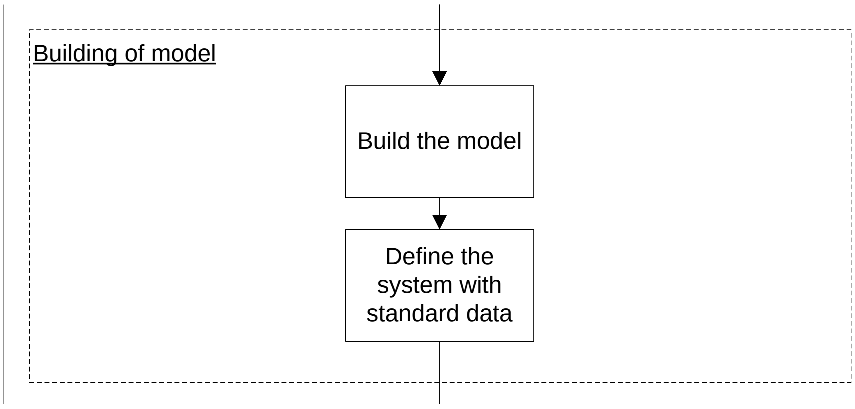


**Figure 2-4: Model building flow sheet***

### 2.3.4 Calibration

Conventional methods define the system with standard parameters and incorporate manual iteration to determine unknown parameters. Figure 2-5 shows the calibration flow sheet for conventional simulation methodologies.

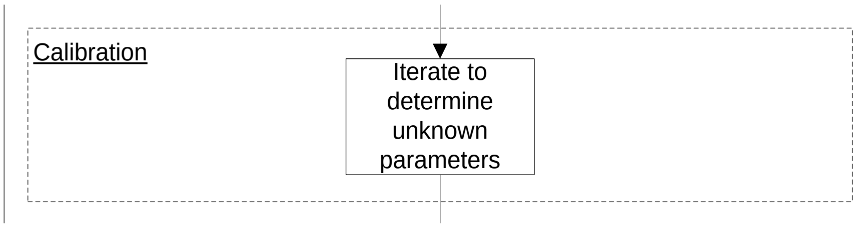


**Figure 2-5: Conventional calibration flow sheet***

#### *i) Incorporate true transient simulation*

The underground temperature data collected for the ventilation system shows the thermal history effect, as seen in Figure 1-4. Historical temperatures are used to prime the model. Figure 2-6 shows the intake temperatures of a deep-level gold mine in South Africa. The temperature history is used to prime the model so that the true transient heat transfer is correct at the start of the calibration period. The calibration should be selected for a period during which the underground operations were running as normal. The length of the calibration period will depend on the amount of thermal history present in the mine. A longer calibration period will improve the accuracy but comes at the cost of longer data collection and simulation times.

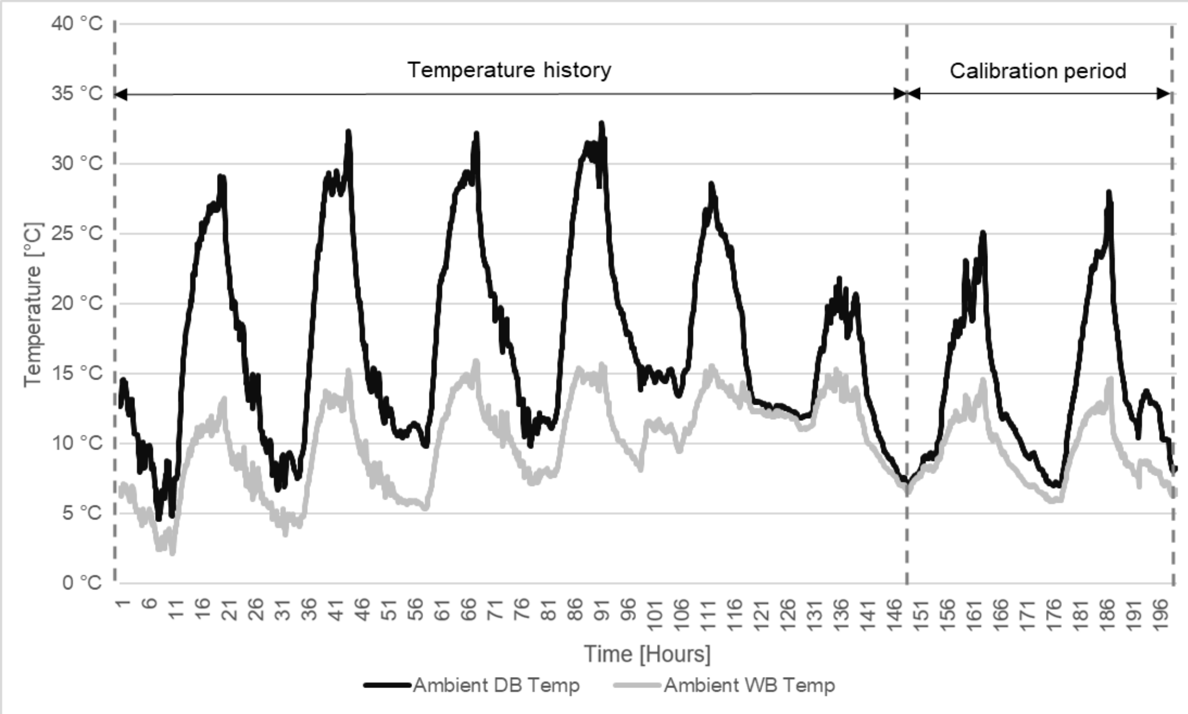


**Figure 2-6: Thermal history calibration example***

### *ii) Be practically applicable*

The calibration should be practical, thus it is crucial to consider the accuracy of the measured data. The calibration of the ventilation and cooling simulation is only as accurate as the accuracy of the measured data, i.e. only iterate for the unknown parameters until the simulation reaches the measured data's accuracy. The accuracy of the measured data was determined in the data collection steps of the method.

The simulation time increases exponentially with more extensive ventilation simulation networks [55]. Solving many iterations to determine unknown parameters can take up an extensive amount of time. In cases where many iterations are required, sections of the simulation can be isolated. The underground measurements are used as inlet boundary conditions for the isolated section. The unknown parameters determined from these iterations are applied to other sections of the mine with similar characteristics, for example, vertical shafts, horizontal tunnels, decline shafts/tunnels and workings areas.

### *iii) A new approach to calibration*

Figure 2-7 shows the adapted calibration methodology flow sheet for the true transient simulation. The additional step ensures that the true transient heat exchange is primed for the calibration period.

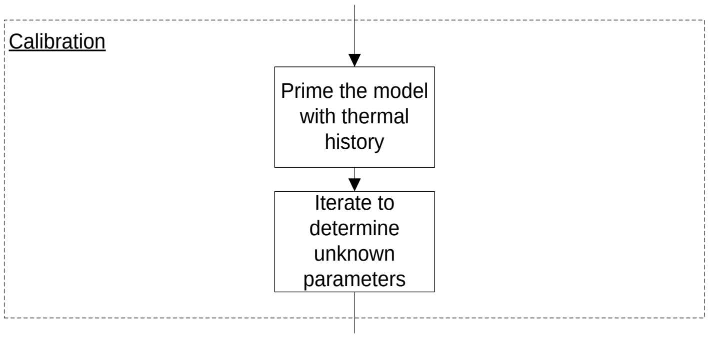


**Figure 2-7: Adapted true transient calibration flow sheet***

### 2.3.5 Verification

Conventional methodologies usually use the mean absolute error, average error ($E_{ave}$), maximum error ($E_{max}$) and minimum error ($E_{min}$) to determine the accuracy of a model [4], [67], [81]. Figure 2-8 shows the flow sheet for the verification steps involved in conventional simulation methodologies. The verification steps of the model will not change when incorporating a true transient simulation.

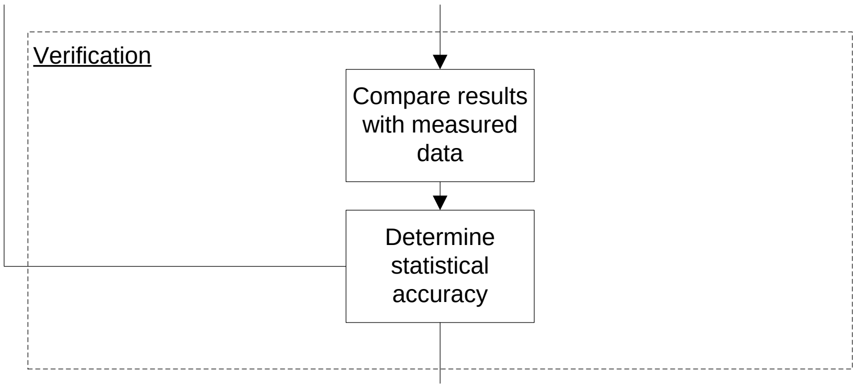


**Figure 2-8: Conventional verification flow sheet***

#### *i) Incorporate true transient simulation*

The most common methods for determining accuracy among the critical true transient studies shown in Table 1-4 are MSE and $R^2$ [52], [70]. These methods are more applicable to continuous data, and using these methods will allow the results from this study to be compared with other true transient simulation studies. The maximum error is further used to compare the environmental predictions of different mine ventilation software [4], [18]. The MSE is calculated with Equation 2-10 [52].

$$MSE = {\left(\sum_{i=1}^{n}(\hat{y}_i - y_i)^2\right)}/{n} \qquad 2\text{-}10$$

Where:

| | | | |
|---|---|---|---|
| $\hat{y}$ | = | Simulation result | – |
| $y$ | = | Measured data | – |
| $n$ | = | Number of data points | – |

A study by Roghanchi and Kocsis [52] used a simulation to predict the environmental conditions at the bottom of vertical shafts. The results from this study indicated that the model still had an acceptable level of accuracy with an MSE of 1.58, $R^2 = 0.73$, and a maximum DB temperature error of 1.93°C. Currently, this is the only indication of the accuracy of transient environmental predictions. These values will be used to indicate whether the simulation has acceptable accuracy. The comparison between steady state and true transient simulation will be used to determine prediction improvements.

***ii) Be practically applicable***

The MSE and $R^2$ indicate the model's performance. As discussed in Section 2.3.4, the accuracy of the measured data must be considered. The model can only be verified practically to the best accuracy of the measurements used to calibrate the model. A study by Mathews et al. [38] confirmed that a transient cooling and water simulation with an average error of less than 5% will represent the actual system accurately.

### 2.3.6 Summary

Figure 2-9 summarises the new methodology for the true transient ventilation and cooling simulation in a flow sheet. Conventional methods were adapted to ensure that the true transient simulation is incorporated while remaining practical. If the accuracy of the model is inadequate, the process will have to start from the start.

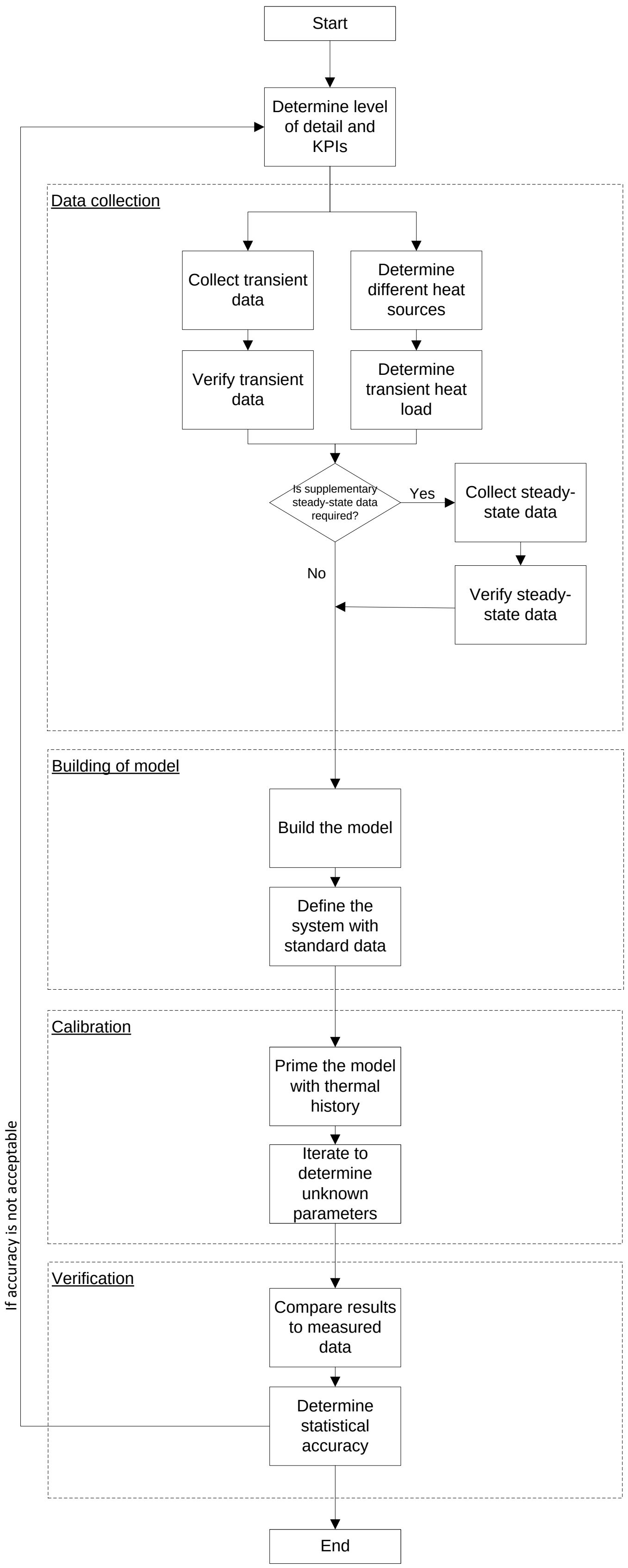


**Figure 2-9: New true transient ventilation and cooling simulation methodology flow sheet***

## 2.4 Process Toolbox

PTB is a simulation software package that uses a one-dimensional computational fluid dynamics code to solve complex thermohydraulic networks. The code includes incompressible (water), compressible (air), and two-phase fluids (steam). Pressure nodes/boundaries are linked to semi-empirical components to form complex networks.

The software uses drag-and-drop components on a 3D GUI to develop large networks to scale. PTB includes a predefined component library to configure simulations. Figure 2-10 illustrates the PTB GUI displaying a complex ventilation network. PTB is designed to be practical in industrial scenarios by combining fundamental principles and empirical parameters. Further detail of PTB is given in references [11], [21], [51].

Two simulation softwares were available to the author at the time of the study, PTB and VUMA. However, VUMA could not incorporate true transient heat exchange. No other simulation was financially available. PTB was selected for this study for the following reasons:

- It is capable of incorporating true transient heat exchange,
- It allows for the integration of ventilation and cooling systems, and
- It is designed for a truly industrial scenario such as complex mine ventilation and cooling systems.

At the time of this study, a limitation of PTB was that the internal heat input was in a steady state. This is the heat added to the ventilation system in the underground tunnels by the secondary sources calculated in the heat load in Section 2.3.1. The impact of this limitation was determined during the application of the simulation to the case studies and is discussed in the case study discussion and conclusion.

***Define the system with standard data using PTB***

During the building of the model, all components are defined with their standard parameters. The remainder of this section investigates the standard parameters required by PTB to define the components listed in Section 2.2.2. These components are linked with air nodes, which connect the components and do not need to be defined.

The standard parameters for the air tunnel component in PTB simulation software are shown in Table 2-6. This information is available from the mining plans and literature. The VRTs differ for rock types and are defined by a gradient. Equation 2-11 shows the VRT formula for the Free State area in South Africa [11], [35], [37].

**Table 2-6: PTB tunnel standard parameters**

| Parameter | Unit | Source |
|---|---|---|
| Flow area | [m²] | Mining plans |
| Flow perimeter | [m²] | Mining plans |
| Friction coefficient | - | Literature |
| VRT gradient | [°C/m] | Literature |
| Tunnel age | [days] | Mining plans |
| Rock thermal conductivity | [kW/m·K] | Literature |
| Rock specific heat | [J/kg] | Literature |
| Rock density | [kg/m³] | Literature |

$$VRT = 20 + 14.6 \times (Depth\ in\ km) \qquad 2\text{-}11$$

Where:

| | | | |
|---|---|---|---|
| $VRT$ | = | Virgin rock temperature | $°C$ |

The standard parameters of air pipes can be found in the product specification. The standard parameters for the air pipe component in PTB simulation software are shown in Table 2-7.

**Table 2-7: PTB air pipe standard parameters**

| Parameter | Unit | Source |
|---|---|---|
| Surface roughness | [mm] | Product specifications |
| Hydraulic diameter | [m] | Product specifications |
| Flow area | [m²] | Product specifications |

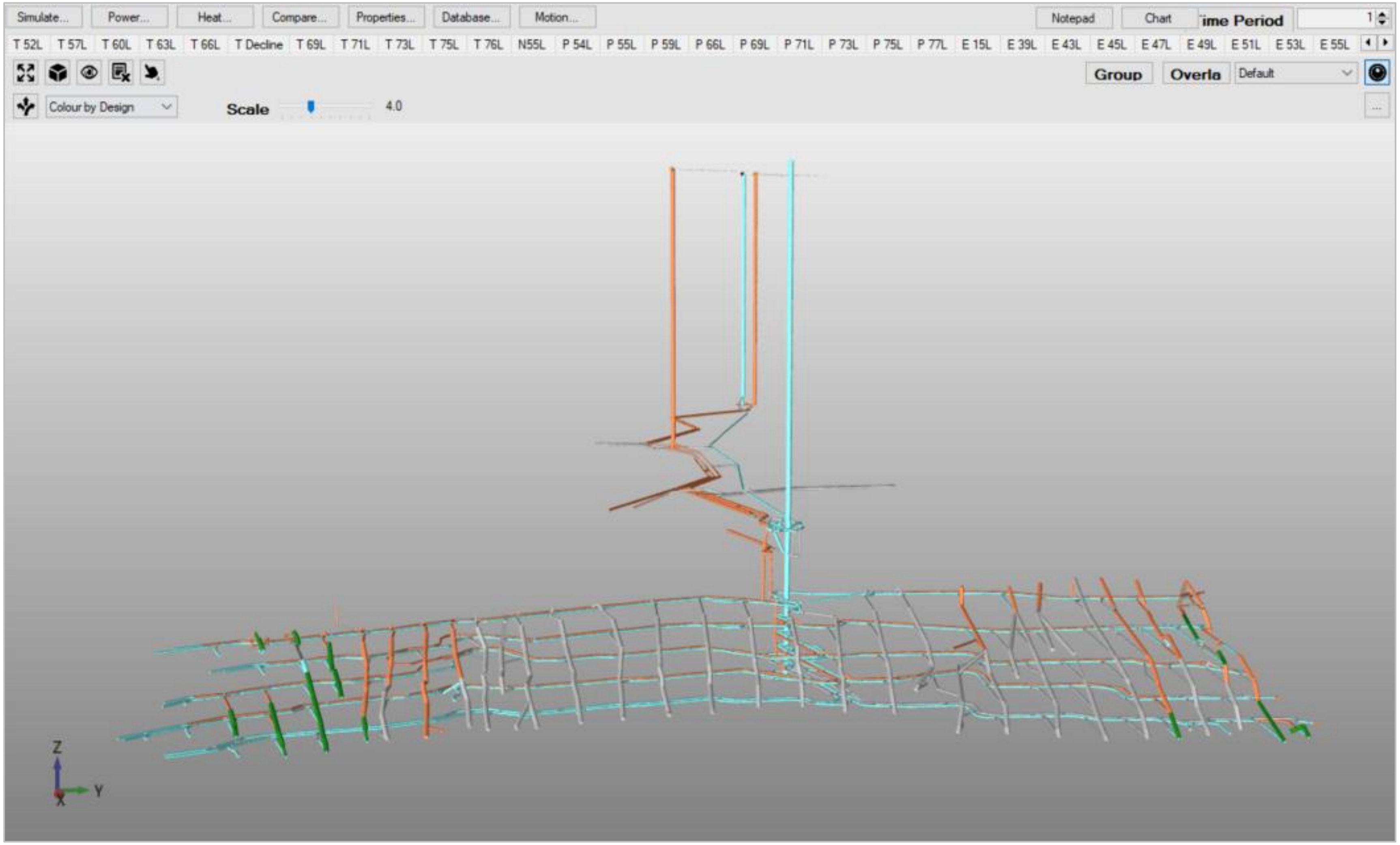


**Figure 2-10: PTB interface***

The final ventilation component is an air fan that is defined by the specification fan curves of the component. Appendix E shows an example of the fan specification and curves of a standard 45 kW booster fan and the defined PTB fan curve with the simulated pressure and flow.

The cooling system simulation components are defined much like the ventilation components. The water-water chiller (fridge plant) component uses measured data to calculate the performance curves of the component. Table 2-8 shows the measured data required to define the component.

**Table 2-8: Fridge plant standard parameters**

| Parameter | Unit | Source |
|---|---|---|
| Evaporator outlet temperature | [°C] | Measured data |
| Evaporator inlet temperature | [°C] | Measured data |
| Evaporator flow rate | [ℓ/s] | Measured data |
| Condenser outlet temperature | [°C] | Measured data |
| Condenser inlet temperature | [°C] | Measured data |
| Condenser flow rate | [ℓ/s] | Measured data |

The water air-cooling tower component, used for BACs, and the water-air heat exchanger component, used for mobile coolers, use specifications and measured data to calculate the overall heat transfer coefficient of the water to air heat exchange. Table 2-9 shows the component specifications and measured data required to define this component. Appendix F shows the heat exchanger specifications for a mobile cooler. The BAC water catchment is included in the simulation as a water dam component and is specified according to the actual size of the catchment dam.

**Table 2-9: Water air-cooling tower and heat exchanger standard parameters**

| Parameter | Unit | Source |
|---|---|---|
| Design water flow rate | [ℓ/s] | Component specifications |
| Design airflow rate | [kg/s] | Component specifications |
| Barometric pressure | [kPa] | Measured data/component specifications |
| Water inlet temperature | [°C] | Measured data/component specifications |
| Water outlet temperature | [°C] | Measured data/component specifications |
| Water flow rate | [ℓ/s] | Measured data/component specifications |
| Air inlet temperature | [°C] | Measured data/component specifications |
| Air inlet relative humidity | [%] | Measured data/component specifications |
| Airflow rate | [kg/s] | Measured data/component specifications |

The water and ice dams require the volume of the dam to define the component. The ice dam further requires the ice mass fraction, which is the percentage of the water that enters the dam as ice. Table 2-10 shows the standard parameters required to define the ice dam component.

**Table 2-10: Ice dam standard parameters**

| Parameter | Unit | Source |
|---|---|---|
| Dam volume | [m³] | Dam specifications |
| Ice mass fraction | [%] | Measured data |

The water pipes are defined the same way as the air pipe. It is crucial to account for heat losses in chilled water pipes that are not covered in insulation. The heat transferred to airflow over the outside of pipes depends on the temperature difference between the water and air. The heat transfer coefficients depend on the material of the pipe and the air temperature and velocity over the pipe [35]. Table 2-11 shows the parameters that are required to define water pipe components.

**Table 2-11: Water pipe standard parameters**

| Parameter | Unit | Source |
|---|---|---|
| Surface roughness | [mm] | Product specifications |
| Hydraulic diameter | [m] | Product specifications |
| Flow area | [m²] | Product specifications |
| Ambient air temperature | [°C] | Measured data |
| Air convective heat transfer coefficient | [kW/m°C] | Literature |
| Conduction heat transfer coefficient | [kW/m°C] | Literature |

The water pumps are defined with each pump's specific pump curves; a process that is similar to the process of defining the air fans. Finally, the water demand components are used to specify the water flow rate required by the working areas and mobile coolers.

***Iterate unknown parameters with PTB***

The parameters that need to be calibrated by iteration in a PTB ventilation simulation are the tunnels' wetness fraction and door fraction. The wetness fraction adds humidity to the air travelling through the tunnels, and the door fraction restricts airflow through the tunnels.

Literature shows that the average wetness fraction of underground tunnels is between 0.1 and 0.25 [26], [31], [83], [85]. All tunnel components in the intake system are given an initial average wetness fraction value of 0.175. This is the baseline from which the door fraction is iterated to calibrate the airflow.

The door fraction of tunnels allows for calibrating leakages over doors, walls and seals. Iterations are required to determine the exact door fraction value for each leak as there is no standard value. The doors, walls and seals in the simulation are started at a door fraction of 0%, representing a fully closed tunnel with no leaks. The door fractions are increased until the leaks correlate with the measured data.

## 2.5 Overview of the application of these methodologies

In Chapter 1, a critical review revealed the shortcomings in the literature for a true transient simulation of mine ventilation and cooling systems. These shortcomings formed the foundation of the need and the novel contributions of this study. The objectives of this study, as seen in Section 1.6, are:

- Development of a methodology for a true transient mine ventilation and cooling simulation for deep underground mines,
- Application of a true transient ventilation simulation to an entire mine ventilation network, and
- Integration of a transient cooling simulation with a true transient ventilation simulation on a deep-level mine.

This chapter developed a methodology to meet the first objective of this study. The methodology incorporates the thermal history effect while remaining practically applicable. This methodology is genuinely novel as the state-of-the-art studies in Section 1.4 do not provide a method for building and calibrating a true transient simulation. Case studies of real-life underground mine ventilation and cooling systems was used to meet this study's other needs and validate the new methodology. The mines in these case studies were also selected according to the information available to the author at the time of this study.

### 2.5.1 Case study 1

This case study applied a true transient ventilation simulation to a conventional underground mine with no cooling system installed. The new methodology developed in this chapter was used to meet the need of the second novel contribution of this study, namely:

- Application of a true transient ventilation simulation to an entire mine ventilation network.

### 2.5.2 Case study 2

In this case study, a true transient simulation was applied to a large underground mine ventilation system with a cooling system. The new methodology developed in this chapter was used in this case study. This case study met the needs of the second and third novel contributions of this study, namely:

- Application of a true transient ventilation simulation to an entire mine ventilation network, and

- Integration of a transient cooling simulation with a true transient ventilation simulation on a deep-level mine.

### 2.5.3 Case study 3

The third case study applied a true transient ventilation and cooling simulation to a mechanised underground mine. This further validated the new methodology by applying it to an underground mine with a different mining technique.

## 2.6 Summary

This chapter aimed to meet the first outcome of this study and started by investigating conventional mine ventilation and cooling simulation methodologies. These conventional methodologies were adapted for integrated true transient mine ventilation and cooling simulations. The flow sheet for the adapted true transient methodology is shown in Figure 2-9. The simulation software used in this study was also discussed. The next chapter applies the new methodology to the case study mine ventilation and cooling systems, as discussed in Section 2.5.

# CHAPTER 3: RESULTS

## 3.1 Preamble

The literature study in Chapter 1 investigated the literature on transient mine ventilation and cooling simulations. The following objectives were determined in Chapter 1:

- Development of a methodology for integrated true transient mine ventilation and cooling simulations,
- Application of a true transient ventilation simulation to an entire deep-level mine, and
- Integration of a transient cooling simulation with a true transient ventilation simulation on a deep-level mine.

Chapter 2 developed a novel method for true transient mine ventilation and cooling simulations. This method incorporates the thermal history effect while remaining practically applicable. This chapter aims at meeting the second and third objectives by a applying true transient simulation to three case studies. The results from these case studies will validate the use of the methodology developed in Chapter 2 and the application of a true transient simulation to an entire mine ventilation and cooling system. The three case studies were summarised in Section 2.5.

## 3.2 Case Study 1

### 3.2.1 The objective of Case Study 1

Case Study 1 investigated the true transient simulation of an underground mine ventilation system. For confidentiality, the mine investigated in this case study is referred to as Mine A. This case study aimed at meeting the second objective of this study.

This case study aimed at verifying that this objective would be met by determining whether a true transient ventilation simulation could produce accurate results. Comparing the new true transient simulation to conventional steady-state simulations would validate using the true transient simulation in the mining industry. The true transient simulation results were compared to actual measured data to determine if it could produce accurate results. These results would further validate the use of the new true transient methodology. The results from this case study were published in an article which is included in Appendix G.

### 3.2.2 Description of Mine A

Mine A is an underground gold mine in Free State, South Africa. This mine started production in 1986 and was mining at an average depth of 1 290 m at the time of the study. The maximum mining depth was 1 370 m underground. The mine produced 1 400 kg of gold per year and had around 2 000 employees.

Figure 3-1 illustrates an overhead view of the underground layout of Mine A. This mine had three shafts, two downcast (intake air) and one upcast (return air). Apart from taking fresh air underground, the main downcast shaft was also used to transport broken rock, while the secondary downcast shaft was used to transport people and materials. The current working areas were on the northeastern section, which was also the deepest section of the mine.

Mine A used a conventional or narrow-reef mining technique. This technique involves the excavation of rock by drilling and blasting in the working areas. An electric tram and conveyor system transported the ore from the working areas to the shaft, where it was hoisted in a skip to the surface with a winder.

A simplified conventional underground mine ventilation system was shown in Figure 1-2. Fresh air entered the mine through the downcast shafts and flowed through a network of tunnels (intake airways) to the working areas. Thereafter, the contaminated air flowed through a network of tunnels (return airways) to the upcast shaft.

On the surface, Mine A used two exhaust fans with a design capacity of 1 MW to exhaust contaminated air from the mine ventilation system. These fans extracted around 500 kg/s of contaminated air from the underground system to surface at an operating static fan pressure of 1.5 kPa.

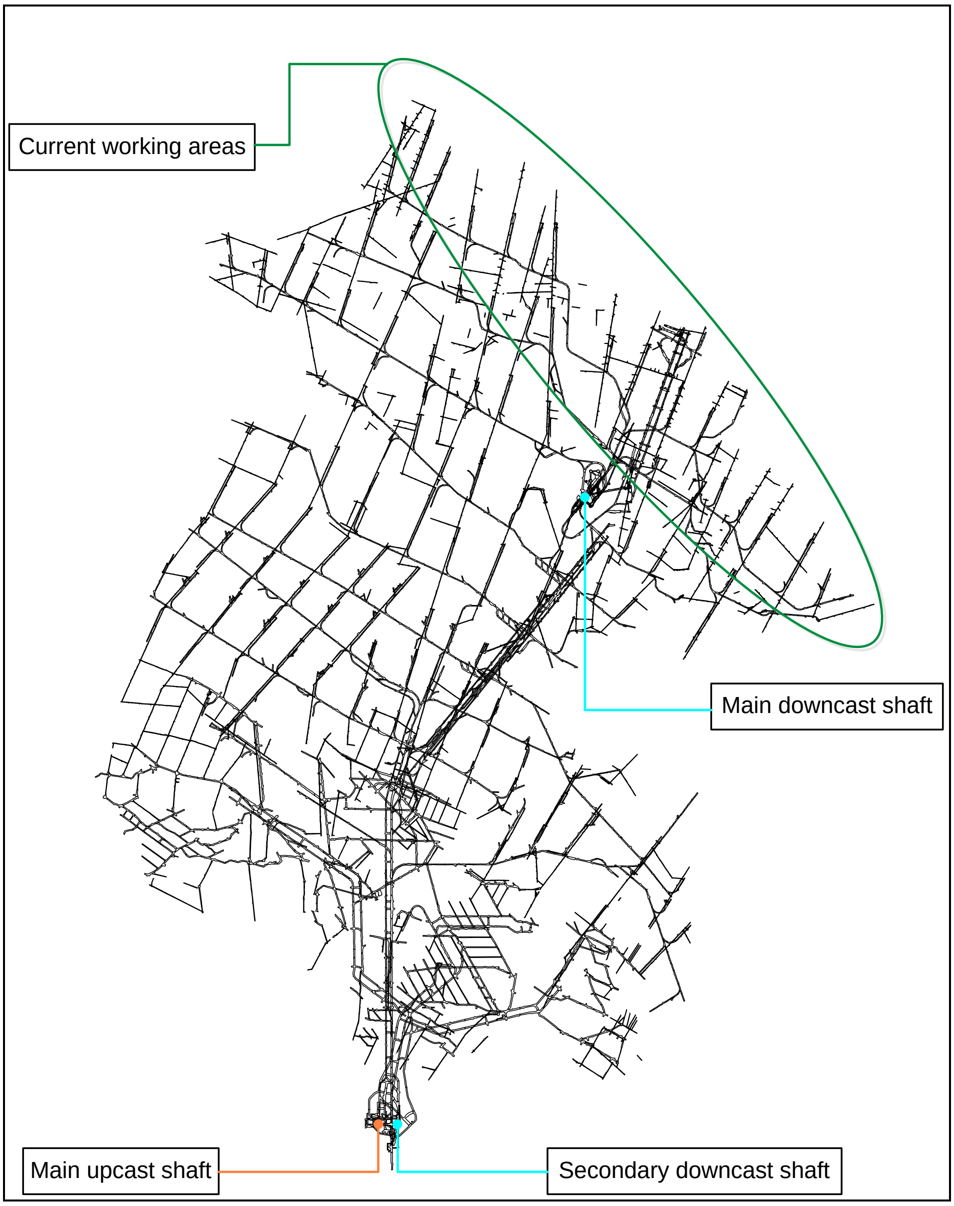


**Figure 3-1: Mine A underground layout***

Mine A used underground ventilation controlling equipment to ensure that adequate fresh air reached the working areas. The controlling equipment such as doors, walls and booster fans was installed on the underground levels as per the ventilation plans. Figure 3-2 illustrates a section of a level ventilation plan for Mine A. The tunnels on the level were used as the intake airways for the working areas and also for transporting people, material, equipment and broken rock. In some cases, the return airways were used to access working areas to reduce travelling time.

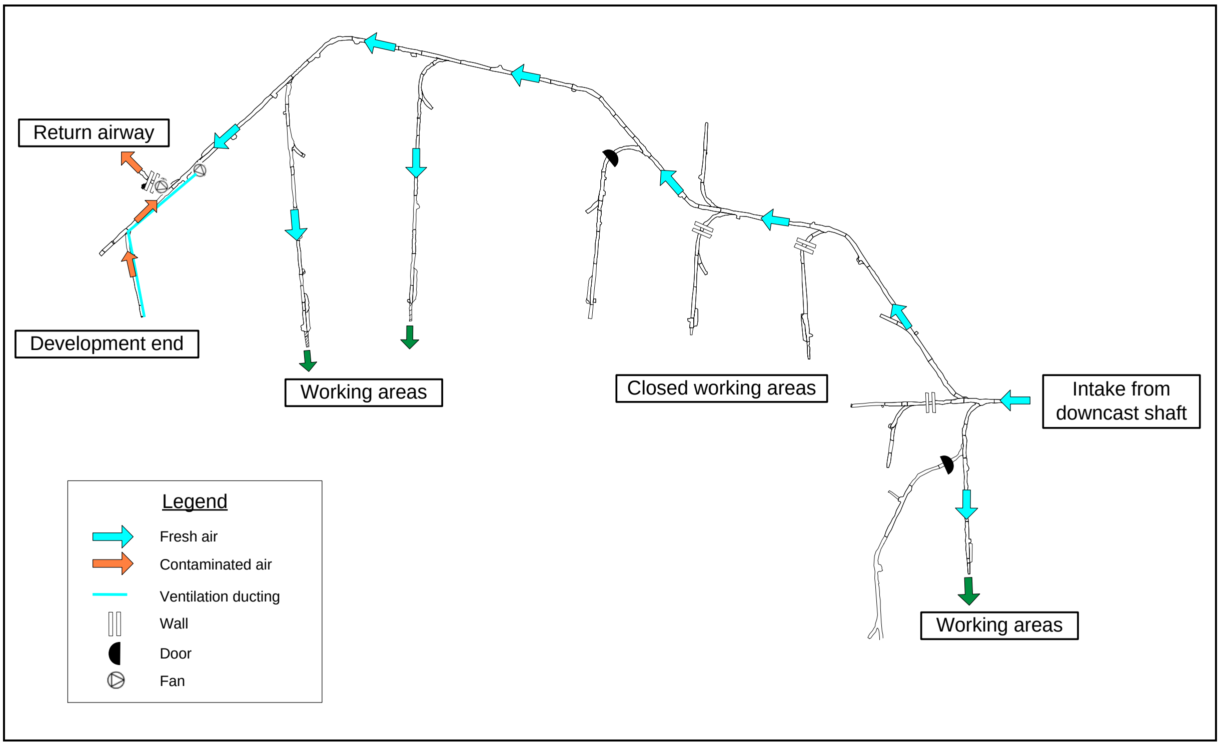


**Figure 3-2: Section of a level ventilation plan for Mine A***

The airflow in the intake and return airways was in a relatively steady state because mine fans and underground booster fans controlled the airflow. During the mining shifts, there was a great deal of movement of people, materials, equipment and broken rock underground. At Mine A this movement often required the ventilation doors to be opened and closed, and in some cases, the booster fans to be turned on and off. The ventilation network at Mine A was very interconnected, and a change in one section could affect other sections. The changes in ventilation controlling equipment caused by the underground operations led to dynamic airflow in the ventilation system during the mining shifts.

Mine A had a variety of heat sources underground. There were no fuel-driven machines underground, thus the heat sources present in the mine were strata heat (geothermal gradient), auto-compression, electric machinery, human metabolism, blasting, and fissure water. The ventilation infrastructure could provide enough ventilation airflow (air-cooling power) to mitigate the heat sources. Mine A did not have refrigeration or cooling systems installed.

### 3.2.3 Data collection

The data was collected according to the steps developed in Section 2.3.1 and Section 2.3.2. Figure 3-3 shows the true transient data collection method flow sheet. This method remained the same when applied to the ventilation system of Mine A, even though it did not have refrigeration or cooling systems installed.

Mine A did not have a SCADA system and no environmental monitoring instruments were installed. All data had to be collected manually with handheld instruments. As stated in Section 2.3.1, only the necessary data had to be collected to meet the desired outcomes of the simulation. However, enough data had to be collected to define the thermal history effect accurately. As mentioned in Section 2.3.1, the required data depends on the mine.

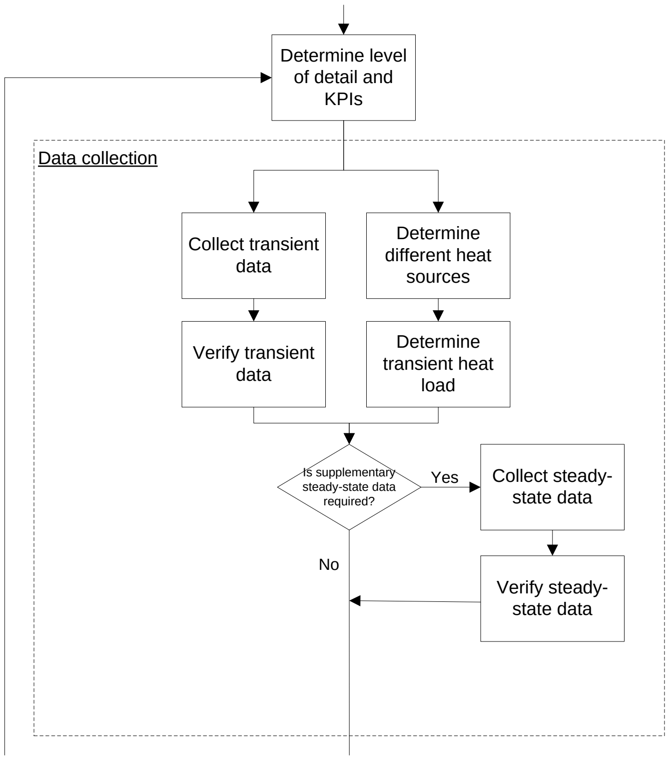


**Figure 3-3: True transient data collection flow sheet***

### *i) Collecting transient data*

Figure 3-4 illustrates the ambient and underground temperature measured at Mine A with temperature loggers placed at a working area intake. The thermal history effect can be seen in the change in temperature as the air travelled in the mine. A temperature logger was placed at a working area intake underground. The temperature loggers were installed for a total of three weeks to ensure that the thermal history was adequate. This data was collected during a time of normal mining operations.

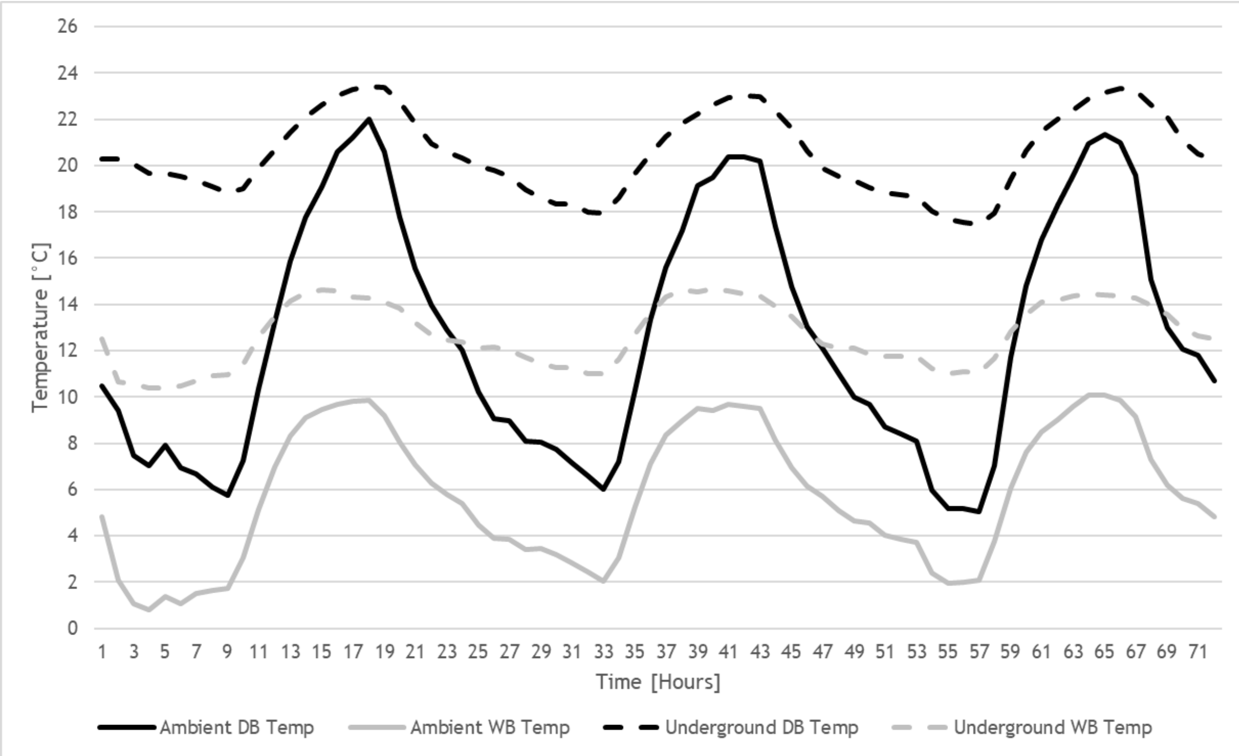


**Figure 3-4: Ambient and underground temperatures at Mine A***

The valid supplier's calibration certificate was used to determine the accuracy of the temperature logger. The temperature loggers were rated to be accurate to within 0.5°C DB temperature and 3% for relative humidity between 0°C to 40°C. Table 3-1 summarises the accuracy of the transient data measured at Mine A.

**Table 3-1: Mine A transient data accuracy**

| Measurement | Unit | Accuracy |
|---|---|---|
| DB Temperature | [°C] | ±0.5 |
| Relative humidity | [%] | ±3.0 |

### *ii) Determining heat load*

The heat load of underground heat sources was used to calibrate the secondary heat added to the ventilation air in the simulation. As discussed in Section 2.4, the limitation of PTB is that the internal heat input is in a steady state. For this case study, the heat from secondary sources was calculated in a steady state. The total heat added to the ventilation system of Mine A by the secondary heat sources is summarised in Table 3-2. The calculation of the heat from these sources is summarised in Appendix H.

**Table 3-2: Total heat load from secondary sources for Mine A**

| Parameter | Unit | Value |
|---|---|---|
| Effective electrical heat load | [kW] | 958 |
| Metabolic heat load | [kW] | 216 |
| Explosive heat load | [kW] | 2 |
| Fissure water heat load | [kW] | 236 |
| **Total heat load from secondary sources** | **[kW]** | **1 412** |

The amount of heat from each category was not constant over time. The heat load of Mine A was dynamic over 24 hours. As an example of how dynamic the heat load could be, Figure 3-5 shows the effective electrical heat load over 24 hours.

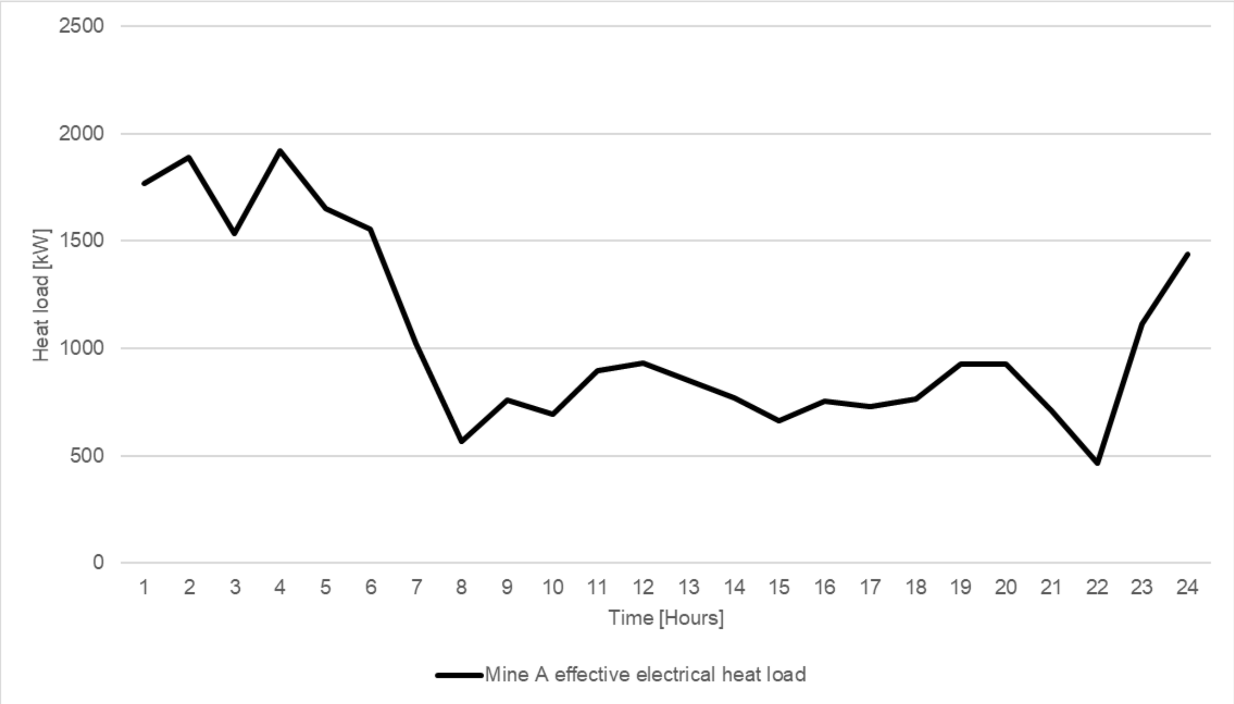


**Figure 3-5: Mine A effective electrical heat load***

#### ***iii) Collecting steady-state data***

The outstanding data that could not be collected using transient methods are listed below:

- Surface and underground barometric pressure,
- Airflow of the mine ventilation network, and
- Return fan static pressure.

These parameters were measured using the techniques discussed in Section 2.3.2. The vane anemometer had a calibration certificate that guaranteed a certain level of accuracy. However, the method for measuring the airflow increased the difficulty of defining the accuracy of airflow measurements. Studies have shown that underground airflow measurements with a vane anemometer can be accurate within 5–23%; therefore, the airflow could not be practically calibrated to more than 95% accuracy [74], [86].

### 3.2.4 Building of the model

Figure 3-6 shows the steps for building a ventilation and cooling simulation in PTB.

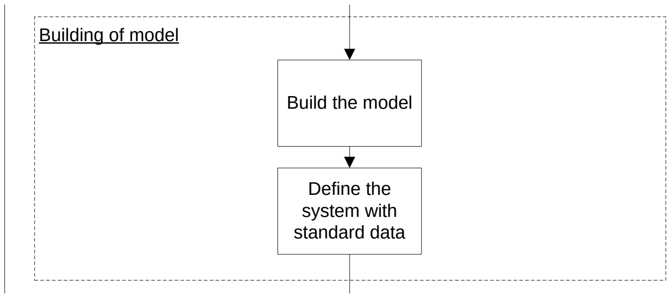


**Figure 3-6: Model building flow sheet***

#### *i) Building the model*

The digital mining layouts seen in Figure 3-1 were imported into PTB and the drag-and-drop function was used to add the components to the layouts. Figure 3-7 illustrates the final 3D PTB ventilation model.

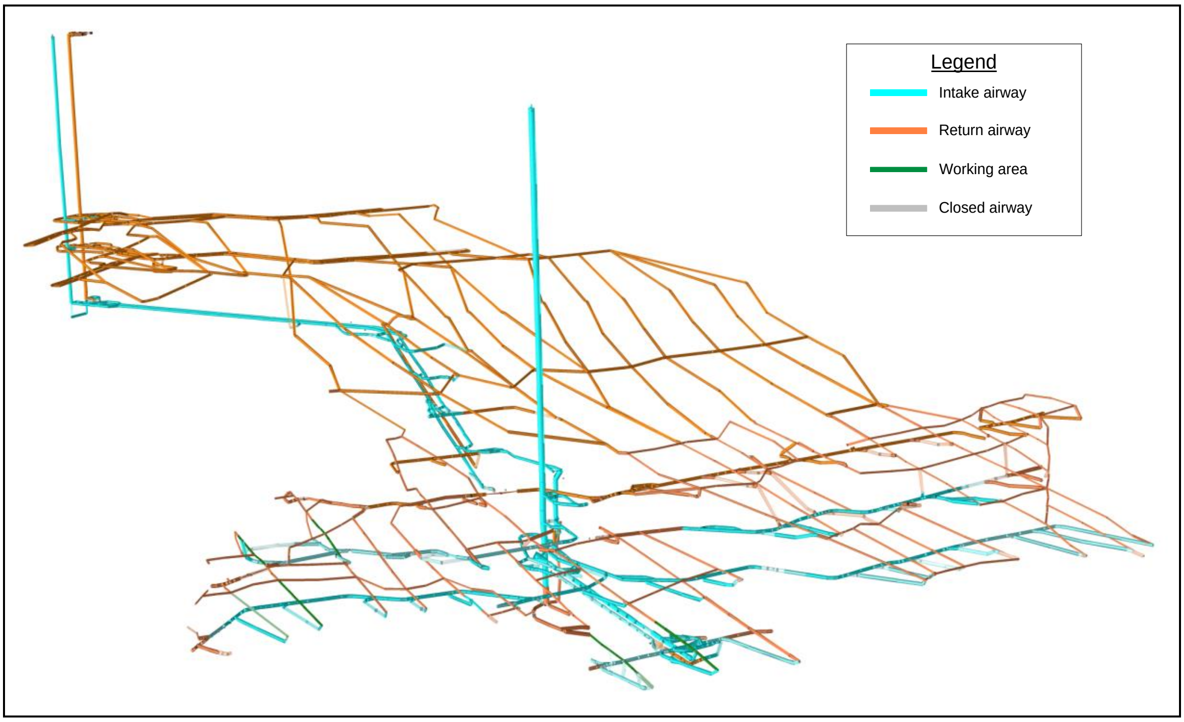


**Figure 3-7: PTB ventilation simulation of Mine A***

### *ii) Defining the system with standard data*

The final step of building the model was to define all the components with their standard parameters. The components used to build the ventilation simulations of Mine A were tunnels, air pipes and air fans. The components were defined according to the standard parameters sources discussed in Section 2.4. The values used to define the system are summarised in Appendix I.

### 3.2.5 Calibration

Figure 3-8 shows the true transient calibration flow sheet developed in Chapter 2. This method remained the same when applied to the ventilation system of Mine A.

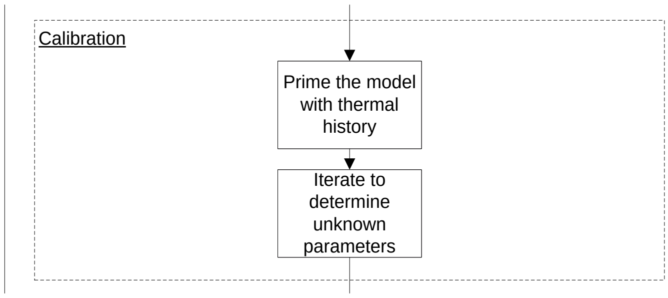


**Figure 3-8: True transient calibration flow sheet***

A description of the heat load is shown in Section 3.2.3, and the heat load is calculated in Appendix H. The secondary heat sources were distributed across the intake airways as a kW/m value. The simulation was simplified by distributing the heat evenly across all active intakes of the mine. The total heat load of 1 412 kW was distributed over the total intake airways length of 12 022 m, resulting in an average heat load of 0.12 kW/m.

The calibration process was simplified by dividing the mine into sections with the same mining characteristics. Each section was extracted from the simulation and calibrated individually, providing that the section's intake and outlet environmental conditions were known. The wetness fraction of that section was applied to similar sections in the mine. Mine A was divided into two sections, namely vertical downcast shafts and horizontal tunnels.

### *i) Priming the model with temperature history*

To incorporate true transient heat exchange for the calibration period, it is essential to prime the model with temperatures leading up to the period. This ensures that the heat exchange is correct at the start of the calibration period. The calibration period was selected for three days during which underground mining continued as usual.

The ambient environmental conditions were recorded for three weeks to provide a suitable temperature history for an accurate heat exchange. The average ambient environmental conditions for the priming period are shown in Table 3-3.

**Table 3-3: Average priming period environmental conditions for Mine A**

| Environmental conditions | Unit | Value |
|---|---|---|
| Average DB temperature | [°C] | 12.3 |
| Average relative humidity | [%] | 47.4 |
| Average barometric pressure | [kPa] | 87.4 |

These averages were used as inputs to the PTB model, and the model was run until the entire model reached a steady state. The simulated temperature of the underground tunnels after priming represented the actual temperature of the tunnels at the start of the calibration period.

***ii) Iterating unknown parameters***

The airflow data could only be measured in a steady state so that the airflow would be calibrated and verified in a steady state. The first step simulated the PTB model with the standard data imported to all components. As discussed in Section 2.4, an average wetness fraction of 0.175 on intake tunnels and a 0% door fraction on closed tunnels were used as the baseline.

The door fractions were adjusted and simulated airflows were compared with the underground tunnels' measured airflows for every iteration. As the airflow calibration improved, the wetness fraction was also changed for each iteration. This process was repeated until the calibration was completed.

After each iteration, the accuracy of each simulated environmental condition was compared with the measured environmental condition at the same location. The data collection determined that the airflow measurements had at least a 5% error. Once a simulated airflow was within 5% of the measured airflow, the calibration was completed for that component.

The temperature data was transient and the simulation was calibrated for a single wetness fraction. This wetness of the underground network could have changed during the data collection period. Thus, the wetness fraction was calibrated to be as close as possible to the measured data for the entire calibration period while taking the accuracy of the measured data into account, as shown in Table 3-1.

### 3.2.6 Verification

Figure 3-9 shows the true transient verification flow sheet developed in Chapter 2.

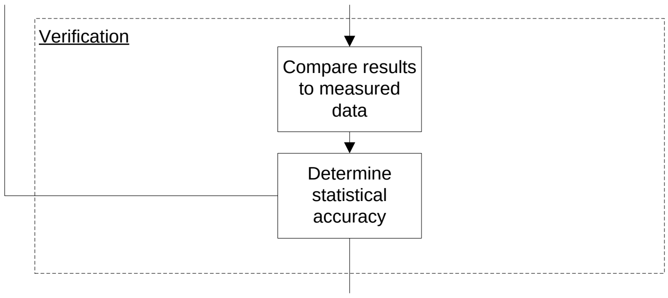


**Figure 3-9: True transient verification flow sheet***

The final simulation had an airflow that represented the actual system accurately. The simulation had an average airflow accuracy of 97%. The airflow calibration had an MSE of 0.77 with a maximum error of 2.11 kg/s, which included the main return fans. The minimum error of the handheld measurement technique was 5%, thus the practical accuracy of the airflow was 95%. The main return fans had a measured operating static pressure of 1.5 kPa and a simulated static pressure of 1.56 kPa, which was an error of less than 4%.

The simulation DB and WB temperatures of a working area intake on the main working level were compared with the measured temperatures. Figure 3-10 illustrates the comparison between the measured and simulated temperatures. The simulation was able to incorporate the thermal history effect as discussed in Section 1.2.4.

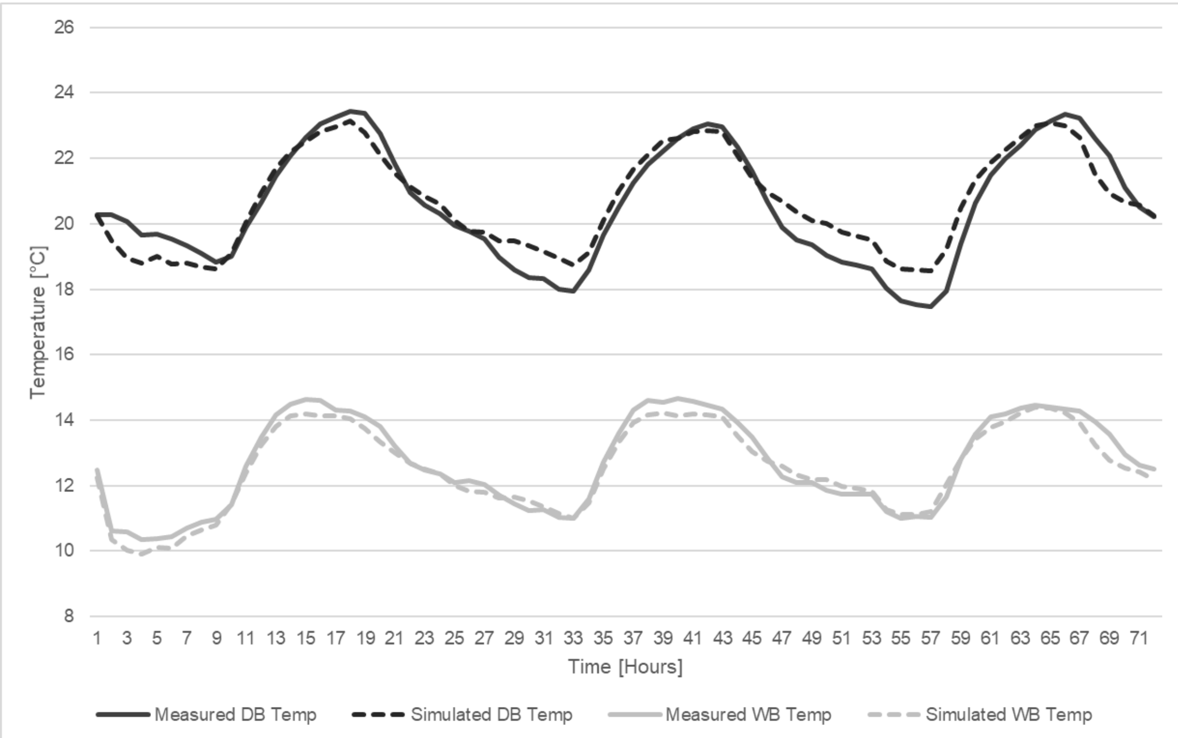


**Figure 3-10: Mine A underground temperature comparison using transient simulation***

As discussed in Section 2.3.5, literature has determined that a true transient ventilation simulation of downcast shafts has an acceptable level of accuracy with an MSE of 1.58, $R^2$ of 0.73 for DB temperature predictions, and a maximum DB temperature error of 1.93°C [52]. Table 3-4 shows the simulation performance for Mine A. These results prove that the true transient simulation predicts the underground environmental conditions with a high level of accuracy when applied to an entire mine ventilation system.

**Table 3-4: Summary of Mine A simulation performance**

| Parameter | Unit | MSE | $R^2$ | Maximum error |
|---|---|---|---|---|
| Airflow | [kg/s] | 0.77 | – | 2.11 |
| DB temperature (transient) | [°C] | 0.38 | 0.99 | 1.53 |
| WB temperature (transient) | [°C] | 0.09 | 0.97 | 0.79 |

The simulation showed accurate results for all the KPIs selected. Maximum temperatures are often used in planning and optimisation to predict limiting underground temperatures [54]. The simulation results demonstrated that the maximum temperatures were within 0.30°C of the actual maximum temperatures i.e..:

- DB temperature of 23.14°C (0.30°C lower than actual)
- WB temperature of 14.39°C (0.27°C lower than actual)

The temperature loggers used were accurate to ±0.5°C for the DB temperature and ±3.0% for the relative humidity, which was equivalent to around ±0.5°C for the WB temperature. The results in this section showed that these loggers had an adequate accuracy for calibrating a true transient simulation.

### 3.2.7 Comparison to quasi-steady-state ventilation simulation

Literature has shown that there are limitations to a steady-state mine ventilation analysis. Some studies used quasi-steady-state simulation, which has improved prediction over standard simulation [43], [54]. PTB has the functionality to switch to a steady-state simulation, which can be used as a standard steady-state or quasi-steady-state simulation.

The simulation was resimulated with a quasi-steady-state analysis. Figure 3-11 compares the actual measurements, transient simulation and quasi-steady-state simulation. These results confirm the limitation of a steady-state ventilation analysis, which is that it tends to overpredict high temperatures.

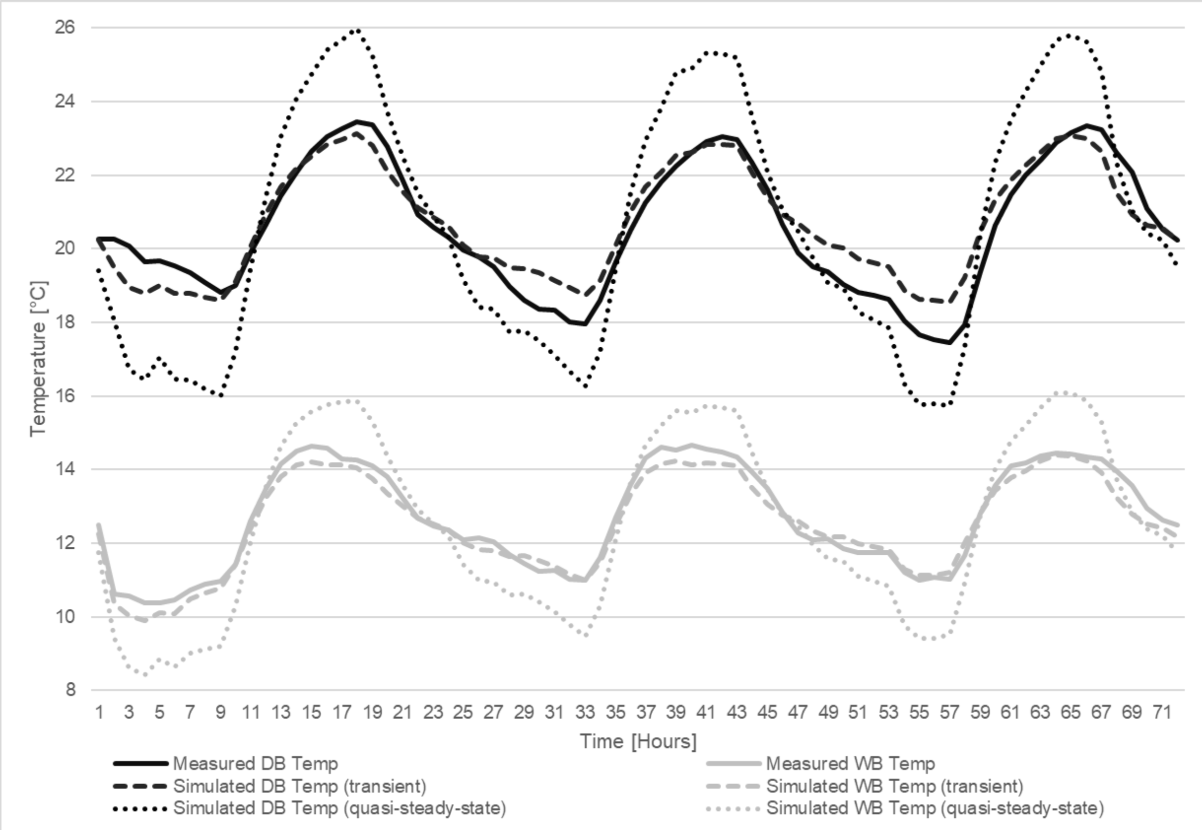


**Figure 3-11: Mine A temperature comparison using a true transient and quasi-steady-state simulation***

The quasi-steady-state results showed the following maximum temperatures:

- DB temperature of 25.98°C (2.54°C higher than actual)
- WB temperature of 16.08°C (1.42°C higher than actual)

When comparing the quasi-steady-state simulation with the transient simulation, the transient showed improved predictions of the underground environment, leading to better accuracy. Table 3-5 compares the simulation results from the transient and quasi-steady-state simulations.

**Table 3-5: Mine A comparison of transient and quasi-steady-state simulation performance**

| Parameter | Unit | MSE | $R^2$ | Maximum error |
|---|---|---|---|---|
| Airflow | [kg/s] | 0.77 | – | 2.11 |
| DB temperature (transient) | [°C] | 0.38 | 0.99 | 1.53 |
| DB temperature (quasi-steady-state) | [°C] | 3.03 | 0.98 | 3.34 |
| WB temperature (transient) | [°C] | 0.09 | 0.97 | 0.79 |
| WB temperature (quasi-steady-state) | [°C] | 1.15 | 0.99 | 1.95 |

### 3.2.8 Discussion

This case study aimed to meet the following objective:

- Application of a true transient ventilation simulation to an entire mine ventilation network.

The new true transient method was applied to Mine A. The results showed that the simulation could predict the underground environment accurately, thereby meeting the first objective of this case study. Mine A did not have a SCADA system and no environmental monitoring instruments were installed. This, combined with the fact that the secondary heat sources could only be applied in PTB in a steady state, validated the practical nature of the methodology. The amount of data collected to prime the model seemed adequate for this case study, but further investigation is required to determine the more detailed impact of the

The application of the true transient simulation to an entire mine ventilation system was also published. The article's main findings were that simulation software could incorporate the thermal history effect into an entire mine ventilation network and that a true transient ventilation simulation could improve environmental predictions used for mine ventilation management. This validated the use of a true transient simulation on mine ventilation systems [1].

## 3.3 Case Study 2

### 3.3.1 The objectives of Case Study 2

Case Study 2 investigated the true transient simulation of an underground mine ventilation and integrated cooling system. For confidentiality, the mine investigated in this case study is referred to as Mine B. This case study aimed to meet the second and third objectives of this case study:

- Application of a true transient ventilation simulation to an entire deep-level mine, and
- Integration of a transient cooling simulation with a true transient ventilation simulation on a deep-level mine.

This case study aimed at verifying that these objectives would be met by determining whether a true transient ventilation and cooling simulation could produce accurate results. The simulation developed in this case study was compared with a conventional steady-state simulation to validate the use of true transient simulations in real-life integrated ventilation and cooling applications. Accurate results would further validate the use of the new true transient methodology.

### 3.3.2 Description of Mine B

Mine B was part of an underground gold mining operation in the Free State, South Africa. This mine started production in 1984 and was mining at an average depth of 2 180 m at the time of the study. The maximum mining depth was 2 280 m underground. The mining operation produced 7 400 kg of gold per year, and Mine B had around 1 800 employees. Conventional narrow-reef mining techniques were used, much like Mine A.

On the surface, Mine B used two exhaust fans with a capacity of 2.5 MW to exhaust contaminated air from underground. These fans extracted around 560 kg/s from the ventilation system at a static pressure of 2.4 kPa. Figure 3-12 illustrates an overhead view of the underground layout of Mine B. The current working areas are shown on the layout.

Mine B had five main working levels with a travelling length of over 5 km at some places. Figure 3-13 illustrates a section of one of the main working levels. Each level had two main parallel drifts. The first drift was the air intake to the working areas, and the second drift was the return airway that removed the contaminated air from the working areas.

Mine B used the same mining technique and types of heat sources as Mine A. The ventilation airflow at Mine B did not provide enough air-cooling power to mitigate the heat from the mine as a result of the depth of the mine. Two cooling systems provided additional cooling. The first was a cooling system situated on the shallowest level (55L) at a depth of 1 670 m. The second was ice plants that provided ice to an ice dam that serviced the mine with chilled water.

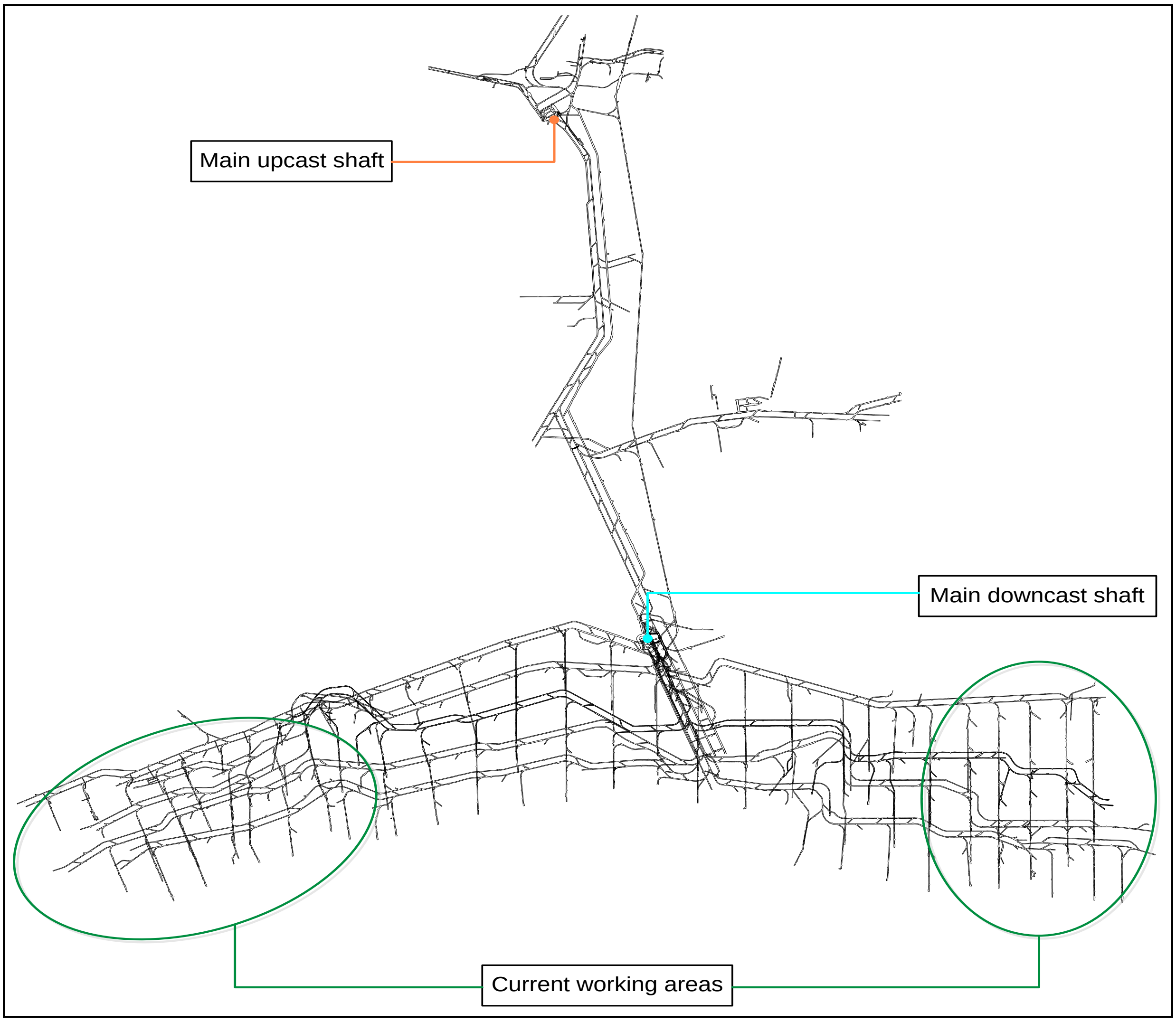


**Figure 3-12: Mine B underground layout***

This cooling system on 55L consisted of refrigeration plants that provided chilled water to a BAC. The BAC cooled the air in the downcast shaft before the air continued to the main working levels. Condenser ponds rejected the heat from the refrigeration plants to the return airway system of the mine. The heat from the condenser ponds was absorbed by the return air, whereafter it was expelled to the atmosphere through the upcast shaft and mine fans.

The ice plants were located on the surface and provided ice to an ice dam on 55L. The ice was mixed in the ice dam with treated service water returning from the working areas. Thereafter, the water from the ice dam was distributed through the mine to mobile coolers that provided localised cooling to working areas.

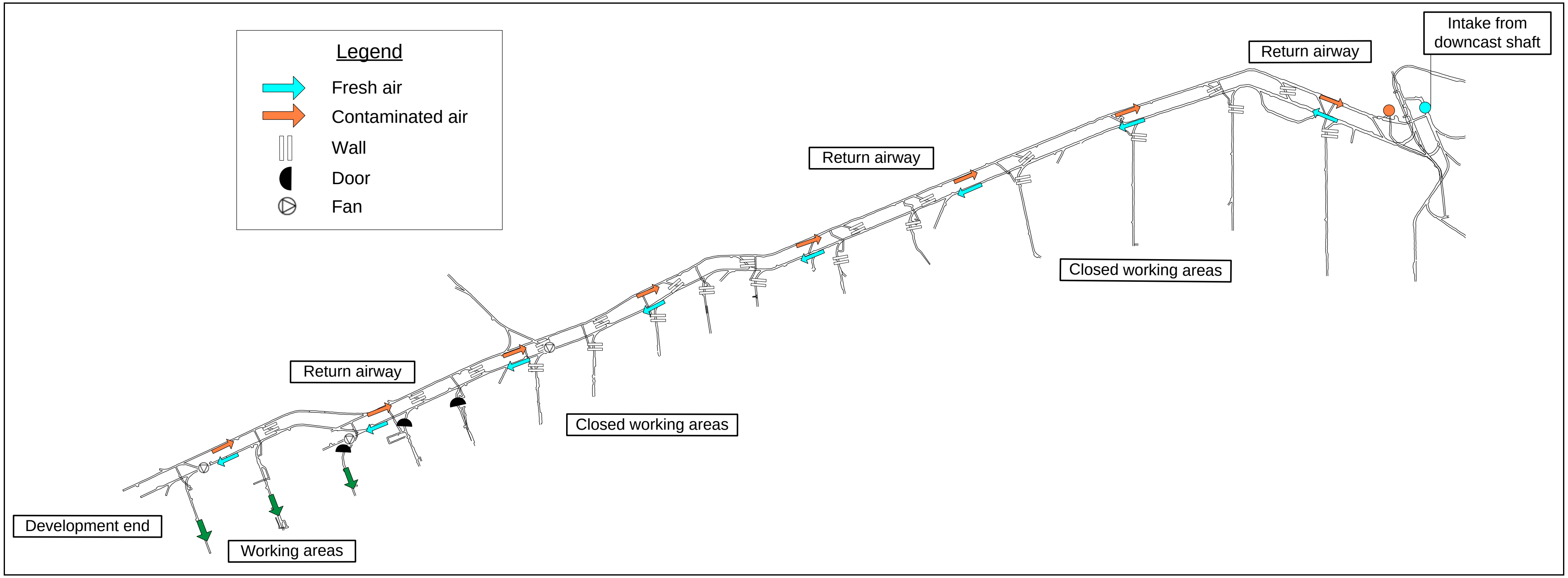


**Figure 3-13: Section of a level ventilation plan for Mine B***

Figure 3-14 illustrates a simplified diagram of the cooling systems on 55L at Mine B. Fans forced the air from the downcast shaft over the BAC. This chilled air travelled down a raise borehole back to the downcast shaft and the working levels. The return airway entered this level via an upcast raise borehole. Thereafter, fans forced this air over the condenser pond. The chilled water from the ice dam flowed to the working levels below.

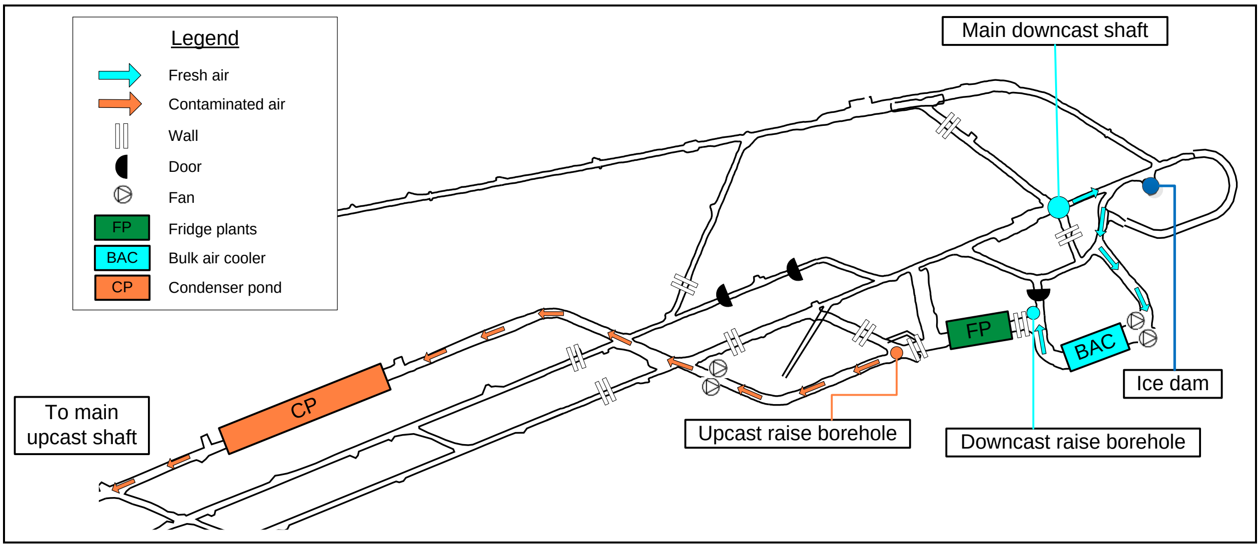


**Figure 3-14: Mine B cooling system diagram 55L***

### 3.3.3 Data collection

Mine B had a SCADA system but no environmental monitoring instruments were installed on the surface or the working levels. All required data needed to calibrate the cooling system was available. The remaining environmental data had to be collected manually with handheld instruments.

#### *i) Collecting transient data*

The data for both cooling systems were obtained from the SCADA system. The data quality was determined by performing checks on the data, which entailed checking the maximum and minimum limits as well as the checking of balance [38].

Mine B operated two of the three fridge plants on 55L at all times. The data was collected when Fridge Plant 1 (FP1) and Fridge Plant 2 (FP2) were in operation. The fridge plants were set to provide a water temperature of 5°C to the BAC. Appendix J gives further details of the refrigeration layout and set points of this system.

Figure 3-15 illustrates the fridge plant temperature under regular operation over 24 hours for FP1. It operated at an average evaporator water flow rate of 64.5 ℓ/s and an average condenser water flow rate of 149.5 ℓ/s. The same data was collected for FP2. Both fridge plants were running at their set points and provided an evaporator outlet temperature of 5°C throughout the day. The result was a BAC that provided a fairly constant outlet air temperature, which reduced the fluctuations in ventilation air temperature provided to the mine.

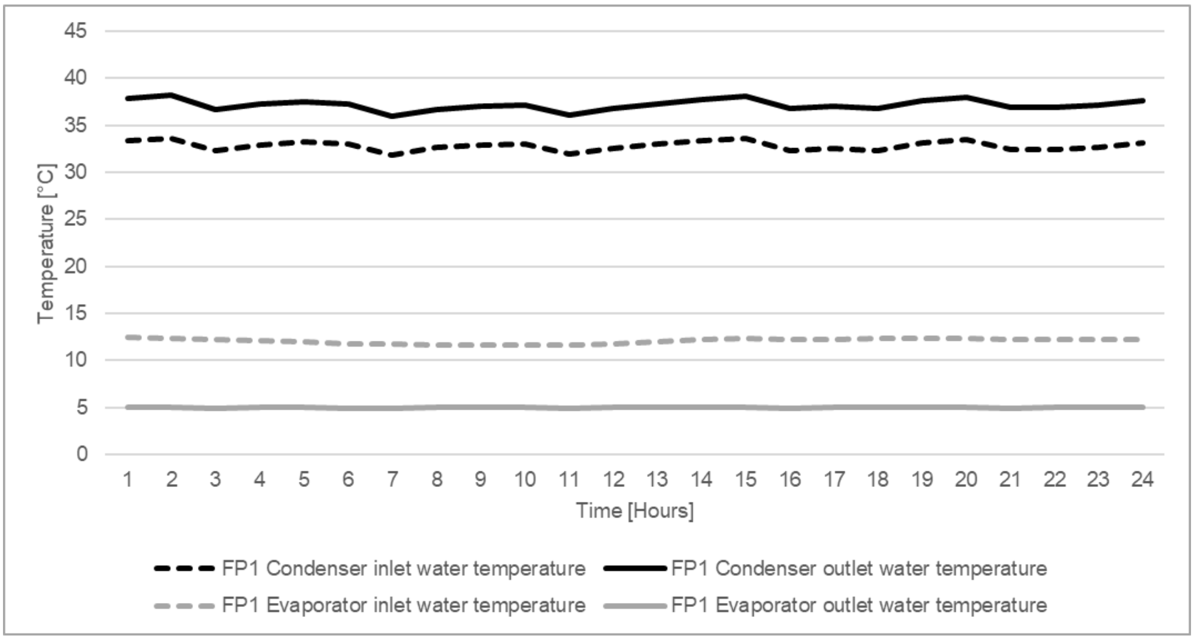


**Figure 3-15: Mine B FP1 temperatures***

Figure 3-16 illustrates the data collected for the chilled water system. The ice plants provided ice at a constant flow rate of 35 kg/s, and the ice was mixed with treated water at 32°C in the ice dam. The mixture ratio between treated water and ice varied throughout the day. Mine B was equipped with water flow instrumentation per working level. This data was collected and compared with the total water flow from the ice dam to verify the flow measurements with a mass balance calculation.

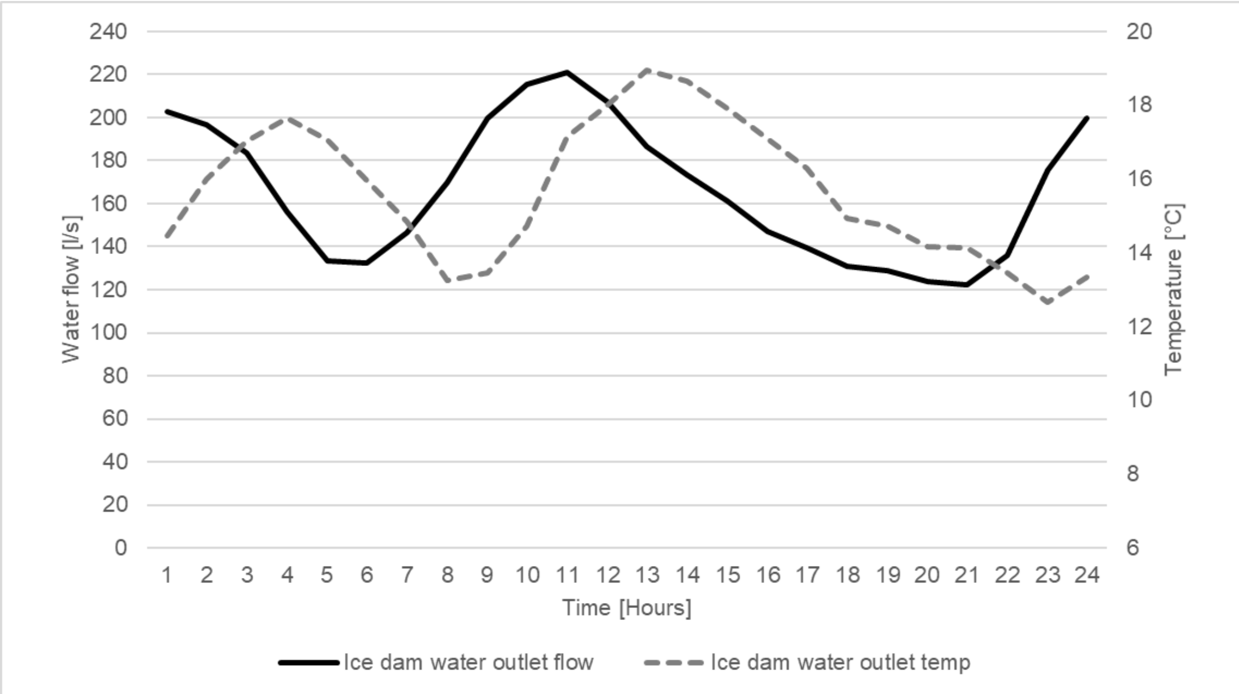


**Figure 3-16: Mine B Ice dam data***

The same method of underground temperature measurement as Case Study 1 was applied at Mine B. Figure 3-17 illustrates an example of the ambient and underground temperature measured at Mine B. The underground temperatures were measured at the intake of the shallowest services level (55L), which was 1 676 m underground. These temperatures were the intake and outlet boundaries of the downcast shaft up to 55L and were used to calibrate the downcast shaft. There was a slight reduction in the temperature fluctuations compared with the data collected at Mine A in Figure 3-4. The thermal history effect was more significant with greater depths and distance.

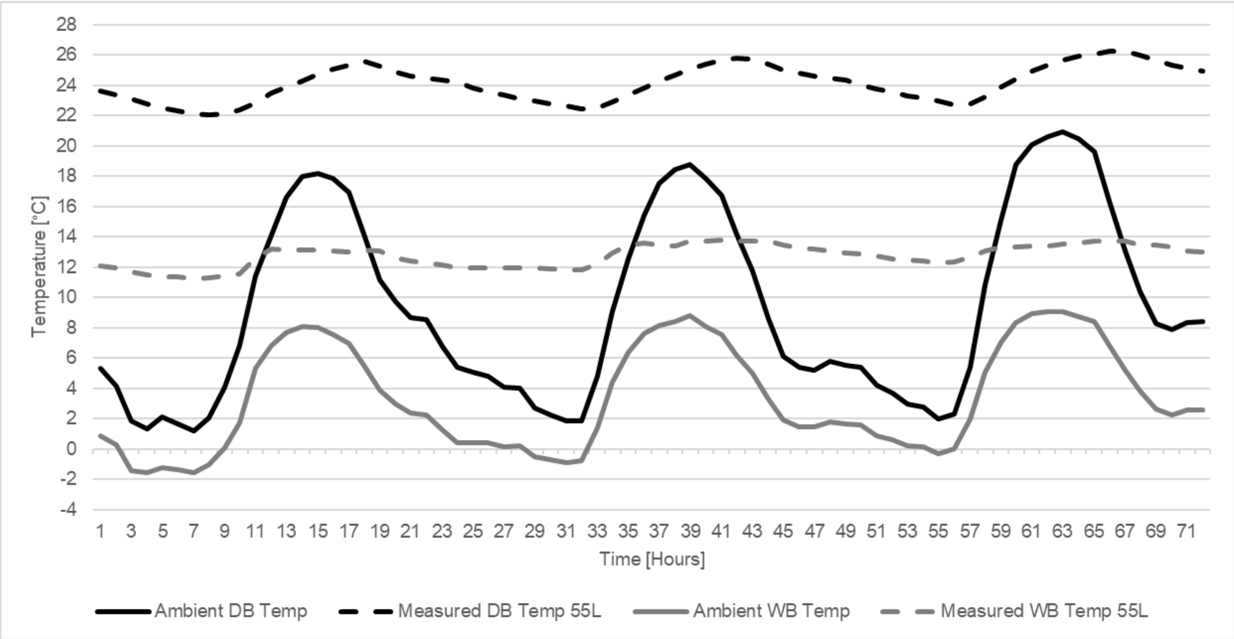


**Figure 3-17: Ambient and underground temperature on 55L at Mine B***

Figure 3-18 illustrates the measurement locations on the shallowest mining level (66L). The first location (Point 1) was in the main intake drift, approximately halfway between the downcast shaft and the working areas. The second location (Point 2) was the working area intake. The third location (Point 3) was in the return airway after the working areas. Similar locations were selected for the deepest mining level (75L).

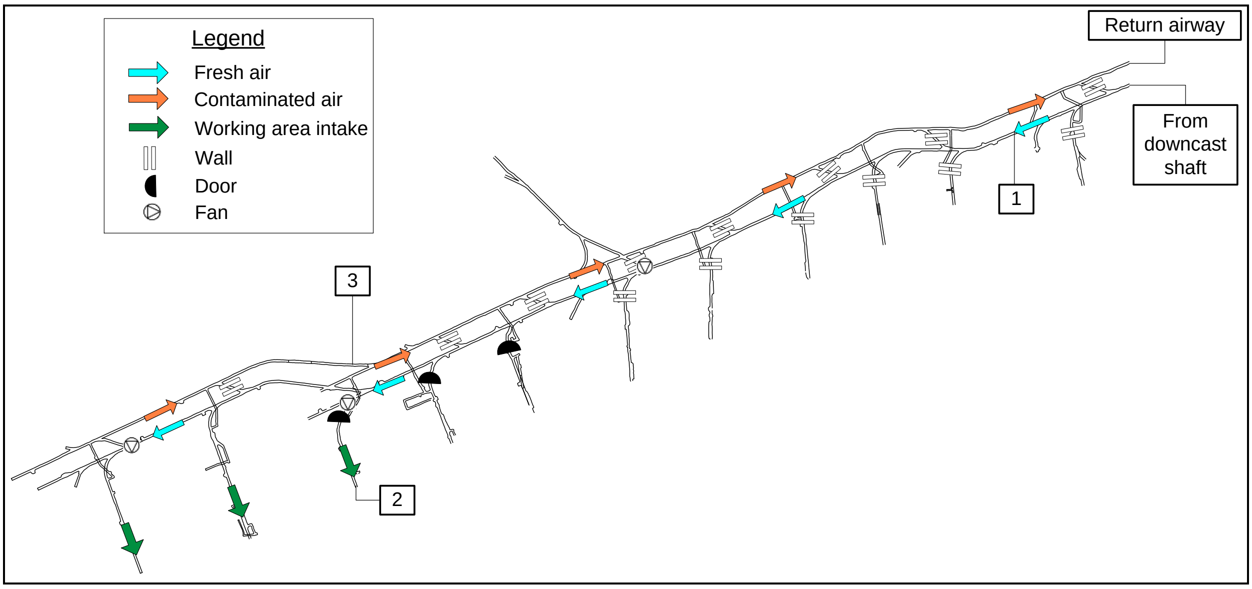


**Figure 3-18: Underground temperature measurement locations at Mine B (66L)***

Figure 3-19 illustrates the DB temperatures measured at these locations over 24 hours. At this depth, the thermal damping was so significant that the temperatures had minimal variation over the 24 hours. The low airflow in the main drift of this level and the constant cooling further increased the thermal damping impact. Therefore, the fluctuations in the temperatures resulted from the dynamic nature of mining operations leading to the working areas.

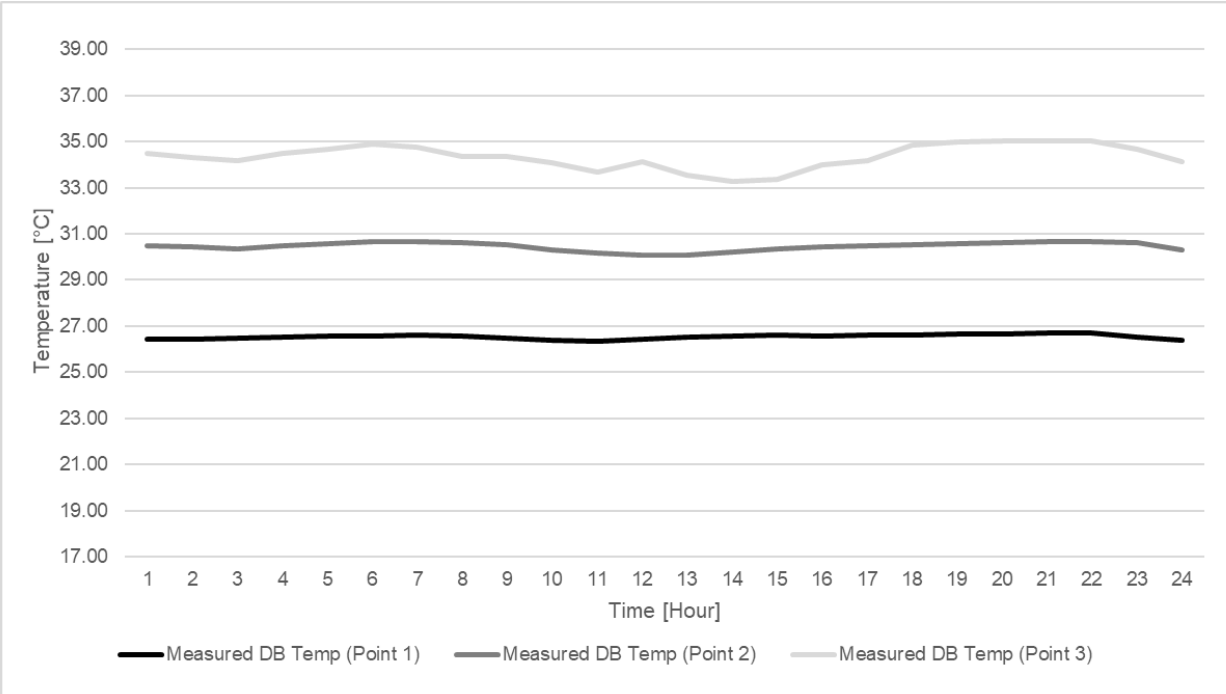


**Figure 3-19: Underground temperature measurement at Mine B (66L)***

The final step of transient data collection was to determine the accuracy of the measured ventilation data. The same temperature loggers as Case Study 1 were used to measure the ambient and underground environmental conditions. The results from Case Study 1 showed that these loggers had adequate accuracy for a true transient simulation calibration.

The outstanding data that could not be collected using transient methods are listed below:

- Surface and underground barometric pressure,
- Airflow of the mine ventilation network,
- Return fan static pressure,
- Chilled water pipe temperatures.

#### *ii) Determining heat load*

Mine B used the same narrow reef mining technique as Mine A, thus the heat load calculation was similar. The heat load was calculated in a steady state due to the limitation of PTB mentioned in

Section 2.4. Table 3-6 summarises the total heat added to the ventilation system of Mine B by the secondary heat sources after the chilled water-cooling duty. The calculation of the heat from these sources is summarised in Appendix K.

**Table 3-6: Total heat load from secondary sources for Mine B**

| Parameter | Unit | Value |
|---|---|---|
| Effective electrical heat load | [kW] | 4 348 |
| Metabolic heat load | [kW] | 450 |
| Explosive heat load | [kW] | 3 |
| Fissure water heat load | [kW] | 999 |
| Chilled water pipes cooling duty | [kW] | −4 829 |
| **Total heat load from secondary sources** | **[kW]** | **970** |

#### *iii) Collecting steady-state data*

The same handheld measuring instruments and methods as with Case Study 1 were applied to Mine B. The final step was to determine the accuracy of the measured data. As with Case Study 1, the simulation airflow could not practically be calibrated to more than 95% accuracy since the airflow measurements had a minimum error of 5% [74], [86].

### 3.3.4 Building of the model

#### *i) Building the model*

The digital mining layouts seen in Figure 3-12 were imported into PTB, and the drag-and-drop function was used to add components to the layouts. Figure 3-20 illustrates the final 3D PTB ventilation model. This model had over 10 000 individual simulation components and took approximately 45 minutes to solve a 24-hour period simulation.

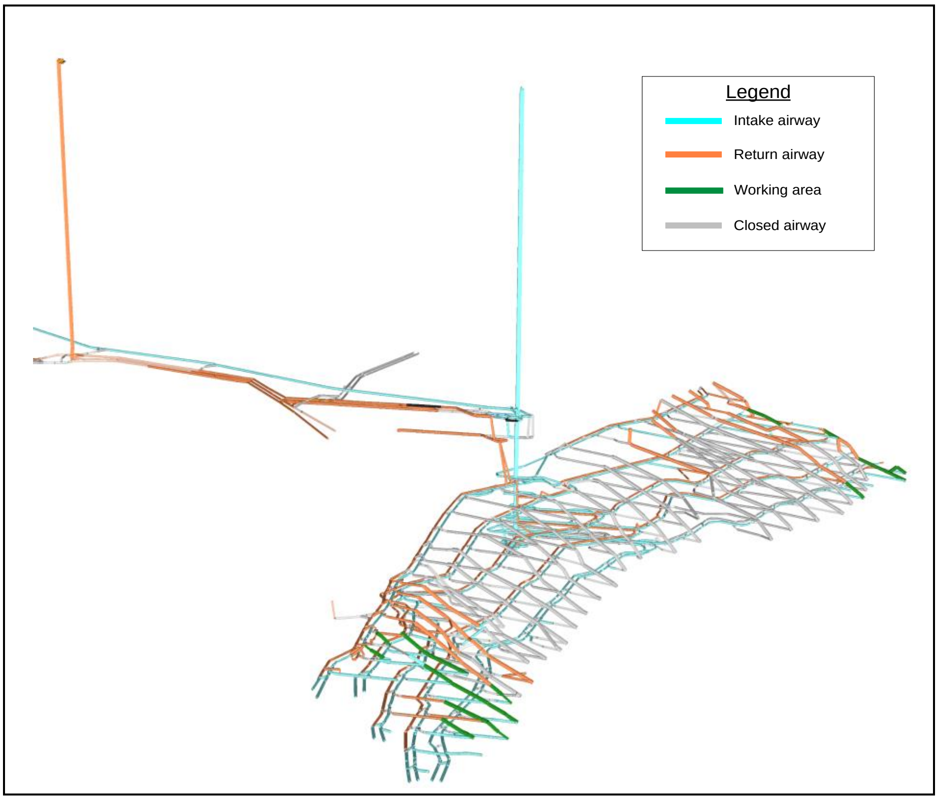


**Figure 3-20: PTB ventilation simulation of Mine B***

Figure 3-21 illustrates the cooling system simulation integrated into the ventilation simulation of Mine B.

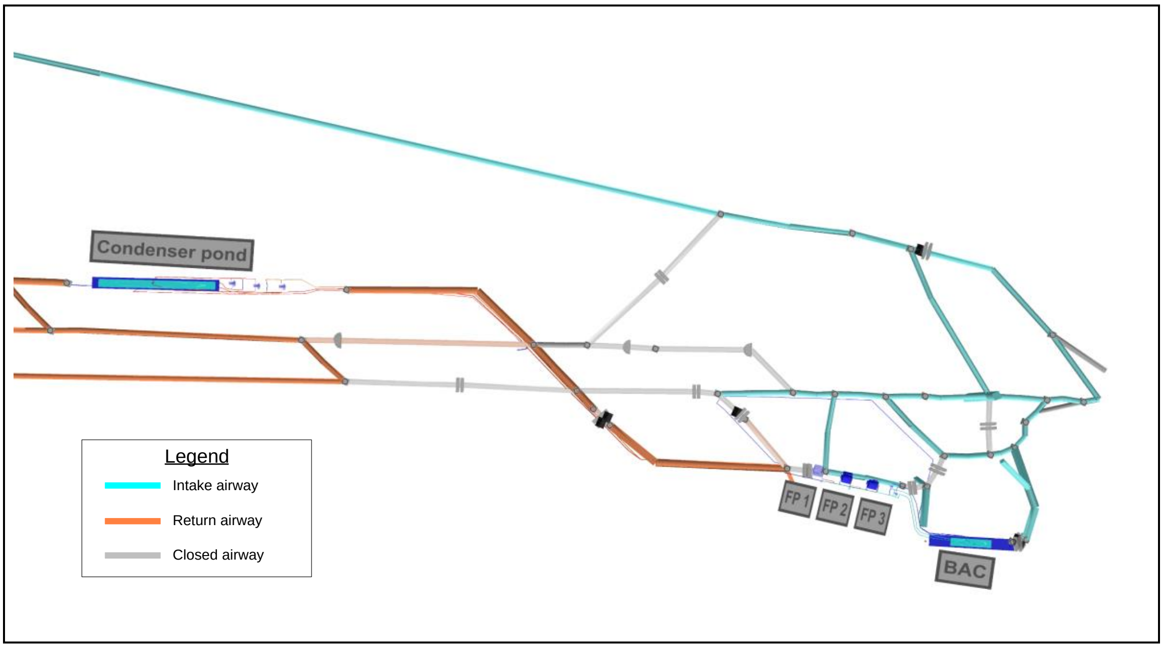


**Figure 3-21: PTB integrated cooling simulation of Mine B***

At the time of this study, PTB did not have an ice plant component and the chilled water supply had to be simplified. The simplified chilled water system included the ice dam and water network up to the mobile coolers. The ice dam had to be calibrated according to the actual ice production and water temperatures, and this system provided the same impact as the actual cooling system on the ventilation system.

#### *ii) Defining the system with standard data*

The ventilation components were defined using the same method as the first case study discussed. The cooling components were defined with standard data from the sources in Section 2.4. The values used as inputs are summarised in Appendix L. The ice mass fraction on the inlet of the ice dam could not practically be measured at Mine B, thus it had to be calibrated using iterations.

### 3.3.5 Calibration

The calibration of the system was similar to Mine A, with the addition of the ice mass fraction as an unknown parameter. Different sections of the mine had different types of water usage, which resulted in different wetness fractions. For the calibration of the wetness fraction, the mine was divided into the downcast shaft (55L), main drift (66L), and main drift (75L).

The secondary heat load for Mine B was calculated to be 970 kW, as shown in Section 3.3.3, which included the cooling duty of the chilled water pipes. The secondary heat was distributed across the intake airways, as with Case Study 1. The heat was distributed across the total length of the intake airways as a kW/m value.

#### *i) Prime the model with temperature history*

The cooling system operation and ambient environmental conditions were recorded for three weeks to provide a suitable temperature history for accurate heat exchange. The average ambient environmental conditions and cooling system operation for the priming period are shown in Table 3-7.

**Table 3-7: Average priming period parameters for Mine B**

| Priming parameters | Unit | Value |
|---|---|---|
| Average ambient DB temperature | [°C] | 10.8 |
| Average ambient relative humidity | [%] | 37.0 |
| Average ambient barometric pressure | [kPa] | 87.5 |
| Average ice flow rate | [kg/s] | 35.9 |
| Evaporator outlet temperature | [°C] | 5.0 |

These averages were used as inputs to the model, and the model was run until it reached a steady state. The model was at a steady state when there were no fluctuations in any parameters. The simulated temperature of the underground tunnels after priming represented the actual temperature of the tunnels at the start of the calibration period. The calibration period was three days for smaller sections and one day (24 hours) for larger sections to reduce simulation times.

#### *ii) Iteration of unknown parameters*

The airflow data could only be measured in a steady state so that the airflow would be calibrated and verified in a steady state. The same iteration process as in Case Study 1 was used for this case study. A wetness fraction of 0.175 and door fraction of 0% on closed tunnels was used as the baseline. Iterations showed that an ice mass fraction of 58% produced accurate results on the outlet water temperature.

### 3.3.6 Verification

The final simulation had airflow that accurately represented the actual system. The final simulation had an average accuracy of 86% when all ventilation doors and fans were operating as planned. When the actual unplanned operation of doors and fans was simulated during the measurement, the two calibration levels had an air intake accuracy of 91%. Although this was not as accurate as Mine A, it fell within the error margin of the measurement technique, which was 5–23% [87], [88]. These levels had an MSE of 10.4 and a maximum error of 7.7 kg/s.

The ventilation system of Mine B was dynamic due to the travel of people and equipment through doorways that were installed to prevent recirculation. These temporary changes in airflow resulted in less accurate spot measurements, which also affected the airflow and environmental conditions across levels.

The simulated DB and WB temperatures on 55L were compared with the measured temperatures to verify the downcast shaft. Figure 3-22 illustrates the comparison between these temperatures over 72 hours. As with Case Study 1, the simulation could incorporate the thermal history effect.

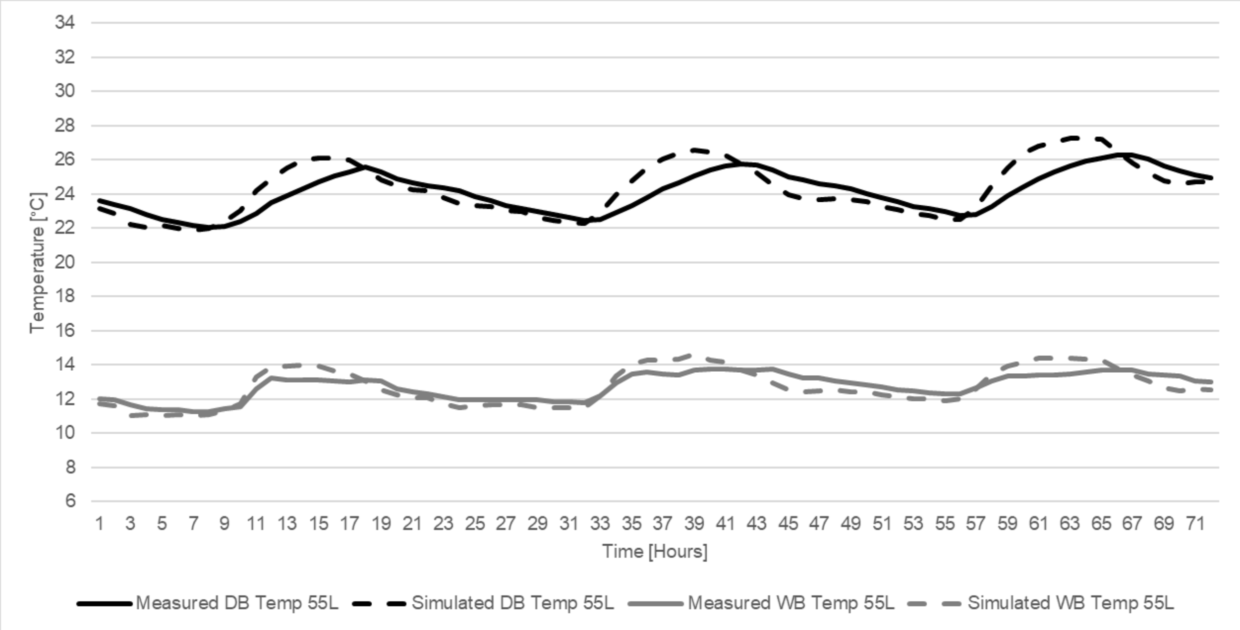


**Figure 3-22: Mine B transient temperature comparison (55L)***

Table 3-8 demonstrates the simulation performance for Mine B for the downcast shaft. The results showed that the downcast shaft in the simulation was calibrated accurately. The results were similar to the results from the literature discussed in Section 2.3.5, which were for a downcast shaft calibrated to an acceptable level of accuracy.

**Table 3-8: Summary of Mine B shaft simulation performance (55L)**

| Parameter | Unit | MSE | R² | Maximum error |
|---|---|---|---|---|
| DB temperature (transient) | [°C] | 0.87 | 0.66 | 1.97 |
| WB temperature (transient) | [°C] | 0.30 | 0.79 | 1.02 |

These results had lower accuracy than the simulation in Case Study 1. The main downcast shaft at Mine B was used for transporting materials, broken rock, and people. The underground operation was also more dynamic than at Mine A. These factors negatively affected the accuracy of the predicted temperatures.

The cooling system simulation accurately represented the actual system with an average accuracy of 95.6% [38]. Appendix M shows the average cooling system conditions measured and simulated. These results had low $R^2$ values and adequate maximum error, indicating that the simulation predicted values close to the actual values, but the trend did not closely represent the actual system.

The 55L environmental conditions were supplied directly to the BAC, as seen in Figure 3-14. The condenser circuit of the cooling system on 55L rejected heat to the main return airway to the upcast shaft. The environmental conditions in the return airways were the result of the mining operation, which was dynamic.

The $R^2$ between the measured and simulation temperatures was low due to the actual fluctuating temperature experienced by the condenser ponds in the return airway. However, the chilled air provided to the underground operations was the main output of this cooling system and affected the rest of the ventilation system after that point. The simulation accurately represented the BAC outlet temperature with an MSE of 0.02, an $R^2$ of 0.83, and a maximum error of 0.3°C.

Figure 3-23 illustrates the measured and simulated outlet WB temperatures on 55L. The refrigeration plants provided water at 5.0°C with a flow rate of 132 kg/s to the BAC, allowing the BAC to provide a constant airflow rate of 250.2 kg/s at an average WB temperature of 9.9°C.

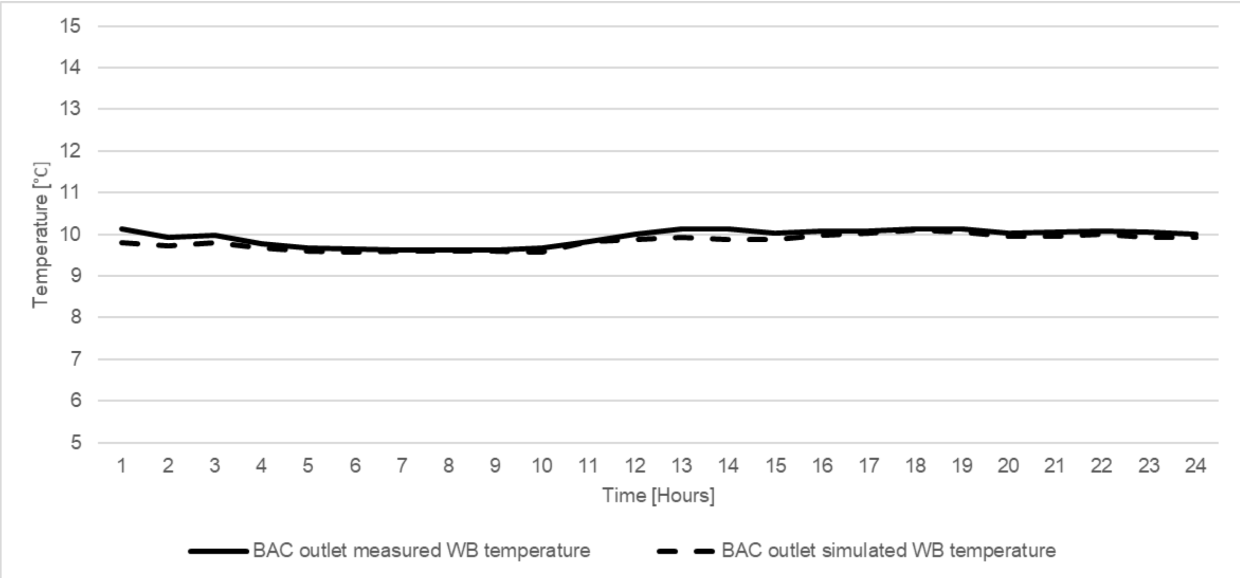


**Figure 3-23: Mine B BAC transient temperature comparison (55L)***

The ice dam supplied chilled water to the mine. The chilled water was transported throughout the mine with a piping network. Figure 3-24 compares the measured and simulated ice dam outlet water temperature. The ice dam outlet temperature had an average accuracy of 97%. The simulation performance is shown in Table 3-9.

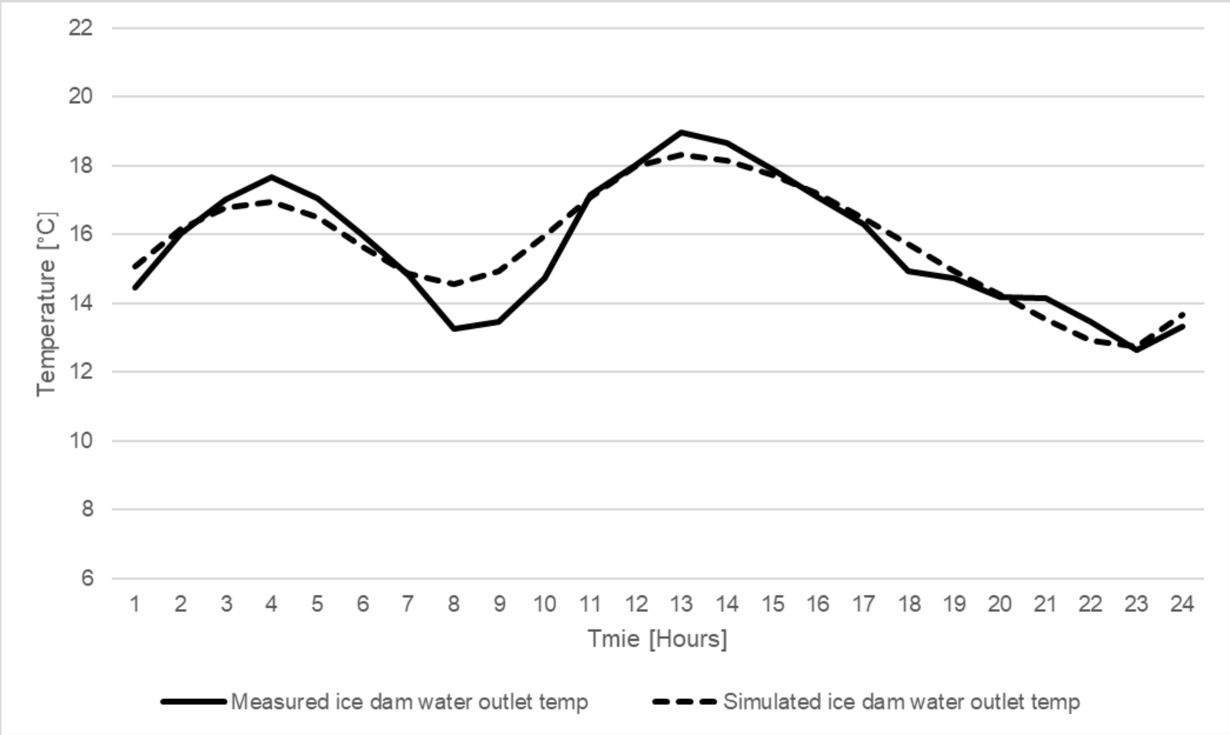


**Figure 3-24: Mine B ice dam transient temperature comparison (55L)***

**Table 3-9: Summary of Mine B ice dam simulation performance**

| Parameter | Unit | MSE | $R^2$ | Maximum error |
|---|---|---|---|---|
| Ice dam outlet temperature | [°C] | 0.37 | 0.90 | 1.45 |

With the shaft and cooling system calibrated, the simulation provided environmental conditions to the main working levels that represented the actual measured values accurately. Figure 3-18 in Section 3.3.3 illustrates the measuring locations on 66L. The rise of temperature from Point 1 to Point 3 represented the air heat pickup on a working level. The environmental conditions at Point 3 were prioritised when iterating for unknown parameters in the calibration process.

Figure 3-25 illustrates the measured and simulated DB temperatures on 66L and shows how they increased as the air travelled on the level. The figures that compare the WB and DB temperatures for all three points on 66L are attached in Appendix N.

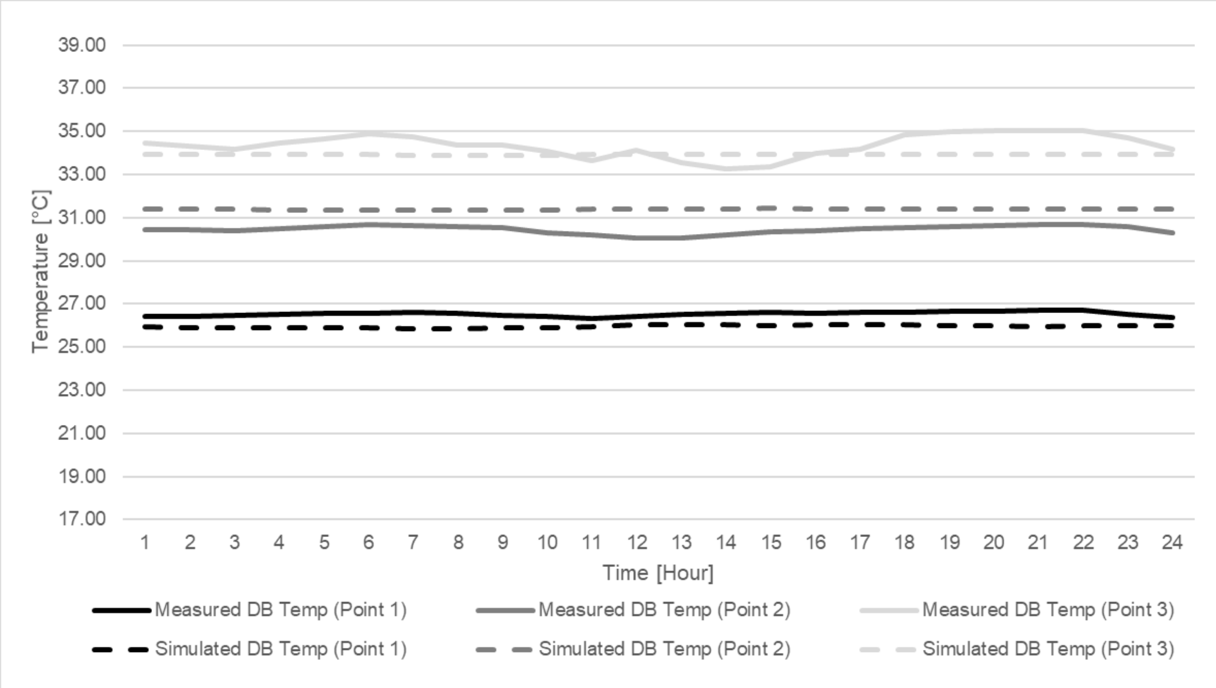


**Figure 3-25: Mine B transient DB temperature comparison (66L)***

At this depth, the thermal history effect had almost completely removed the temperature fluctuations due to the changing ambient conditions. The BAC on 55L provided fairly consistent temperatures to the mining levels at an airflow rate of 250 kg/s. The total airflow rate in the main downcast shaft was around 475 kg/s, thus the BAC chilled around 53% of the downcast air. This resulted in more consistent temperatures on the working levels.

The measured DB temperature at Point 1 was the intake of the section of the ventilation system and was relatively consistent. The DB at Point 3 varied over the 24 hours, which meant that the fluctuations in measured data were due to the dynamic nature of the mining operations closer to the working areas.

Table 3-10 summarises the simulation performance on a working level (66L). These results confirm a decrease in simulation accuracy as the intake air travelled deeper and further into the mine [4]. The results were, however, still better than conventional steady-state simulations. This resulted from the system's increasing complexity and dynamic nature as the mine expanded. The maximum error of 2.06°C on 66L was only 0.13°C higher than the maximum acceptable error from the literature (1.93°C) [52].

**Table 3-10: Summary of Mine B simulation performance (66L)**

| Location | Parameter | Unit | MSE | $R^2$ | Maximum error |
|---|---|---|---|---|---|
| Point 1 | DB temperature (transient) | [°C] | 0.35 | 0.04 | 0.75 |
| | WB temperature (transient) | [°C] | 2.28 | 0.05 | 2.06 |
| Point 2 | DB temperature (transient) | [°C] | 0.92 | 0.12 | 1.35 |
| | WB temperature (transient) | [°C] | 0.11 | 0.06 | 0.56 |
| Point 3 | DB temperature (transient) | [°C] | 0.45 | 0.04 | 1.11 |
| | WB temperature (transient) | [°C] | 1.14 | 0.10 | 1.55 |

The true transient simulation of Mine B was further verified by comparing the environmental predictions on another level, 75L, with the same calibration as 66L. The unknown parameters on 66L determined in Section 3.3.5 were applied directly to 75L.

Table 3-11 summarises the simulation performance on 75L. The measurement locations and figures that compare the WB and DB temperatures for all three points on 75L are attached in Appendix O. These results verify the results in Table 3-10 and show that a similar accuracy can be expected when calibration parameters are applied throughout the mine.

**Table 3-11: Summary of Mine B simulation performance (75L)**

| Location | Parameter | Unit | MSE | $R^2$ | Maximum error |
|---|---|---|---|---|---|
| Point 1 | DB temperature (transient) | [°C] | 0.49 | 0.56 | 1.78 |
| | WB temperature (transient) | [°C] | 2.78 | 0.35 | 2.27 |
| Point 2 | DB temperature (transient) | [°C] | 0.77 | 0.64 | 1.61 |
| | WB temperature (transient) | [°C] | 1.78 | 0.46 | 1.90 |
| Point 3 | DB temperature (transient) | [°C] | 0.44 | 0.13 | 1.00 |
| | WB temperature (transient) | [°C] | 0.82 | 0.28 | 1.19 |

The low $R^2$ values seen in Table 3-10 and Table 3-11 show that the simulation had a low correlation to the data trend, even though the maximum errors were within the normal values for similar simulations [52]. This results from unknown variables which cause minor variations in the data that the simulation does not fully take into account. These variations can be caused by the movement of people and equipment, opening and closing ventilation doors, blasting, or changes in the electrical heat load at Mine B.

The results from this section show that the simulation was able to provide environmental predictions with an acceptable level of accuracy for most sections of the mine according to the KPIs. From the results it was noted that the accuracy of the simulation decreased with increasing depth and distance from the intake shafts. This could be due to the increased distance that the air is in contact with the rock and the increased equipment used underground. The results further show that the measurement equipment had adequate accuracy for the purpose of calibration.

### 3.3.7 Comparison to steady-state simulation

The simulation was resimulated with a quasi-steady-state analysis for 55L and the two working levels, 66L and 75L. These results were compared with Case Study 1 results to determine the effect of thermal history on underground environmental conditions at different depths. Figure 3-26 compares the actual measurements, transient simulation and quasi-steady-state simulation on 55L, which represents the downcast shaft calibration.

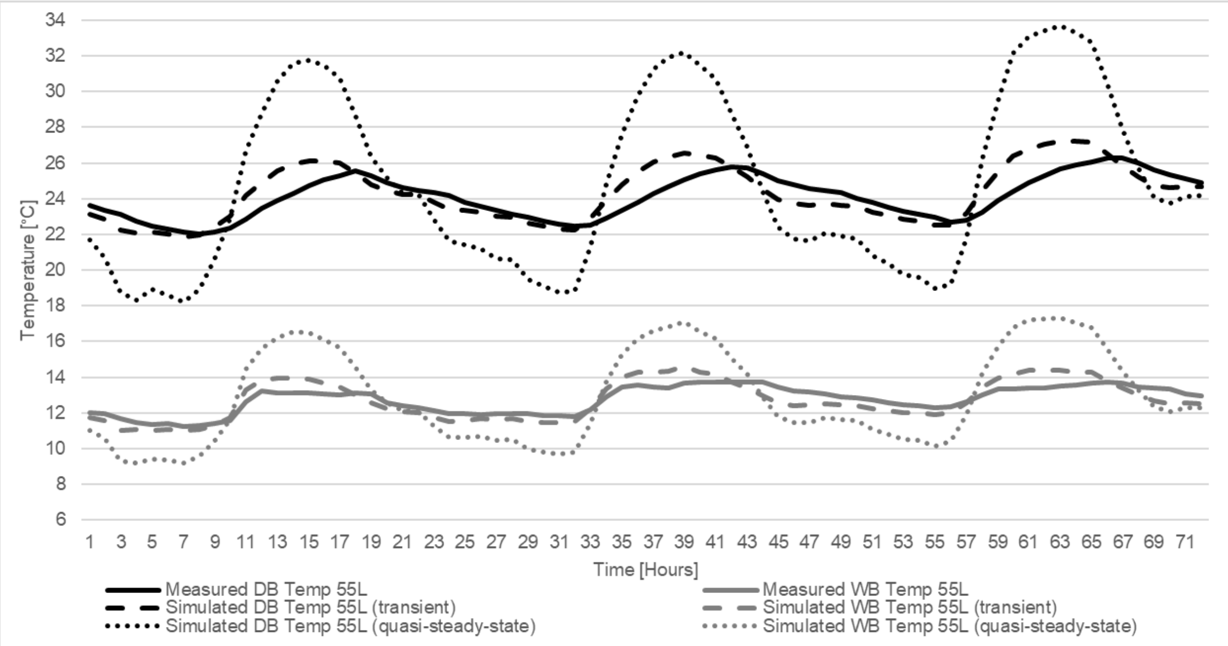


**Figure 3-26: Mine B transient and quasi-steady-state temperature comparison (55L)***

This comparison shows similar results to the comparison of the underground temperatures in Case Study 1, in Figure 3-11. Table 3-12 compares the simulation results from the transient and quasi-steady-state simulations. These results show an advantage with true transient at this depth.

**Table 3-12: Mine B comparison of transient and quasi-steady-state simulation performance (55L)**

| Parameter | Unit | MSE | R² | Maximum error |
|---|---|---|---|---|
| DB temperature (transient) | [°C] | 0.87 | 0.66 | 1.97 |
| DB temperature (quasi-steady-state) | [°C] | 17.84 | 0.47 | 8.16 |
| WB temperature (transient) | [°C] | 0.30 | 0.79 | 1.02 |
| WB temperature (quasi-steady-state ) | [°C] | 4.24 | 0.67 | 3.90 |

Figure 3-27 illustrates the measured and simulated DB temperatures on 66L. The measured temperatures showed little to no fluctuations due to changing ambient conditions, as seen at Point 1. The true transient simulation corroborated the fairly steady DB temperatures at all the points. The quasi-steady-state simulation showed some fluctuation as a result of fluctuating ambient conditions.

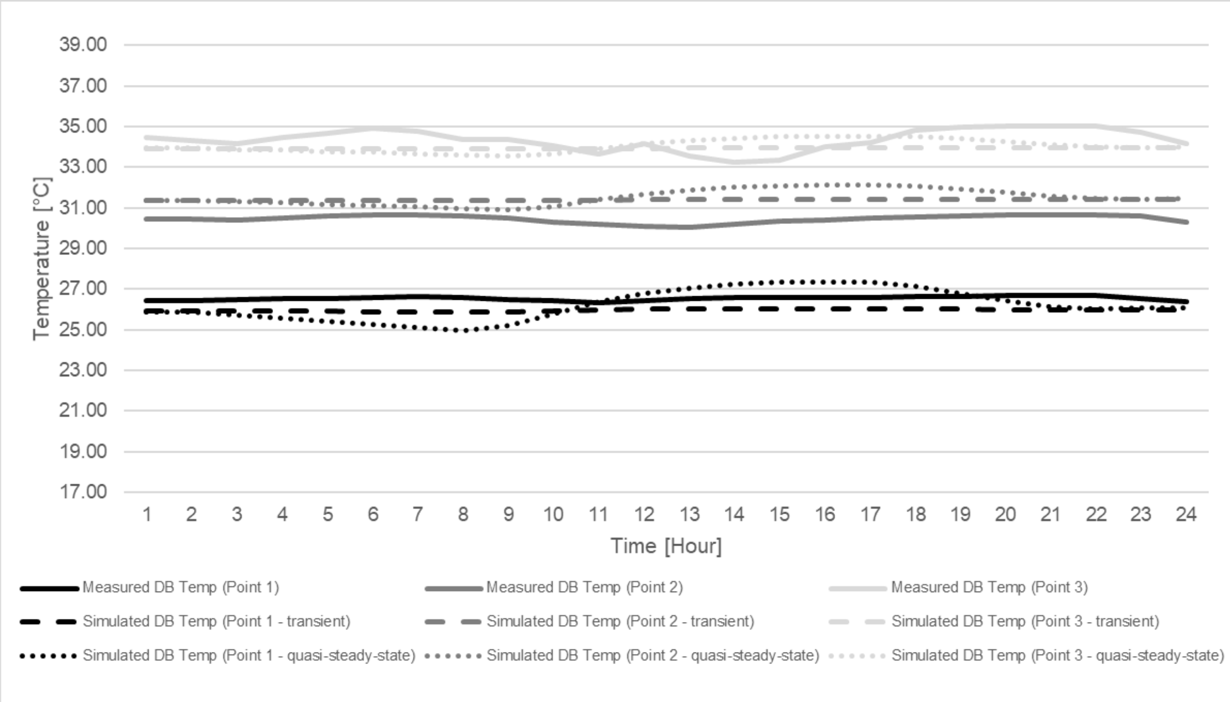


**Figure 3-27: Mine B transient and quasi-steady-state DB temperature comparison (66L)***

Table 3-13 summarises the simulation performances on 66L. The figures and tables that compare the WB and DB temperatures for all three points on 66L are attached in Appendix N. The true transient simulation provided the most accurate environmental conditions on the entire 66L.

**Table 3-13: Mine B comparison of transient and quasi-steady-state simulation performance (66L)**

| Location | Parameter | Unit | MSE | $R^2$ | Maximum error |
|---|---|---|---|---|---|
| 66L | Average DB (transient) | [°C] | 0.57 | 0.07 | 1.35 |
| | Average DB (quasi-steady-state) | [°C] | 0.86 | 0.07 | 1.82 |
| | Average WB (transient) | [°C] | 1.18 | 0.07 | 2.06 |
| | Average WB (quasi-steady-state) | [°C] | 1.88 | 0.05 | 3.06 |

The results on 75L confirm the result recorded on 66L. The figures and tables that compare the WB and DB temperatures for all three points on 75L are attached in Appendix O. Table 3-14 summarises the simulation performances on 75L. Again, the true transient simulation provided the most accurate environmental conditions on the entire 75L.

Table 3-14: Mine B comparison of transient and quasi-steady-state simulation performance (75L)

| Location | Parameter | Unit | MSE | $R^2$ | Maximum error |
|---|---|---|---|---|---|
| 75L | Average DB (transient) | [°C] | 0.57 | 0.44 | 1.78 |
| | Average DB (quasi-steady-state) | [°C] | 0.67 | 0.25 | 1.89 |
| | Average WB (transient) | [°C] | 1.79 | 0.36 | 2.27 |
| | Average WB (quasi-steady-state) | [°C] | 1.78 | 0.25 | 2.66 |

This section shows that even though the true transient simulation accuracy decreased with depth and distance from the shaft, it still had improved accuracy over conventional simulation for all areas at Mine B.

### 3.3.8 Discussion

#### *i) Transient cooling simulations*

The refrigeration system on 55L produced BAC outlet temperatures that accurately represented the actual temperatures. The simulated BAC outlet WB temperature could not be calibrated more accurately as it had a maximum error of 0.3°C, which was less than the temperature loggers' accuracy.

The ice dam was calibrated to provide chilled water per the measured water temperatures and had an average accuracy of 97%. The ice dam and chilled water simulation represented the actual system accurately.

Mine B's transient cooling systems simulations were integrated successfully into the true transient mine ventilation simulation. The simulation provided the ventilation simulation with cooling that represented the conditions experienced by the actual system accurately.

#### *ii) True transient ventilation simulation*

This case study verified the results from the first case study that proved a true transient simulation could be applied to an underground ventilation system and could produce accurate results while incorporating the thermal history effect.

The results were more accurate than conventional steady-state simulations in both case studies. The accuracy of the true transient simulation decreased for areas that were deeper and further away from the downcast shaft. The environmental conditions at the working areas' intakes resulted from the aggregation of heat and cooling sources up to that point. Therefore, the accuracy was expected to decrease since the error in the heat and cooling was also aggregated.

The methodology developed in Chapter 2 was specifically adapted to be practical so that it could be applied to mine ventilation systems with different infrastructure and cooling. A few factors in this case study contributed to the errors in the heat and cooling supplied to the simulation:

- Steady-state airflow measurements,
- Steady-state tunnel internal heat load,
- Average heat load applied to the entire intake system, and
- Average wetness fraction applied to the entire intake system.

Mine B is a large and dynamic mine that did not have ventilation measurement instrumentation installed underground. The airflow was measured using spot checks, thus the airflow of this case study had to be calibrated in a steady state.

Steady-state manual airflow measurements have an error of between 5% and 23% [74], [86]. The dynamic operation of ventilation doors and fans made it difficult to measure a steady-state snapshot of the airflow in the mine. The aggregation of the errors in heat and cooling due to errors in airflow calibration significantly affected the environmental conditions at the working areas' intakes. This was more evident in this case study as Mine B was much larger and more complicated than Mine A from the first case study.

The second factor that affected the underground environmental predictions was the steady-state simulation of the internal heat, which was the heat from secondary sources. The largest contributor to the internal heat for Mine B was the electrical heat load, which varied with up to 1 MW in 24 hours. This was a 4% variation in the total heat added to Mine B and would have a notable impact on simulated environmental conditions.

The final two factors were implemented to make the development of the simulation more practical. Measuring and calibrating each section of the mine individually would require extensive time and resources. The distribution of average internal heat load and wetness fraction across the mine decreased the accuracy of the environmental predictions.

The actual internal heat and wetness of underground tunnels varied between the different mining areas. This was visible on 66L in Figure 3-25, where the average simulated DB temperature was too high for Point 1 and too low for Point 2. There was too much heat leading up to Point 1 and not enough heat between Point 1 and Point 2 due to the average internal heat load.

Applying the average internal heat and wetness fraction to the entire mine reduced the calibration time. The unknown wetness fraction determined by the calibration of 66L was applied to 75L and produced results with similar accuracy. This verified that the true transient simulation would have accurate results on all mine sections with similar infrastructure.

#### *iii) Objectives*

This case study aimed to meet the following objectives:

- Application of a true transient ventilation simulation to an entire deep-level mine, and
- Integration of a transient cooling simulation with a true transient ventilation simulation on a deep-level mine.

The new true transient method was applied to Mine B's ventilation and cooling system. The results showed that the simulation could take the thermal history effect into account and could determine the underground environmental conditions to an acceptable level of accuracy. The results further demonstrated that the true transient simulation was more accurate than conventional steady-state simulations, which validated the true transient simulation of real-life applications.

## 3.4 Case Study 3

### 3.4.1 The objective of Case Study 3

Case Study 3 investigated a true transient simulation of an underground mine ventilation and cooling system that used a block-caving mining method with fuel-driven mechanised machinery. For confidentiality, the mine investigated in this case study is referred to as Mine C. This case study aimed to meet and validate the second and third objectives of this case study.

The focus was to compare the true transient simulation of mines with different mining techniques. Previous case studies used conventional narrow-reef mining, but this case study used block-caving and fuel-driven mechanised machinery. Most of the data collection and calibration of this case study were similar to Case Study 2 and were simplified.

This case study aimed at verifying that the objectives were met by determining whether a true transient ventilation and cooling simulation could produce accurate results. The simulation developed in this case study was compared with a conventional steady-state simulation to validate the use of true transient simulations in real-life integrated ventilation and cooling applications. Accurate results would also validate the use of the new true transient methodology.

### 3.4.2 Description of Mine C

Mine C was an underground gold mine in Free State, South Africa. This mine started production in 2002 and was mining at an average depth of 2 300 m at the time of the study, with a maximum mining depth of 2 430 m underground. Mine C produced 1 600 kg of gold per year and had around 1 900 employees.

Figure 3-28 illustrates an overhead view of the underground layout of Mine C. This mine had one downcast and one upcast shaft. The current mining areas were on the northern side of the mine and were up to 6.5 km away from the main intake shaft.

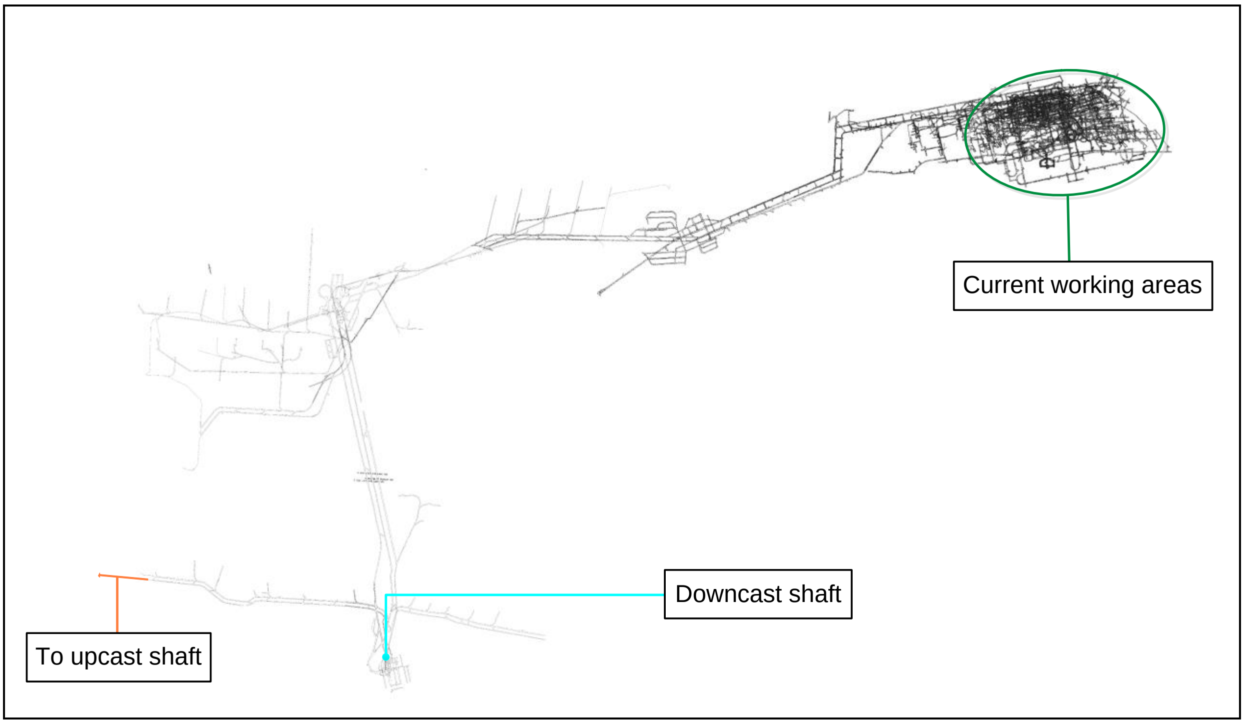


**Figure 3-28: Mine C underground layout***

Mine C used a block-caving mining method to mine large vertical ore deposits. Mobile fuel-driven machinery was used for drilling and moving broken rock. The rock was moved to electric conveyor belts, where it was transported to the intake shaft and the surface with a skip. Fuel-driven machinery can be a significant contributor to the overall heat load of an underground mine [11], [31]. The machine operating times determine the heat from fuel-driven machinery [11]. The dynamic operation of fuel-driven machinery contributes to fluctuating underground environmental conditions.

Mine C utilised an underground cooling system on 255L to mitigate the heat produced in the mine. The cooling systems consisted of ten fridge plants that supplied chilled water to BACs and working areas. Condenser ponds rejected the heat to the return airway, which was upcast to the surface and rejected to the atmosphere. Figure 3-29 illustrates a simplified schematic of the cooling system at Mine C.

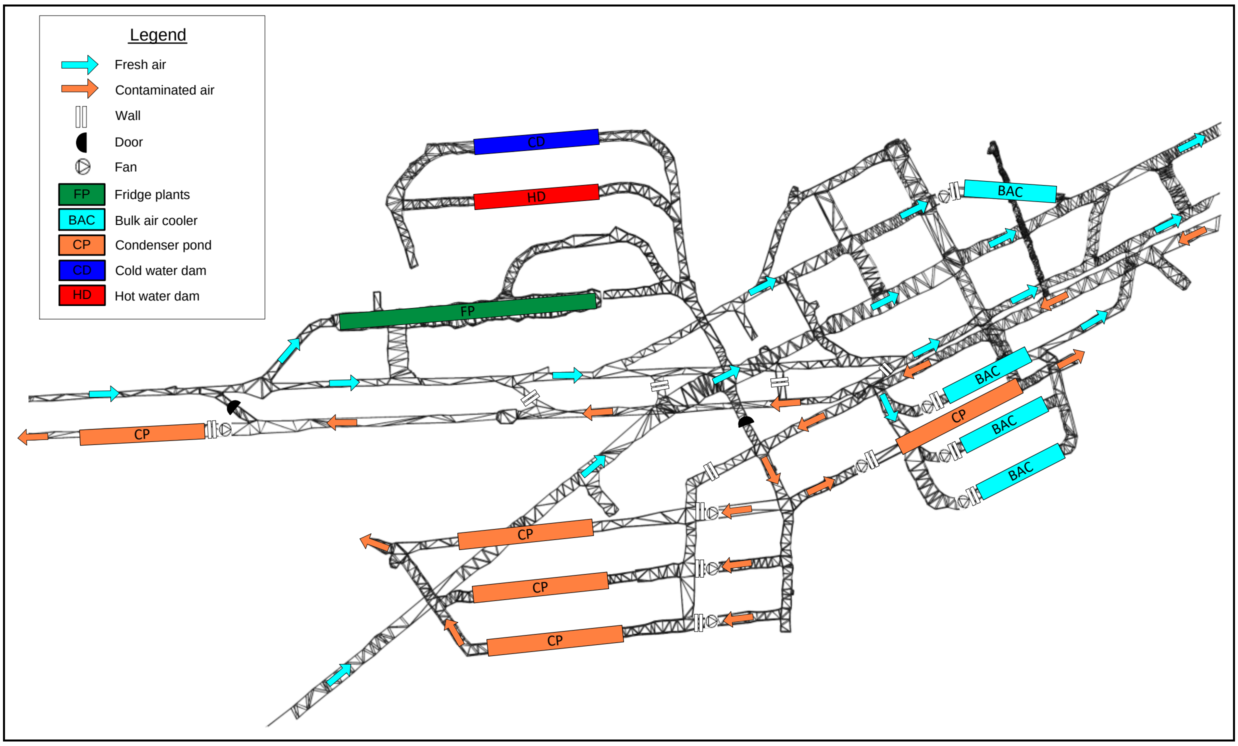


**Figure 3-29: Mine C cooling system schematic 255L***

### 3.4.3 Data collection

#### *i) Collecting the transient and steady-state data*

The data collection steps for this case study were similar to Case Study 2. This included the same level of detail and KPIs, except for the ice dam KPIs. The transient and steady-state data collection was similar as both mines had SCADA systems with similar infrastructure. Most data required to calibrate the cooling system was available, and the remaining environmental data had to be collected manually with handheld instruments. The KPIs and collected data are shown in Appendix P.

#### *ii) Determining heat load*

The heat load was also calculated in a steady state due to the limitation of PTB mentioned in Section 2.4. The heat from the fuel-driven machinery was the only additional heat source compared with Case Study 2. Table 3-15 summarises the total heat load from secondary sources at Mine C. The calculation of the heat from these sources is summarised in Appendix Q.

Table 3-15: Total heat load from secondary sources for Mine C

| Parameter | Unit | Value |
|---|---|---|
| Effective electrical heat load | [kW] | 4 357 |
| Effective mechanised heat load | [kW] | 5 104 |
| Metabolic heat load | [kW] | 303 |
| Explosive heat load | [kW] | 105 |
| Fissure water heat load | [kW] | 0 |
| Chilled water pipes cooling duty | [kW] | −1 883 |
| **Total heat load from secondary sources** | **[kW]** | **7 987** |

### 3.4.4 Building of the model

#### *i) Building the model*

The digital mining layouts seen in Figure 3-28 were imported into PTB, and the drag-and-drop function was used to add the components to the layouts. Figure 3-30 illustrates the final 3D PTB ventilation model. This model had over 6 550 individual simulation components.

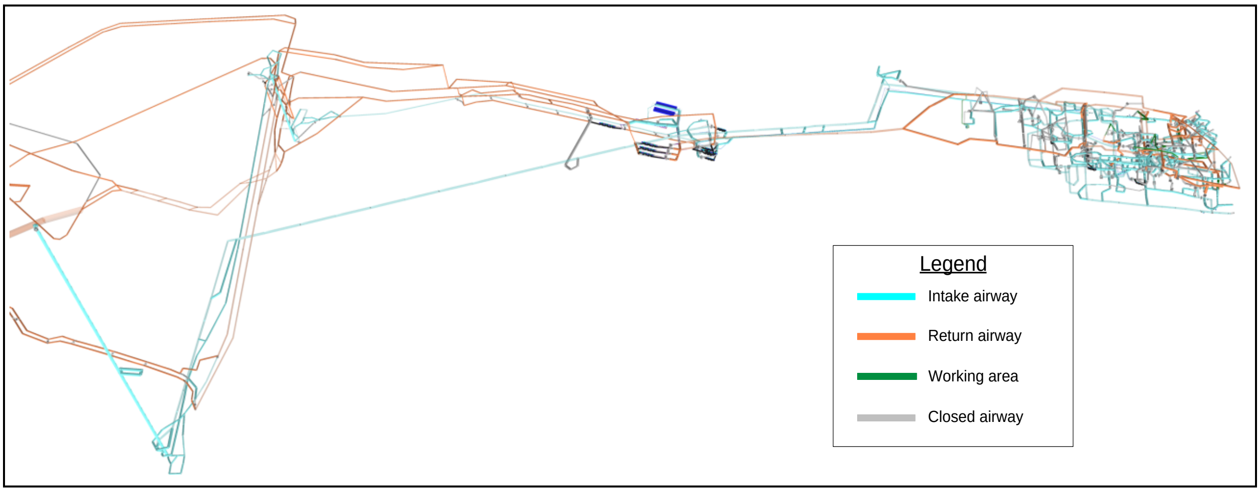


**Figure 3-30: PTB ventilation simulation of Mine C***

Figure 3-31 illustrates the cooling system simulation integrated into the ventilation simulation of Mine C.

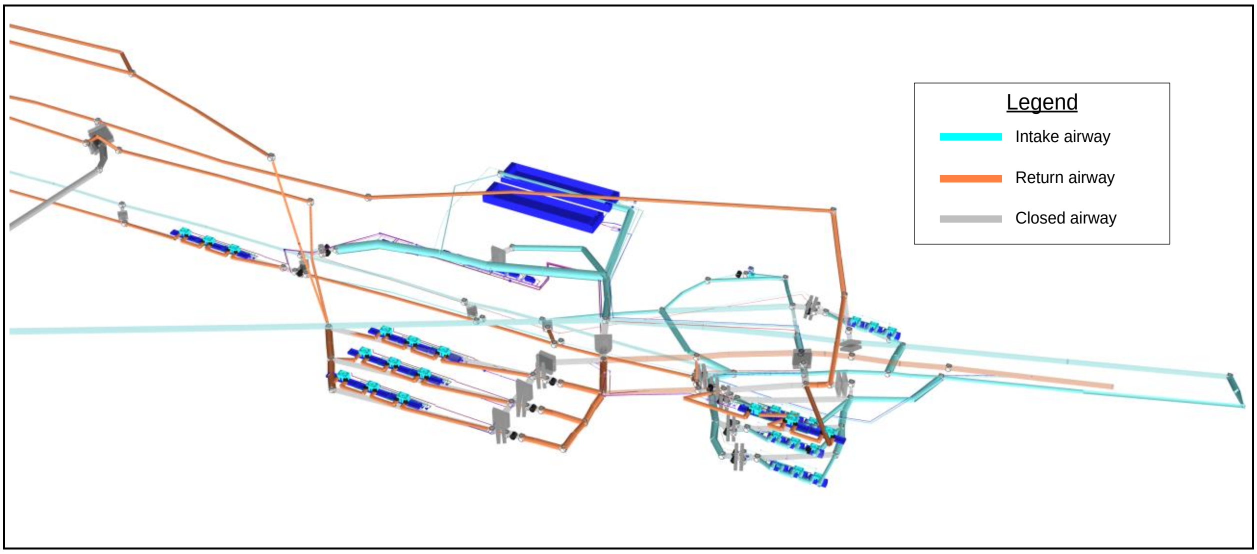


**Figure 3-31: PTB integrated cooling simulation of Mine C***

#### *ii) Defining the system with standard data*

The standard parameters from Section 2.4 were used to define the components, much like the first two case studies.

### 3.4.5 Calibration

The simulation for Mine C had the same components as Mine A and B, thus the calibration remained the same. The average ambient environmental conditions and cooling system operation for the priming period are shown in Table 3-16.

**Table 3-16: Average priming period parameters for Mine C**

| Priming parameters | Unit | Value |
|---|---|---|
| Average ambient DB temperature | [°C] | 24.9 |
| Average ambient relative humidity | [%] | 65.6 |
| Average ambient barometric pressure | [kPa] | 85.6 |
| Average cold dam temperature | [°C] | 14.0 |

These averages were used as inputs to the model, and the model was run until it reached a steady state. Thereafter, the model was iterated to determine the unknown parameters.

### 3.4.6 Verification

The underground environment of Mine C was dynamic due to the movement of large mechanised machines throughout the mine. The final simulation had an airflow accuracy of 87%, which fell within the error margin of the measurement technique, which was 5–23% [74], [86].

The cooling system on 255L was calibrated to represent the actual system accurately, with an average accuracy of 97.3% [38]. The main output of this system was the chilled water dam temperature that provided chilled water to the BACs and underground mining. The simulation accurately represented the cold water dam temperature with an MSE of 0.72, an $R^2$ of 0.17, and a maximum error of 1.54°C. Further details on the calibration accuracy of the fridge plants are included in Appendix R.

The simulation was calibrated for the working area intakes on the lower levels. Figure 3-32 illustrates the measured and simulated temperatures on a working area intake on 287L West. The operation of the mechanised machinery during the mining shifts resulted in increased temperatures between 9 to 16 hours and hours 20 to 24 hours. The summary of the simulation performance of this location and other locations is attached in Appendix S.

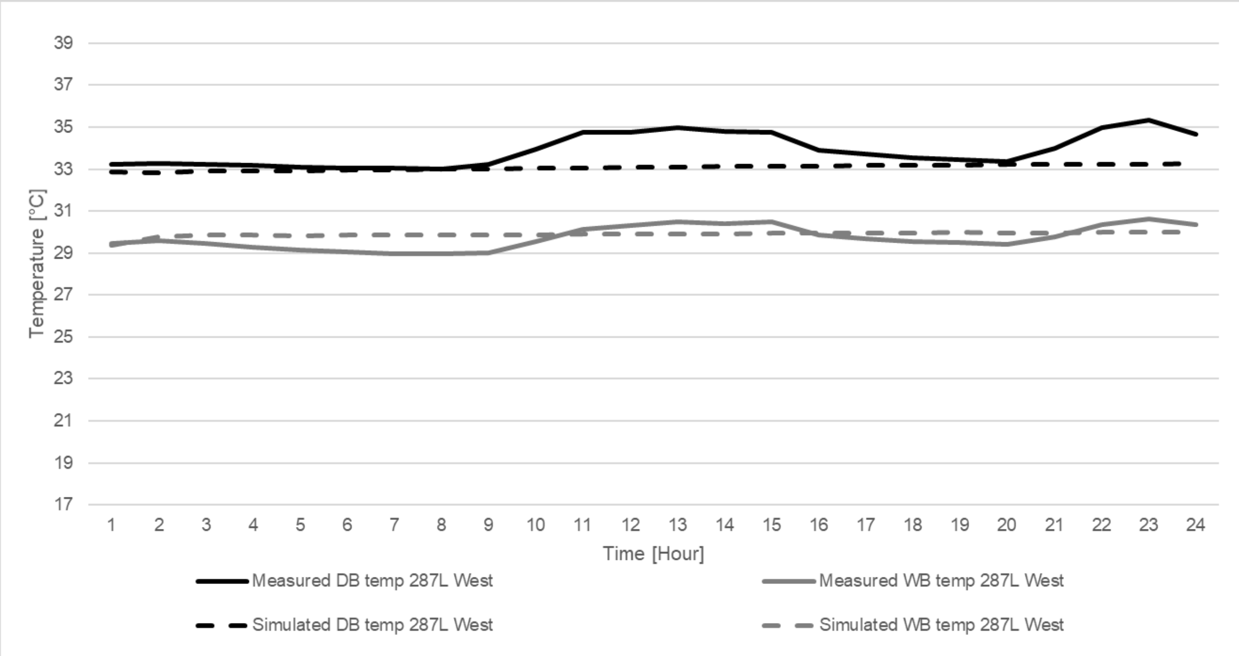


**Figure 3-32: Mine C transient temperature comparison (287L West)***

Table 3-17 summarises the simulation performance for all the points measured in the mining block. These results fell just above the acceptable level of accuracy as recommended by the literature [52].

**Table 3-17: Summary of Mine C simulation performance**

| Parameter | Unit | MSE | $R^2$ | Maximum error |
|---|---|---|---|---|
| Average DB (transient) | [°C] | 0.69 | 0.21 | 2.11 |
| Average WB (transient) | [°C] | 2.03 | 0.30 | 2.30 |

The results from this section showed that the simulation was able to provide environmental predictions with an acceptable levels of accuracy for most sections of the mine according to the KPIs selected. The simulation again had low $R^2$ values as a result of dynamic mining operation and unknown variables as discussed for Mine B in Section 3.3.6.

### 3.4.7 Comparison to steady-state simulation

The simulation was resimulated with quasi-steady-state analysis. Figure 3-33 compares the actual measurements, transient simulation and quasi-steady-state simulation temperatures on 287L West. None of the simulations could fully incorporate the temperature fluctuations due to the mechanised machinery. The summary of the simulation performance of this location and other locations is attached in Appendix S.

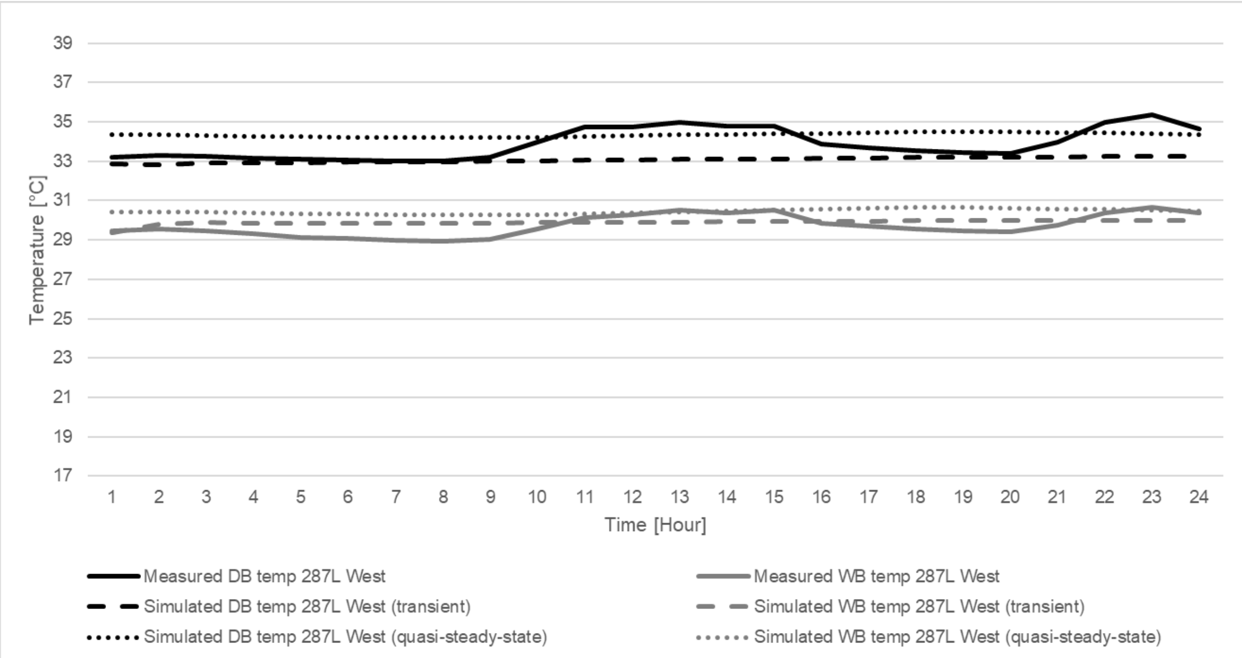


**Figure 3-33: Mine C transient and quasi-steady-state temperature comparison (287L West)***

Table 3-18 summarises the simulation performance for all the measurement locations at Mine C. In some cases, the quasi-steady-state simulation had better results than the true transient simulation. As seen in Case Study 2, there are minimum temperature variations at a depth of 2 300 m, thus the measured temperature variations resulted from mining operations.

**Table 3-18: Mine C comparison of transient and quasi-steady-state simulation performance (287L West)**

| Parameter | Unit | MSE | $R^2$ | Maximum error |
|---|---|---|---|---|
| Average DB (transient) | [°C] | 0.69 | 0.21 | 2.11 |
| Average DB (quasi-steady-state) | [°C] | 1.36 | 0.26 | 2.02 |
| Average WB (transient) | [°C] | 2.03 | 0.30 | 2.30 |
| Average WB (quasi-steady-state) | [°C] | 1.54 | 0.47 | 1.74 |

The steady-state internal heat input in PTB averaged the heat from secondary heat sources throughout the day. The simulation results showed this with the steady temperatures over the 24 hours. The larger maximum error for the true transient simulation could result from different environmental conditions experienced in the priming period.

Figure 3-34 illustrates the intake conditions for 287L West at Mine C during the last week of the priming period. The temperatures varied significantly due to the mechanised machinery, and temperature variations of up to 2.5°C per day resulted in dynamic heat transfer from the strata. These dynamic conditions led to incorrect priming of the model and reduced the accuracy of the true transient simulation.

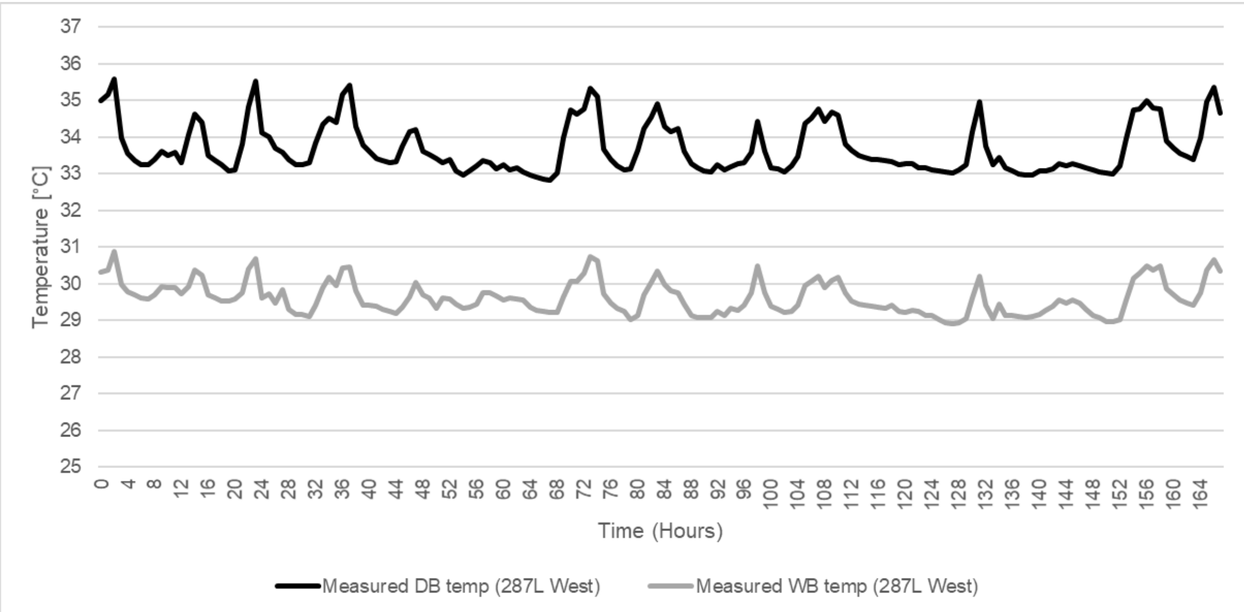


**Figure 3-34: Mine C underground temperatures (287L West)***

### 3.4.8 Discussion

This case study aimed at meeting the second and third objectives of this study. The results showed that the simulation could take the thermal history effect into account but that the accuracy was lower than the previous case studies.

Mine C used a different mining method that added more heat to the system from the secondary heat sources. The fluctuation in the heat from the mechanised machinery resulted in dynamic temperatures at the working area intakes, and the temperature fluctuations reduced the accuracy of the result. This resulted in true transient simulation performance comparable to the conventional simulation performance.

The steady-state secondary heat input of the PTB meant that the simulation could not simulate the temperature fluctuations in the mining shifts. Transient secondary heat input is therefore required in mines with significant and dynamic secondary heat sources such as fuel-driven machinery.

## 3.5 Conclusion

Chapter 1 showed the importance of mine ventilation and cooling simulations and how the state-of-the-art true transient simulations have improved the prediction of underground environmental conditions. A study of the critical literature led to the following objectives for this study:

- Development of a methodology for integrated true transient mine ventilation and cooling simulations,
- Application of a true transient ventilation simulation to an entire deep-level mine, and
- Integration of a transient cooling simulation with a true transient ventilation simulation on a deep-level mine.

Chapter 2 developed a novel method for true transient mine ventilation and cooling simulations to meet the first objective of this study. This chapter used this methodology to apply the true transient simulations to three case study mines. All the case study mines were located in Free State, South Africa, but had different infrastructure and mining techniques.

### 3.5.1 Case Study 1

This case study applied a true transient simulation to Mine A, which did not have a cooling system installed. This case study focused on the second objective of this study.

The results showed that the simulation could accurately predict the underground environment. Compared with conventional steady-state simulations, the true transient simulation was able to improve the prediction of underground temperatures. This validated that the methodology developed in Chapter 2 could be applied to a real-life application to produce accurate results.

A summary of the results from this case study was also published as an article. This publication showed that a true transient ventilation simulation accurately simulated the sensitivity that underground mines have to fluctuating ambient conditions [1]. The results from this case study validated the improved accuracy that true transient simulations can provide when applied to a mine ventilation system.

### 3.5.2 Case Study 2

This case study was similar to the first case study, with the major difference being the integration of cooling systems. This case study aimed to meet the second and third objectives of this case study.

The results showed that the simulation could take the thermal history effect into account and could determine the underground environmental conditions to an acceptable level of accuracy. Compared with conventional steady-state simulations, the true transient simulation was able to improve the prediction of underground temperatures. This validated the integration of transient cooling simulation with true transient ventilation simulation on deep-level mines.

### 3.5.3 Case Study 3

The third case study applied a true transient ventilation and cooling simulation to a fuel-driven mechanised underground mine. The focus was to compare the true transient simulation of mines with different mining methods. The results showed that the simulation could take the thermal history effect into account but that the accuracy was lower than for the previous case studies. The large fraction of heat contributing to the system from secondary heat sources meant that the limitations of PTB resulted in lower accuracy.

### 3.5.4 Case studies accuracy

These case studies compared the accuracy of true transient simulation to conventional steady-state simulations. Table 3-19 below compares temperature prediction accuracy and shows improvement over conventional simulations.

**Table 3-19: Case study temperature results accuracy comparison**

| Parameter | Unit | True transient simulation | Quasi-steady-state simulation | Simulation improvement |
|---|---|---|---|---|
| Case study 1 average DB temp MSE | [°C] | 0.38 | 3.03 | 2.65 |
| Case study 2 average DB temp MSE | [°C] | 0.67 | 6.46 | 5.79 |
| Case study 3 average DB temp MSE | [°C] | 0.69 | 1.36 | 0.67 |
| Case study 1 average DB temp Max error | [°C] | 1.53 | 3.34 | 1.81 |
| Case study 2 average DB temp Max error | [°C] | 1.70 | 3.96 | 2.26 |
| Case study 3 average DB temp Max error | [°C] | 1.35 | 1.50 | 0.15 |
| Case study 1 average WB temp MSE | [°C] | 0.09 | 1.15 | 1.06 |
| Case study 2 average WB temp MSE | [°C] | 1.09 | 2.63 | 1.54 |
| Case study 3 average WB temp MSE | [°C] | 2.03 | 1.54 | -0.49 |
| Case study 1 average WB temp Max error | [°C] | 0.79 | 1.95 | 1.16 |
| Case study 2 average WB temp Max error | [°C] | 1.78 | 3.21 | 1.42 |
| Case study 3 average WB temp Max error | [°C] | 1.83 | 1.55 | -0.28 |

# CHAPTER 4: CONCLUSION

## 4.1 Introduction

Ventilation and cooling systems are essential in the operations of underground mines. These systems provide the underground system with adequate environmental temperatures and airflows to ensure that mines comply with the regulations set out by mine ventilation council.

Mines are becoming deeper in South Africa, with an average depth of over 2 km already. Ensuring good environmental conditions is becoming increasingly difficult with the increasing depth and associated infrastructure requirements. The increasing cost of ventilating and cooling adds to the financial strain and uncertainties of the future of mining operations.

Underground mines have various heat sources, and adequate cooling must be supplied to mitigate the heat and provide an environment conducive to work. Fluctuating ambient temperatures, heat sources and underground operations lead to a system that is seldomly in a steady state.

Simulations have proved vital to the planning and optimisation of mine ventilation and cooling systems. The underground rock provides cyclic time-based heat dampening in mines, resulting in complex heat transfer, known as the thermal history effect. State-of-the-art simulations have shown the benefit of incorporating the thermal history effect when simulating underground environmental conditions.

An in-depth review of the literature in Section 1.4 showed that a true transient simulation improves the environmental predictions of mine ventilation simulations. The gaps in literature from this section formed the foundations of the need and objectives of this study. The novel contributions of this study, as discussed in Section 1.6, were:

- Development of a methodology for integrated true transient mine ventilation and cooling simulations,
- Application of a true transient ventilation simulation to an entire deep-level mine, and
- Integration of a transient cooling simulation with a true transient ventilation simulation on a deep-level mine.

Chapter 2 met the first outcome of the study by developing a methodology that incorporated the thermal history effect found in underground mines. The new true transient methodology process was shown in Figure 2-9. This methodology was genuinely novel as the state-of-the-art studies in Section 1.4 did not provide a method for building and calibrating a true transient simulation.

Chapter 3 used the new methodology to apply a true transient simulation to three real-life underground mines. The case studies were on entire mines with different infrastructure and mining methods. The case studies aimed to meet this study's second and third objectives while validating the methodology developed in Chapter 2.

This chapter aims to conclude this study by reviewing the novel contributions that were set out in Chapter 1. The study's limitations will also be discussed, and recommendations for further work will be made.

## 4.2 Key findings of the research

The following sections will discuss the key findings from developing a new methodology in Chapter 2 and the key results from applying this methodology to case study mines in Chapter 3.

### 4.2.1 Methodology

Chapter 2 reviewed the literature on steady-state and transient mine ventilation and cooling simulation methodologies. The four main tasks of conventional simulation methodologies are data collection, model building, calibration and verification. These tasks were adapted to account for the thermal history effect.

The conventional methodology flow sheet is shown in Figure 2-1, and the adapted true transient flow sheet is shown in Figure 2-9. Comparing these flow sheets shows that most tasks required an adaptation to account for the thermal history effect.

The main changes in the data collection task show that transient data is vital to the calibration of true transient simulations. This is especially true for underground temperature data, which is required to determine if the simulation accurately predicts the thermal history effect. Further changes included heat load calculations and collections of steady-state data when necessary.

The model building task remained relatively unchanged as this step depends on the simulation software that is used. The main change in the calibration of these simulations was the priming of the simulated rock model by simulating the historical temperatures that the mine experienced before the calibration period. This ensures that the simulated heat transfer from the rock accurately represents the actual heat transfer.

The verification task was adapted to account for the fact that simulated values are compared to large sets of transient measured data instead of a single steady state comparison in conventional methods.

### 4.2.2 Case Study 1

This case study applied true transient simulation to a mine ventilation system without a cooling system. The key results showed that the true transient simulation had improved accuracy over conventional steady-state simulations. This validated the use of a true transient simulation on mine ventilation systems.

### 4.2.3 Case Study 2

This case study applied true transient simulation to a mine ventilation system with a cooling system. The key results showed that the simulation could incorporate the thermal history effect when integrating a transient cooling simulation. The results also showed that the true transient simulation was more accurate than conventional steady-state simulations but that the accuracy of the simulation decreased with larger and more dynamic mine ventilation and cooling systems.

### 4.2.4 Case Study 3

This case study was similar to the second case study but was applied to a mine with a different mining technique, namely block caving with fuel-driven mechanised machinery. The key results showed that the true transient simulation could not accurately predict the temperature fluctuations caused by the machinery. The simulation accuracy was comparable to conventional steady-state simulation in this case study.

## 4.3 Research contributions

Chapter 1 revealed shortcomings in the literature on a true transient simulation of mine ventilation and cooling systems. These shortcomings formed the foundation of the need and the novel contributions of this study. The following sections discuss each novel contribution and the objectives met in this study.

### 4.3.1 Development of a methodology for integrated true transient mine ventilation and cooling simulations

Chapter 2 reviewed and adapted conventional simulation methodologies for integrated true transient mine ventilation and cooling simulations. The true transient simulation methodologies needed to incorporate true transient simulation and be practically applicable.

This methodology is genuinely novel as the studies in Section 1.4 did not provide a method for building and calibrating a true transient simulation. The true transient methodology was applied to three case studies with different infrastructure and mining methods.

The first case study showed that the true transient simulation improved the prediction of underground temperatures by incorporating thermal damping and the phase shift associated with the thermal history effect. The second and third case studies showed similar results when integrating the transient cooling simulations. The true transient simulations incorporated the thermal history effect and had better results than conventional steady-state simulations.

These case study simulations were calibrated accurately according to the transient data collection and priming methods described in the new methodology. This calibration would not have been possible using the conventional mine ventilation and cooling simulation methodologies described in Section 2.2.

The case study results demonstrated the advantages of using a true transient simulation and validated the new true transient simulation methodology when applied to mine ventilation and cooling systems.

### 4.3.2 Application of a true transient ventilation simulation to an entire deep-level mine

The true transient ventilation simulations of South African gold mines were built using the methodology developed in Chapter 2. Chapter 3 demonstrated that the simulations could predict the underground environments accurately. These results further showed that the true transient simulation was more accurate than conventional steady-state simulations, which validated the true transient simulation of real-life applications.

The first case study focused on applying the true transient simulation to an entire mine ventilation system and was applied to a mine that did not have a cooling system installed. The results from this case study showed that the true transient simulation improved the maximum error of the working area intake temperature predictions by up to 1.8°C when compared with conventional simulations.

### 4.3.3 Integration of a transient cooling simulation with a true transient ventilation simulation on a deep-level mine

In Chapter 3, transient cooling systems simulations were integrated successfully with a true transient mine ventilation simulation. The cooling simulation accurately represented the actual systems, and the results showed that the integrated true transient simulation was more accurate than conventional integrated simulations. These results validated the use of integrated true transient mine ventilation and cooling systems.

The second case study focused on integrating a transient cooling simulation into a true transient ventilation simulation. The case study mine had a similar mining method as the first case study but had two cooling systems installed to mitigate the heat produced in the mine. This case study showed that the true transient simulation improved the maximum error of the working area intake temperature predictions by an average of 0.54°C when compared with conventional simulations.

The third case study applied an integrated transient cooling simulation into a true transient ventilation simulation on a mine that used a mechanised block-caving mining method. The simulation incorporated the thermal history effect and showed the simulation software's limitations.

## 4.4 Research limitations

### 4.4.1 Steady-state inputs of PTB

A limitation of the simulation software used in this study (PTB) was that it only had steady-state input of secondary heat load and wetness fractions. The third case study showed that the simulation could not accurately predict the fluctuations in temperature caused by the dynamic secondary heat sources. This can be seen in Figure 3-32, where the simulation showed fairly steady-state temperatures while the actual measured temperatures had fluctuations during the mining shifts.

### 4.4.2 VRT gradients

A limitation of this study was that it was only applied to deep-level gold mines in the Free State, South Africa, mining predominantly quartzite. The VRT gradient is different for regions with different rock types. Geothermal heat can significantly impact the underground environment.

#### 4.4.3 Chilled water pipe losses

The simulation software used in this study (PTB) could not integrate chilled water pipes into the air tunnel components. Having an integrated water pipe and air tunnel model could simplify the calibration process and allow for detailed studies on the dynamic cooling transferred between the two.

### 4.5 Recommendations for further research

#### 4.5.1 Steady-state inputs of PTB

There is a need for a true transient ventilation and cooling simulation with transient secondary heat load and wetness fraction. This will allow the transient simulation to fully incorporate the temperature fluctuations experienced from significant changes in secondary heat sources and wetness. The incorporation of these transient inputs will further improve the priming of the model during calibration, leading to improved environmental predictions.

#### 4.5.2 VRT gradients

Future work should apply a true transient ventilation simulation to other regions to determine whether it can be used across other regions and rock types. This would also give insight into the impact of geothermal heat on the thermal history effect.

#### 4.5.3 Chilled water pipe losses

Future work should develop software to integrate the chilled water and ventilation simulation for more accurate cold water pipe loss calculations. This would decrease the required calibration time and simplify optimisation and planning simulations.

#### 4.5.4 Priming period length

The amount of data required to prime the models for true transient simulation in this study was determined by trial-and-error. The length of the priming period was increased until the model had the correct conditions according at the start of the priming period. Further research is required to create a guideline for determining priming period length, and this would reduce the amount of time required to calibrate the model.

### 4.6 Final conclusion

Literature showed that true transient simulations have significantly more benefits than conventional steady-state simulations on mine ventilation and cooling systems. A literature study determined that there were a few gaps in the literature and that there was a need for:

- Development of a methodology for integrated true transient mine ventilation and cooling simulations,
- Application of a true transient ventilation simulation to an entire deep-level mine, and
- Integration of a transient cooling simulation with a true transient ventilation simulation on a deep-level mine.

This study developed a methodology for a true transient simulation of integrated deep-level mine ventilation and cooling systems. This method was applied to three case study mines with different infrastructure and mining methods. The results showed that the true transient simulation predicted the underground working area intake temperatures accurately. Comparisons with a conventional steady-state simulation showed that a true transient simulation improved the accuracy of environmental predictions used for optimisation and planning of deep-level mines. These results validated the true transient methodology and simulation of real-life mine ventilation and cooling systems.

## REFERENCE LIST

[1] R. Fair, J. H. van Laar, K. Nell, D. Nell, and E. H. Mathews, "Simulating the sensitivity of underground ventilation networks to fluctuating ambient conditions," *S. Afr. J. Ind. Eng.*, vol. 32, no. 3, pp. 42–51, 2021.

[2] K. A. Scalise, M. B. Teixeira, and K. C. Kocsis, "Managing heat in underground mines: The importance of incorporating the thermal flywheel effect into climatic modeling," *Mining, Metall. Explor.*, vol. 38, no. 1, pp. 575–579, 2020, doi: 10.1007/s42461-020-00323-5.

[3] J. Janus and J. Krawczyk, "Measurement and simulation of flow in a section of a mine gallery," *Energies*, vol. 14, no. 16, p. 4894, 2021, doi: 10.3390/en14164894.

[4] C. Lu, "Analysis of the effects of thermal history of the strata upon temperature variations in underground airways," PhD dissertation, University of Nevada, Reno, NV, 2019.

[5] K. Carpenter, P. Roghanchi, and K. C. Kocsis, "Investigating the importance of climatic monitoring and modeling in deep and hot US underground mines," in *Proc. 15th N. Am. Mine Vent. Symp*, 2015, pp. 1–4.

[6] G. L. Danko, W. K. Asante, D. Bahrami, and C. Stewart, "Dynamic models in atmospheric monitoring signal evaluation for safety, health and cost benefits," *Mining, Metall. Explor.*, vol. 36, no. 6, pp. 1235–1252, 2019, doi: 10.1007/s42461-019-0099-x.

[7] K. C. Kocsis, R. Hall, and S. G. Hardcastle, "The integration of mine simulation and ventilation simulation to develop a 'life-cycle' mine ventilation system," *J. South. Afr. Inst. Min. Met.*, pp. 223–230, 2003.

[8] K. C. Kocsis, S. G. Hardcastle, and R. Hall, "The benefit of using mine process simulators to design a 'life-cycle' mine ventilation system," *2004 SME Annu. Meet. Prepr.*, no. January 2004, pp. 381–387, 2004.

[9] P. Goosen, "The development and implementation of an energy management information system for industries," PhD thesis, North-West University, Potchefstroom, 2020.

[10] Mine Health and Safety Council, *Mine Health and Safety Act 29 of 1996 and Regulations*, no. 29. South Africa, 2018, pp. 199–203.

[11] D. Nell, "Practical determination of heat loads for existing deep level gold mines," PhD

thesis, North-West University, Potchefstroom, 2020.

[12] M. Bascompta, J. M. Rossell, L. Sanmiquel, and H. Anticoi, “Temperature prediction model in the main ventilation system of an underground mine,” *Appl. Sci.*, vol. 10, no. 20, pp. 1–11, 2020, doi: 10.3390/app10207238.

[13] R. Anderson and E. De Souza, “Heat stress management in underground mines,” *Int. J. Min. Sci. Technol.*, vol. 27, no. 4, pp. 651–655, 2017, doi: 10.1016/j.ijmst.2017.05.020.

[14] B. Samatemba, L. Zhang, and B. Besa, “Evaluating and optimizing the effectiveness of mining equipment: The case of Chibuluma South underground mine,” *J. Clean. Prod.*, vol. 252, p. 119697, 2020, doi: 10.1016/j.jclepro.2019.119697.

[15] E. Smoorenburg, O. Ogunomedede, S. Nichols, A. Newman, and G. Bogin Jr., “Incorporating ventilation and heat in an underground mine production scheduling model,” *Mine Vent.*, pp. 349–356, 2021, doi: 10.1201/9781003188476-36.

[16] A. F. Kuyuk, S. A. Ghoreishi-Madiseh, and A. P. Sasmito, “Design of mine bulk air cooling systems: Numerical, empirical and experimental validation,” in *Proc. 18th N. Am. Mine Vent. Symp.*, 2021, pp. 168–176.

[17] P. G. Ranjith, J. Zhao, M. Ju, R. V. S. De Silva, T. D. Rathnaweera, and A. K. M. S. Bandara, “Opportunities and challenges in deep mining: A brief review,” *Eng.*, vol. 3, no. 4, pp. 546–551, 2017, doi: 10.1016/J.ENG.2017.04.024.

[18] G. Danko, D. Bahrami, and C. Stewart, “Applications and verification of a computational energy dynamics model for mine climate simulations,” *Int. J. Min. Sci. Technol.*, vol. 30, no. 4, pp. 483–493, 2020, doi: 10.1016/j.ijmst.2020.03.019.

[19] P. N. Neingo and T. Tholana, “Trends in productivity in the South African gold mining industry,” *J. South. Afr. Inst. Min. Met.*, vol. 116, no. 3, pp. 283–290, 2016, doi: 10.17159/2411-9717/2016/v116n3a10.

[20] Eskom Holdings SOC LTD, “Eskom interim financial report,” 2020. [Online]. Available: https://www.eskom.co.za/IR2020/Interim/Pages/default.aspx.

[21] P. Maré, “Novel simulations for energy management of mine cooling systems,” PhD thesis, North-West University, Potchefstroom, 2017.

[22] J. J. L. du Plessis, W. M. Marx, and C. Nell, “Efficient use of energy in the ventilation and cooling of mines,” *J. South. Afr. Inst. Min. Met.*, vol. 114, no. June, pp. 26–30, 2014.

[23] P. Goosen, M. J. Mathews, and J. C. Vosloo, “Automated electricity bill analysis in South Africa,” *S. Afr. J. Ind. Eng.*, vol. 28, no. 3 Special Edition, pp. 66–77, 2017, doi: 10.7166/28-3-1840.

[24] D. Nell, E. H. Mathews, and P. Maré, “Industry 4.0 roll-out strategy for dynamic mine heat load management,” *S. Afr. J. Ind. Eng.*, vol. 30, no. 3, pp. 106–114, 2019.

[25] G. J. Maasz and H. Darwish, “Towards an initiative-based industry 4.0 maturity improvement process: Master drilling as a case study,” *South African J. Ind. Eng.*, vol. 29, no. 3, pp. 92–107, 2018, doi: 10.7166/29-3-2052.

[26] T. Imgrund, A. Bischoff, and S. Spürk, “Comparison of mine ventilation software tools for underground coal in harsh conditions,” *Proc. 17th N. Am. Mine Vent. Symp.,* vol. 1985, p. 10, 2019.

[27] N. K. Dumakor-Dupey, S. Arya, D. Atambila, and M. Anselmi, “Numerical evaluation of a spot cooling technique for underground metal mines,” *Mine Vent.*, pp. 177–186, 2021, doi: 10.1201/9781003188476-18.

[28] E. Develo, M. Pillalamarry, and E. Garab, “Improving the ventilation system at Rosh Pinah zinc mine,” *J. South. Afr. Inst. Min. Met.*, vol. 116, no. 4, pp. 301–305, 2016, doi: 10.17159/2411-9717/2016/v116n4a1.

[29] N. Saeidi and C. Allen, “Underground hard-rock mine ventilation considerations for battery electric mobile equipment,” *Mine Vent.*, pp. 548–555, 2021, doi: 10.1201/9781003188476-56.

[30] C. Ding, X. He, and B. Nie, “Numerical simulation of airflow distribution in mine tunnels,” *Int. J. Min. Sci. Technol.*, vol. 27, no. 4, pp. 663–667, 2017, doi: 10.1016/j.ijmst.2017.05.017.

[31] M. J. McPherson, *Subsurface Ventilation and Environmental Engineering*, 2nd ed. Blacksburg, VA: Springer Science & Business Media, 1993.

[32] S. Bluhm and H. Smit, “Important basics of mine ventilation and cooling planning,” *Mine Vent. Soc. S. Afr. Ann. Conf.*, vol. 57, no. 1, pp. 15–24, 2004.

[33] J. C. Tien, “Chapter 9: Mine ventilation systems,” in *Practical Mine Ventilation Engineering*, no. 1, Fresno, CA: Intertec Pub., 1999, pp. 167–189.

[34] B. Ünver, “Analysis of a possible root cause and mechanism for Soma mine disaster,” *J. Min. Environ.*, vol. 10, no. 1, pp. 1–26, 2019, doi: 10.22044/jme.2018.7391.1594.

[35] J. J. L. du Plessis, *Ventilation and occupational environment engineering in mines*. Mine Ventilation Society of South Africa, 2014.

[36] A. Jha, Y. Pan, P. Tukkaraja, and S. J. Sridharan, “Scale model investigation of ventilation parameters in a block cave mine,” *Mine Vent.*, pp. 556–562, 2021, doi: 10.1201/9781003188476-57.

[37] M. J. McPherson, *Subsurface Ventilation Systems*. Blacksburg, VA: Springer, 1993.

[38] I. Mathews, J. H. van Laar, D. Arndt, J. C. Vosloo, and G. Seetal, “Integrated dynamic simulation method for deep-level mine cooling systems planning,” in *Proc. SAIIE32*, 2021, pp. 669–686.

[39] A. Greth, P. Roghanchi, and K. C. Kocsis, “A review of cooling system practices and their applicability to deep and hot underground US mines,” *Proc. 16th N. Am. Mine Vent. Symp.*, vol. 11, no. June, pp. 1–9, 2017.

[40] J. J. L. du Plessis, D. Hoffman, W. M. Marx, and R. van der Westhuizen, “Optimising ventilation and cooling systems for an operating mine using network simulation models,” in *Assoc. Mine Manag. S. Afr.*, 2013, pp. 1–16.

[41] S. Bluhm, R. G. Moreby, F. von Glehn, and C. Pascoe, “Life-of-mine ventilation and refrigeration planning for resolution copper mine,” *J. South. Afr. Inst. Min. Met.*, vol. 114, no. 6, pp. 497–503, 2014.

[42] M. C. Şuvar, C. Lupu, V. Arad, D. Cioclea, V. M. Păsculescu, and N. Mija, “Computerized simulation of mine ventilation networks for sustainable decision making process,” *Environ. Eng. Manag. J.*, vol. 13, no. 6, pp. 1445–1451, 2014.

[43] P. Roghanchi, K. C. Kocsis, G. Danko, and A. Powell, “Underground climatic monitoring and modeling: Are we missing something?,” *Qual. Access to Success*, vol. 18, no. S1, pp. 133–139, 2017.

[44] K. G. Wallace, "Comparison of air velocity measurement techniques," *Mine Vent.*, pp. 469–478, 2021, doi: 10.1201/9781003188476-48.

[45] L. Zhou, R. A. Thomas, L. Yuan, and D. Bahrami, "Improving calibration of a mine ventilation network using continuous airflow monitoring," *Mine Vent.*, pp. 518–528, 2021, doi: 10.1201/9781003188476-53.

[46] A. N. Sarvestani, "Mine ventilation circuits in an underground mine in Northern Italy," Politecnico di Torino, Torina TO, Italy, 2021.

[47] O. Haitham Kanam and M. Obaid Ahmed, "A review on underground mine ventilation system," *J. Mines, Met. Fuels*, vol. 69, no. 2, p. 62, 2021, doi: 10.18311/jmmf/2021/27334.

[48] J. Prinsloo, J. C. Vosloo, and E. H. Mathews, "Towards Industry 4.0: A roadmap for the South African heavy industry sector," *S. Afr. J. Ind. Eng.*, vol. 31, no. 3, pp. 174–186, 2019.

[49] P. Roghanchi, K. C. Kocsis, and A. Powell, "Evaluation of the atmospheric and underground environmental conditions by means of continuous climatic monitoring systems: Lessons learned," *Proc. 16th N. Am. Mine Vent. Symp.*, no. June, pp. 9–16, 2017.

[50] F. H. von Glehn and I. Ox, "Monitoring and control of underground ventilation systems using VUMA-network," in *Proc. 10th US/N. Am. Mine Vent. Symp.*, 2004, pp. 16–19.

[51] I. Mathews, E. H. Mathews, J. H. van Laar, W. Hamer, and M. Kleingeld, "A simulation-based prediction model for coal-fired power plant condenser maintenance," *Appl. Therm. Eng.*, vol. 174, pp. 1–10, 2020, doi: 10.1016/j.applthermaleng.2020.115294.

[52] P. Roghanchi and K. C. Kocsis, "Quantifying the thermal damping effect in underground vertical shafts using the nonlinear autoregressive with external input (NARX) algorithm," *Int. J. Min. Sci. Technol.*, vol. 29, no. 2, pp. 255–262, 2018, doi: 10.1016/j.ijmst.2018.06.002.

[53] E. de Souza, "Optimization of complex mine ventilation systems with computer network modelling," in *IFAC Proc.*, 2007, pp. 323–329, doi: 10.3182/20070821-3-CA-2919.00049.

[54] C. Stewart, S. M. Aminossadati, M. S. Kizil, and T. Andreatidis, "Diurnal thermal flywheel influence on ventilation temperatures in large underground mines," in *Proc. 16th N. Am. Mine Vent. Symp.*, 2017, pp. 9.1–9.8.

[55] C. M. Stewart, “Rapid dynamic ventilation modelling for improving health and safety in underground mining,” PhD thesis, University if Queensland, Brisbane, 2021.

[56] G. Danko, “Quality evaluation and error mitigation for mine climate models,” *Qual. Access to Success*, vol. 20, no. January, pp. 123–128, 2019.

[57] H. C. Hoover and L. H. Hoover, *De Re Metallica*. New York: Dover Publications, Inc., 1950.

[58] J. J. Atkinson, “On the theory of the ventilation of mines,” *North Engl. Inst. Min. Eng.*, p. 118, 1854.

[59] L. W. Laage, R. E. Greuer, and W. H. Pomroy, “MFIRE users manual,” Twin Cities Research Center, Minneapolis, MN, 1995.

[60] C. Stewart, S. Aminossadati, and M. Kizil, “Use of live sensor data in transient simulations of mine ventilation models,” *Min. Rep.*, vol. 153, no. 4, pp. 356–363, 2017.

[61] R. L. Grayson, M. Georgiana, J. M. Dean, L. Zhao, and T. J. Wang, “Computer and software use in the U.S. coal industry,” in *21st APCOM*, 1989, pp. 730–745.

[62] L. Zhou, A. C. Smith, and L. Yuan, “New improvements to MFIRE to enhance fire-modeling capabilities,” *Min. Eng.*, vol. 68, no. 6, pp. 45–50, 2016, doi: 10.19150/me.6628.

[63] M. S. Morar, S. M. Radu, D. Cioclea, and I. Gherghe, “Use of IT equipment and specialized programs for solving ventilation networks,” *Qual. Access to Success*, vol. 18, no. S1, pp. 121–126, 2017.

[64] G. L. Danko, D. Bahrami, W. K. Asante, R. Grymko, and P. Rostami, “Temperature variations in underground tunnels,” in *Proc. 14th US/N. Am. Mine Vent. Symp.*, 2012, pp. 365–373.

[65] G. L. Danko, “Subsurface flow and transport process model for time dependent mine ventilation simulations,” *Trans. Institutions Min. Metall. Sect. A Min. Technol.*, vol. 122, no. 3, pp. 134–144, 2013, doi: 10.1179/147490013X13639459465691.

[66] W. Bouwer, “Designing a dynamic thermal and energy system simulation scheme for cross industry applications,” PhD thesis, Potchefstroomse Universiteit vir Christelike Hoer Ondenwys, Potchefstroom, 2004.

[67] A. J. H. Nel, J. C. Vosloo, and M. J. Mathews, “Evaluating complex mine ventilation

operational changes through simulations," *J. Energy South. Afr.*, vol. 29, no. 3, pp. 22–32, 2018.

[68] S. J. Bluhm, W. M. Marx, F. H. von Glehn, and M. Biffi, "Vuma mine ventilation software," *J. Mine Vent. Soc. S. Afr.*, vol. 54, no. 3, 2001.

[69] K. Wallace, B. Prosser, and J. D. Stinnette, "The practice of mine ventilation engineering," *Int. J. Min. Sci. Technol.*, vol. 25, no. 2, pp. 165–169, 2015, doi: 10.1016/j.ijmst.2015.02.001.

[70] P. Roghanchi, "Managing and controlling the thermal environment in underground metal mines," PhD Dissertation, University of Nevada, Reno, NV, 2017.

[71] K. A. Scalise and K. C. Kocsis, "Utilizing nonlinear autoregressive with exogenous input neural networks to evaluate the thermal flywheel effect along intake shafts at Nevada mines," *Min. Metall. Explor.*, vol. 38, no. 3, pp. 1–16, 2021.

[72] W. Feng, F. Zhu, and H. Lv, "The use of 3D simulation system in mine ventilation management," *Procedia Eng.*, vol. 26, pp. 1370–1379, 2011, doi: 10.1016/j.proeng.2011.11.2313.

[73] R. H. Howell and H. J. Sauer, "Field measurement of air velocity. Pitot traverse or vane anemometer," *ASHRAE J.*, vol. 32, no. 3, 1990.

[74] I. D. Unwin, *The Measurement of Air Flow in British Coal Mines: A Historical Review*. Philippines: NONESCOST, 1998.

[75] M. D. Griffith and C. M. Stewart, "Ventilation model calibration from limited survey data," *Mine Vent.*, pp. 509–517, 2021, doi: 10.1201/9781003188476-52.

[76] S. Maleki, F. Sotoudeh, and F. Sereshki, "Application of VENTSIM 3D and mathematical programming to optimize underground mine ventilation network: A case study," *J. Min. Environ.*, vol. 9, no. 3, pp. 741–752, 2018, doi: 10.22044/jme.2018.6793.1503.

[77] E. Widzyk-Capehart and B. Watson, "Agnew gold mine expansion mine ventilation evaluation using VentSim," in *Proc. 7th Int. Mine Vent. Congr*, 2001, pp. 345–352.

[78] B. Belle and W. Marx, "Simulating airflow conditions in a South African coal mine, using the VUMA-Network simulation software," *Mine Vent.*, 2002, doi:

10.1201/9781439833742.ch36.

[79] Y. Shen and H. N. Wang, “Study and application on simulation and optimization system for the mine ventilation network,” *Procedia Eng.*, vol. 26, pp. 236–242, 2011, doi: 10.1016/j.proeng.2011.11.2163.

[80] W. Feng, F. Zhu, and H. Lv, “The use of 3D simulation system in mine ventilation management,” *Procedia Eng.*, vol. 26, pp. 1370–1379, 2011, doi: 10.1016/j.proeng.2011.11.2313.

[81] N. J. Smit, “Reducing electrical costs for a mine ventilation system with the aid of simulation software,” Masters Dissertation, North-West University, Potchefstroom, 2017.

[82] F. Michelin, C. M. Stewart, M. D. Griffith, and T. Andreatidis, “Calibrating model airway size and resistance with survey asbuilt data,” in *Aust. Mine Vent. Conf.*, 2019, pp. 363–368.

[83] C. A. Nixon, A. D. S. Gilliest, and M. J. Howes, “Analysis of heat sources in a large mechanized development,” in *Proc. 5th Int. Mine Vent. Cong.*, 1992, pp. 109–117.

[84] A. J. Schutte, “An integrated energy efficiency strategy for deep mine ventilation and refrigeration,” PhD thesis, North-West University, Potchefstroom, 2014.

[85] J. Swanepoel, “Quantifying the impact of water mismanagement on latent heat in deep-level mines,” Masters dissertation, North-West University, Potchefstroom, 2019.

[86] B. Belle, “Real-time air velocity monitoring in mines: A quintessential design parameter for managing major mine health and safety hazards,” in *13th Coal Operators’ Conf .*, 2013, pp. 184–198.

[87] X. Chang, “The transient-state simulation of mine ventilation systems,” PhD dissertation, Mischigan Technological University, Houghton, MI, 1987.

[88] R. E. Greuer, “Computer models of underground mine ventilation and fires,” in *US Bureau of Mines Information Circular*, 1988, pp. 6–14.

[89] T. R. Roy and B. Singh, “Computer simulation of transient climatic conditions in underground airways,” *Min. Sci. Technol.*, vol. 13, no. 3, pp. 395–402, 1991.

[90] T. R. Roy, “A simplified computational approach for prediction of transient climatic conditions in underground mine airways,” *Geotech. Geol. Eng.*, vol. 11, no. 1, pp. 15–23,

1993.

[91] E. J. Jacques, “Transient flows in ventilation networks,” in *7th US Mine Vent. Symp.*, 1995, p. 525.

[92] W. Dziurzynski, S. T. Nawrat, J. Roszkowski, and W. Trutwin, “Computer simulation of mine ventilation disturbed by fires and the use of fire extinguishers,” *Proc. 6th Int. Mine Vent. Congr.*, 1997, doi: 10.1007/978-981-13-1420-9.

[93] A. D. S. Gillies, H. Wu, D. Reece, and R. Hosking, “Use of mine fire simulation for emergency preparedness,” in *Proc. Queensland Mining Ind. Health. Saf. Conf.*, 2004, pp. 1–23.

[94] M. Biffi, D. Stanton, H. Rose, and D. Pienaar, “Ventilation strategies to meet future needs of the South African platinum industry,” *J. South. Afr. Inst. Min. Met.*, vol. 107, no. 1, pp. 59–66, 2007.

[95] G. Danko, D. Bahrami, and P. Mousset-Jones, “Ventilation and climate simulation with the Multiflux code,” *J. Coal Sci. Eng.*, vol. 17, no. 3, pp. 243–250, 2011, doi: 10.1007/s12404-011-0304-0.

[96] W. Kai, Z. Aitao, and L. Shan, “Computer simulation of dynamic influence of outburst gas flow on mine ventilation network,” *Disaster Adv.*, vol. 6, no. 9, pp. 69–76, 2013.

[97] D. Brake, “Fire modelling in underground mines using Ventsim Visual VentFIRE software,” *Aust. Mine Vent. Conf.*, no. July, pp. 1–3, 2013.

[98] C. M. Stewart, S. M. Aminossadati, and M. S. Kizil, “Predictive network modelling with live sensor data,” *2nd Int. Conf. Fibre-Optic Photonic Sensors Ind. Saf. Appl.*, pp. 63–69, 2017, doi: 10.1109/OFSIS.2017.16.

[99] M. D. Griffith and C. M. Stewart, “Sensitivity analysis of ventilation models: Where not to trust your simulation,” in *Proc. 17th N. Am. Mine Vent. Symp.*, 2019, p. 1.

[100] C. M. Stewart, S. M. Aminossadati, and M. S. Kizil, “Improving the performance of the Hardy Cross algorithm for large ventilation models,” *Proc. 17th N. Am. Mine Vent. Symp.*, p. 9, 2019.

[101] M. D. Griffith and C. M. Stewart, “Predicting annual underground thermal flywheel effects,”

in *Aust. Mine Vent. Conf.*, 2019, pp. 284–291.

[102] S. Zhu *et al.*, “Using seasonal temperature difference in underground surrounding rocks to cooling ventilation airflow: A conceptual model and simulation study,” *Energy Sci. Eng.*, vol. 8, no. 10, pp. 3457–3475, 2020, doi: 10.1002/ese3.619.

[103] C. M. Stewart, *Challenges and Solutions in the Development of the VentFIRE Mine Network Fire Simulator*. Brisbane: CRC Press, 2021.

[104] J. E. Fox and K. C. Kocsis, “Development of energy efficient and sustainable cooling strategies for hot underground mines,” *Mine Vent.*, pp. 153–167, 2021, doi: 10.1201/9781003188476-16.

[105] D. Nell, E. H. Mathews, and P. Maré, “Industry 4.0 roll-out strategy for dynamic mine heat load management,” *S. Afr. J. Ind. Eng.*, vol. 30, no. 3, pp. 106–114, 2019, doi: 10.7166/30-3-2232.

[106] I. J. Duckworth, “A heat balance study for a mechanized cut-and-fill stope,” Masters thesis, University of Nevada, Reno, NV, 1993.

# APPENDIX A: TRANSIENT VENTILATION SIMULATION

Table A-1 summarises all the literature in Figure 1-6.

**Table A-1: Summary of literature on transient mine ventilation simulation**

| Number | Name | Year | Reference | Description |
|---|---|---|---|---|
| 1 | The transient-state simulation of mine ventilation systems | 1987 | [87] | This dissertation was the first to explore the digital simulation of a non-steady-state mine ventilation under thermal disturbances. |
| 2 | Computer models of underground mine ventilation and fires | 1988 | [88] | This study describes the principal features of steady-state and transient simulations developed by the Bureau of Mines. |
| 3 | Computer simulation of transient climatic conditions in underground airways | 1991 | [89] | This study describes the development of CLIMA, a time-dependent mine temperature prediction computer program. |
| 4 | A simplified computational approach for prediction of transient climatic conditions in underground mine airways | 1993 | [90] | This study developed a simplified approach for predicting transient climatic conditions using a pseudo-based-temperature approach. |
| 5 | MFIRE users manual | 1995 | [59] | User manual for the MFIRE mine fire and ventilation simulator. |
| 6 | Transient flows in ventilation networks | 1995 | [91] | This paper aimed to present a model that simulates one-dimensional compressible flows in unsteady-state conditions, specifically for systems with multiple fans. |
| 7 | Computer simulation of mine ventilation disturbed by fires and the use of fire extinguishers | 1997 | [92] | This paper gives an account of the principles on which VentGraph has been based to solve non-steady mine ventilation processes. |
| 8 | VUMA mine ventilation software | 2001 | [68] | This paper describes the development of VUMA mine ventilation simulation software. |
| 9 | The integration of mine simulation and ventilation simulation to develop a 'life-cycle' mine ventilation system | 2003 | [7] | This study describes the integration of discrete-event simulation and mine planning with mine dynamic ventilation planning. |
| 10 | Use of mine fire simulation for emergency preparedness | 2004 | [93] | This study used the transient mine ventilation simulation software, VentGraph, to model various mitigation strategies. |
| 11 | Monitoring and control of underground ventilation systems using VUMA-network | 2004 | [50] | This study linked the VUMA mine ventilation network simulation to climatic monitoring systems to verify predictions and examine areas without instrumentation. |
| 12 | Ventilation strategies to meet future needs of the South African platinum industry | 2007 | [94] | This paper provides an overview of the future of ventilation systems and real-life simulations in both steady and transient states. |
| 13 | The use of 3D simulation system in mine ventilation management | 2011 | [72] | This study used a 3D dynamic mine ventilation simulation to optimise the Donghai mine ventilation system to save on expenses. |

| Number | Name | Year | Reference | Description |
|---|---|---|---|---|
| 14 | Ventilation and climate simulation with the Multiflux code | 2011 | [95] | This study used the Multiflux mine ventilation software to simulate development-end models to show the flexibility of the software. |
| 15 | Temperature variations in underground tunnels | 2012 | [64] | This study analysed time history in transient mine ventilation simulation and applied it to a theoretical 3 km long underground tunnel. |
| 17 | Computer simulation of dynamic influence of outburst gas flow on mine ventilation network | 2013 | [96] | This study simulated the dynamic outburst of gas on a mine ventilation networking simulation to determine the optimal ventilation technique. |
| 18 | Fire modelling in underground mines using Ventsim Visual VentFIRE software | 2013 | [97] | This paper describes the dynamic modelling of underground fire scenarios and the application thereof. |
| 19 | Subsurface flow and transport process model for time dependent mine ventilation simulations | 2013 | [65] | This paper discusses the use of Multiflux to solve time-dependent heat transport of heat, humidity and gas. |
| 20 | Investigating the importance of climatic monitoring and modeling in deep and hot US underground mines | 2015 | [5] | This paper discusses the best practices of underground mine environmental modelling and dynamic modelling of various cooling strategies. |
| 21 | New improvements to MFIRE to enhance fire modelling capabilities | 2016 | [62] | This paper reports on improvements made to MFIRE mine ventilation software used for the dynamic simulation of ventilation networks and fires. |
| 22 | Underground climatic monitoring and modelling: Are we missing something? | 2017 | [43] | This paper discusses the importance of underground climatic modelling and how this can be used to develop a dynamic ventilation model. |
| 23 | Managing and controlling the thermal environment in underground metal mines | 2017 | [70] | This dissertation discusses the best practices of climatic monitoring and artificial neural networks to incorporate the thermal damping effect in dynamic ventilation simulations. |
| 24 | Predictive network modelling with live sensor data | 2017 | [98] | This paper discusses using a predictive modelling tool to incorporate real-time actual and simulated data. |
| 25 | Diurnal thermal flywheel influence on ventilation temperatures in large underground mines | 2017 | [54] | This paper measured and simulated the influence of diurnal temperature variations on an underground mine. |
| 26 | Reducing electrical costs for a mine ventilation system with the aid of simulation software | 2017 | [81] | This dissertation investigated the use of VUMA3D-Transient to simulate different scenarios. |
| 27 | Use of IT equipment and specialised programs for solving ventilation networks | 2017 | [63] | This paper provides an overview of mine ventilation simulation software and its specifications when it was published. |
| 28 | Use of live sensor data in transient simulations of mine ventilation models | 2017 | [60] | This study demonstrates a transient simulation computer model technique to predict the time-based changes to the atmosphere downstream from sensors. |
| 29 | Quantifying the thermal damping effect in underground | 2018 | [52] | This paper aimed to quantify the thermal damping effect using an algorithm and |

| Number | Name | Year | Reference | Description |
|---|---|---|---|---|
| | vertical shafts using the nonlinear autoregressive with external input (NARX) algorithm | | | quantify the damping coefficient of a mine ventilation system. |
| 30 | Sensitivity analysis of ventilation models – where not to trust your simulation | 2019 | [99] | The study used sensitivity analysis to explore examples of the variability of simulated airflow due to small resistance, heat and natural ventilation changes. |
| 31 | Improving the performance of the hardy cross algorithm for large ventilation models | 2019 | [100] | This paper investigated the improvement of traditionally used algorithms that solve quasi-steady-state ventilation models. |
| 32 | Dynamic models in atmospheric monitoring signal evaluation for safety, health and cost benefits | 2019 | [6] | This paper describes an early warning system that analyses real-time data to recognise dangerous trends. |
| 33 | Analysis of the effects of thermal history of the strata upon temperature variations in underground airways | 2019 | [4] | This dissertation reviews the commercial mine ventilation simulation software available at the time and advanced models with a thermal history effect. |
| 34 | Quality evaluation and error mitigation for mine climate models | 2019 | [56] | This study aimed to find the best way of using the simple thermal-humidity simulation models without the thermal history component for reduced simulation error in the thermal design of mine ventilation. |
| 35 | Predicting annual underground thermal flywheel effects | 2019 | [101] | This study simulated the seasonal temperature variations in a cold climate underground mine ventilation system. |
| 36 | Using seasonal temperature difference in underground surrounding rocks to cooling ventilation airflow: A conceptual model and simulation study | 2020 | [102] | This study proposes a mathematical model to simulate heat regulation and energy storage in underground mine tunnels. |
| 37 | Applications and verification of a computational energy dynamics model for mine climate simulations | 2020 | [18] | This study describes the computational energy dynamics model that is capable of simulating transient heat transfer in underground mines. |
| 38 | Managing heat in underground mines: The importance of incorporating the thermal flywheel effect into climatic modeling | 2020 | [2] | This paper analyses the WB and DB temperatures at the bottom of an intake shaft using different mine ventilation simulation software. |
| 39 | Utilizing nonlinear autoregressive with exogenous input neural networks to evaluate the thermal flywheel effect along intake shafts at Nevada mines | 2021 | [71] | This study used neural networks to determine the WB temperatures at the bottom of an intake shaft while considering the thermal flywheel effect. |
| 40 | Rapid dynamic ventilation modelling for improving health and safety in underground mining | 2021 | [55] | This dissertation developed a new method to improve the speed and effectiveness of dynamic ventilation modelling. |

| Number | Name | Year | Reference | Description |
|---|---|---|---|---|
| 41 | Challenges and solutions in the development of the VentFIRE mine network fire simulator | 2021 | [103] | This paper highlights the key outcomes in developing a new fire simulator VentFIRE that was integrated into Ventsim. |
| 42 | Development of energy efficient and sustainable cooling strategies for hot underground mines | 2021 | [104] | This paper investigated alternative cooling storage with propylene glycol as the coolth source. |

# APPENDIX B: CRITICAL LITERATURE CITATION HISTORY

Figure B-1 illustrates how the studies were cited to reach the current state-of-the-art practices. The arrows represent where the studies were cited in the following studies.

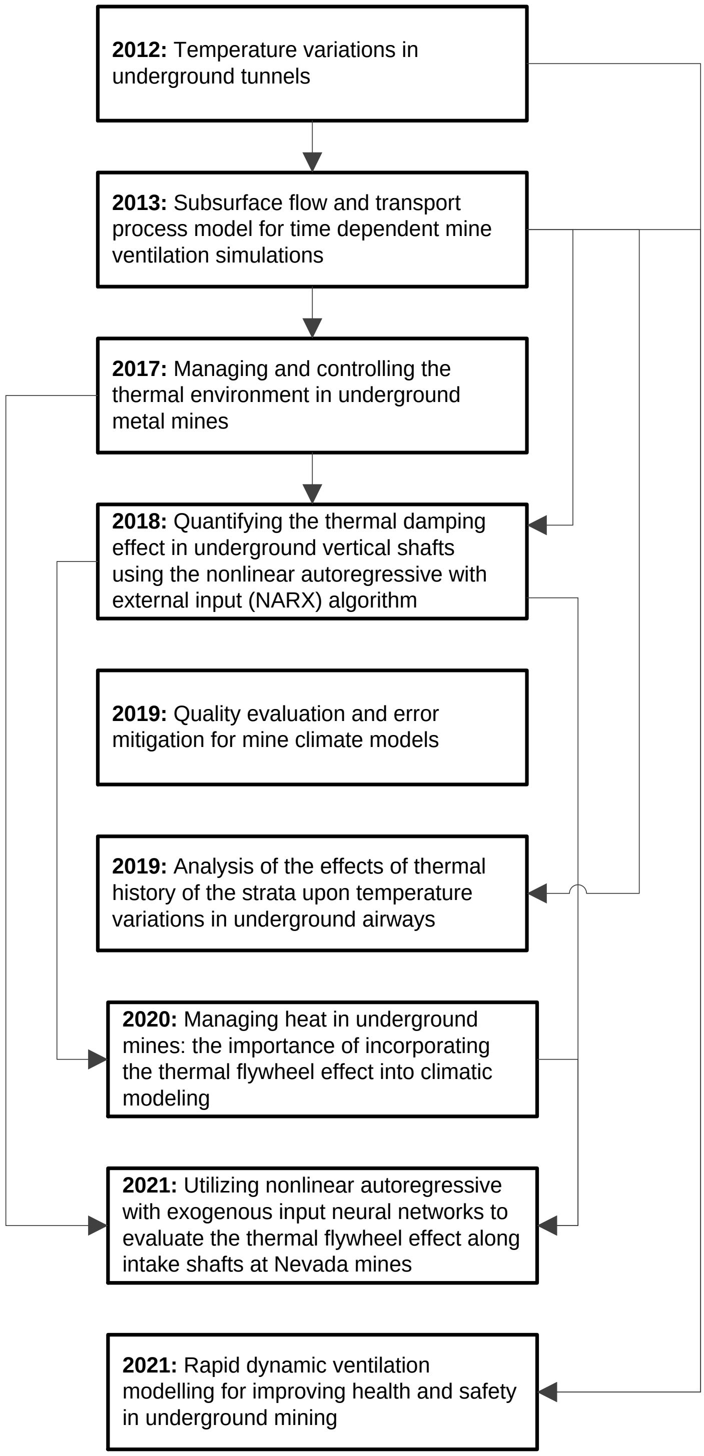


**Figure B-1: Citation history of the literature***

# APPENDIX C: SIMULATION METHODOLOGIES

Table C-1 summarises the literature used in the timeline in Table 2-2.

**Table C-1: Summary of literature on mine ventilation and cooling simulation methodologies**

| Number | Name | Year | Reference | Description |
|---|---|---|---|---|
| 1 | Agnew gold mine expansion mine ventilation evaluation using Ventsim | 2001 | [77] | This study optimised the ventilation system of Redeemer Gold Mine using Ventsim simulation software. |
| 2 | Simulating airflow conditions in a South African coal mine, using the VUMA-Network simulation software | 2002 | [78] | This paper describes VUMA simulation software and its application in "what-if" scenarios in a coal mine. |
| 3 | Monitoring and control of underground ventilation systems using VUMA-network | 2004 | [50] | This paper describes the linking of ventilation monitoring systems with ventilation simulations using VUMA-network. |
| 4 | Important basics of mine ventilation and cooling planning | 2004 | [32] | This paper reviews the important basics of mine ventilation and cooling planning. |
| 5 | Optimisation of complex mine ventilation systems with computer network modelling | 2007 | [53] | This study used computer network modelling for the optimisation of a ventilation network for the purpose of saving costs. |
| 6 | Study and application on simulation and optimisation system for the mine ventilation network | 2011 | [79] | This study developed an all-purpose ventilation simulation software using Visual Basic language. |
| 7 | The use of 3D simulation system in mine ventilation management | 2011 | [72] | This study applied Ventsim ventilation simulation software to Donghai mine to provide reliable data for decision-making. |
| 8 | Life-of-mine ventilation and refrigeration planning for resolution copper mine | 2014 | [41] | This study explains the life-of-mine ventilation planning for a copper mine, which includes ventilation and cooling simulations. |
| 9 | Computerised simulation of mine ventilation networks for sustainable decision making process | 2014 | [42] | This study used the simulation software 3D-Canvent to simulate different situations in a mine ventilation network. |
| 10 | Underground climatic monitoring and modeling: Are we missing something? | 2017 | [43] | This study discusses the importance of continuous climatic monitoring and how it is used to calibrate ventilation simulations. |
| 11 | Managing and controlling the thermal environment in underground metal mines | 2017 | [70] | This dissertation discusses the best practices of climatic monitoring and the use of artificial neural networks to incorporate the thermal damping effect in dynamic ventilation simulations. |
| 12 | Novel simulations for energy management of mine cooling systems | 2017 | [21] | This dissertation developed and applied a novel transient cooling simulation to case studies. |

| Number | Name | Year | Reference | Description |
|---|---|---|---|---|
| 13 | Reducing electrical costs for a mine ventilation system with the aid of simulation software | 2017 | [81] | This dissertation used transient mine ventilation software to predict changes in fan configurations. |
| 14 | Diurnal thermal flywheel influence on ventilation temperatures in large underground mines | 2017 | [54] | This study undertook to quantify and simulate the thermal flywheel behaviour of a mine ventilation system with simplified transient software. |
| 15 | Evaluating complex mine ventilation operational changes through simulations | 2018 | [67] | A scalable method was developed for the optimisation and evaluation of ventilation networks. |
| 16 | Application of Ventsim 3D and mathematical programming to optimise underground mine ventilation network: A case study | 2018 | [76] | This study optimised mine ventilation fan efficiency with Ventsim 3D ventilation simulation software. |
| 17 | Quantifying the thermal damping effect in underground vertical shafts using the nonlinear autoregressive with external input (NARX) algorithm | 2018 | [52] | An algorithm is developed to predict transient underground temperatures. |
| 18 | Dynamic models in atmospheric monitoring signal evaluation for safety, health and cost benefits | 2019 | [6] | This paper describes an early warning system integrated into a dynamic numerical ventilation model to provide real-time recognition and prediction of dangerous trends. |
| 19 | Industry 4.0 roll-out strategy for dynamic mine heat load management | 2019 | [105] | This paper proposed a roll-out strategy for Industry 4.0 instrumentation to improve the data collection for mine heat load management. |
| 20 | Calibrating model airway size and resistance with survey asbuilt data | 2021 | [82] | This study examined the merits of using an algorithm to convert 3D survey information to correct airway size automatically and observed the effect on model accuracy. |
| 21 | A review on underground mine ventilation system | 2021 | [47] | This study reviews the previous studies of ventilation system design and optimisation methods. |
| 22 | Rapid dynamic ventilation modelling for improving health and safety in underground mining | 2021 | [55] | This thesis discusses the development of new methods of improved dynamic ventilation modelling. |
| 23 | Ventilation model calibration from limited survey data | 2021 | [75] | This study investigated a numerical method to calculate the resistances of underground tunnels with limited surveying automatically. |
| 24 | Improving calibration of a mine ventilation network using continuous airflow monitoring | 2021 | [45] | This study investigated the use of continuously measured air velocities to calibrate the resistance of a mine ventilation network. |
| 25 | Managing heat in underground mines: The importance of incorporating the thermal flywheel effect into climatic modelling | 2021 | [2] | This paper investigated the temperature prediction of different ventilation software to determine the consequence and importance of taking the thermal damping and flywheel effect into account. |

# APPENDIX D: AIR PSYCHROMETRIC CALCULATOR

Figure D-1 illustrates an example of a psychrometric properties outputs of air calculated at a DB temperature of 26°C, relative humidity of 55% and a barometric pressure of 87.5 kPa.

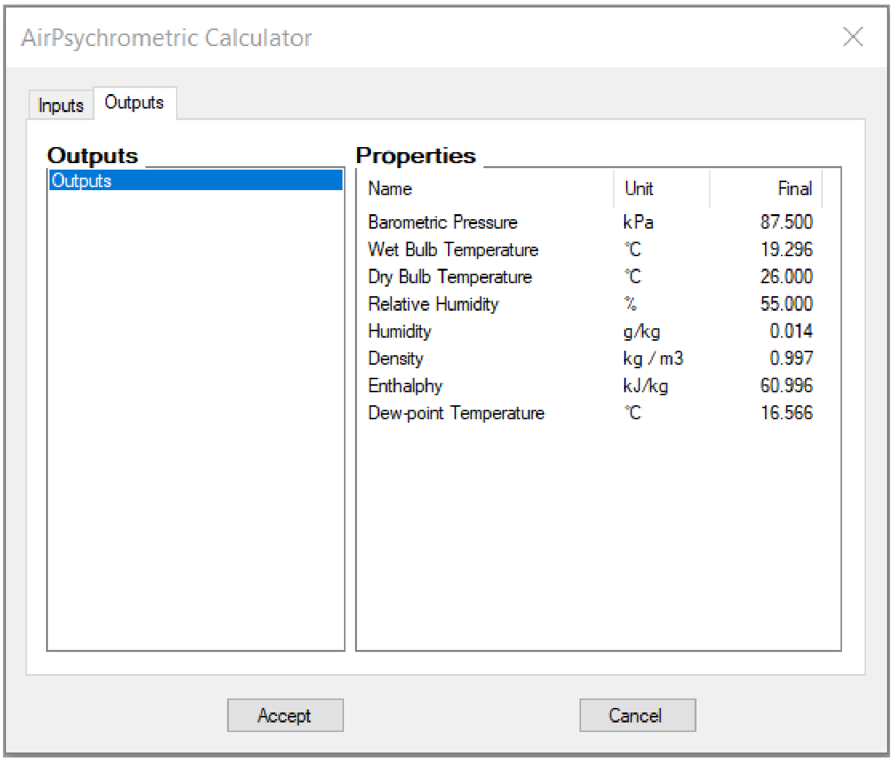


**Figure D-1: PTB air psychrometric calculator outputs***

# APPENDIX E: 45 KW FAN CURVE

Figure E-1 shows an example of a fan curve for a 45 kW booster fan. The specification shows that at standard operating conditions, the fan should produce an airflow rate of 12.00 m$^3$/s at a static pressure of 2.20 kPa with a power consumption of 39.99 kW.

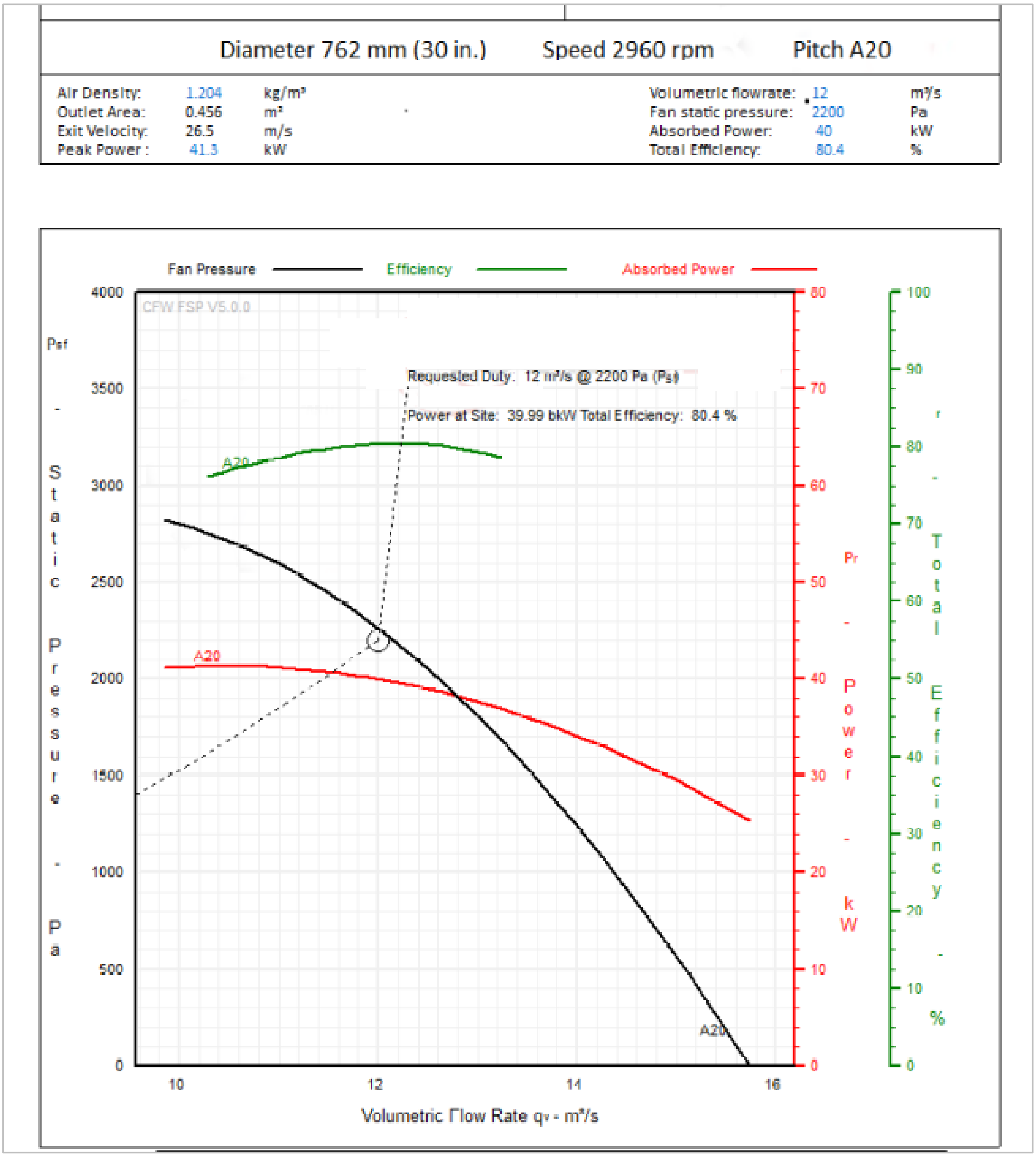


**Figure E-1: 45 kW Fan curves***

Figure E-2 shows the fan curves calculated by the simulation program using the standard parameters. The simulation component produced an airflow rate of 11.97 $m^3/s$ at a static pressure of 2.20 kPa with a power consumption of 40.12 kW.

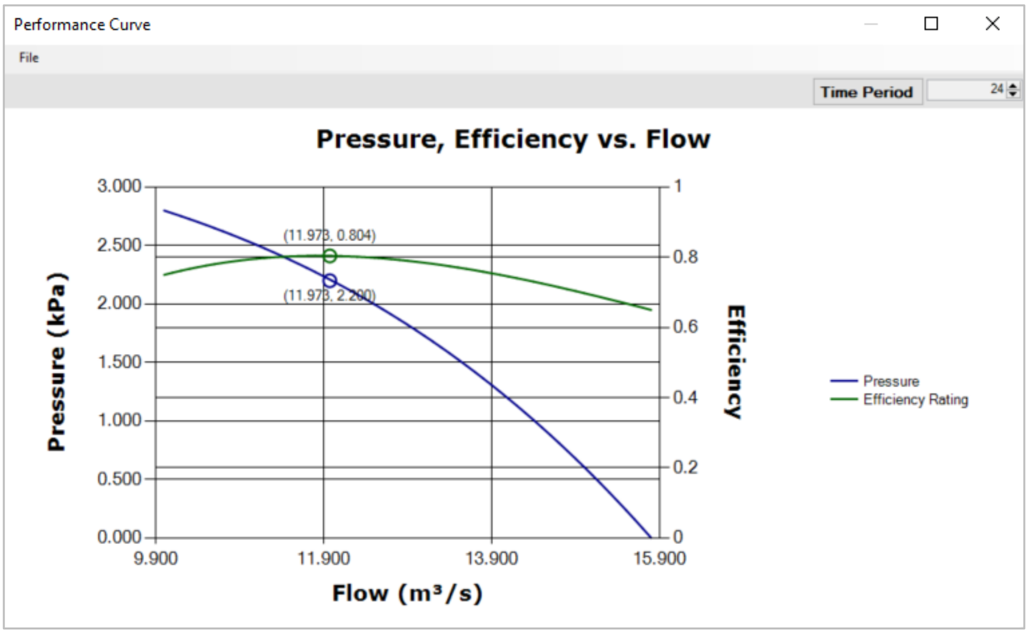


**Figure E-2: Example 45 kW PTB fan curve***

# APPENDIX F: MOBILE COOLER SPECIFICATIONS

Figure F-1 show an example of a mobile cooler cooling duty curve.

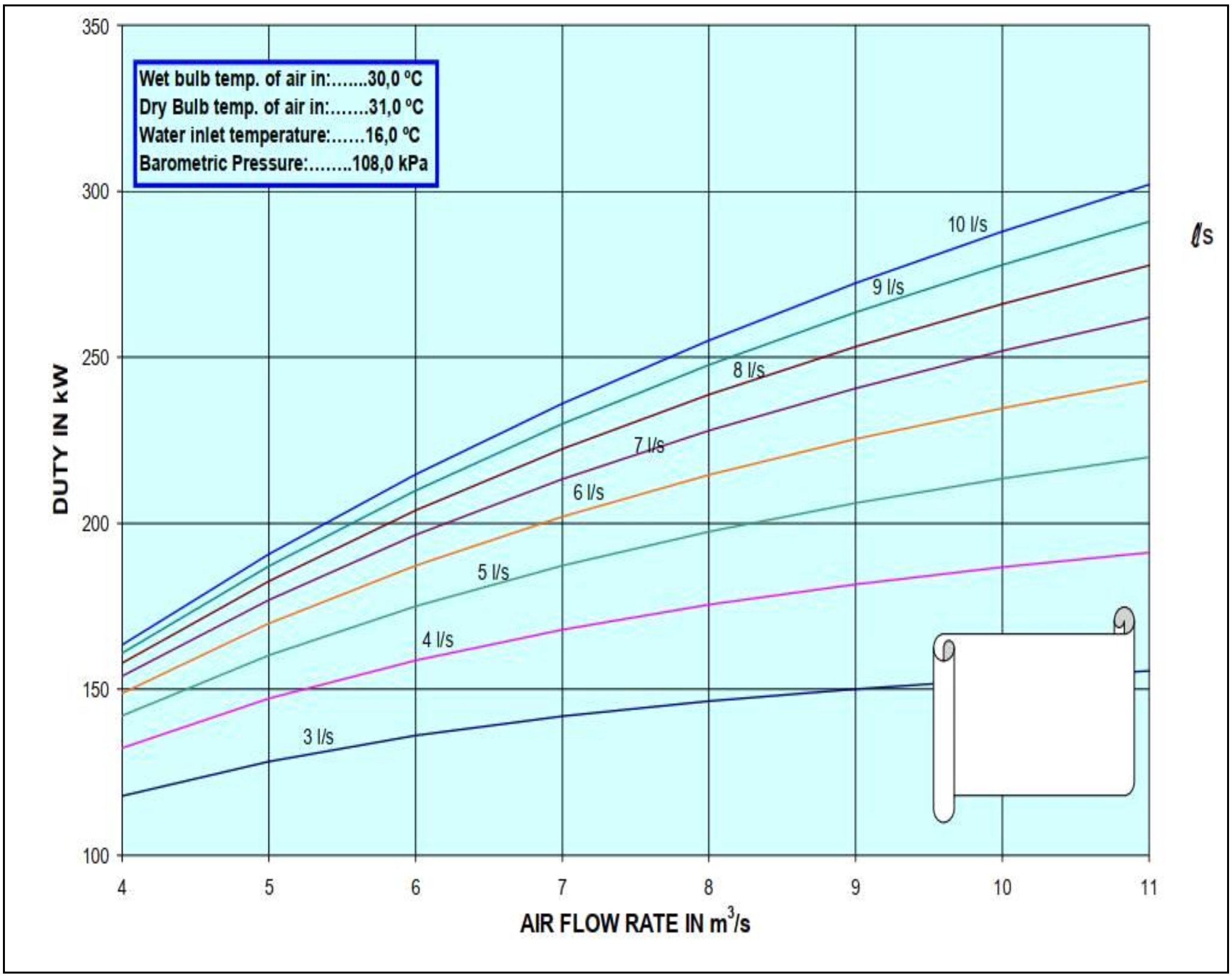


**Figure F-1: Mobile cooler specifications***

# APPENDIX G: SAJIE PUBLICATION [1]

South African Journal of Industrial Engineering November 2021 Vol 32(3) Special Edition, pp 42-51

## SIMULATING THE SENSITIVITY OF UNDERGROUND VENTILATION NETWORKS TO FLUCTUATING AMBIENT CONDITIONS

R. Fair[1]*, J.H. van Laar[2], K. Nell[1], D. Nell[1] & E.H. Mathews[1]

ARTICLE INFO

*Article details*
Presented at the 32nd annual conference of the Southern African Institute for Industrial Engineering (SAIIE), held from 4-6 October 2021 in Muldersdrift, South Africa.

Available online 29 Nov 2021

*Contact details*
* Corresponding author
rfair@rems2.com

*Author affiliations*
1 Centre for Research and Continued Engineering Development (CRCED), North West University, South Africa

2 Department of Industrial Engineering, University of Stellenbosch, South Africa

*ORCID® identifiers*
R. Fair1
https://orcid.org/0000-0002-5286-9045

J.H. van Laar
https://orcid.org/0000-0003-0457-328X

K. Nell
https://orcid.org/0000-0002-0670-045X

D. Nell
https://orcid.org/0000-0002-2817-9343

E.H. Mathews
https://orcid.org/0000-0001-5425-6368

*DOI*
http://dx.doi.org/10.7166/32-3-2616

ABSTRACT

The weather directly impacts ventilation systems, especially large industrial systems found in underground mines. Underground mine ventilation systems have high cost implications that add to the financial strains and uncertainties of future mining operations. In addition, the dynamic nature of underground ventilation systems makes the accurate prediction of underground conditions extremely difficult using traditional steady-state methods. Therefore, improved prediction methods of dynamic underground environmental conditions are needed to ensure cost-effective ventilation systems. This paper investigates simulating the sensitivity that underground ventilation systems have to fluctuating ambient conditions. Simulation software was applied to a case study on a gold mine in South Africa. The results showed that transient software can now be applied to entire mine ventilation systems, and can improve predicting the underground environment because of fluctuating ambient conditions.

OPSOMMING

Die weer het 'n direkte impak op ventilasiestelsels, veral by groot industriële stelsels soos in gebruik in ondergrondse myne. Ondergrondse mynventilasie-stelsels het hoë koste-implikasies wat bydra tot die finansiële druk en onsekerheid van toekomstige mynbedrywighede. Die dinamiese aard van ondergrondse mynventilasiestelsels bemoeilik die voorspelling van die ondergrondse toestande met tradisionele, gestadigdetoestand metodes aansienlik. Daarom word verbeterde voorspellingsmetodes van die dinamiese ondergrondse omgewingstoestande benodig; dit mag ook die kostedoeltreffendheid van mynventilasiestelsels verseker. Hierdie artikel ondersoek die moontlikheid om die faktore wat die verandering van ondergrondse omgewingstoestande beïnvloed, te simuleer. Simulasie sagteware is toegepas in 'n gevallestudie van 'n goudmyn in Suid-Afrika. Die resultate toon dat die oorgangsgedrag gesimuleer kan word en dat dit gebruik kan word om die veranderende omgewingstoestande te voorspel.

## 1 INTRODUCTION

### 1.1 Background

Underground mine ventilation systems provide an underground working environment that is conducive to productive work [1], [2]. In South Africa, the Mine Health and Safety Council enforces environmental standards [3].

These ventilation systems generally consist of underground tunnels in which ventilation equipment controls the airflow [2]. Figure 1 illustrates a simplified ventilation system on a conventional underground mine.

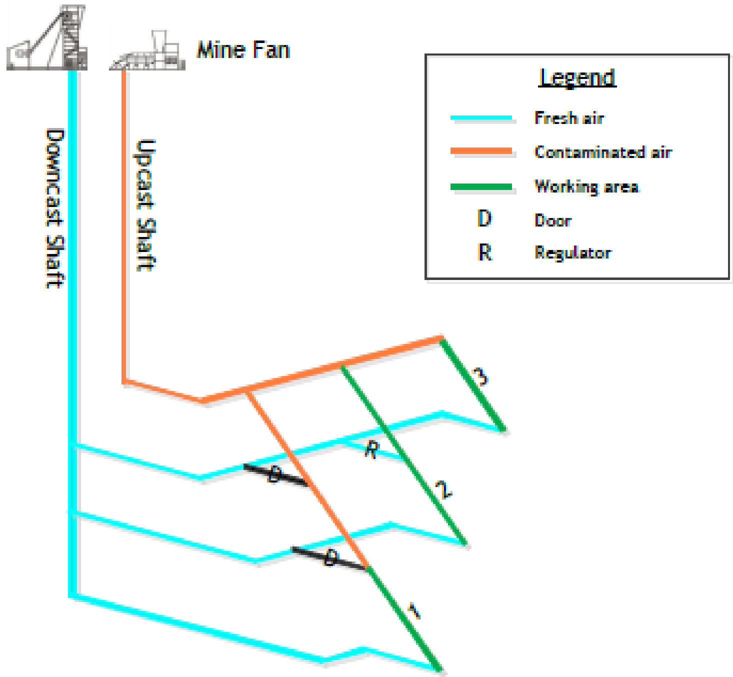


Figure 1: Simplified mine ventilation system (adapted from [2])

The amount of heat transferred to the ventilation system increases as the mining network expands to both new depths and extended distances from the shaft. Underground mines have many potential heat sources, such as [4]:

- Strata heat (geothermal gradient),
- Auto-compression,
- Machinery,
- Human metabolism,
- Oxidation,
- Blasting, and
- Fissure water.

These heat sources increase the limiting temperature of the working areas. Consequently, cooling systems are needed to mitigate the heat and achieve required temperatures. The cooling requirements are balanced with the cost of refrigeration when planning a ventilation system [5].

The high cost implications of ventilating mining networks add to the financial strains and uncertainties of the future of mining operations [6]. Industry 4.0 is becoming a crucial paradigm to ensure that the mining sector remains profitable [7]. Tools such as real-time climatic monitoring systems and simulations are used for ventilation system management [6], [8], [9], [10].

### 1.2 Dynamic nature of mine ventilation systems

The main intake of an underground ventilation system is directly from the ambient environment. Fluctuating ambient temperatures can have a significant impact on underground conditions [11]. The changing ambient conditions and the dynamic nature of an underground mine result in a complex system that is never steady-state. The heat exchange between the ventilation air and the underground rock is always transient [12].

Figure 2 shows the intake dry-bulb (DB) temperatures of a South African mine and the DB temperatures at 1 290 m below the surface over 24 hours. The decrease in the temperature fluctuation as the air travels down the mine is known as the thermal damping effect (TDE). The time lag in temperature peaks as the air travels down the mine is the thermal flywheel effect (TFE) [12].

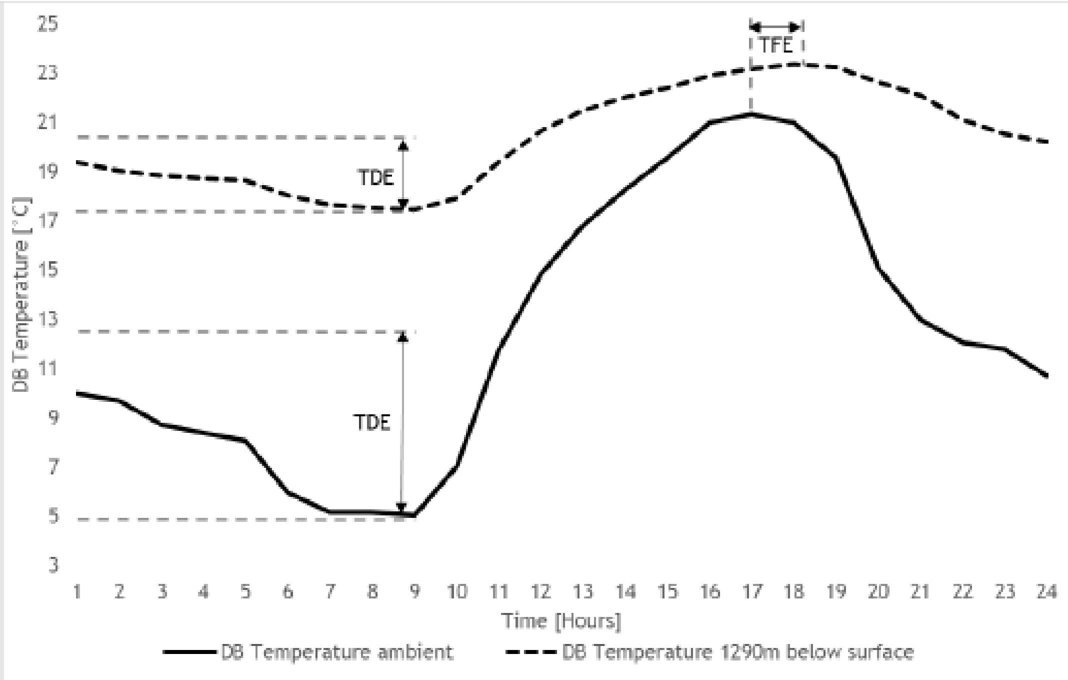


**Figure 2: DB temperature damping at 1 290 m below surface over a 24h period**

### 1.3 Mine ventilation simulation software

Simulation software is widely used on mine ventilation systems [13]. These simulation programs are a crucial part of mine ventilation systems' planning and energy optimisation processes [10], [14]. A wide range of software is available, a number of which are commercially available, such as [13], [15]:

- Process Toolbox (PTB),
- VentSim,
- Vuma-3D,
- ClimSim,
- VnetPC,
- MineFire,
- DuctSIM,
- VentGraph,
- MULTIFLUX,
- VenPri, and
- 3D-Canvent.

Most of these software packages have an intuitive setup with a three-dimensional (3D) visualiser to allow for the rapid assessment of underground network sizing [13].

Studies have shown the limitations of steady-state analysis in underground ventilation networks [11], [12]. Steady-state simulations tend to over-predict the high temperatures and under-predict the low temperatures that are traditionally used to plan future underground operations [11]. Therefore, time-dependent or transient simulation software is required to simulate the dynamic heat transfer processes such as the TDE and the TFE [16], [17].

Few simulation software packages are capable of incorporating true transient heat exchange calculations into an entire mine ventilation system [11], [17], [18].The MULTIFLUX model can simulate the TDE and TFE, but it is not yet commercially available, and it has not been applied to an entire mine ventilation network [12]. VUMA-transient was developed to simulate temperature variations, but no literature was found on the application thereof to an entire mining network [19], [20]. PTB is a thermodynamic simulation software that is capable of incorporating transient heat exchange processes, but it has not yet been applied to an entire mine ventilation system [15].

## 1.4 Need and objective

With the limitations of the steady-state simulation of ventilation systems seen in the literature, there is a need to model the entire ventilation system of an underground mine using transient simulations. This study will construct and calibrate a transient simulation of a complete underground gold mine ventilation system in South Africa. Ambient conditions will be used as an input to predict underground temperatures, accounting for complex heat exchange processes and the sensitivity of an underground mine ventilation network.

The accuracy of the underground temperature predictions will be compared with that of steady-state analysis. This will determine whether the use of transient simulation could improve the prediction of underground limiting-temperatures used in life-of-mine planning and optimisation processes.

# 2 METHODOLOGY

## 2.1 Technical overview of Process Toolbox

The thermohydraulic simulation software Process Toolbox (PTB) was used for this study. PTB is a one-dimensional computational fluid dynamics (CFD) code that is capable of solving complex thermo-hydraulic networks, such as mine ventilation systems [15], [21], [22].

The software has a 3D interface that assists with the intuitive construction and calibration of ventilation systems. The simulation is constructed on the actual digital layouts to ensure accurate dimensions of the underground system.

The PTB code solves steady-state and transient solutions of energy, mass, and momentum balances for any number of periods and period sizes. Transient flow is solved with a quasi-steady-state semi-implicit algorithm. The pressure matrix is linearised to guarantee convergence for every step so that no iterations are required. This is valuable in industrial scenarios such as mine ventilation systems [15].

The components of PTB are designed to represent an underground mine ventilation system as closely as possible. Actual rock heat transfer properties are used to ensure that the heat capacity of the simulation is as accurate as possible. Design specifications and measurements are used to calibrate underground ventilation equipment such as fans and heat exchangers.

## 2.2 Method

### *2.2.1 Data acquisition*

Continuous and accurate data is required for the calibration of transient heat transfer processes [17]. A wide range of technology is available that allows for the continuous monitoring of an underground ventilation network. Nell *et al.* [6] described the different levels of detail to which a mine ventilation system can be instrumented. Increased levels of detail would result in the increased accuracy of the simulation.

Mines that have not yet been instrumented with data collection technology require manual measurements. Hand-held data-loggers that allow for the continuous monitoring of temperature, humidity, and barometric pressure are available [11], [12], [17]. The number of data measurement points is mainly dependent on the mine ventilation system, the instrumentation available, and the required outcomes of the simulations [10]. In general, the following information is required for all main airways and working areas:

- Air mass flow (kg/s),
- Dry-bulb (DB) temperature (°C), and
- Wet-bulb (WB) temperature (°C).

The information about and specification of all environmental control devices should be collected from mining personnel and measurements. The simulation is built on the digital layouts of the underground mining network.

### 2.2.2 *Calibration and verification*

The complex nature of an underground ventilation system means that an iterative approach is required to calibrate the simulation model [10]. First, the underground system model must be constructed as accurately as possible in respect of the actual system dimensions. Second, all known component parameters must be programmed into the model. The calibration process can then be broken down into the following steps:

1. Build ventilation system in digital layouts.
2. Use continuous measured ambient data as inputs to air boundaries on the surface.
3. Simulate the model.
4. Compare measured points in the mine with the simulation results.
5. Adjust calibration parameters.
6. Repeat steps 2-4 until the desired accuracy is achieved.

The performance of the model is calculated using the mean square error (MSE) and the coefficient of determination ($R^2$) [17]. The MSE is calculated with Equation 1:

$$MSE = \left(\sum_{i=1}^{n}(\hat{y}_i - y_i)^2\right)/n \quad (1)$$

Here:

- $\hat{y}_i$ is the simulation result,
- $y_i$ is the measured data, and
- $n$ is the number of data points.

PTB has the functionality to switch to a steady-state solver. This allows the simulation to solve for the same parameters and input conditions.

## 3 RESULTS AND DISCUSSION

The results show how the method is applied to a real-life case study on an underground gold mine ventilation system. The calibrated results are shown and compared with those of traditional methods.

### 3.1 Case study overview

A gold mine in Free State Province, South Africa, was selected as a case study. It is mining at an average depth of 1 290 m underground. It follows a conventional mining setup, as shown in Figure 1.

The mine ventilation system has two downcast shafts and a single upcast shaft, and does not have secondary cooling systems. Therefore, the environmental conditions recorded underground are only influenced by the ambient conditions and by the heat sources in the underground network.

### 3.2 Data acquisition

At the time of this study, the mine did not have ventilation instrumentation installed, and all data had to be collected with hand-held instruments. Continuous loggers were placed on the surface and underground to measure the change in temperature as the air flowed through the mine ventilation system.

A logger was placed 1 290 m below the surface on the main working level. The difference between surface temperatures and underground temperatures will be due to heat sources in the ventilation system. This indicates how sensitive the mine is to changing ambient conditions. Figure 3 illustrates the ambient and underground DB temperatures and WB temperatures recorded over three days.

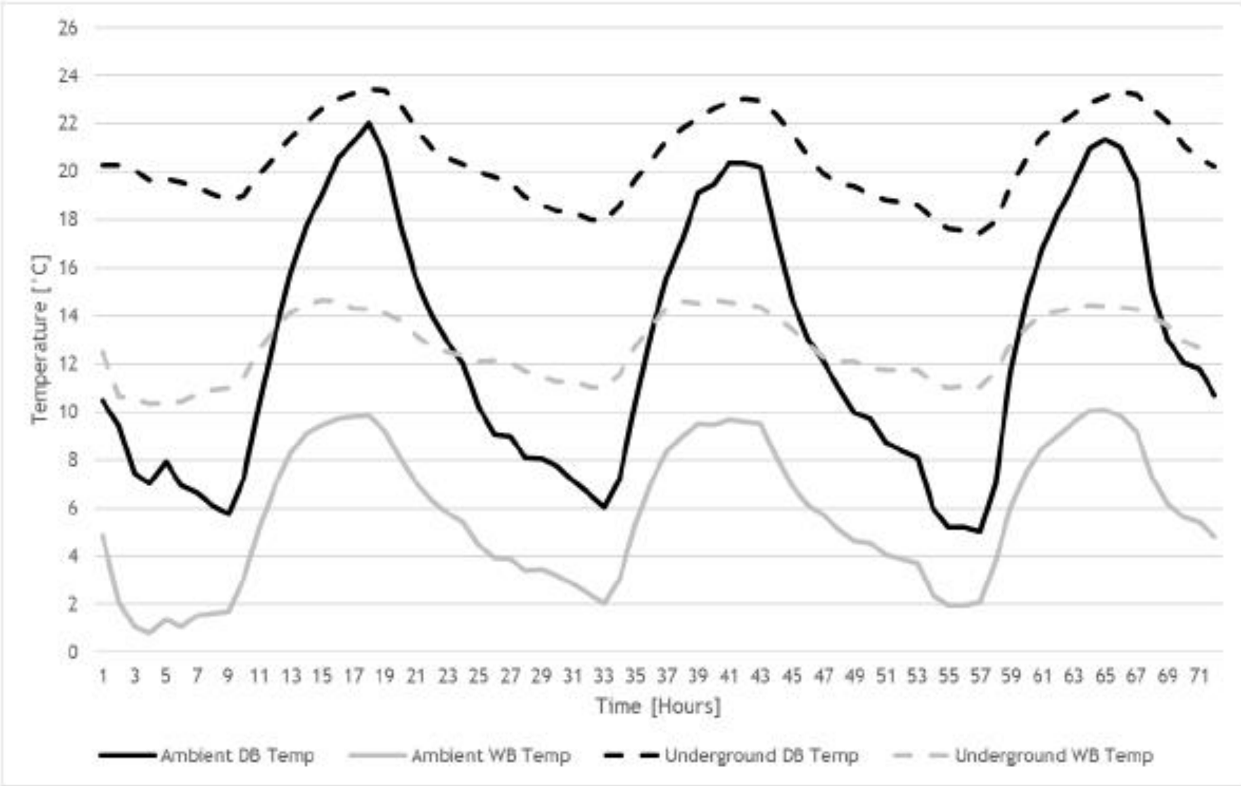


**Figure 3: Ambient and underground temperatures at the case study mine**

The simulation software was used to build the ventilation system according to the mine plan. All known parameters were programmed into the model. Figure 4 shows a screenshot of the PTB ventilation system model of the mine.

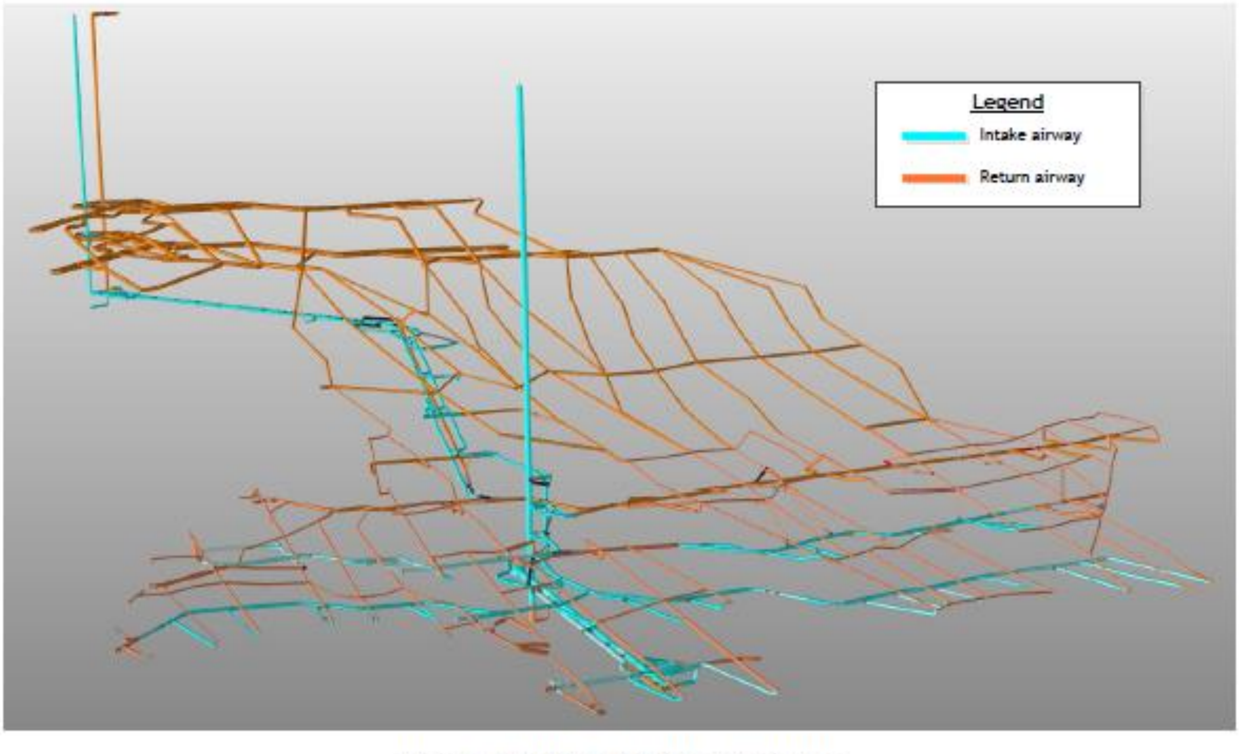


**Figure 4: PTB ventilation simulation**

### 3.3 Calibration and verification

The temperature data was collected over three weeks. This provided a suitable temperature history that allowed for accurate heat exchange [18]. The iterative process discussed in Section 2.2.2 was followed to calibrate the model.

The measured air mass flow through the ventilation network was compared with the simulation results at the same points. The MSE was calculated to be 0.77, with a maximum error of 2.11 kg/s.

The measured DB and WB temperatures on the main working level underground were compared with the simulated DB and WB temperatures. Figure 5 illustrates how the simulated temperature predictions compared with the actual measurements. The transient simulation was able to incorporate the TDE and TFE.

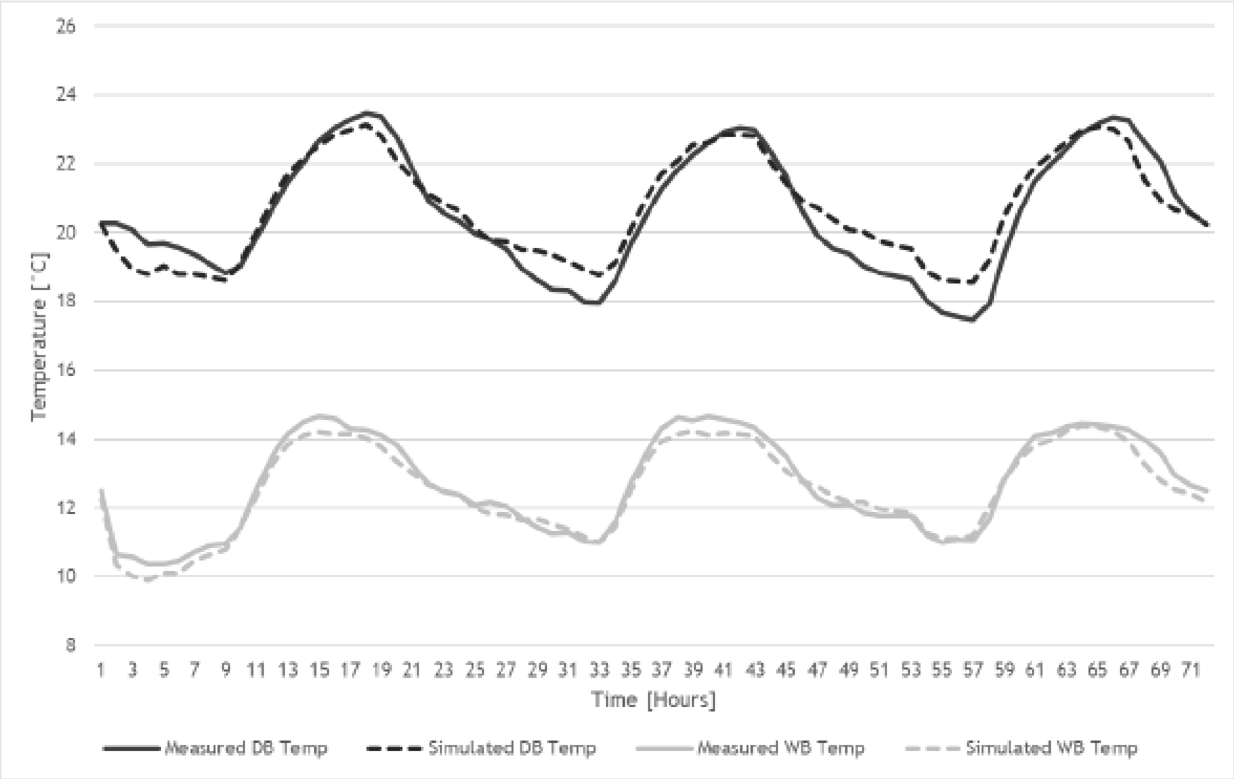


Figure 5: Underground temperature comparison using transient simulation

The simulation predicted the DB temperature with a performance accuracy of MSE = 0.38, $R^2$ = 0.99, and a maximum error of 1.5°C. The WB temperature performance was even better, with an MSE = 0.09, $R^2$ = 0.97 and a maximum error of 0.8°C. Table 1 shows a summary of the transient simulation performance. These results show that it is possible to apply transient ventilation simulation to an entire mine ventilation system.

Table 1: Summary of simulation performance

| | MSE | $R^2$ | Maximum error |
|---|---|---|---|
| Air mass flow | 0.77 | - | 2.11 |
| DB temperature (transient) | 0.38 | 0.99 | 1.53 |
| WB temperature (transient) | 0.09 | 0.97 | 0.79 |

Maximum temperatures are traditionally used to predict limiting underground temperatures [11]. The results showed the following maximum underground temperatures:

- DB temperature of 23.14°C (0.30°C lower than actual)
- WB temperature of 14.39°C (0.27°C lower than actual)

### 3.4 Comparison with steady-state simulation

From the literature, there are limitations to steady-state ventilation analysis. Quasi-steady-state simulations have been shown to provide more accurate results when compared with steady-state methods [11], [12].

The ventilation model was re-simulated with traditional steady-state analysis. The maximum ambient temperatures shown in Figure 3 were used to determine the limiting mine temperatures. The results showed the following maximum temperatures at a depth of 1 290 m:

- DB temperature of 26.09°C (2.65°C higher than actual)
- WB temperature of 16.13°C (1.47°C higher than actual)

The ventilation model was re-simulated with quasi-steady-state analysis. Figure 6 illustrates the transient and quasi-steady-state simulation results compared with the transient prediction and actual measurements.

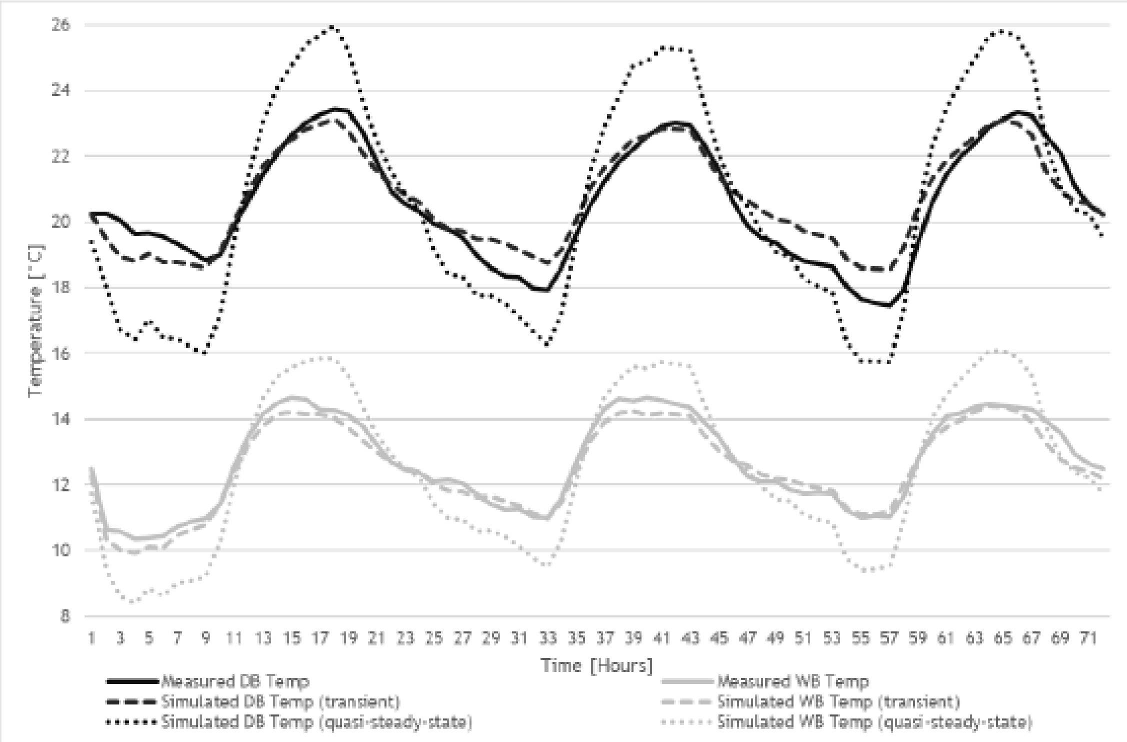


Figure 6: Comparison of transient and quasi-steady-state simulations

Comparing the steady-state and quasi-steady-state analyses showed a slight improvement in predictions. The results showed the following maximum temperatures at a depth of 1 290 m:

- DB temperature of 25.98°C (2.54°C higher than actual)
- WB temperature of 16.08°C (1.42°C higher than actual)

Compared with the transient solution, the quasi-steady-state solution had a higher MSE, with 3.03 for the DB temperature and 1.15 for the WB temperature. The quasi-steady-state model had a maximum error of 3.34 for DB temperature and 1.95 for WB temperature. A summary comparison of the simulation performance is shown in Table 2.

Table 2: Comparison of transient and quasi-steady-state simulation performance

| | MSE | $R^2$ | Maximum error |
|---|---|---|---|
| Air mass flow | 0.77 | - | 2.11 |
| DB temperature (transient) | 0.38 | 0.99 | 1.53 |
| DB temperature (quasi-steady) | 3.03 | 0.98 | 3.34 |
| WB temperature (transient) | 0.09 | 0.97 | 0.79 |
| WB temperature (quasi-steady) | 1.15 | 0.99 | 1.95 |

## 3.5 Discussion

The results showed that the simulation could accurately predict the underground environment as a result of fluctuating ambient temperatures. The transient simulation was then compared with traditional steady-state analysis. This showed that the transient simulation had a clear advantage when simulating complex heat transfer processes such as the TDE and TFE.

From the results and the literature, steady-state simulations over-predict high temperatures and under-predict low temperatures. Inaccurate predictions have a detrimental impact on the life-of-mine planning and optimisation of a ventilation system, because cooling requirements are determined from the predicted underground temperatures.

The over-prediction of underground temperatures would result in over-predicted cooling requirements. In this study, the steady-state analysis over-predicted the limiting underground temperatures by 2.65°C for DB and by 1.47°C for WB compared with the actual temperatures. This would result in 1.1 MW of over-cooling when planning or optimising this ventilation system. 1.1 MW of cooling on a typical bulk air cooler is equivalent to an additional electrical cost of up to R1.8 million per year [23], [24].

**The under**-prediction of underground temperatures would result in under-predicting the cooling requirements. If environmental standards are not met because of under-cooling, the mine can be forced to terminate all work in areas that exceed the temperature standards. The gold mine in this study has an average daily revenue of R4 million. The termination of underground workings would therefore lead to substantial financial losses.

The improved prediction of underground temperatures with transient simulations would result in better life-of-mine planning and optimisation. When paired with Industry 4.0 real-time climatic monitoring systems, this opens the doors to other applications. Some of these applications include ventilation-on-demand, live predictive modelling, and dynamic heat load management.

# 4 CONCLUSION

The literature points to the need to apply a transient simulation to an entire underground mine ventilation system. The objective of this study was to develop a transient model of an entire underground mine ventilation system. This transient model needed accurately to represent the ventilation system and its sensitivity to fluctuating ambient conditions.

A PTB simulation was successfully applied to a gold mine in Free State Province, South Africa. The transient simulation incorporated complex heat exchange processes and the sensitivity of an underground mine ventilation system to varying ambient conditions.

The results showed that the transient analysis improved the predictions of the underground environment compared with traditional steady-state analysis. The transient simulation had an error of 0.30°C for the DB temperature and 0.27°C for the WB temperature when predicting the limiting underground conditions. Steady-state analysis had an error of 2.54°C for the DB temperature and 1.42°C for the WB temperature for the same prediction.

Improved predictions allow for the improved management of mine ventilation systems. This is especially true for mine ventilation planning and optimisation, as they depend on the accurate prediction of underground temperatures.

This study was applied to a gold mining case study. Applying this study to underground mines with different depths, infrastructure, and geographical locations or in different seasons would give further insight into complex mine ventilation systems simulation. This would also give further indications of the sensitivity that mine ventilation systems have to different parameters.

# REFERENCES


[1] J. J. L. du Plessis, *Ventilation and occupational environment engineering in mines*, 3rd ed., Johannesburg: Mine Ventilation Society of South Africa, 2014.

[2] J. C. Tien, "Chapter 9 — Mine ventilation systems," in *Practical Mine Ventilation Engineering*, no. 1, Intertec Pub., 1999, pp. 167-189.

[3] Mine Health and Safety Council, *Mine Health and Safety Act 29 of 1996 and Regulations*, no. 29. South Africa, 2018, p. 199-203.

[4] K. Carpenter, P. Roghanchi, and K. C. Kocsis, "Investigating the importance of climatic monitoring and modeling in deep and hot US underground mines," in *Proceedings of 15th North American Mine Ventilation Symposium*, 2015, pp. 1-4.
[5] S. Bluhm, R. G. Moreby, F. von Glehn, and C. Pascoe, "Life-of-mine ventilation and refrigeration planning for resolution copper mine," *J. South. African Inst. Min. Metall.*, vol. 114, no. 6, pp. 497-503, 2014.
[6] D. Nell, E. H. Mathews, and P. Mare, "Industry 4.0 roll-out strategy for dynamic mine heat load management," *South African J. Ind. Eng.*, vol. 30, no. 3, pp. 106-114, 2019.
[7] J. Prinsloo, J. Vosloo, and E. H. Mathews, "Towards Industry 4.0: A roadmap for the South African heavy industry sector," *South African J. Ind. Eng.*, **vol. 31, no. 3, pp. 174**-186, 2019.
[8] A. Ryan and D. S. Euler, "Heat stress management in underground mines," *Int. J. Min. Sci. Technol.*, vol. 27, no. 4, pp. 651-655, 2017, doi: https://doi.org/10.1016/j.ijmst.2017.05.020.
[9] C. Gherghel and E. De Souza, "Ventilation requirements for uranium mines," in *12th US/North American Mine Ventilation Symposium*, pp. 65-70, 2008.
[10] A. J. H. Nel, J. C. Vosloo, and M. J. Mathews, "Evaluating complex mine ventilation operational changes through simulations," *J. Energy South. Africa*, vol. 29, no. 3, pp. 22-32, 2018.
[11] C. Stewart, S. M. Aminossadati, M. S. Kizil, and T. Andreatidis, "Diurnal thermal flywheel influence on ventilation temperatures in large underground mines," in *16th North American Mine Ventilation Symposium*, pp. 9.1-9.8, 2017.
[12] P. Roghanchi, K. C. Kocsis, G. Danko, and A. Powell, "Underground climatic monitoring and modeling: Are we missing something?" *Qual. — Access to Success*, vol. 18, no. S1, pp. 133-139, 2017.
[13] M. S. Morar, S. M. Radu, D. Cioclea, and I. Gherghe, "Use of IT equipment and specialized programs for solving ventilation networks," *Qual. — Access to Success*, vol. 18, no. S1, pp. 121-126, 2017.
[14] S. Bluhm and H. Smit, "Important basics of mine ventilation and cooling planning," *Mine Vent. Soc. South Africa*, vol. 57, no. 1, pp. 15-24, 2004.
[15] I. Mathews, E. H. Mathews, J. H. van Laar, W. Hamer, and M. Kleingeld, "A simulation-based prediction model for coal-fired power plant condenser maintenance," *Appl. Therm. Eng.*, vol. 174, pp. 1-10, 2020, doi: https://doi.org/10.1016/j.applthermaleng.2020.115294.
[16] K. A. Scalise, M. B. Teixeira, and K. C. Kocsis, "Managing heat in underground mines: The importance of incorporating the thermal flywheel effect into climatic modeling," *Mining, Metall. Explor.*, vol. 38, no. 1, pp. 575-579, 2021, doi: https://doi.org/10.1007/s42461-020-00323-5.
[17] P. Roghanchi and K. C. Kocsis, "Quantifying the thermal damping effect in underground vertical shafts using the nonlinear autoregressive with external input (NARX) algorithm," *Int. J. Min. Sci. Technol.*, vol. 29, no. 2, pp. 255-262, 2018, doi: https://doi.org/10.1016/j.ijmst.2018.06.002.
[18] G. L. Danko, "Subsurface flow and transport process model for time dependent mine ventilation simulations," *Trans. Institutions Min. Metall. Sect. A Min. Technol.*, vol. 122, no. 3, pp. 134-144, 2013, doi: https://doi.org/10.1179/147490013X13639459465691.
[19] F. H. von Glehn and I. Ox, "Monitoring and control of underground ventilation systems using VUMA-network," in *Proceedings of the 10th US/North American Mine Ventilation Symposium*, pp. 16-19, 2004.
[20] N. J. Smit, "Reducing electrical costs for a mine ventilation system with the aid of simulation software," Master's dissertation, Department of Electrical and Electronic Engineering, North-West University, 2017.
[21] B. M. Friedenstein, C. Cilliers, and J. van Rensburg, "Simulating operational improvements on mine compressed air systems," *South African J. Ind. Eng.*, vol. 29, no. 3, pp. 69-81, 2018, doi: https://doi.org/10.7166/29-3-2049.
[22] D. Nell, "Optimising production through improving the efficiency of mine compressed air networks with limited infrastructure," Master's dissertation, Department of Mechanical Engineering. North-West University, 2017.
[23] G. E. du Plessis, "A variable water flow strategy for energy savings in large cooling systems", PhD dissertation, Department of Mechanical Engineering, North-West University, 2013.
[24] Eskom Ltd, *Tariffs & charges booklet 2021/2022*, 2021. [Online].
Available: https://www.eskom.co.za/CustomerCare/TariffsAndCharges/Pages/Tariffs_And_Charges.aspx.

# APPENDIX H: MINE A SECONDARY HEAT SOURCES

Mine A did not have fuel-driven machinery, thus the first heat source to be quantified was electrical heat. The effective electrical heat load was calculated using Equation 2-4. The data for the total electrical load supplied to the mine was collected from the electric supply loggers of the different sections of the mine.

It is essential to account for the useful work completed and equipment that must be excluded. Therefore, the potential energy gained from useful work completed by electric equipment was calculated using Equation 2-1. The results for Mine A are shown in Table H-1.

**Table H-1: Electrical potential energy gain for Mine A**

| Parameter | Amount [kg/s] | Elevation gain [m] | Potential energy gain [kW] |
|---|---|---|---|
| Water pumped out of the mine | 34.0 | 1 290 | 430 |
| Rock transported out of the mine | 17.8 | 1 290 | 225 |
| **Total** | | | **656** |

PTB includes the heat added to the system by booster fans. The sum of the electrical energy users excluded for the supplied electrical load equated to 222 kW, which included the booster fans. Each booster fan's heat added to the system was determined by the operating conditions and fan curves where electrical data was unavailable. Table H-2 summarises the calculation of the effective electrical load of Mine A.

**Table H-2: Effective electrical load for Mine A**

| Parameter | Value [kW] |
|---|---|
| Average total supply | 1 836 |
| Average potential energy gained | 656 |
| Excluded equipment | 222 |
| **Effective electrical heat load** | **958** |

An average metabolic rate of 250 W was assumed for heavy manual work for 70% of the shift [11], [106]. Mine A had around 864 employees underground during the drilling shift. The metabolic heat load was calculated using Equation 2-5, and the results are shown in Table H-3.

**Table H-3: Metabolic heat load for Mine A**

| Parameter | Unit | Value |
|---|---|---|
| Employees | [–] | 864 |
| Average metabolic rate | [kW] | 0.25 |
| **Metabolic heat load** | **[kW]** | **216** |

The heat produced by explosives in the working areas was calculated using Equation 2-6. Mine A used an average of 1 340 kg of explosive per month with 4 030 kJ of energy produced per kilogram. This method assumes that the heat energy released by the explosion is absorbed by the rock and released over an entire day [11], [31]. Table H-4 summarises the calculation of the explosive heat load.

**Table H-4: Explosive heat load for Mine A**

| **Parameter** | **Unit** | **Value** |
|---|---|---|
| Explosive used (monthly) | [kg] | 1 340 |
| Heat produced per kilogram | [MJ/kg] | 4 030 |
| Blast frequency | [days] | 1 |
| **Explosive heat load** | **[kW]** | **2** |

Finally, the heat added to the ventilation system by fissure water was calculated using Equation 2-7. The mass flow of the fissure water was determined from the difference of water entering and leaving the mine. The temperature of the fissure water that enters the system is equal to the VRT at the depth that the water enters the mine. Therefore, the temperature at which the fissure water exited the mine was assumed to be equal to the rejected air WB temperature of the mine working areas [11]. Table H-5 summarises the calculation of the fissure water heat load.

**Table H-5: Fissure water heat load for Mine A**

| **Parameter** | **Unit** | **Value** |
|---|---|---|
| Mass flow of fissure water | [kg/s] | 6 |
| Exit fissure water temperature | [°C] | 29.5 |
| Inlet fissure water temperature | [°C] | 38.9 |
| **Fissure water heat load** | **[kW]** | **236** |

It was not necessary to include the cooling duty of cold water pipes as the water was not chilled before entering the mine.

# APPENDIX I: MINE A KPIS AND STANDARD PARAMETERS

Table I-1 shows the KPIs for Mine A.

**Table I-1: Mine A KPIs**

| Area | KPI | Unit |
|---|---|---|
| Working area intakes | Air mass flow | [kg/s] |
| | DB temperature | [°C] |
| | WB temperature | [°C] |
| Return fans | Air mass flow | [kg/s] |
| | Static pressure | [kPa] |

The underground tunnels sizes were obtained from mining plans and are shown in Table I-2. Drifts are the main travel ways on an underground level, and cross-cuts are travelways to a specific working area. These were used as the standard input on all tunnels of each type. In cases where the tunnel size significantly deviated from the standard, the tunnel size was input manually from data obtained from manual measurements. The working area sizes depended on the current mining progress of each working area and ranged between 4 $m^2$ and 25 $m^2$.

**Table I-2: Tunnel sizes for Mine A**

| Tunnel type | Area [m²] | Perimeter [m] |
|---|---|---|
| Main downcast shaft | 50.3 | 25.1 |
| Secondary downcast shaft | 29.2 | 19.2 |
| Main upcast shaft | 29.2 | 19.2 |
| Drifts | 12.0 | 14.0 |
| Cross-cuts | 9.0 | 12.0 |
| Working areas | Working area-specific | |

The tunnel's age was programmed into the simulation tunnels as per the historical mining plans. Mine A was in the Free State in South Africa, mining predominately quartzite. The VRT formula for this region and rock type was shown in Equation 2-11, which had a temperature gradient of 0.0146°C/m. The tunnel friction coefficients and rock properties used for Mine A are shown in Table I-3 [11], [37], [35]. The rock density was confirmed by the measured volume and mass of rock extracted from the mine.

**Table I-3: Tunnel friction coefficients and rock properties**

| Parameter | Unit | Value |
|---|---|---|
| Friction coefficient (Concrete lined shaft empty) | [$Ns^2/m^4$] | 0.0037 |
| Friction coefficient (Concrete lined shaft equipment) | [$Ns^2/m^4$] | 0.009 |
| Friction coefficient (Underground rock-lined tunnel) | [$Ns^2/m^4$] | 0.011 |
| VRT gradient | [°C/m] | 0.0146 |
| Rock thermal conductivity | [W/m·K] | 5.74 |
| Rock density | [$kg/m^3$] | 2 690 |
| Rock specific heat | [J/kg] | 837 |

Table I-4 shows the calibration parameters of the air pipe components. The air fan components were calibrated as discussed in Section 2.4.

**Table I-4: Air pipe calibration parameters**

| Parameter | Unit | Source |
|---|---|---|
| Surface roughness | [mm] | Product specifications |
| Hydraulic diameter | [m] | Product specifications |
| Flow area | [$m^2$] | Product specifications |

# APPENDIX J: MINE B 55L REFRIGERATION SIMULATION

Table J-1 shows the set points for the Mine B refrigeration system on 55L, and these are the standard operating conditions and targets for the chillers. Figure J-1 illustrates the refrigeration system on 55L level and shows the piping network between the refrigeration components.

**Table J-1: Mine B 55L refrigeration set points**

| Area | KPI | Unit | Value |
|---|---|---|---|
| Fridge plants | Condenser water flow | [ℓ/s] | 130.0 |
| | Evaporator water flow | [ℓ/s] | 65.0 |
| | Evaporator outlet water temperature | [°C] | 5.0 |

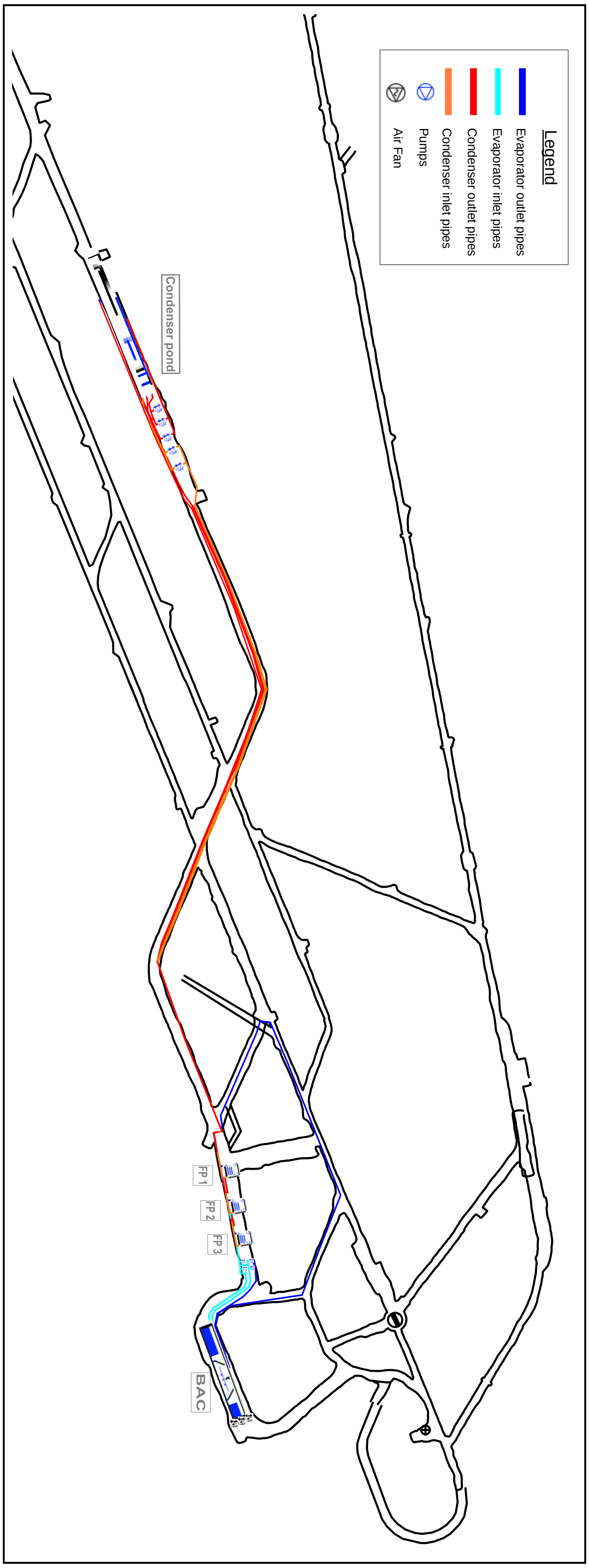


**Figure J-1: Mine B 55L PTB refrigeration simulation***

# APPENDIX K: MINE B SECONDARY HEAT SOURCES

First, the effective electrical heat load was calculated using Equation 2-4. The potential energy gained by useful work was calculated using Equation 2-1. Table K-1 shows the results for the potential energy gain at Mine B. The electrical load of the water pumps was not included in the electrical load supplied, thus it had to be excluded from the calculation.

**Table K-1: Electrical potential energy gain for Mine B**

| Parameter | Amount [kg/s] | Elevation gain [m] | Potential energy gain [kW] |
|---|---|---|---|
| Water pumped out of ventilation district | 0 | 0 | 0 |
| Rock transported out of ventilation district | 23.5 | 499 | 115 |
| **Total** | | | **115** |

The sum of the electrical energy users that had to be excluded from the supplied electrical load equalled 1 055 kW. Table K-2 shows the results for Mine B's effective electrical heat load.

**Table K-2: Effective electrical load for Mine B**

| Parameter | Value [kW] |
|---|---|
| Average electrical load supplied | 5 518 |
| Average potential gained | 115 |
| Excluded equipment | 1 055 |
| **Effective electrical heat load** | **4 348** |

Mine B had around 1 800 employees underground during a drilling shift. The metabolic heat load was calculated using Equation 2-5, and the results are shown in Table K-3.

**Table K-3: Metabolic heat load for Mine B**

| Parameter | Unit | Value |
|---|---|---|
| Employees | [–] | 1 800 |
| Average metabolic rate | [kW] | 0.25 |
| **Metabolic heat load** | **[kW]** | **450** |

The heat produced by explosives in the working areas was calculated using Equation 2-6. Mine A used an average of 1 758 kg of explosive per month with 3 820 kJ of energy produced per kilogram [35]. Table K-4 summarises the calculation of the explosive heat load.

**Table K-4: Explosive heat load for Mine B**

| Parameter | Unit | Value |
|---|---|---|
| Explosive used (monthly) | [kg] | 1 758 |
| Heat produced per kilogram | [kJ/kg] | 3 820 |
| Blast frequency | [days] | 1 |
| **Explosive heat load** | **[kW]** | **3** |

The heat added to the ventilation system by fissure water was calculated using Equation 2-7. Table K-5 summarises the calculation of the fissure water heat load.

**Table K-5: Fissure water heat load for Mine B**

| Parameter | Unit | Value |
|---|---|---|
| Mass flow of fissure water | [kg/s] | 10.7 |
| Exit fissure water temperature | [°C] | 29.5 |
| Inlet fissure water temperature | [°C] | 51.8 |
| **Fissure water heat load** | **[kW]** | **999** |

Mine B had a chilled water piping network that was not insulated adequately, resulting in heat transfer between the ventilation air and piping. The cooling duty supplied by the chilled water piping was determined with Equation 2-8. Transient water temperature data was not available for the working areas, thus the cooling duty was determined from an average of multiple manual measurements. Table K-6 summarises the calculation of the average chilled water-cooling duty as a result of the poorly insulated pipes.

**Table K-6: Total chilled water-cooling duty for Mine B**

| Parameter | Unit | Value |
|---|---|---|
| Average mass flow of chilled water | [kg/s] | 190.3 |
| Average ice dam outlet temperature | [°C] | 10.4 |
| Average working area water intake temperature | [°C] | 16.5 |
| **Chilled water pipes cooling duty** | **[kW]** | **4 829** |

## APPENDIX L: MINE B KPIS AND STANDARD PARAMETERS

Table L-1 shows the KPIs for Mine B.

**Table L-1: Mine B KPIs**

| Area | KPI | Unit |
|---|---|---|
| Working area intakes | Air mass flow rate | [kg/s] |
| | DB temperature | [°C] |
| | WB temperature | [°C] |
| Return fans operating condition | Air mass flow rate | [kg/s] |
| | Static pressure | [kPa] |
| Fridge plants | Condenser water flow rate | [ℓ/s] |
| | Condenser inlet water temperature | [°C] |
| | Condenser outlet water temperature | [°C] |
| | Evaporator water flow rate | [ℓ/s] |
| | Evaporator inlet water temperature | [°C] |
| | Evaporator outlet water temperature | [°C] |
| BAC | Air outlet WB temperature | [°C] |
| Ice dam | Outlet water temperature | [°C] |

The ventilation components used the same standard parameters from literature as Mine A, as both these mines were in the Free State, South Africa. These parameters were shown in Appendix I. Table L-2 shows the tunnel sizes for Mine B. The working area sizes depended on the current mining progress of each working area and ranged between 4 $m^2$ and 25 $m^2$.

**Table L-2: Tunnel sizes for Mine B**

| Tunnel | Area [m²] | Perimeter [m] |
|---|---|---|
| Main downcast shaft | 39.6 | 22.3 |
| Main upcast shaft | 46.5 | 24.2 |
| Drifts | 9.0 | 12.0 |
| Cross-cuts | 9.0 | 12.0 |
| Working areas | Working area-specific | |

The fridge plants and heat exchangers were all defined using measured data that was available on the SCADA. The ice dam volume was specified according to the actual size of the dam, 2 350 $m^3$. The mobile coolers were fitted with valves that controlled the water flow to 7 ℓ/s, and this was used as the input for water demand components.

# APPENDIX M: MINE B COOLING SYSTEM SIMULATION ACCURACY

Table M-1 shows the accuracy of the cooling system components, which had an average accuracy of 95.6%.

**Table M-1: Mine B 55L cooling system average operating conditions (55L)**

| Parameter | Unit | Measured | Simulated | MSE | $R^2$ |
|---|---|---|---|---|---|
| FP1 Condenser inlet water temperature | [°C] | 32.83 | 33.00 | 0.36 | 0.01 |
| FP1 Condenser outlet water temperature | [°C] | 37.18 | 37.14 | 0.39 | 0.00 |
| FP1 Condenser water flow rate | [ℓ/s] | 149.46 | 150.00 | 0.14 | 0.22 |
| FP1 Evaporator inlet water temperature | [°C] | 12.10 | 12.18 | 0.38 | 0.51 |
| FP1 Evaporator outlet water temperature | [°C] | 5.02 | 5.02 | 0.37 | 0.00 |
| FP1 Evaporator water flow rate | [ℓ/s] | 64.52 | 65.10 | 0.97 | 0.09 |
| FP2 Condenser inlet water temperature | [°C] | 33.18 | 33.00 | 0.36 | 0.01 |
| FP2 Condenser outlet water temperature | [°C] | 37.10 | 37.08 | 0.39 | 0.00 |
| FP2 Condenser water flow rate | [ℓ/s] | 150.47 | 150.00 | 0.14 | 0.22 |
| FP2 Evaporator inlet water temperature | [°C] | 12.26 | 12.18 | 0.38 | 0.51 |
| FP2 Evaporator outlet water temperature | [°C] | 5.03 | 5.02 | 0.37 | 0.00 |
| FP2 Evaporator water flow rate | [ℓ/s] | 65.77 | 65.10 | 0.97 | 0.09 |
| BAC outlet WB temperature | [°C] | 9.93 | 9.83 | 0.02 | 0.83 |
| BAC air mass flow rate | [kg/s] | 250.20 | 251.20 | 1.04 | – |

# APPENDIX N: MINE B 66L SIMULATION RESULTS

This appendix contains the measured and simulated temperatures at three locations seen in Figure 3-18. These results were summarised in Section 3.3.6 and Section 3.3.7. Figure N-1, Figure N-2, and Figure N-3 illustrate the WB and DB temperatures at Points 1 to 3, respectively. These include the measured temperature compared with the true transient simulated temperature and quasi-steady-state simulated temperature.

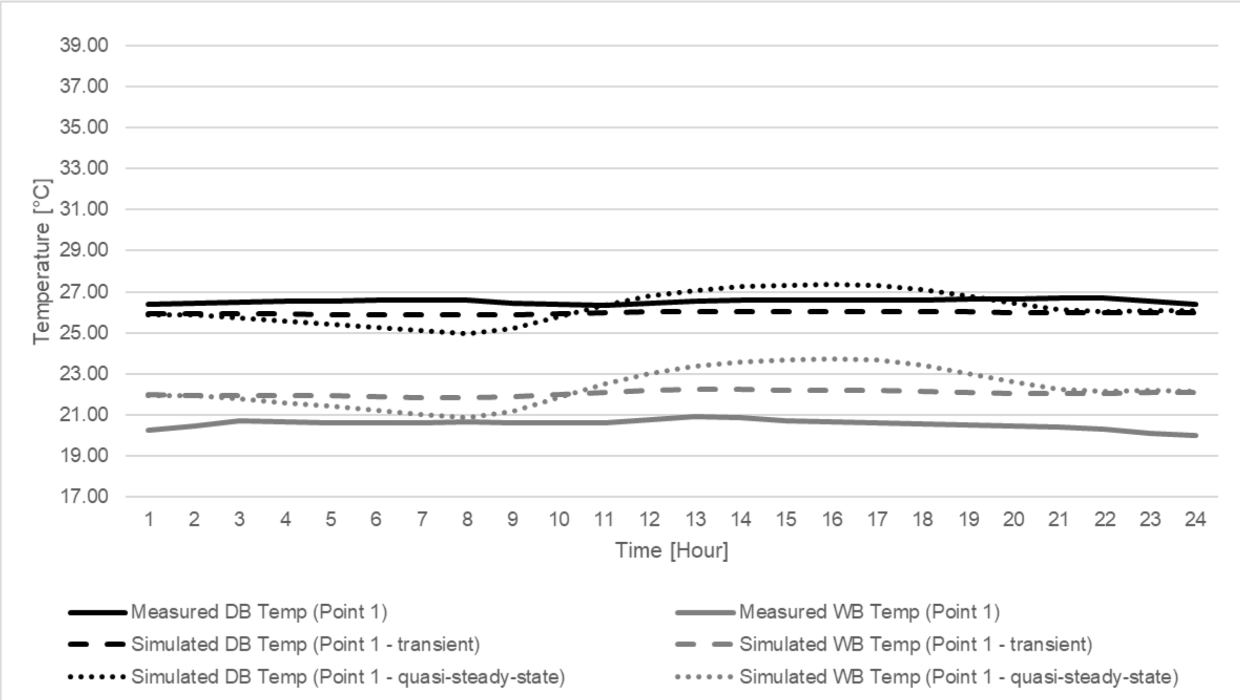


**Figure N-1: Mine B transient and quasi-steady-state temperature comparison (66L – Point 1)***

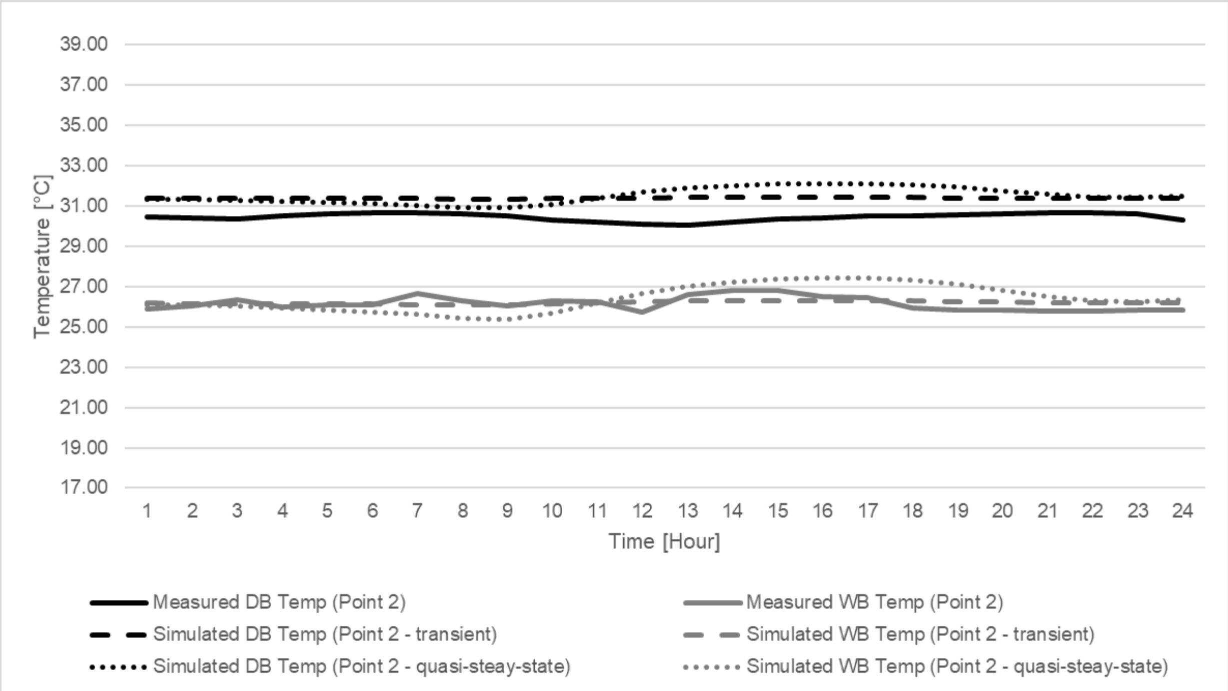


**Figure N-2: Mine B transient and quasi-steady-state temperature comparison (66L – Point 2)***

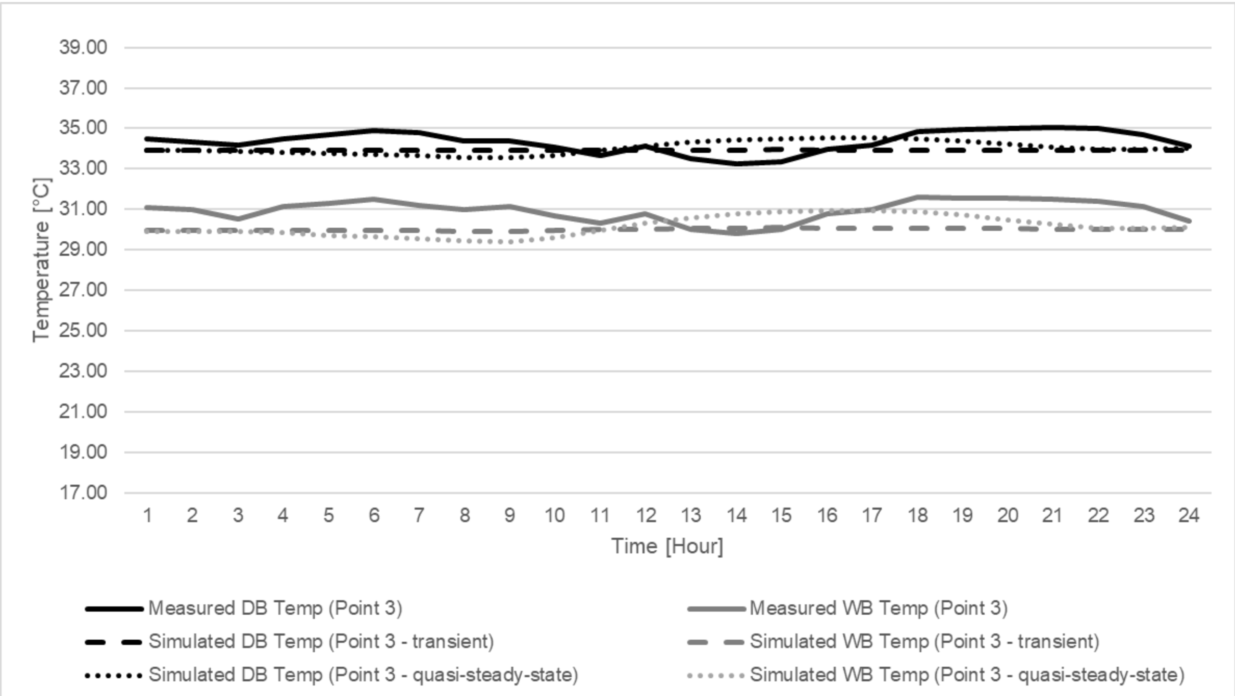


**Figure N-3: Mine B transient and quasi-steady-state temperature comparison (66L – Point 3)***

Table N-1 summarises the simulation performance for the three measurement points on 66L.

**Table N-1: Mine B comparison of transient and quasi-steady-state simulation performance (66L)**

| Location | Parameter | Unit | MSE | $R^2$ | Maximum error |
|---|---|---|---|---|---|
| Point 1 | DB temperature (transient) | °C | 0.35 | 0.04 | 0.75 |
| | DB temperature (quasi-steady-state) | °C | 0.66 | 0.03 | 1.61 |
| | WB temperature (transient) | °C | 2.28 | 0.05 | 2.06 |
| | WB temperature (quasi-steady-state) | °C | 3.93 | 0.06 | 3.06 |
| Point 2 | DB temperature (transient) | °C | 0.92 | 0.12 | 1.35 |
| | DB temperature (quasi-steady-state) | °C | 1.37 | 0.09 | 1.82 |
| | WB temperature (transient) | °C | 0.11 | 0.06 | 0.56 |
| | WB temperature (quasi-steady-state) | °C | 0.50 | 0.05 | 1.43 |
| Point 3 | DB temperature (transient) | °C | 0.45 | 0.04 | 1.11 |
| | DB temperature (quasi-steady-state) | °C | 0.55 | 0.08 | 1.18 |
| | WB temperature (transient) | °C | 1.14 | 0.10 | 1.55 |
| | WB temperature (quasi-steady-state) | °C | 1.22 | 0.05 | 1.84 |

The average maximum error improvement between the true transient and quasi-steady-state simulation was 0.59°C.

# APPENDIX O: MINE B 75L SIMULATION RESULTS

This appendix contains the measured and simulated temperatures at three locations on Mine B 75L. Figure O-1 illustrates the measurement locations on Mine B 75L.

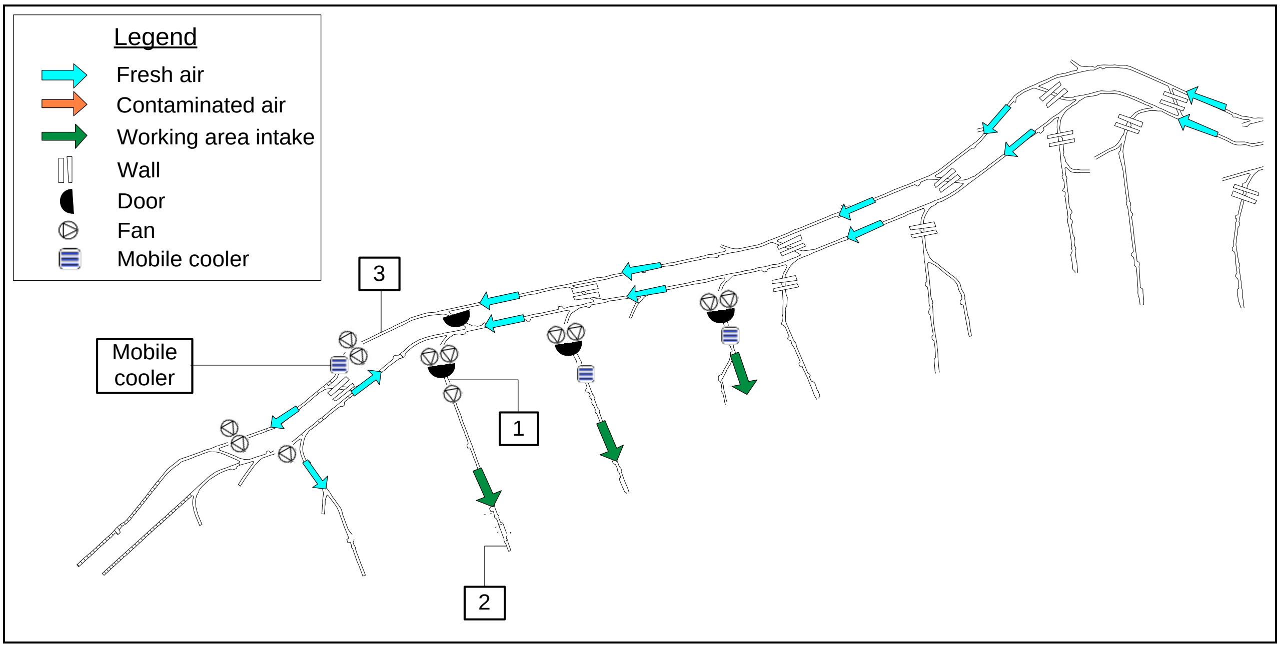


**Figure O-1: Underground temperature measurement locations at Mine B (75L)***

These results were summarised in Section 3.3.6 and Section 3.3.7. Figure O-2, Figure O-3 and Figure O-4 illustrate the WB and DB temperatures at Points 1 to 3, respectively. These include the measured temperature compared with the transient simulated temperature and quasi-steady-state simulated temperature.

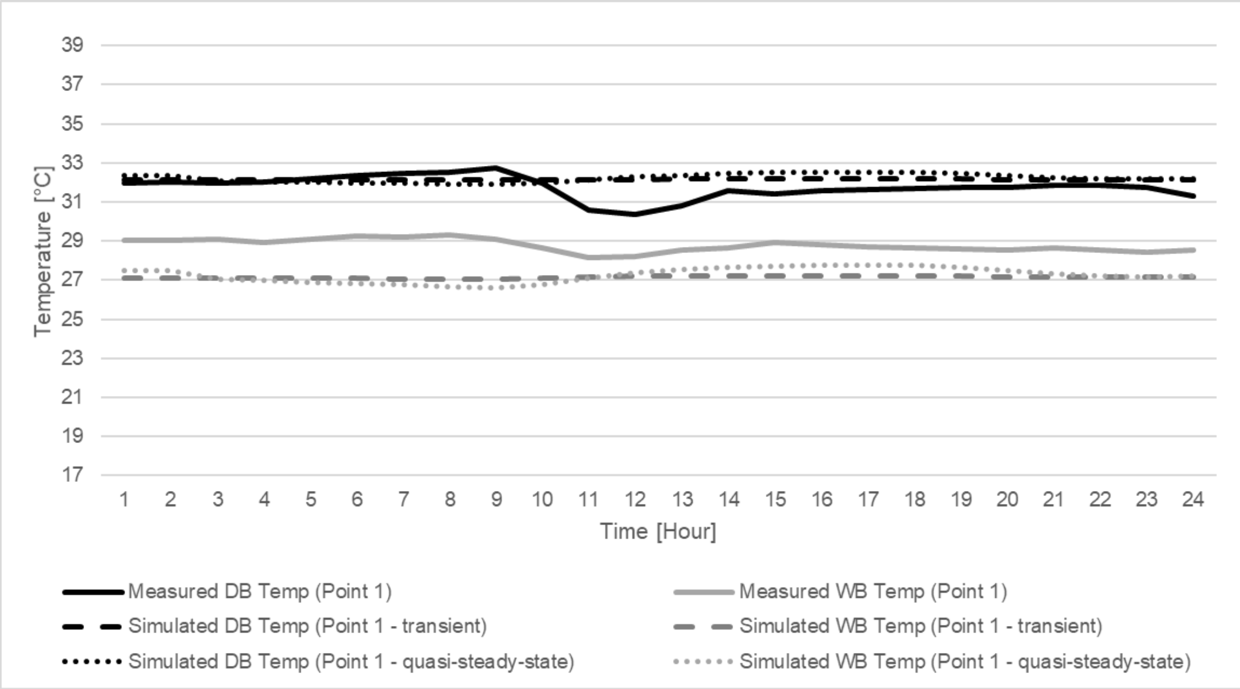


**Figure O-2: Mine B transient and quasi-steady-state temperature comparison (75L – Point 1)***

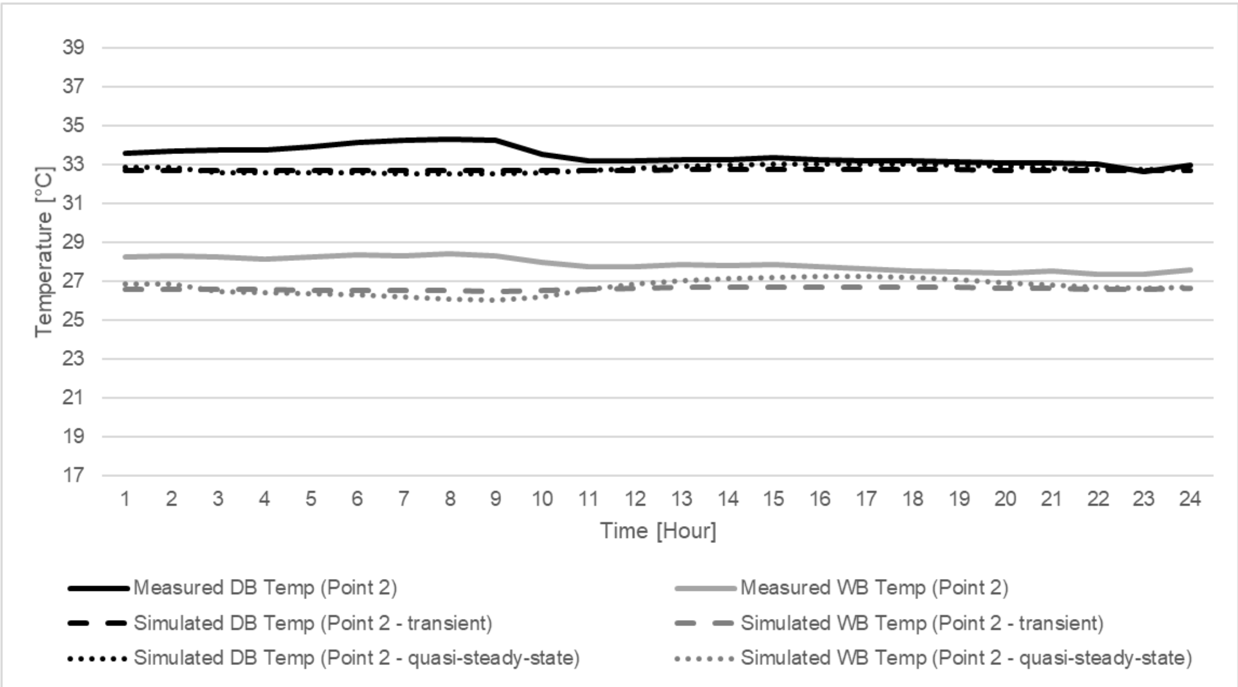


**Figure O-3: Mine B transient and quasi-steady-state temperature comparison (75L – Point 2)***

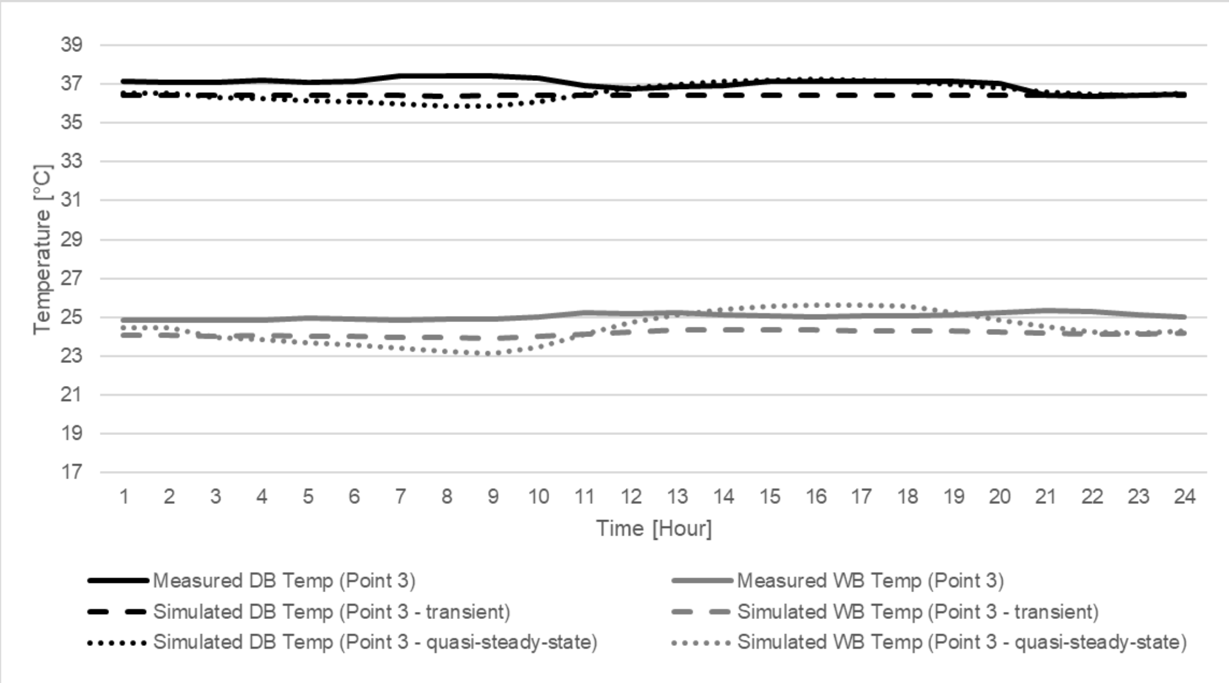


**Figure O-4: Mine B transient and quasi-steady-state temperature comparison (75L – Point 3)***

Table O-1 summarises the simulation performance for the three measurement points on 75L.

**Table O-1: Mine B comparison of transient and quasi-steady-state simulation performance (75L)**

| Location | Parameter | Unit | MSE | $R^2$ | Maximum error |
|---|---|---|---|---|---|
| Point 1 | DB temperature (transient) | °C | 0.49 | 0.56 | 1.78 |
| | DB temperature (quasi-steady-state) | °C | 0.70 | 0.25 | 1.89 |
| | WB temperature (transient) | °C | 2.78 | 0.35 | 2.27 |
| | WB temperature (quasi-steady-state) | °C | 2.64 | 0.17 | 2.66 |
| Point 2 | DB temperature (transient) | °C | 0.77 | 0.64 | 1.61 |
| | DB temperature (quasi-steady-state) | °C | 0.79 | 0.44 | 1.76 |
| | WB temperature (transient) | °C | 1.78 | 0.46 | 1.90 |
| | WB temperature (quasi-steady-state) | °C | 1.78 | 0.38 | 2.31 |
| Point 3 | DB temperature (transient) | °C | 0.44 | 0.13 | 1.00 |
| | DB temperature (quasi-steady-state) | °C | 0.53 | 0.05 | 1.76 |
| | WB temperature (transient) | °C | 0.82 | 0.28 | 1.19 |
| | WB temperature (quasi-steady-state) | °C | 0.91 | 0.20 | 2.31 |

The average maximum error improvement between the true transient and quasi-steady-state simulation was 0.49°C.

# APPENDIX P: MINE C KPIS AND DATA

The KPIs for Mine C are shown in Table P-1.

**Table P-1: Mine C KPIs**

| Area | KPI | Unit |
|---|---|---|
| Working area intakes | Air mass flow rate | [kg/s] |
| | DB temperature | [°C] |
| | WB temperature | [°C] |
| Return fans operating condition | Air mass flow rate | [kg/s] |
| | Static pressure | [kPa] |
| Fridge plants | Condenser water flow rate | [ℓ/s] |
| | Condenser inlet water temperature | [°C] |
| | Condenser outlet water temperature | [°C] |
| | Evaporator water flow rate | [ℓ/s] |
| | Evaporator inlet water temperature | [°C] |
| | Evaporator outlet water temperature | [°C] |
| BAC | Air outlet WB temperature | [°C] |
| Cold dam | Outlet water temperature | [°C] |

Figure P-1 illustrates the ambient and underground temperature measured at Mine C with temperature loggers placed at a working area intake.

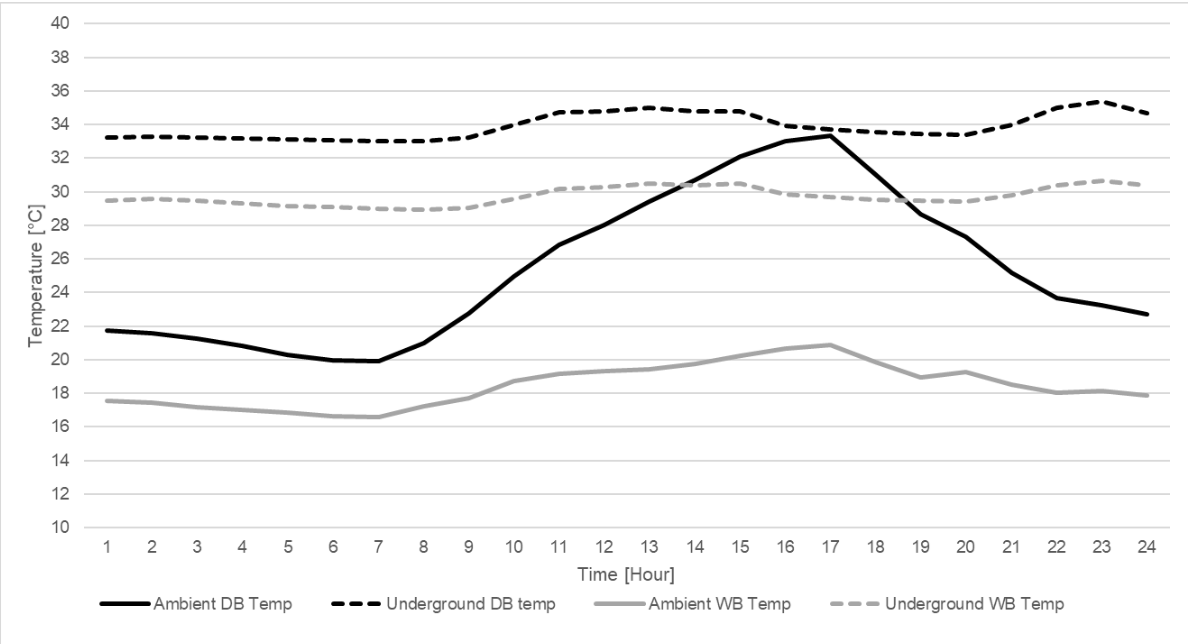


**Figure P-1: Ambient and underground temperatures at Mine C***

Figure P-2 illustrates the water flow supplied to the cold dam and the cold dam water outlet temperature. These are the main outputs and KPIs of the cooling system.

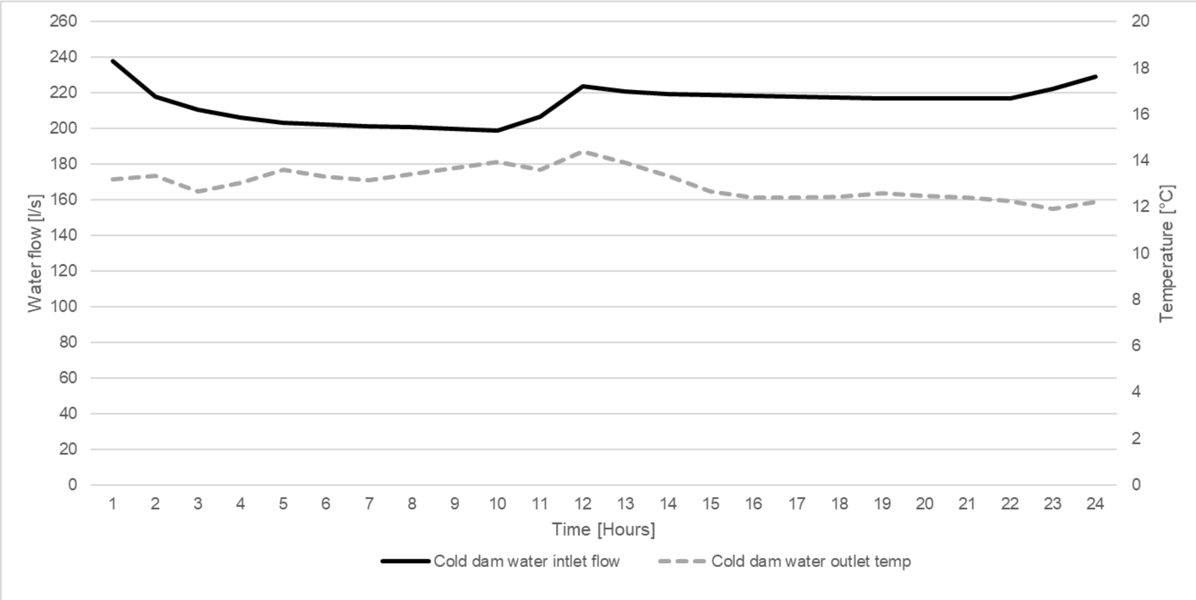


**Figure P-2: Mine C 255L cooling system main outputs***

# APPENDIX Q: MINE C SECONDARY HEAT SOURCES

Mine C did not record the machine operating times in detail, thus the fuel-driven machinery heat load was determined with the fuel consumption using Equation 2-2. Table Q-1 shows how the heat was calculated according to the fuel consumption. A multiplication factor of 2.5 was used to account for inefficiencies [35].

**Table Q-1: Fuel-driven machinery heat for Mine C**

| Parameter | Unit | Value |
|---|---|---|
| Total diesel consumption | [ℓ/month] | 146 109 |
| Calorific value of diesel | [MJ/kg] | 45.6 |
| Diesel density | [kg/m³] | 0.85 |
| Combustion efficiency | [%] | 0.95 |
| Multiplication factor | – | 2.5 |
| **Mechanised heat load** | **[kW]** | **5 104** |

Thereafter, the effective mechanised heat was calculated by excluding the potential energy gained, as seen in Equation 2-3. The machinery generally operated on the same levels, thus the average potential energy was negligible over 24 hours. Table Q-2 summarises the calculation of the heat from fuel-driven mechanised machinery.

**Table Q-2: Mine B effective mechanised machinery heat load for Mine C**

| Parameter | Unit | Value |
|---|---|---|
| Average mechanised heat load | [kW] | 5 104 |
| Average potential gained | [kW] | 0 |
| **Effective mechanised heat load** | **[kW]** | **5 104** |

The effective electrical heat load was calculated using Equation 2-4. The potential energy gained by useful work was calculated using Equation 2-1. Table Q-3 shows the results for the potential energy gain at Mine B.

**Table Q-3: Electrical potential energy gain for Mine C**

| Parameter | Amount [kg/s] | Elevation gain [m] | Potential energy gain [kW] |
|---|---|---|---|
| Water pumped out of ventilation district | 30 | 2 310 | 678 |
| Rock transported out of ventilation district | 21 | 790 | 162 |
| **Total** | | | **840** |

The sum of the electrical energy users that had to be excluded from the supplied electrical load equalled 10 106 kW. Table Q-4 shows the results for Mine B's effective electrical heat load.

**Table Q-4: Effective electrical load for Mine C**

| Parameter | Unit | Value |
|---|---|---|
| Average electrical load supplied | [kW] | 15 303 |
| Average potential gained | [kW] | 840 |
| Excluded equipment | [kW] | 10 106 |
| **Effective electrical heat load** | **[kW]** | **4 357** |

Mine B had 1 212 employees underground during a drilling shift. The metabolic heat load was calculated using Equation 2-5, and the results are shown in Table Q-5.

**Table Q-5: Metabolic heat load for Mine C**

| Parameter | Unit | Value |
|---|---|---|
| Employees | [–] | 1 212 |
| Average metabolic rate | [kW] | 0.25 |
| **Metabolic heat load** | **[kW]** | **303** |

The heat produced by explosives in the working areas was calculated using Equation 2-6. Mine A used an average of 68 880 kg of explosive per month with 4 030 kJ of energy produced per kilogram [35]. Table Q-6 summarises the calculation of the explosive heat load.

**Table Q-6: Explosive heat load for Mine C**

| Parameter | Unit | Value |
|---|---|---|
| Explosive used (monthly) | [kg] | 68 880 |
| Heat produced per kilogram | [kJ/kg] | 4 030 |
| Blast frequency | [days] | 1 |
| **Explosive heat load** | **[kW]** | **105** |

Mine C did not have fissure water underground, thus it was not included as a heat source.

# APPENDIX R: MINE C COOLING SYSTEM SIMULATION ACCURACY

Some water temperatures and airflow could only be measured in a steady state. The cooling system simulation was first calibrated in a steady state, thereafter an accurate cold water dam temperature was provided when integrated into the true transient ventilation model. Table R-1 shows the accuracy of the cooling system components, which had an average accuracy of 97.3%. When integrated into the transient ventilation model, the simulation produced a cold water dam temperature with an MSE of 0.72, an $R^2$ of 0.17, and a maximum error of 1.54°C.

**Table R-1: Mine C cooling system accuracy**

| Parameter | Unit | Measured | Simulated | Error |
|---|---|---|---|---|
| FP1 Condenser inlet water temperature | [°C] | 41.2 | 40.9 | 0.8 |
| FP1 Condenser outlet water temperature | [°C] | 44.3 | 43.7 | 1.3 |
| FP1 Condenser water flow rate | [ℓ/s] | 154.8 | 154.6 | 0.1 |
| FP1 Evaporator inlet water temperature | [°C] | 16.4 | 16.4 | 0.1 |
| FP1 Evaporator outlet water temperature | [°C] | 9.7 | 10.2 | 4.7 |
| FP1 Evaporator water flow rate | [ℓ/s] | 60.0 | 60.0 | 0.0 |
| FP3 Condenser inlet water temperature | [°C] | 43.8 | 41.9 | 4.4 |
| FP3 Condenser outlet water temperature | [°C] | 53.9 | 50.6 | 6.1 |
| FP3 Condenser water flow rate | [ℓ/s] | 145.2 | 144.9 | 0.2 |
| FP3 Evaporator inlet water temperature | [°C] | 16.4 | 16.9 | 2.9 |
| FP3 Evaporator outlet water temperature | [°C] | 6.7 | 7.0 | 4.5 |
| FP3 Evaporator water flow rate | [ℓ/s] | 141.8 | 137.8 | 2.8 |
| FP4 Condenser inlet water temperature | [°C] | 42.2 | 40.7 | 3.6 |
| FP4 Condenser outlet water temperature | [°C] | 46.9 | 46.0 | 2.0 |
| FP4 Condenser water flow rate | [ℓ/s] | 111.0 | 111.0 | 0.0 |
| FP4 Evaporator inlet water temperature | [°C] | 16.4 | 16.9 | 2.9 |
| FP4 Evaporator outlet water temperature | [°C] | 9.3 | 9.6 | 3.2 |
| FP4 Evaporator water flow rate | [ℓ/s] | 62.3 | 62.1 | 0.3 |
| FP5 Condenser inlet water temperature | [°C] | 42.2 | 40.7 | 3.5 |
| FP5 Condenser outlet water temperature | [°C] | 48.0 | 47.5 | 1.1 |
| FP5 Condenser water flow rate | [ℓ/s] | 90.6 | 90.6 | 0.0 |
| FP5 Evaporator inlet water temperature | [°C] | 16.4 | 16.9 | 2.9 |
| FP5 Evaporator outlet water temperature | [°C] | 9.8 | 9.4 | 4.1 |
| FP5 Evaporator water flow rate | [ℓ/s] | 57.1 | 57.0 | 0.3 |
| FP10 Condenser inlet water temperature | [°C] | 41.6 | 40.5 | 2.7 |
| FP10 Condenser outlet water temperature | [°C] | 49.3 | 48.8 | 1.0 |
| FP10 Condenser water flow rate | [ℓ/s] | 191.7 | 191.7 | 0.0 |
| FP10 Evaporator inlet water temperature | [°C] | 21.1 | 21.7 | 3.0 |
| FP10 Evaporator outlet water temperature | [°C] | 14.8 | 14.0 | 5.2 |
| FP10 Evaporator water flow rate | [ℓ/s] | 163.7 | 163.7 | 0.0 |
| BAC 289L outlet WB temperature | [°C] | 21.8 | 21.8 | 0.2 |
| Cold dam temperature | [°C] | 9.2 | 8.7 | 5.8 |
| Hot dam temperature | [°C] | 20.9 | 21.7 | 3.9 |

Figure R-1 illustrates the measured and simulated cold dam water temperature on 255L.

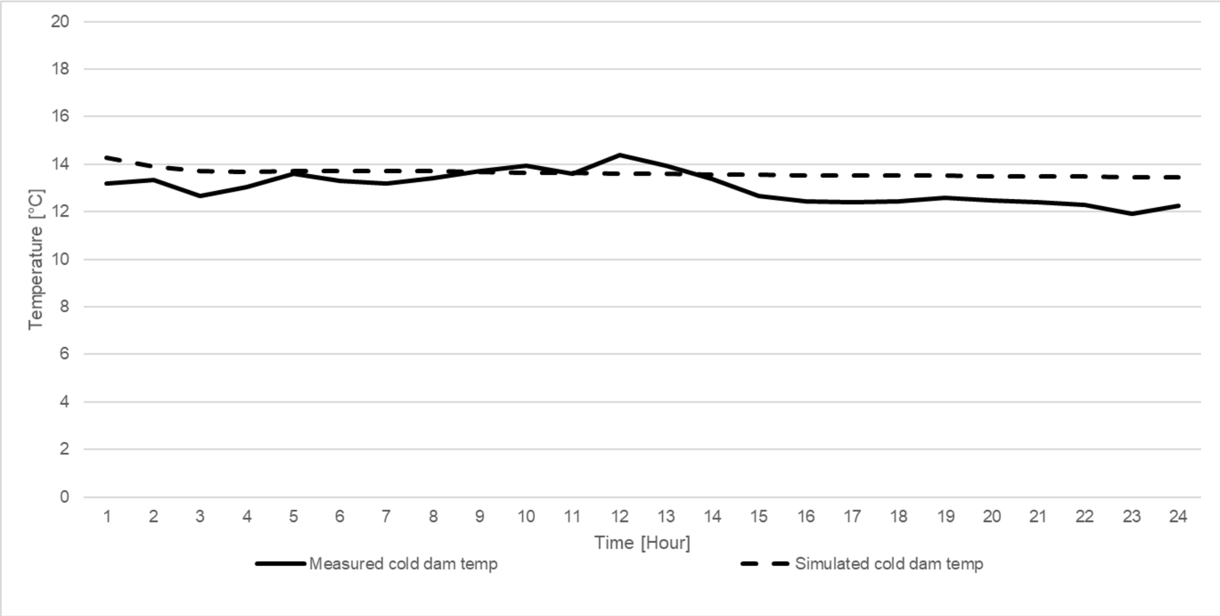


**Figure R-1: Mine C cold dam temperature comparison***

# APPENDIX S: MINE C SIMULATION RESULTS

This appendix contains the measured and simulated temperatures at working area intakes of Mine C. These results were summarised in Section 3.4.6 and Section 3.4.7. Figure S-1 and Figure S-2 illustrate the WB and DB temperatures at 287L East and 289L East, respectively. These include the measured temperature compared with the transient simulated temperature and quasi-steady-state simulated temperature.

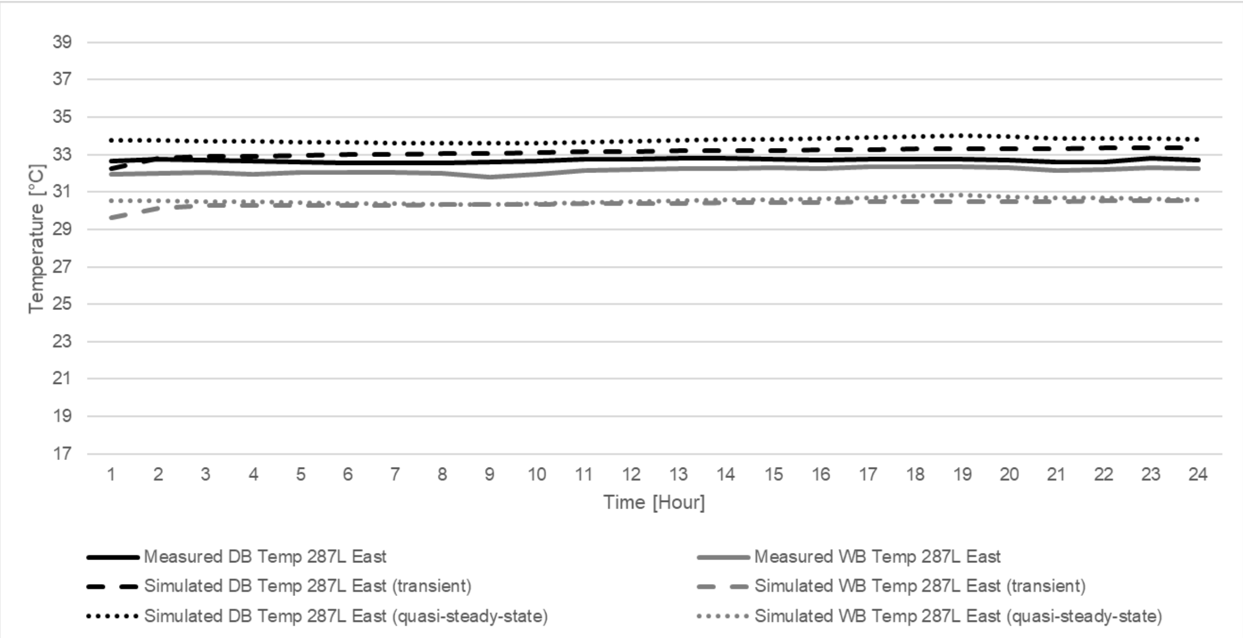


**Figure S-1: Mine C transient and quasi-steady-state temperature comparison (287L East)***

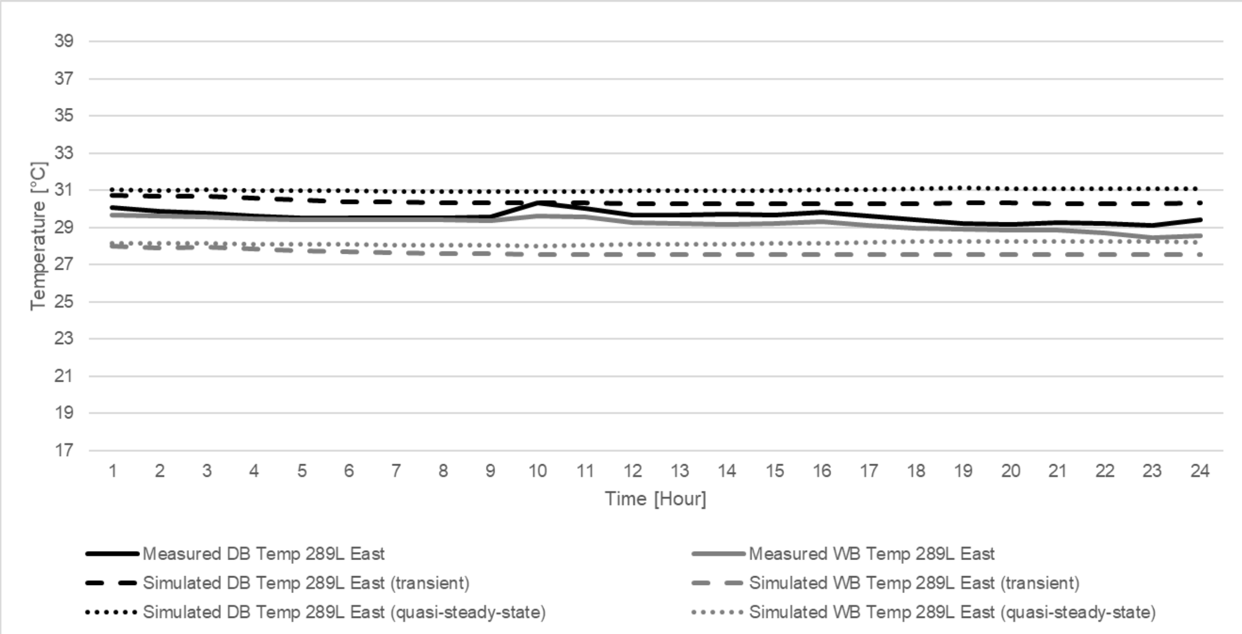


**Figure S-2: Mine C transient and quasi-steady-state temperature comparison (289L East)***

Table S-1 summarises the simulation performance for the three locations at Mine C.

**Table S-1: Mine C comparison of transient and quasi-steady-state simulation performance**

| Location | Parameter | Unit | MSE | $R^2$ | Maximum error |
|---|---|---|---|---|---|
| 287L West | DB temperature (transient) | [°C] | 1.14 | 0.38 | 2.11 |
| | DB temperature (quasi-steady-state) | [°C] | 0.75 | 0.08 | 1.20 |
| | WB temperature (transient) | [°C] | 0.28 | 0.12 | 0.90 |
| | WB temperature (quasi-steady-state) | [°C] | 0.76 | 0.16 | 1.31 |
| 287L East | DB temperature (transient) | [°C] | 0.24 | 0.10 | 0.75 |
| | DB temperature (quasi-steady-state) | [°C] | 1.21 | 0.27 | 1.29 |
| | WB temperature (transient) | [°C] | 3.22 | 0.39 | 2.30 |
| | WB temperature (quasi-steady-state) | [°C] | 2.55 | 0.67 | 1.74 |
| 289L East | DB temperature (transient) | [°C] | 0.69 | 0.14 | 1.20 |
| | DB temperature (quasi-steady-state) | [°C] | 2.13 | 0.44 | 2.02 |
| | WB temperature (transient) | [°C] | 2.59 | 0.39 | 2.30 |
| | WB temperature (quasi-steady-state) | [°C] | 1.31 | 0.60 | 1.61 |